LEVEL II (2)

AD NO.
FUNDING PROJECT 1L161101A91A
TECOM PROJECT (TRMS) 7-CO-ILO-AP1-001 (TASK 5)
TEST ACTIVITY REPORT APG-MT-5481
TEST SPONSOR US ARMY TEST AND EVALUATION COMMAND

AD A096638

IMPROVEMENT OF AIR BLAST MEASUREMENT

ILIR TASK 5

BY

W. SCOTT WALTON

MARCH 1981

DISTRIBUTION UNLIMITED

US ARMY ABERDEEN PROVING GROUND
ABERDEEN PROVING GROUND, MARYLAND
21005

REPRODUCTION LIMITATIONS

NONE

DTIC is authorized to reproduce this document
Government purposes.

DISPOSITION INSTRUCTIONS

Destroy this report in accordance with appropriate regulations when no longer needed. Do not return it to the originator.

DISCLAIMER

Information and data contained in this document are based on input available at the time of preparation. Because the results may be subject to change, this document should not be construed to represent the official position of the US Army Materiel Development Readiness Command unless so stated.

The use of trade names in this report does not constitute an official indorsement or approval of the use of such commercial hardware or software. This report may not be cited for purposes of advertisement.

Unclassified

SECURITY CLASSIFICATION OF THIS PAGE (When Data Entered)

REPORT DOCUMENTATION PAGE

READ INSTRUCTIONS BEFORE COMPLETING FORM

1. REPORT NUMBER: TECOM Project 7-CO-ILO-AP1-001	2. GOVT ACCESSION NO.: AD-A096 638
3. RECIPIENT'S CATALOG NUMBER:	
4. TITLE (and Subtitle): IMPROVEMENT OF AIR BLAST MEASUREMENT ILIR TASK 5	5. TYPE OF REPORT & PERIOD COVERED: Final, May 1978 to Dec 1980
	6. PERFORMING ORG. REPORT NUMBER: APG-MT-5481
7. AUTHOR(s): W. Scott Walton	8. CONTRACT OR GRANT NUMBER(s): None
9. PERFORMING ORGANIZATION NAME AND ADDRESS: Materiel Testing Directorate, ATTN: STEAP-MT-G, Aberdeen Proving Ground, MD 21005	10. PROGRAM ELEMENT, PROJECT, TASK AREA & WORK UNIT NUMBERS: None
11. CONTROLLING OFFICE NAME AND ADDRESS: Commander, TECOM, ATTN: DRSTE-AD-M, Aberdeen Proving Ground, MD 21005	12. REPORT DATE: March 1981
	13. NUMBER OF PAGES: 206
14. MONITORING AGENCY NAME & ADDRESS(if different from Controlling Office): None	15. SECURITY CLASS. (of this report): Unclassified
	15a. DECLASSIFICATION/DOWNGRADING SCHEDULE: None

16. DISTRIBUTION STATEMENT (of this Report)

Distribution Unlimited.

17. DISTRIBUTION STATEMENT (of the abstract entered in Block 20, if different from Report)

None

18. SUPPLEMENTARY NOTES

None

19. KEY WORDS (Continue on reverse side if necessary and identify by block number)

Air blast overpressure
Blast gages
Explosive blasts
Muzzle blasts
Overpressure measurement
Pressure measurement
Transducers

20. ABSTRACT (Continue on reverse side if necessary and identify by block number)

A study was conducted to improve the accuracy of air blast measurements in the range of 170 to 190 dB (6 to 60 kPa or 1 to 10 psi). The primary application of these measurements is to determine human tolerance to muzzle blast produced by Army weapons. A variety of electrical, mechanical, and environmental sources of measurement problems are documented. Extensive testing of a variety of transducers and calibration techniques were conducted in the laboratory. Outdoor field tests were also conducted, several examples of field test data

DD FORM 1 JAN 73 1473 EDITION OF 1 NOV 65 IS OBSOLETE

Unclassified

SECURITY CLASSIFICATION OF THIS PAGE (When Data Entered)

20. are provided. It was concluded that when the best possible measurement techniques are used, single channel, laboratory measurements using hand picked transducers could be made to an accuracy of ±2%. Accuracy for meticulously conducted, multi-channel field tests can be as good as ±5 to ±10%.

TABLE OF CONTENTS

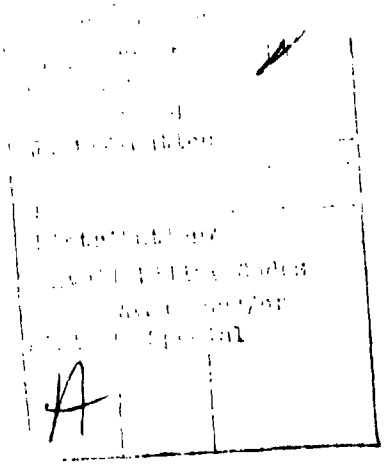

PAGE

SECTION 4. CALIBRATION TECHNIQUES

SECTION 5. EXTRANEOUS EFFECTS

SECTION 6. RECORDING, PLAYBACK, AND ANALYSIS OF DATA

SECTION 7. APPENDICES

FOREWORD

The Materiel Testing Directorate (MTD), Aberdeen Proving Ground (APG), Maryland conducted this investigation and prepared this report in order to improve accuracy of air blast pressure measurement. Work began in May 1978 and was completed in December 1980. Funds for this study were provided by the In-House Laboratory Independent Research Program (ILIR).

In documenting the various error sources that affect accuracy, a certain negative flavor permeates the discussion. Many plots of erroneous measurements have been included; some of the errors were intentionally introduced, and some were discovered by accident. Normally, such measurements would be discarded, and a footnote reading "Data lost at this location" would be inserted.

It is hoped that documentation of these errors will allow such problems to be quickly recognized in the field so that corrective action can be taken. The intent is to show that careful attention to detail can produce accurate blast measurements. It is hoped that this objective has been achieved without leading the reader to believe that all blast measurements are inherently plagued by errors.

Reference to pressure in the text of this report is expressed in units of kilopascals (kPa). Unfortunately, many of the calculator programs written for plotting pressure versus time use pounds per square inch. Usually the plots are presented to illustrate the shape of a curve rather than read a specific value. It is hoped that the conversion nomagraph shown in section 2.1 will alleviate inconveniences caused by use of different units.

Appreciation is expressed to the people who have provided data, ideas, and motivation for this report. They are: George Coulter, Edward Schmidt, Edmund Gion, and George Teel of the US Army Ballistic Research Laboratory; James Patterson and Benjamin Mozo of the Aeromedical Research Laboratory; George Garinther, Joel Kalb, and Benjamin Cummings of the Human Engineering Laboratory. Appreciation is also expressed to John D. Reynolds, who initiated this study.

(Page 2 Blank)

SECTION 1. SUMMARY

1.1 BACKGROUND

The Materiel Testing Directorate (MTD) at Aberdeen Proving Ground (APG) routinely makes air blast measurements. If the peak pressure level is expected to be below 170 dB (6 kPa or 1 psi), microphones are used. Pressures above 170 dB require use of a more rugged pressure transducer.

The transducers available at MTD for measuring blast overpressure were designed more than 20 years ago for measuring large explosions simulating conventional and nuclear bomb detonation, and have changed very little.

Although the transducers and procedures have not changed much in 20 years, the type of workload has changed. Most measurements are now made to determine human tolerance to existing muzzle blast. These measurements generally fall in the range of 170 to 190 dB (6 to 60 kPa or 1 to 10 psi).

Muzzle blast measurements of earlier weapons were evaluated by a criterion stating that the peak pressure must be less than 3 psi (20.7 kPa) in the crew area. This criterion was usually met. Since muzzle blast was not a critical area, it did not generate much managerial interest in the accuracy of the measurements being made.

The Army's effort to make weapons shoot farther and weigh less has created a situation that makes muzzle blast in the crew areas critical. Because training restrictions, and even acceptance or rejection of a weapon may be based on muzzle blast overpressure measurements, it is desirable that these measurements be as accurate as possible. Errors as large as 15 to 20% that could be tolerated in measurement of a bomb explosion are not acceptable in measurement of muzzle blast.

A weapon that has been a focal point for muzzle blast overpressure problems is the M198 howitzer firing the M203 propelling charge shown in figure 1.1-1. Tests conducted by TECOM indicated that with minor exceptions, this weapon passed the human tolerance criteria. Surgeon General testing indicated that the weapon failed. Both sets of measurements could be replicated. This discrepancy indicated the need for improved, standardized measuring techniques.

1.1 (Cont'd)

Figure 1.1-1. M198 Howitzer.

1.2 OBJECTIVE

The objective of this study is to improve the accuracy of airblast overpressure measurements in the range of 170 to 190 dB from ±20% to ±5%.

1.3 SUMMARY OF PROCEDURES

The original plan for this study was to replace the LC-33 pencil gages with two LC-70 miniature transducers placed in a large, pencil-shaped ojive, and to replace pentolite calibration with shock tube calibration. The new transducers were to be qualified using pentolite explosions and comparing their performance to the performance of the LC-33 transducer.

For a variety of reasons, it was determined necessary to adopt a new approach. Several different transducers and calibration techniques were examined.

In addition to laboratory tests performed specifically for this study, valuable data were gathered while making field blast measurements for specific weapons, such as the 81-mm mortar, the M198 howitzer, and the 105-mm tank gun. Data were also obtained from other organizations at APG, such as the Human Engineering Laboratory and the Ballistics Research Laboratory.

The culmination of this study was a 3-day field test using pentolite that was known as the "Swan song shoot." This testing was accomplished 20 to 22 August 1980. It provided confirmation and documentation of the effects of mounting technique, sensitivity to extraneous effects, and calibration.

1.4 SUMMARY OF RESULTS

Figure 1.4-1 shows blast overpressure produced by an 8-inch howitzer as measured with an LC-33 pencil gage. The physical implications of this plot are rather unusual.

Note that ambient pressure seems to increase after the muzzle blast ceases. Such drastic changes in ambient pressure are associated with severe weather. This rapid change in ambient pressure could possibly be observed in an aircraft flying through the eye of a hurricane.

Note the large pressure oscillations indicated after the muzzle blast. Pressure oscillations of this magnitude would be perceived as an unbearably loud noise such as one might encounter next to a foghorn.

It seems rather unlikely that one would make a muzzle blast measurement while firing an 8-inch howitzer from an airplane flying next to a foghorn located in the eye of a hurricane! For a more plausible explanation of what may have happened, refer to the sections of the report on acceleration error and thermal drift (5.2 and 5.6).

Twenty years ago, a measurement like the one shown in figure 1.4-1 might have been considered acceptable. At that time, only the positive phase of a blast measurement was analyzed. In figure 1.4-1 the positive phase only lasts 7 milliseconds, and appears to be a reasonable representation of what occurs during the positive portion of a blast wave.

The rarefaction phase of the blast wave was almost totally ignored in earlier years for two reasons. First, it was assumed that most damage occurred during the positive phase. Second, difficulties such as those shown in figure 1.4-1 were typical of instrumentation available twenty years ago, making measurement of the rarefaction phase difficult.

The current method of analyzing human tolerance to blast makes measurement of the rarefaction phase important. Instrumentation now available makes more accurate measurement of the rarefaction phase possible.

Measuring the output of an electrical pressure transducer to ±1% is a relatively straightforward matter. Insuring that this signal corresponds to ±5% of the true side-on pressure is much more difficult.

Agreement among several methods of calibrating the same transducer was ±2% at best and typically ±5%. This performance can be improved by selecting the best transducers from a lot, repeating the calibration several times and discarding the outliers. Such techniques are only practical when measurements of only 1 or 2 channels are required, and sufficient time for preparation is available.

1.4 (Cont'd)

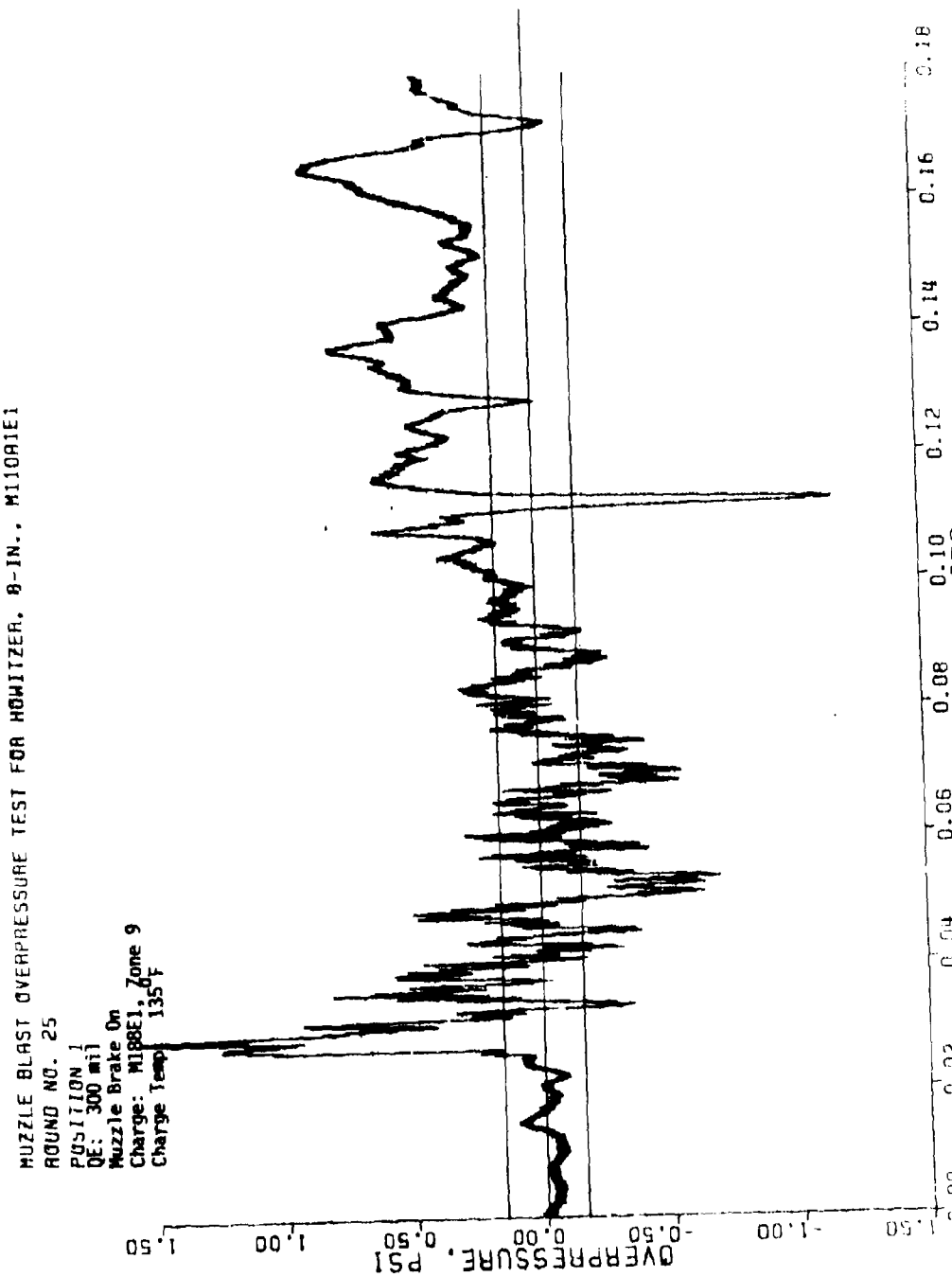

Figure 1.4-1. Example of a poor measurement of muzzle blast overpressure.

In addition to tolerances as large as ±5% for calibration, allowances must be made for other errors such as those caused by:

a. Acceleration (sections 5.1, 5.2, and 5.3)

b. Misalignment and mounting configuration (section 3.3)

c. Transducer anomalies (section 3.2 and 3.4)

d. Thermal drift (section 5.6)

e. Ambient temperature effects (section 5.4)

f. Thermal transients (section 5.5)

g. Aerodynamic cleanliness (section 5.8)

h. Effects of filters and tape recorders (sections 6.2, 6.3, and 6.4)

i. Reflections from objects at the test site (section 5.7)

j. Electrical noise (section 6.5)

As discussed elsewhere in this report, each of these extraneous phenomena can become an indistinguishable part of the pressure measurement. Careful attention to measurement technique can reduce, but not completely eliminate these factors.

All transducers tested were found to have specific advantages and disadvantages; no single transducer was shown to be best for all situations. Recording instrumentation available, the measurement situation, and the specific type of measurement required influence the choice of transducer type and mounting arrangement.

1.5 ANALYSIS

Careful attention must be given to test set-up and data analysis to insure that the results are representative of the blast wave that is present, rather than anomalies caused by extraneous effects. Choice of instrumentation and measurement techniques affects sensitivity to extraneous effects.

Based on the technical problems discussed in this study, the following estimates of expected level of accuracy are presented:

Type of Measurement	Expected Level of Agreement
Laboratory conditions, hand-picked transducers Measurement of only one or two channels	1 to 2%
Typical laboratory equipment	2 to 5%
Field conditions	5 to 10%

In addition to tolerances based on technical problems, further allowances must often be made for non-technical matters which have a significant effect on measurement accuracy. There is an inevitable conflict between the desire to obtain the best possible measurement and the desire to complete the test as quickly as possible with the lowest grade qualified personnel.

The cost and time required to conduct a test are visible, intensively managed factors. The accuracy of the data is a much less tangible factor which occasionally suffers in deference to more practical matters of time and cost.

If an anomaly is noticed in the measurement while testing is in progress, troubleshooting the cause of the problem and fixing it become very expensive tasks. A typical test may involve as many as 15 people. At current labor rates of $15 to $20 per hour, it costs more than $4 per minute to check cables, look for loose connections, or remount and aline a transducer.

Due to thermal considerations, certain tests require that rounds be fired at or above a specified rate. In this situation, data anomalies cannot be remedied if they are discovered while firing, even if the problem requires only minor adjustment.

Because of these reasons, needed changes to test set-up are often not made once testing has begun. In such situations, it is easy to rationalize that a competent analyst will be able to distinguish the valid portions of the waveform from anomalies caused by extraneous effects.

In complex tests, which involve many measurements, or several different kinds of measurements, these problems become acute. The probability of all instrumentation working properly all of the time becomes small. Certain measurements will inevitably be sacrificed so that the test can be completed in a reasonable time.

1.6 CONCLUSIONS

a. Measurement and evaluation of muzzle blast has become a critical operation because many weapons produce blast levels that approach or exceed human tolerance limits.

b. Accurate blast measurements require careful attention to test set-up and data analysis to insure that the results are representative of the blast wave that is present, and not anomalies caused by extraneous effects.

c. Choice of instrumentation and measurement technique can dramatically affect test results. For example, if measurements of a marginal weapon are made with a noisy tape recorder, using a transducer that amplifies when misaligned, and filters that overshoot, the results may indicate that the weapon fails the human tolerance criteria, when in fact it should pass. Another weapon, when tested with a digital recorder, with a large signal to noise ratio, a transducer that attenuates when misaligned, and filters that are set too low, may be shown to pass the human tolerance criteria when the blast wave present in fact exceeds the criteria.

d. Because blast measurements are often both critical and difficult, particular attention must be given to the nontechnical compromises that must be made. Long set-up time and the need to repeat tests when data has anomalies should be anticipated.

e. Calibration of transducers is a critical operation. Many transducers exhibited large discrepancies (5%) between different transducers. This problem illustrates the need for more consistent transducers as well as the fact that there is no perfect technique for calibrating AC coupled transducers.

f. The overpressure levels observed from Pentolite explosions were quite different from what was expected (10%). Sufficient time to determine the reason for this discrepancy was not available.

g. Based on the testing workload, equipment available, and weather conditions encountered at APG, the low impedance, quartz element transducers with suppressed resonance have the best compromise of transducer characteristics for use by MTD.

1.7 RECOMMENDATIONS

a. Pressure transducers should be checked on three devices (static pulse calibrator, sine wave calibrator, and shock tube) before critical blast overpressure tests.

It is felt that these tests will cost less than the old pentolite calibration technique, and provide traceability to NBS, which did not exist before.

b. Further study should be conducted to accomplish the following objectives:

(1) Develop a better way to mount miniature transducers that isolates the transducer from acceleration and allows accurate alinement.

(2) Determine why the pentolite results disagreed so greatly with the laboratory calibration results.

(3) Develop techniques to improve agreement among laboratory calibration techniques.

(4) Explore development of an improved transducer with commercial manufacturers.

c. Selection of a transducer for critical blast overpressure tests should be based on thorough testing of the transducer's characteristics under known conditions. Particular attention should be given to the following characteristics:

(1) Blast wave response (overshoot, ringing, flow effects).

(2) Acceleration sensitivity.

(3) Temperature sensitivity.

(4) Ease and repeatability of calibration.

d. For critical blast overpressure tests, an on-site inspection of the data as they are acquired should be made to insure that the best possible measurement is obtained. This process will obviously increase the cost and time required for the test. If severe anomalies are noted in the data, the test should be repeated.

(Page 12 Blank)

SECTION 2. GENERAL DISCUSSION OF BLAST OVERPRESSURE

2.1 UNITS OF PRESSURE MEASUREMENT

Pressure is force per unit area, and should be expressed in units of force divided by length squared. Various units are used; the four most frequently cited are:

a. Pounds per square inch (psi).

b. Pascals (Newtons per square meter).

c. Atmospheres (dimensionless ratio of measured pressure to standard, sea level atmospheric pressure).

d. Decibels (dimensionless logarithmic ratio of measured pressure to a reference pressure).

Figure 2.1-1 shows the relationship between these four ways of expressing pressure. Most equipment in the United States is calibrated in psi.

In the interest of international standardization, the Army has adopted the pascal as the standard unit of pressure. The pressure levels discussed in this report are expressed in kilopascals (kPa). Many of the plots of pressure versus time are presented in psi rather than kPa because the plotting programs are written for units of psi.

The decibel (dB) is a unit commonly associated with hearing. The reference pressure for dB is 20 micropascals which is estimated to be the lowest pressure detectable by the human ear.

A few convenient relationships should be remembered when using decibels:

a. A difference of 0.1 dB is a 1% discrepancy.

b. A difference of 1 dB is a 12% discrepancy.

c. A 2:1 ratio of pressure (which is either a 50% discrepancy or a 100% discrepancy, depending on whether the small number or the large number is used as a reference) is a difference of 6 dB.

Units of Pressure

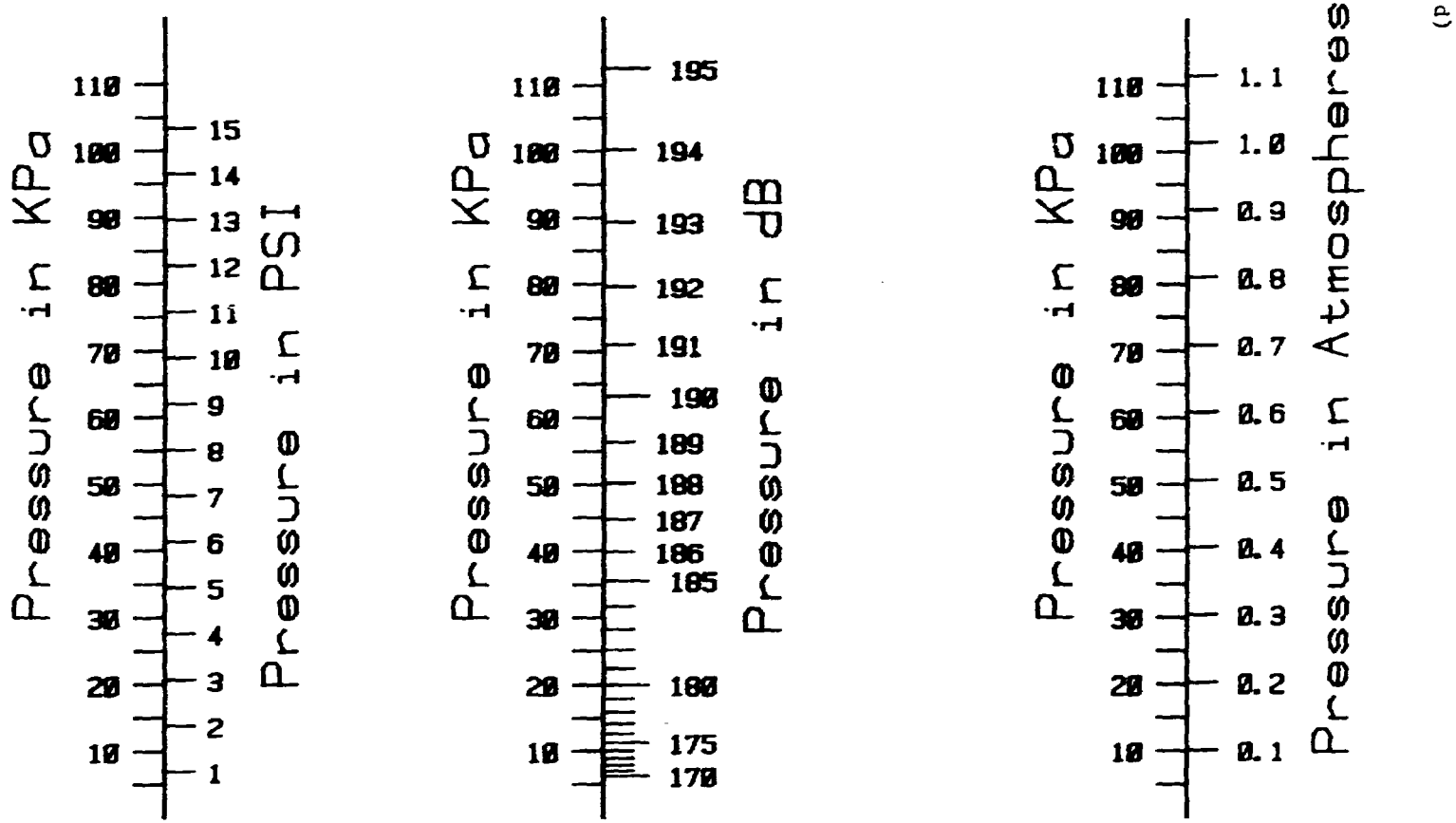

1 PSI = 6.895 KPa

$$dB = 20 \log \frac{KPa}{20 \times 10^{-9}}$$

1 ATMOSPHERE = 101.35 KPa

Figure 2.1-1. Comparison of units of pressure.

2.2 SHOCK WAVES

Most concern about blast pressure is associated with events that occur outdoors in open air. A convenient means of simulating blast experiments in the laboratory is the shock tube. As shown in figure 2.2-1, the pressure versus time waveforms of these two pressure sources is different.

The shock tube produces a flat-topped pressure versus time curve. The duration of the flat portion is a function of the length of the driver portion of the shock tube.

Free air explosions produce a pressure versus time curve that begins to decay immediately after peak pressure is obtained. In outdoor explosions, reflection of the blast wave from the ground plane produces a second pressure wave. This reflected wave travels faster than the incident wave because it is traveling through air already heated by the incident wave. When the reflected wave catches up with the incident wave, the two combine to form what is known as the Mach stem.

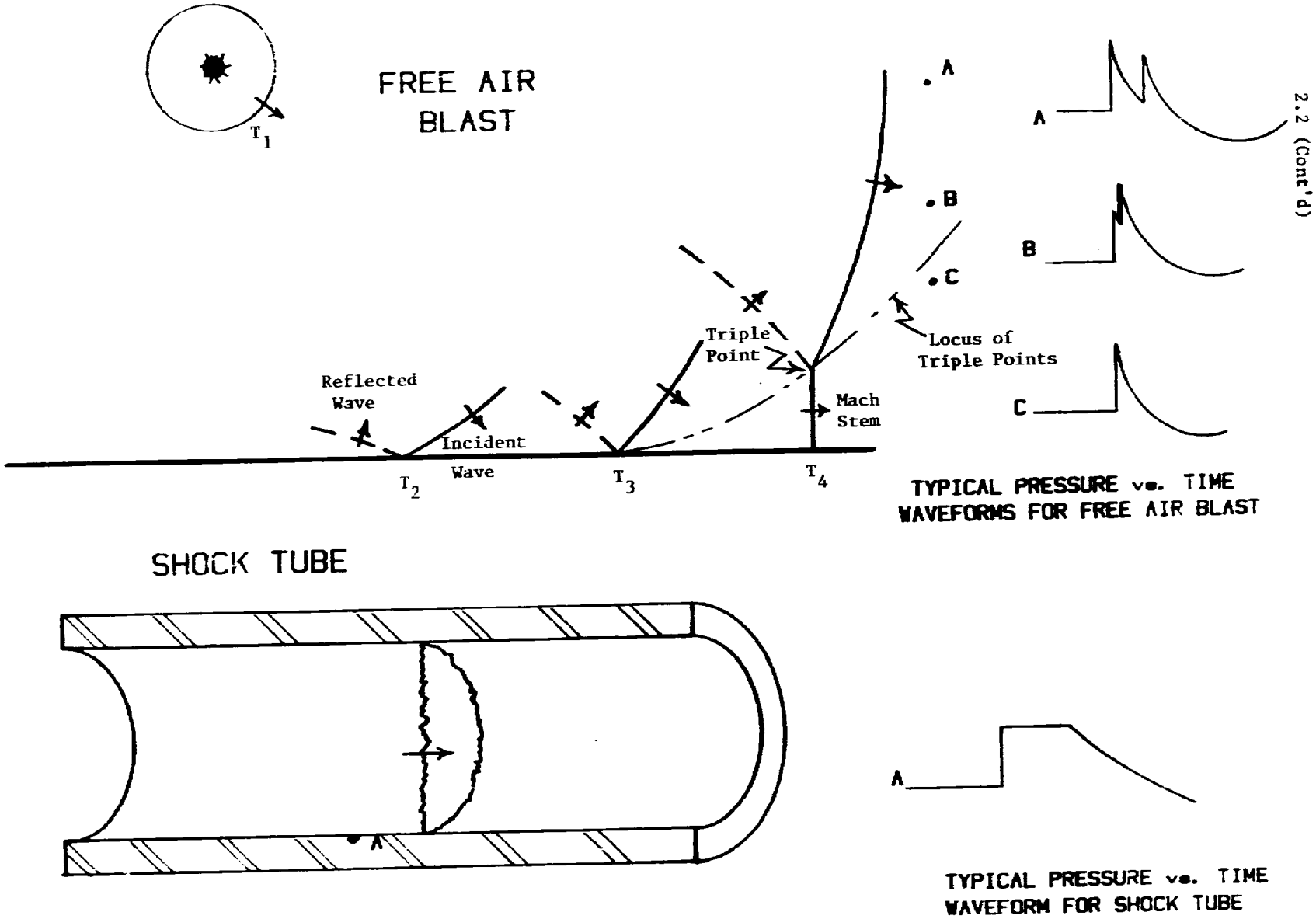

Figure 2.2-1. Examples of classical pressure versus time waveforms.

2.2 (Cont'd)

There are two types of pressure associated with subsonic flow of air: static pressure and dynamic pressure. The sum of static pressure plus dynamic pressure is called stagnation pressure. A blast wave travels supersonically and has three types of pressure associated with it: Side-on pressure (static pressure), face-on pressure (reflected pressure), and stagnation pressure (sum of static and dynamic pressure). Figure 2.2-2 gives pictorial descriptions of the three types of blast pressure, examples of their relative values, and typical waveforms that could be expected in a shock tube.

Side-on or static pressure is the pressure behind the blast wave. It must be measured by a transducer mounted perpendicular to the direction of wave propagation, and the transducer must not interfere with the propagation of the wave. The wave velocity is related to the side-on pressure by the Rankine-Hugoniot Equation for air:

$$P_s = P_o \frac{7}{6} (m^2-1)$$

where

P_s = side-on pressure

P_o = ambient pressure

m = Mach number of wave.

Mach number is a dimensionless expression of velocity. It is the ratio of the wave velocity divided by the speed of sound in ambient air. Mach number can be found by measuring the velocity of the wave and the temperature of the air:

$$m = \frac{v}{a}$$

where

m = Mach number

v = wave velocity

a = speed of sound in ambient air

but

$$a = 20.09 \sqrt{T}$$

where

T = ambient temperature in degrees Kelvin.

2.2 (Cont'd)

Reflected or face-on pressure is that pressure developed when a blast wave strikes an infinitely large wall which is perpendicular to wave propagation and reflects back in the exact opposite direction. Reflected pressure is related to side-on pressure by the following equation:

$$P_r = 2\ P_s\ \left(\frac{7P_o + 4P_s}{7P_o + P_s}\right)$$

where

P_r = Reflected pressure

P_s = Side-on pressure

P_o = Ambient pressure.

Stagnation pressure is the sum of the static pressure (side-on) plus dynamic pressure which is caused by particle flow behind the wave. Propagation of the blast wave alone involves no significant displacement of the air molecules. Behind the wave, the air molecules are displaced, but at a much slower velocity than the supersonic blast wave. The relationship between particle velocity and side-on pressure is:

$$u = \frac{5P_s}{7P_o} \cdot \frac{a}{\left(1 + \frac{6P_s}{7P_o}\right)^{\frac{1}{2}}}$$

where

u = Particle velocity

P_s = Side-on pressure

P_o = Ambient pressure

a = Speed of sound in ambient air.

Stagnation pressure can be expressed as the sum of side-on pressure plus dynamic pressure:

$$P_{stag} = P_s + \frac{\rho\ u^2}{2}$$

where

P_{stag} = Stagnation pressure

P_s = Side-on pressure

ρ = Density of ambient air

u = Particle velocity.

2.2 (Cont'd)

A more convenient expression for calculating stagnation pressure in terms of side-on pressure and ambient pressure alone is:

$$P_{stag} = P_s + \frac{5}{2} \cdot \frac{P_s^2}{7P_o + P_s}$$

where

P_{stag} = Stagnation pressure

P_s = Side-on pressure

P_o = Ambient pressure.

Practical measurement of stagnation pressure can be made by constructing a probe that will allow the blast wave to travel over it. As shown in figure 2.2-2, the transducer mounted in the point of the probe will instantaneously register reflected pressure when struck by the blast wave, but will register stagnation pressure once the wave continues past the tip of the probe.

The duration of the period during which reflected pressure is registered is called relief time. Relief time is a function of the diameter of the flat tip of the probe.

The equations given in this section are based on air behaving as an ideal gas with constant specific heats. For the pressure levels described in this report (less than 100 kPa), this assumption is valid. At higher pressures, the thermodynamic properties of real air must be used and the simplified equations are no longer valid.

2.2 (Cont'd)

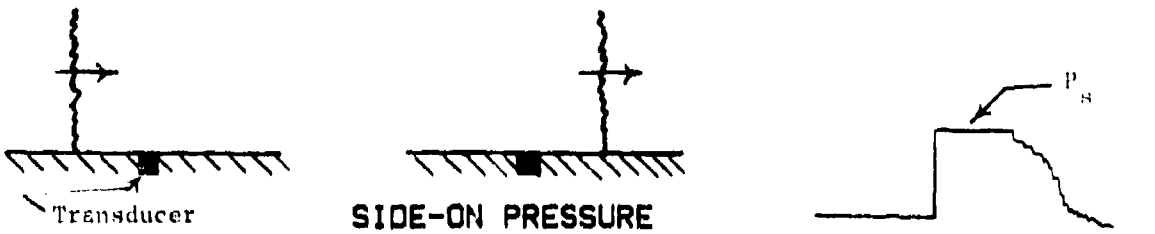

SIDE-ON PRESSURE

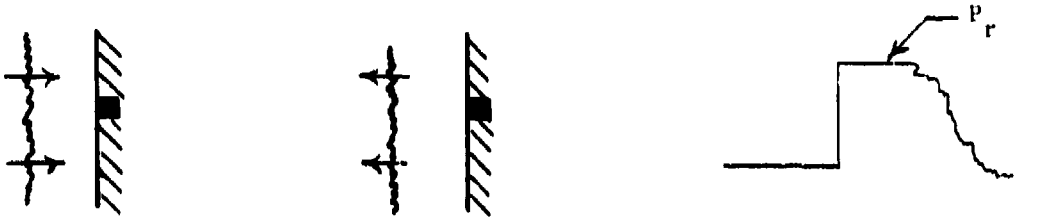

REFLECTED PRESSURE

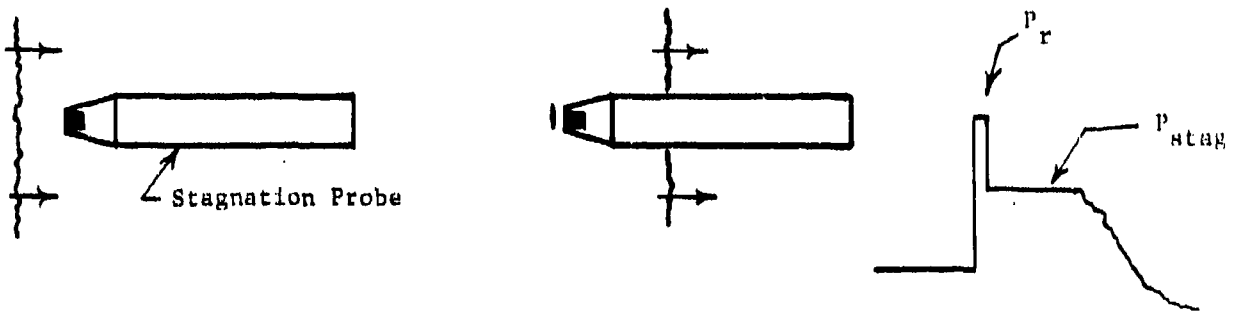

$$P_{stag} = P_s + \frac{\rho U^2}{2}$$

STAGNATION PRESSURE

P_s (KPa)	P_r (KPa)	P_{stag} (KPa)	SHOCK VELOCITY (Meters/Sec)	PARTICLE VELOCITY (Meters/Sec)
10.0	20.8	10.4	355.0	23.1
30.0	67.3	33.0	381.7	64.4
50.0	119.8	58.2	406.6	100.7
70.0	177.7	85.7	430.1	133.3
100.0	274.1	130.9	463.1	176.8

Figure 2.2-2. Types of pressure associated with a shock wave.

2.3 DIRECTIONAL EFFECTS

Blast overpressure is a directional phenomenon. Figure 2.3-1 is an excerpt from The Effects of Nuclear Weapons by Glasstone (ref 1). It shows how overpressure changes as the angle of a blast wave striking a surface is varied. In this plot, 0 degrees represents face-on and 90 degrees represents side-on. It should be noted that this information is for surfaces that are large with respect to the sensing transducer. If the sensor represents a significant portion of the surface, the results in figure 2.3-1 will not be duplicated.

Because of the directional nature of blast waves, it is important that transducers be carefully aligned in the proper direction. In complicated measurement situations, blast waves are reflected from many objects from different directions. In these situations, only certain portions of the pressure time history can be measured accurately.

An omnidirectional pressure sensor would be ideal, but no such gage exists. Some gages are, however, more sensitive to misalignment than others. This characteristic will be examined later in this report.

2.3 (Cont'd)

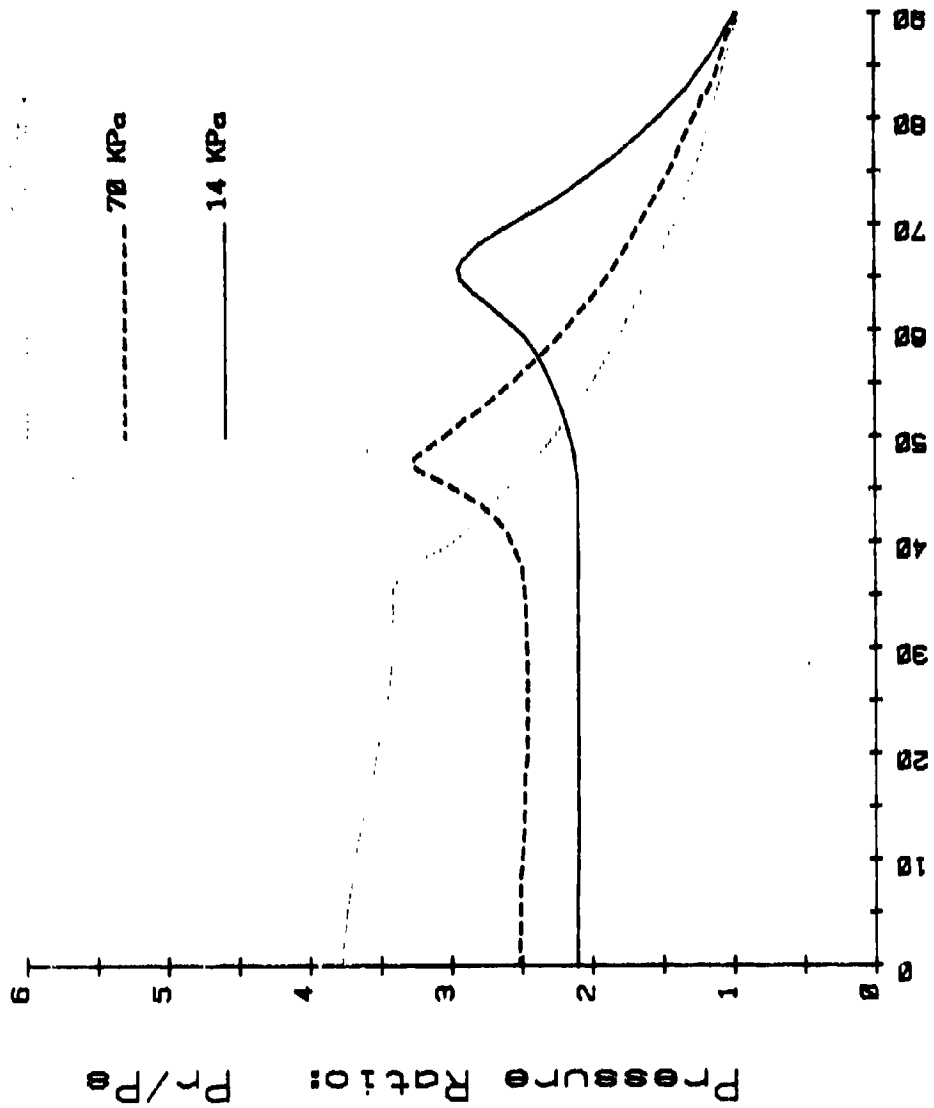

Figure 2.3-1. Reflected overpressure ratios as function of angle of incidence for various side-on overpressures. Pr = reflected overpressure, Ps = side-on overpressure, 0° = perfect reflection, 90° = side-on pressure. Reproduced from reference 1.

2.4 HUMAN TOLERANCE TO BLAST OVERPRESSURE

At the time this report is being written, human tolerance to blast overpressure is a subject of intense study by the Army. At present, it is not known how much blast overpressure can be tolerated and what parts of the body are most sensitive to blast.

In the past, it was assumed that damage to the ear occurred before any other type of damage. Noise limits for Army materiel are specified in MIL-STD-1474B (ref 2). The limits are prescribed in terms of peak side-on pressure and B duration. B duration has an explicit definition, but is essentially the time required for the pressure versus time curve to decay to 10% of the peak value. Figure 2.4-1 shows the limits prescribed by MIL-STD-1474B.

The authors of MIL-STD-1474 have pointed out in reference 3 why side-on rather than face-on pressure was chosen. It is stated that various transducers differed by as much as 3 to 10 dB when measuring face-on pressure. Good agreement between various transducers was observed for side-on pressure measurement.

Until current research is completed, the Army Surgeon General has stated that crew positions for new weapons will be chosen so that the worst case observed shall not exceed the "Z" curve shown in figure 2.4-1. Measurement techniques are proposed in standardization of muzzle blast overpressure measurements (ref 4). Many of the experiments and examples presented in this report provide justification for the guidance presented in reference 4.

2.4 (Cont'd)

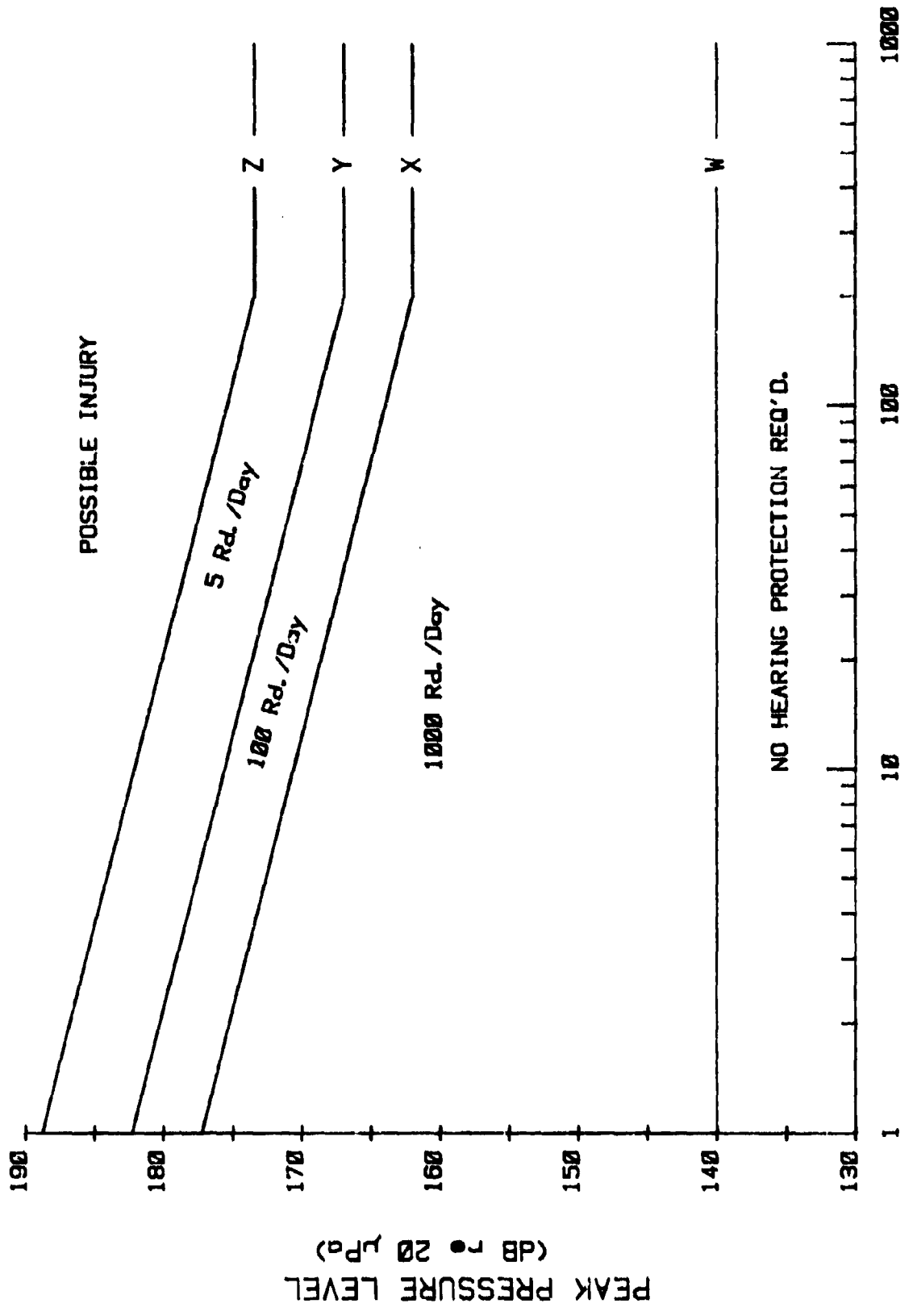

Figure 2.4-1. Limits for impulse noise prescribed in MIL-STD-1474 (ref 2).

2.5 MUZZLE BLAST

Energy released by propellant combustion launches the projectile and creates muzzle blast. The pressure field created by muzzle blast is symetrical about the line of fire but is not spherically symetrical. As shown in figure 2.5-1, the center of pressure moves along the line of fire.

It has been suggested by Cummings (ref 5) that near the muzzle, the center of pressure moves at the velocity of the projectile. Figure 2.5-5 shows the shape of equal pressure contours based on this prediction. Note that these predicted contours agree well with the measured contour.

The above discussion affects muzzle blast measurement in two significant ways. First, as shown in figure 2.5-2, steep gradients exist near the muzzle. Extreme care must be used in placing transducers. With the 81-mm mortar, crew locations are only a few calibers from the muzzle, a difference of 15 cm in locations caused in variation of as much as 50% in peak pressure.

2.5 (Cont'd)

Figure 2.5-1. Photographs of muzzle blast waves. Note that in top photo, projectile has just exited and center of pressure (white dot) is $\sim$2 calibers from the muzzle. In the bottom photo, projectile is $\sim$ 28 calibers from the muzzle, and the center of pressure $\sim$ 8 calibers from the muzzle (photographs courtesy of the US Army Ballistic Research Laboratory).

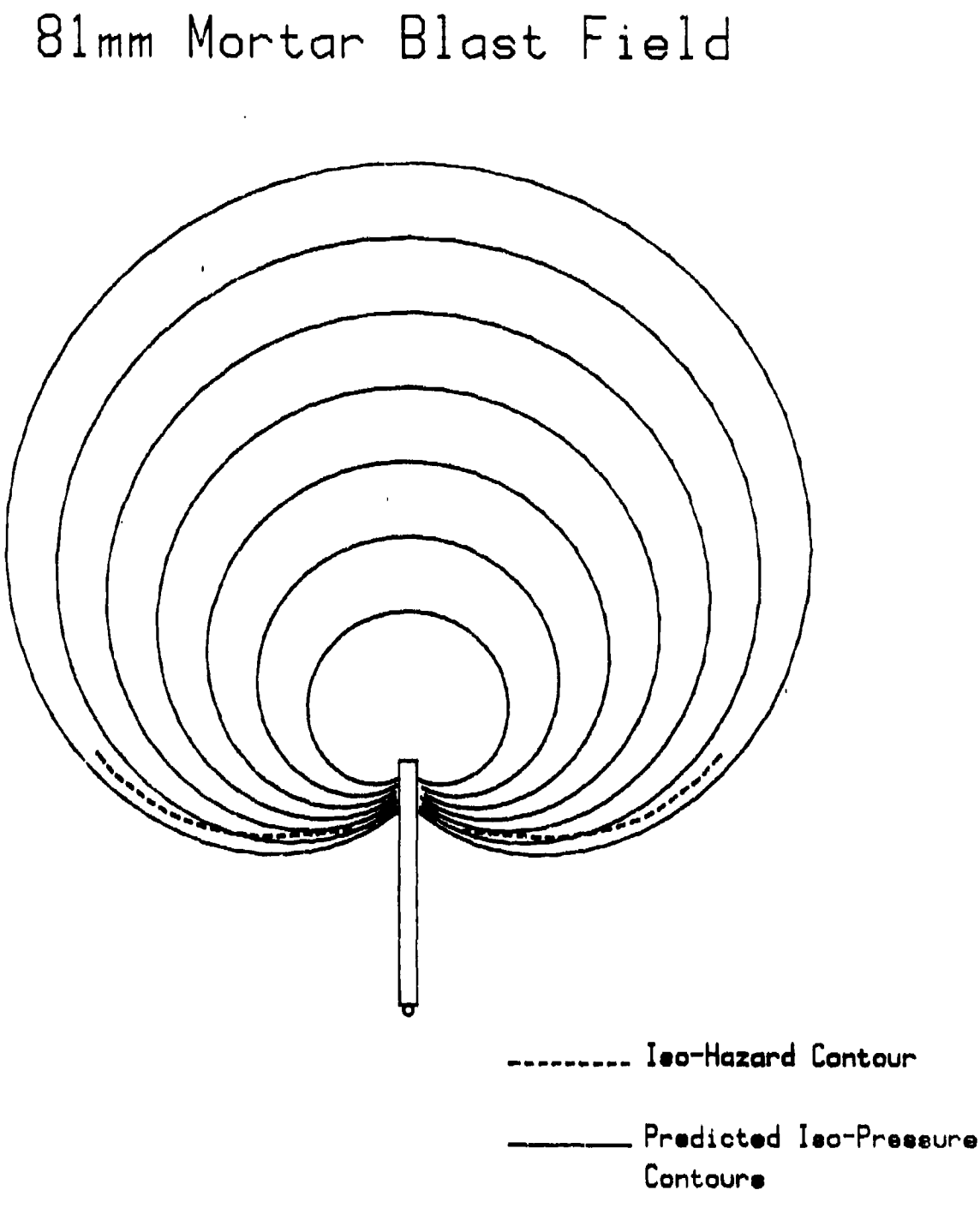

Figure 2.5-2. Comparison of predicted constant pressure contours and measured constant hazard contour. Predicted contours are of the form $C(1 + 0.86 \cos\theta)$ from reference 5.

7.5 (Cont'd)

Second, since the center of pressure moves, there is no single point to which transducers can be aligned. As stated in reference 3, "transducers will be aligned with the plane of the sensitive element passing through the axis of the barrel of the weapon." Figure 7.5-3 shows the process of aligning transducers to the centerline of the weapon. For measurements in near-field muzzle blast, it is desirable to use transducers configured so that they are omnidirectional in one plane.

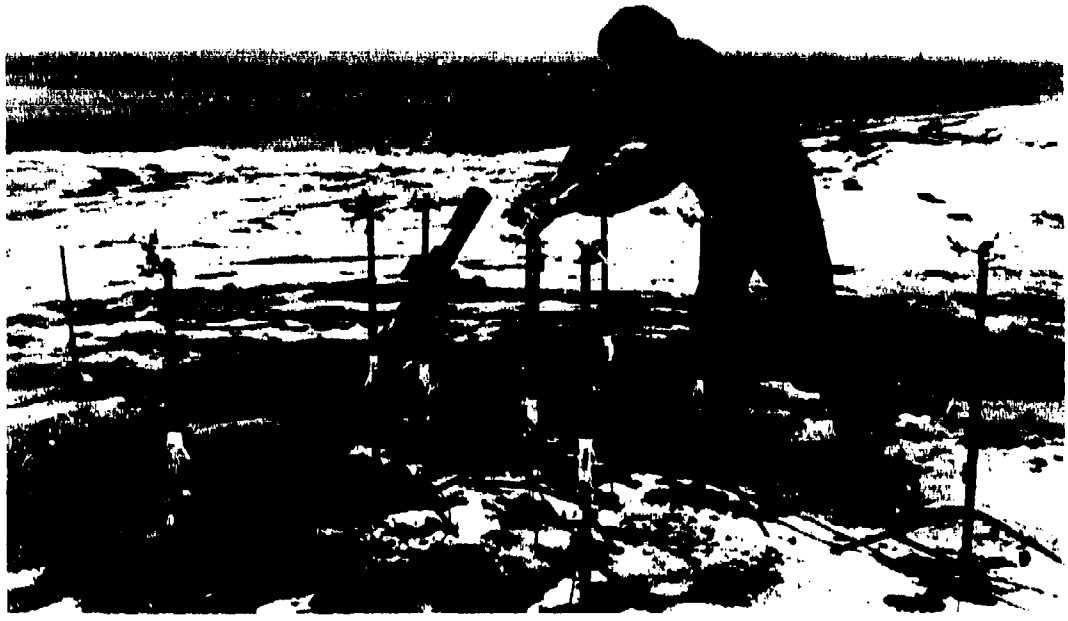

Figure 7.5-3. Aligning transducers to centerline of weapon for measurements in crew area of 81-mm mortar.

2.6 PROJECTILE SHOCK WAVES

A supersonic projectile generates a shock wave as it travels through air. This shock wave produces a classic "N" wave in the pressure versus time history. When a transducer is placed in a location where the projectile shock wave reaches the transducer before the muzzle blast, the transducer will record both the "N" wave and the muzzle blast wave. Figure 2.6-1 shows such a location. Figure 2.6-2 shows a pressure versus time history with both the projectile shock and muzzle blast.

The armor piercing, discarding sabot (APDS) round produces several "N" waves, as shown in figure 2.6-3. This is reasonable because each supersonic object (projectile, sabot, sabot pedals, etc.) produces an independent projectile shock wave. Note that the pressure versus time history measured at the same location produces no "N" waves when a blank is fired, as shown in figure 2.6-4.

When an artillery shell is detonated, each of the thousands of fragments produced will generate an "N" wave as long as the fragment is traveling at supersonic speed. Note the barrage of "N" waves that arrive before the main blast in figure 2.6-5.

Figure 2.6-1. Photograph of muzzle exit. Note that both the muzzle blast wave and the projectile shock wave are visible. A transducer in' location "X" would record both waves (photograph, courtesy of US Army Ballistic Research Laboratory).

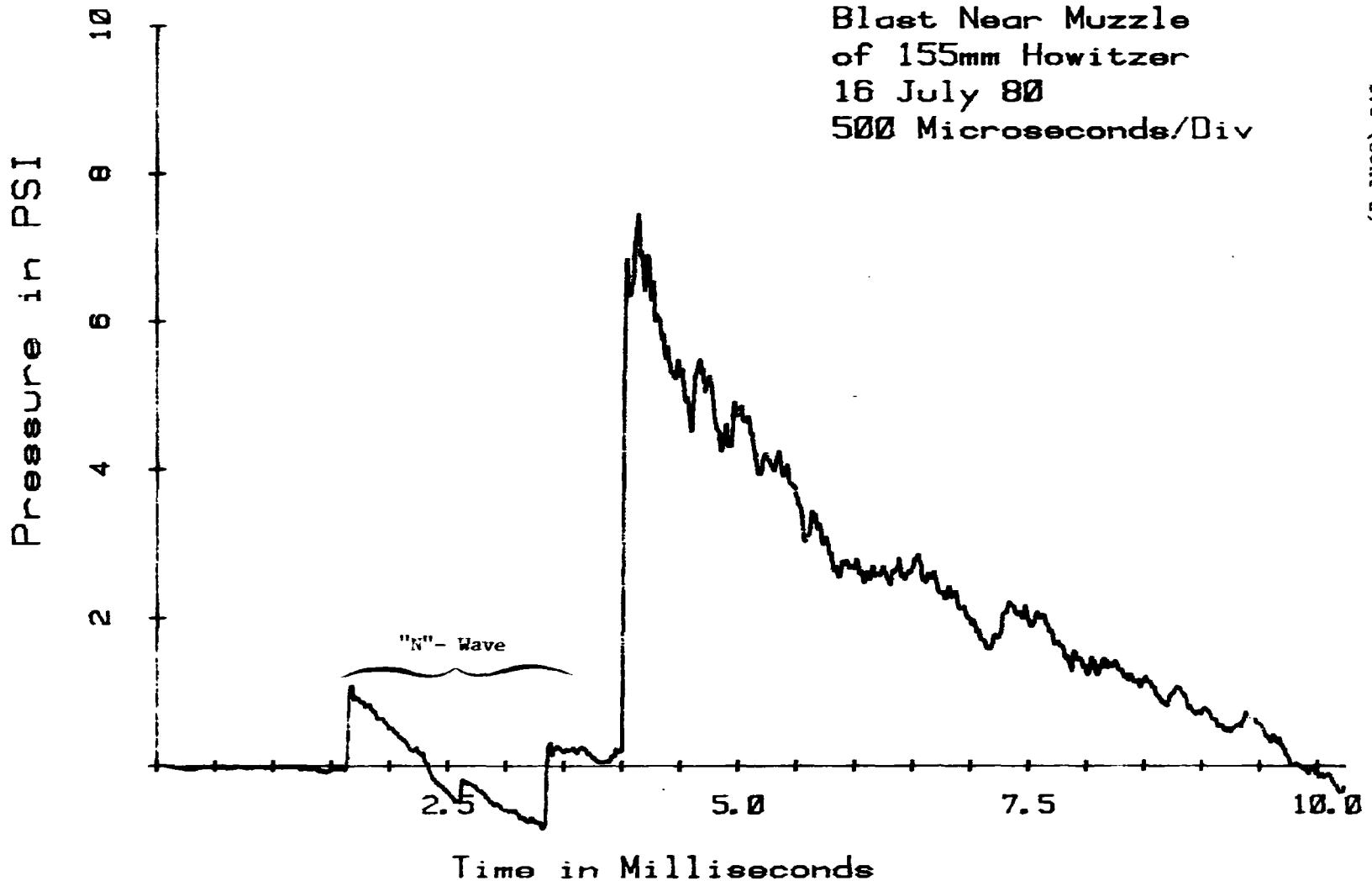

Figure 2.6-2. Pressure measurement showing both projectile "N" wave and muzzle blast wave.

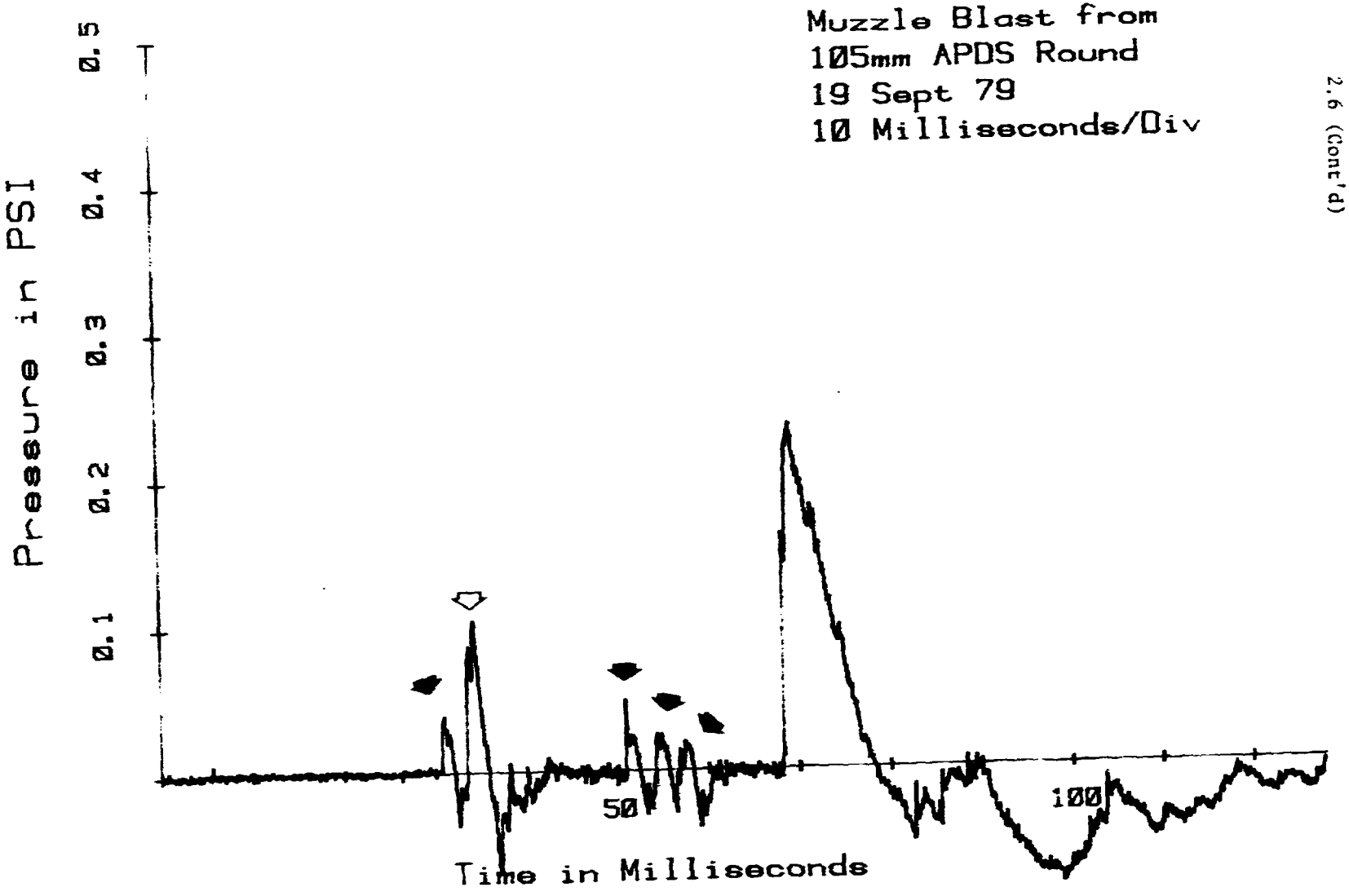

Figure 2.6-3. Measurement of muzzle blast 100 meters from 105-mm tank gun, 45 degrees from the line of fire. Note several "N" waves from various components of APDS round.

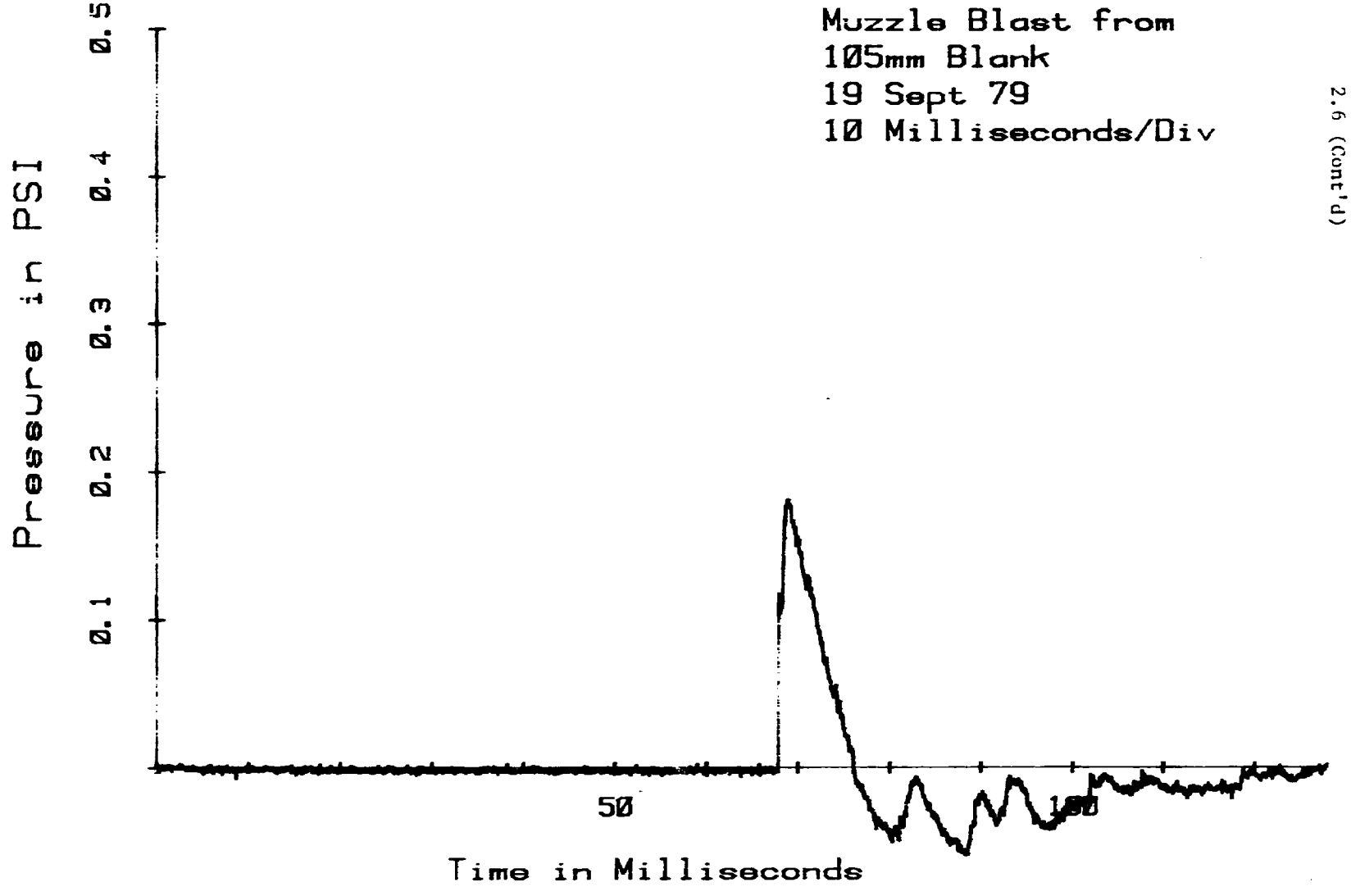

Figure 2.6-4. Measurement of muzzle blast 100 meters from 105-mm tank gun firing a blank. Note the absence of "N" waves.

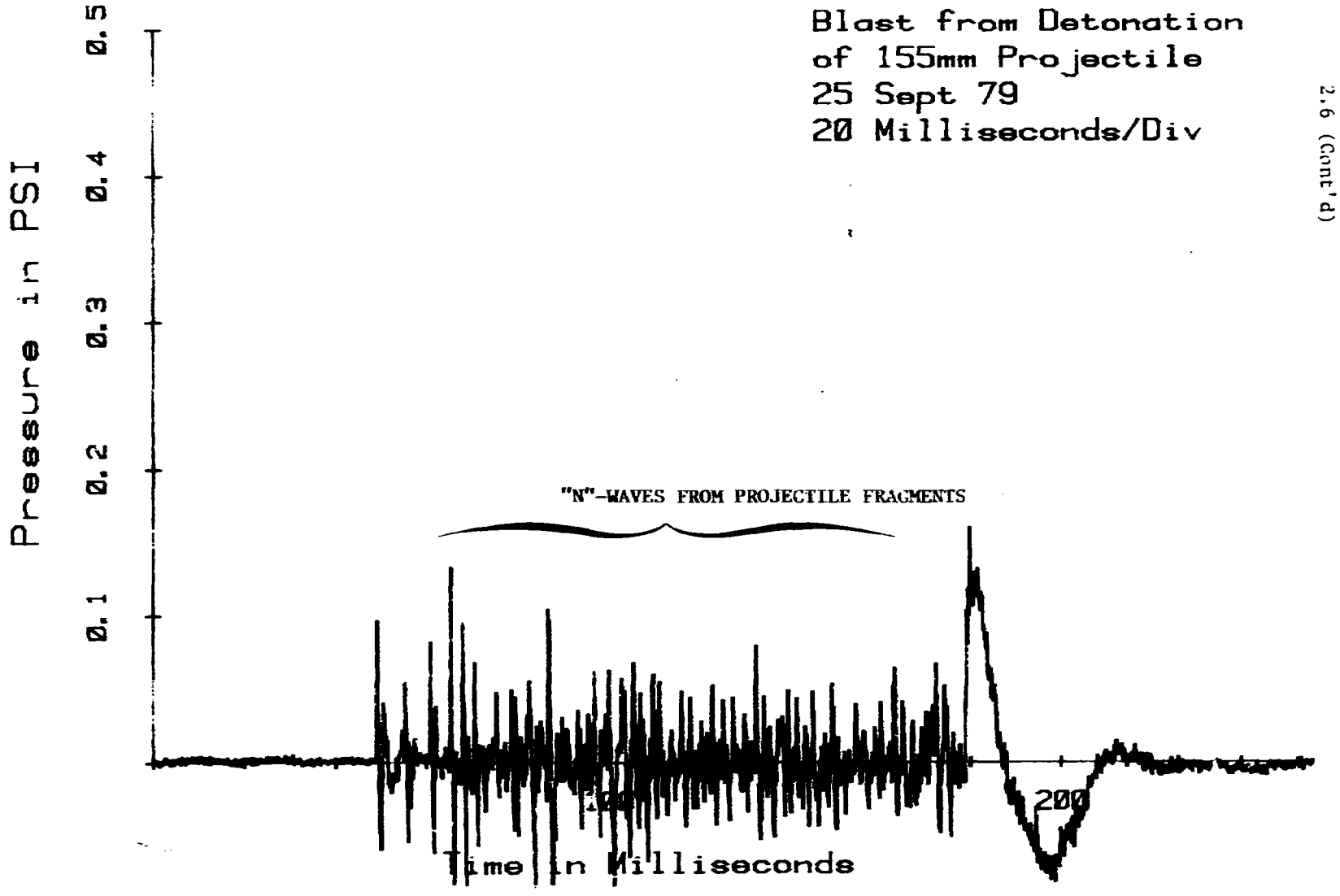

Figure 2.6-5. Measurement of blast overpressure 100 meters from detonation of 155-mm projectile. Note the barrage of "N" waves that precedes main blast wave.

SECTION 3. BLAST OVERPRESSURE TRANSDUCERS

3.1 INTRODUCTION

A variety of transducers are commercially available for measurement of blast pressure. The transducers studied are shown below in figure 3.1-1. A complete sampling of all transducers available was not made.

Transducers can be divided into two broad categories. Some, such as the LC-33 pencil gage and the PCB 113 lollipop are designed specifically to measure side-on pressure and include an aerodynamic housing. Miniature transducers, such as the other four transducers shown in figure 3.1-1 can be used to measure side-on, reflected, or stagnation pressure. The shape of the mounting fixture and its direction of alignment determine what kind of pressure is measured.

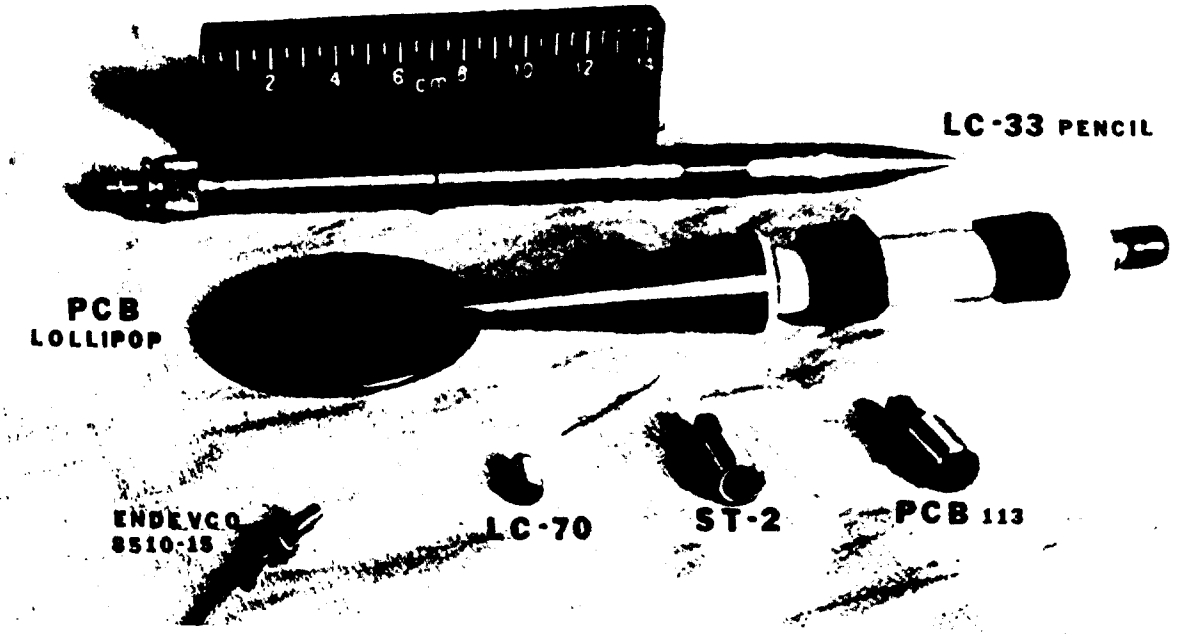

Figure 3.1-1. Side-on and miniature pressure transducers.

3.2 MINIATURE TRANSDUCERS

Miniature pressure transducers can be used for a variety of purposes. The shape and orientation of mounting used determine the type of pressure measured (side-on, face-on, stagnation, etc.). Because the sensing element is small, a blast wave travels over it quickly and a short rise time is observed. This characteristic is important in measurement of small arms blast because the pressure decays rapidly after wave passage. If the sensing element is not small enough, the pressure will begin to decay before the wave has finished traveling across the element. True peak pressure will not be measured in this case.

3.2.1 Susquehanna Instruments Model ST-2

The ST-2 gage was used in gathering the base line data for MIL-STD-1474. Figure 3.2-1 shows the side-on response of the ST-2 gage in the USABRL 58-cm (24-in.) shock tube. It is normally supplied with a screw-on impedance converter and operates in the low impedance, voltage mode. Its specifications are below:

a. Electronics: Voltage mode.

b. Crystal: Lead metaniobate.

c. Resonant frequency: 250 kHz.

d. Crystal diameter: 5.33 mm.

e. Time constant: 200 milliseconds (measured)[a].

f. Acceleration sensitivity: 0.014 kPa/g (0.002 psi/g) (measured)[a].

[a]This quantity was not available in the manufacturer's literature, so it was measured on one sample transducer.

3.2.1 (Cont'd)

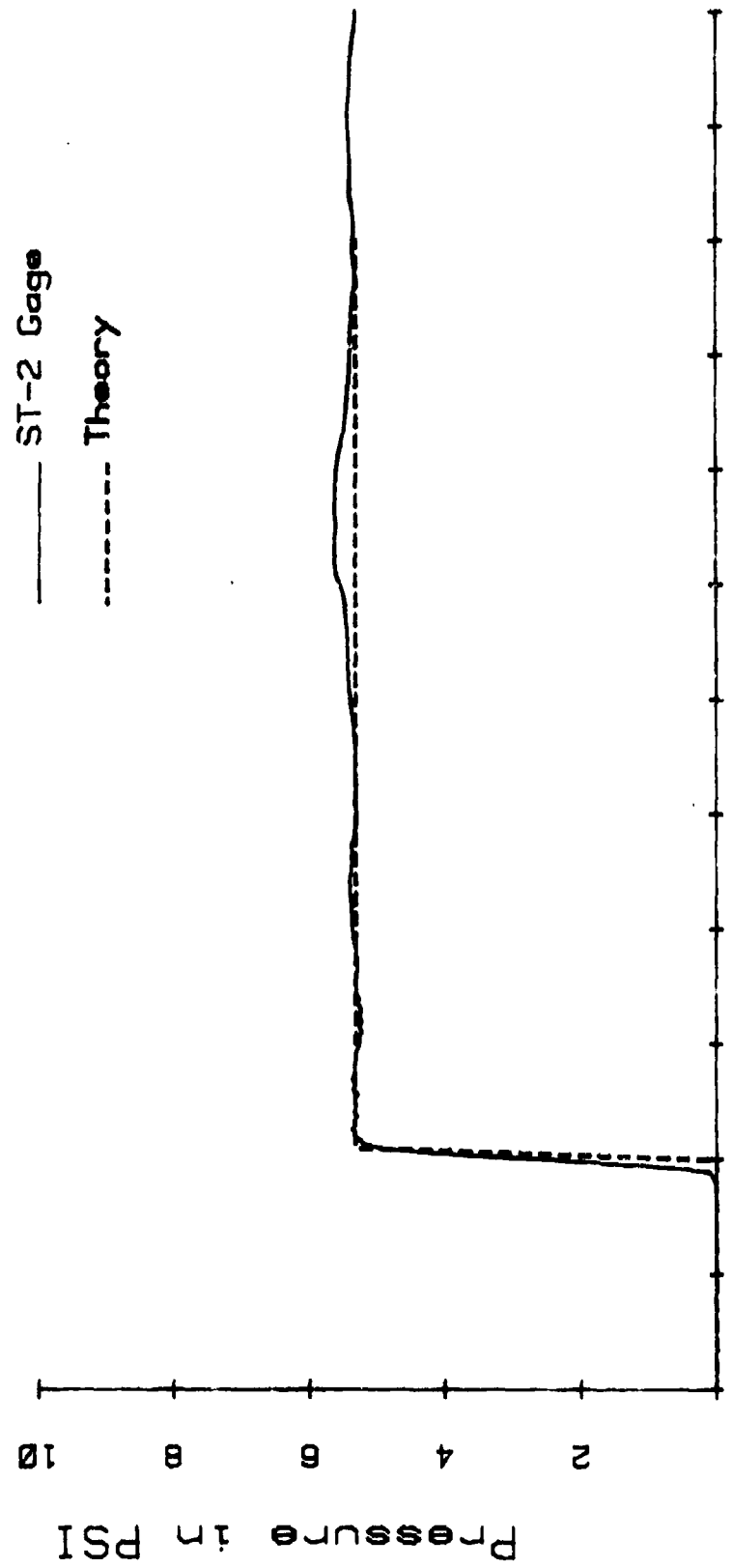

Figure 3.2-1. Side-on response of ST-2 gage in USABRL shock tube. This signal recorded on a digital transient recorder with no filtering (data from ref 6). The theory line represents the pressure level obtained from the measured velocity of the shock wave.

3.2.2 PCB Model 113

The PCB 113 transducer has two crystals, one to sense pressure and one for acceleration compensation. This two degree of freedom system is tuned to produce "frequency tailored response" which suppresses ringing at the resonant frequency. The 113 element is available in a variety of physical configurations and may be purchased as a charge type or low impedance, voltage mode transducer. The side-on response of the PCB gage in the USABRL shock tube is shown in figure 3.2-2. Its specifications are below:

a. Electronics: Voltage mode or charge type.

b. Crystal: Quartz.

c. Resonant frequency: 500 kHz.

d. Crystal diameter: 5.54 mm.

e. Time constant: 10 seconds.

f. Acceleration sensitivity: 0.014 kPa/g (0.002 psi/g).

g. Change in scale factor with temperature: 0.054%/C° (0.03%/°F).

3.2.2 (Cont'd)

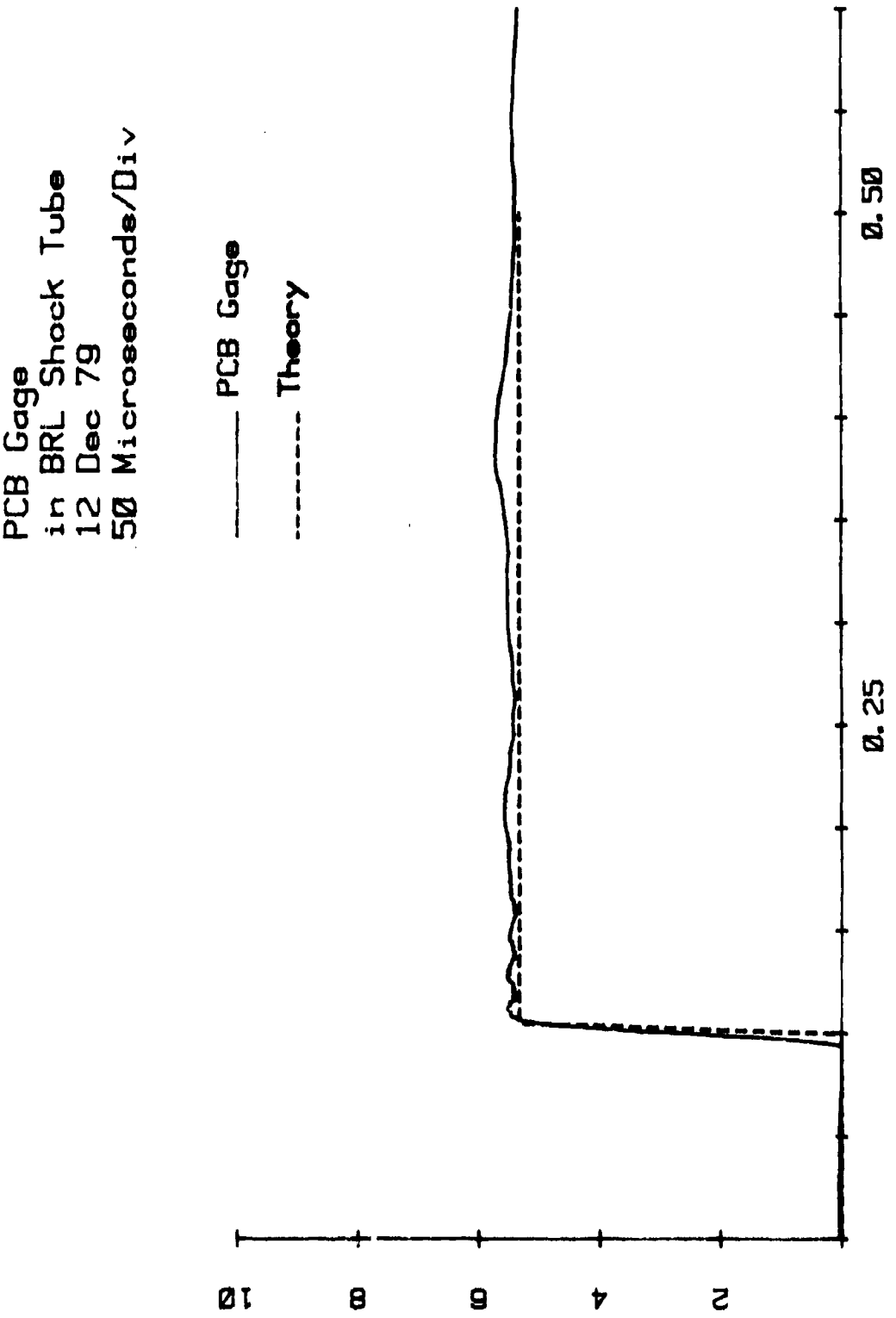

Figure 3.2-2. Side-on response of PCB 113 transducer. This signal was recorded on a digital transient recorder with no filtering (data from ref 6).

3.2.3 Celesco Model LC-70

The LC-70 is the smallest gage tested in this study. Figure 3.2-3 shows different examples of the side-on performance of the LC-70 gage in the USABRL shock tube. Note that the waveforms from the LC-70 are not as clean as the waveform produced by the PCB gage. Because of these anomalies, this gage was used primarily for making velocity measurements rather than peak pressure measurements. Its specifications are below:

a. Electronics: Charge type or voltage mode.

b. Crystal: Lead zirconate titanate.

c. Crystal diameter: 5.28 mm.

d. Time constant: 10 milliseconds.

e. Acceleration sensitivity: 0.09 kPa/g (0.013 psi/g).

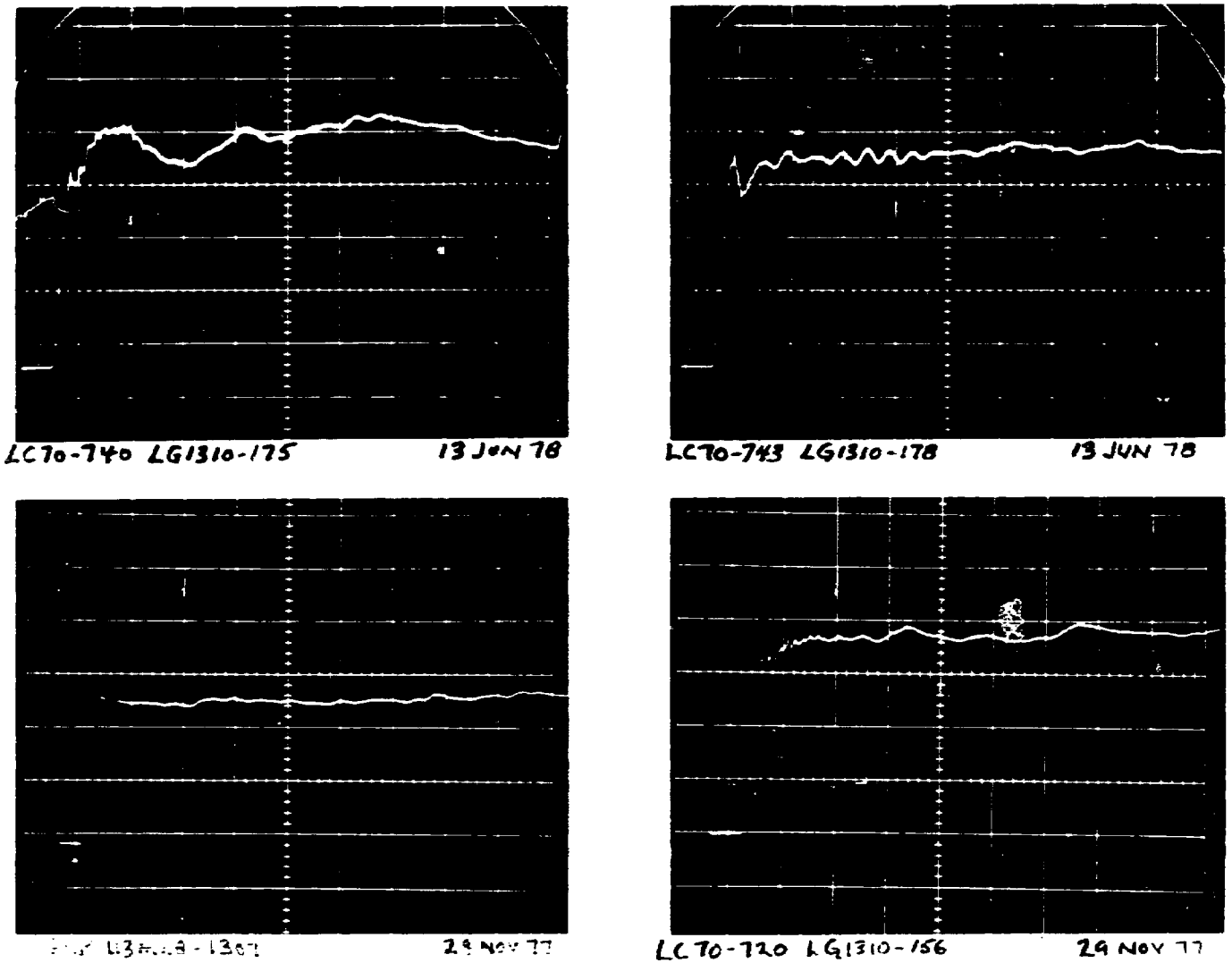

Figure 3.2-3. Side-on performance of LC-70 transducer and PCB 113 transducer in USABEL [illegible] tube. Note the excessive anomalies in the various LC-70 waveforms.

3.2.3 (Cont'd)

3.2.4 Endevco Model 8510

The Endevco 8510 shown in figure 3.2-4, is a newly developed piezoresistive, strain type transducer. It is the only gage tested that had DC response. It is temperature-compensated to minimize response to thermal transients and scale factor change caused by temperature change. Two models of this gage were examined. One model has a full scale range of 1379 kPa (200 psi) and a resonant frequency of 320 kHz, the other had a full scale range of 103 kPa (15 psi) and a resonant frequency of 100 kHz.

Figure 3.2-4. Photograph of Endevco 8510 transducer.

Side-on performance of the 100 kHz model in the USABRL shock tube is shown in figure 3.2-5. Note that the resonant frequency is highly under-damped and is approximately 130 kHz. The reason resonance is excited is because the time required for the blast wave to cross the diaphragm (∿5 microseconds) is close to the rise time of resonant oscillation (∿3 microseconds). The 1379 kPa model has a resonant frequency high enough that side-on pressure waves of the level discussed in this report should not excite resonance.

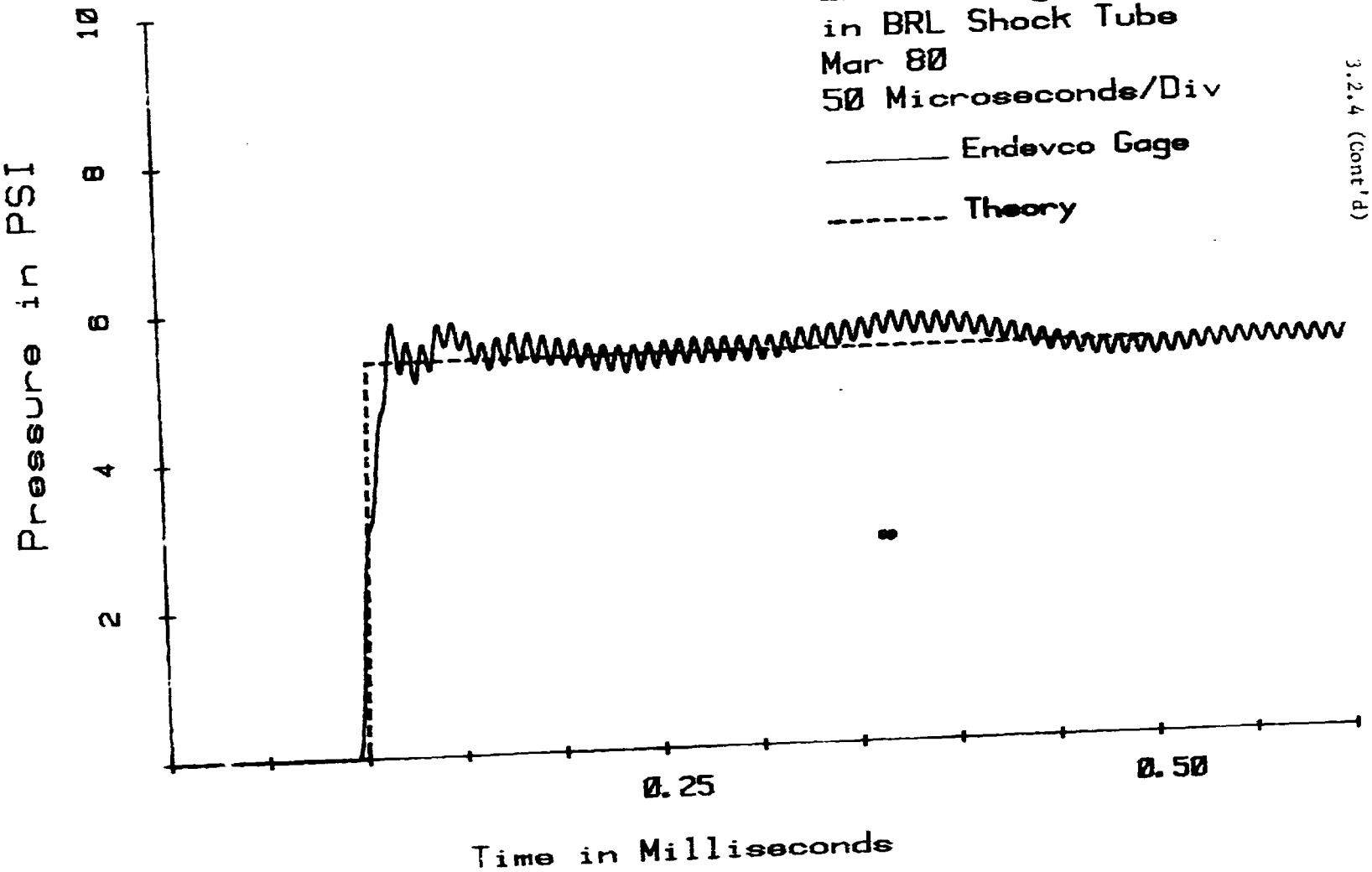

Figure 3.2-5. Side-on response of Endevco 8510-15 transducer (the 100 KHz model) in USABRL shock tube. This signal was recorded on a digital transient recorder with no filtering. Note resonance at 130 kHz (data from ref 6).

3.2.4 (Cont'd)

The specifications of the Endevco gage are listed below:

a. Electronics: 4 arm strain bridge.

b. Sensor: Diffused silicon diaphragm with integral piezoresistive strain gages.

c. Resonant frequency: 100 kHz (103 kPa model), and 320 kHz (1370 kPa model).

d. Diameter of diaphragm: 2-mm.

e. Time constant: ∞ (DC response).

f. Acceleration sensitivity: 0.002 kPa/psi (0.0003 psi/g).

g. Change in scale factor with temperature: 0.036%/°C (0.02%/°F).

The Endevco gage was the easiest gage to calibrate because of its DC response. It showed excellent agreement between the static pulse method of calibration and the sine wave method of calibration.

The Endevco gage has very little response to thermal transients. A room temperature Endevco gage immersed in freezing water produced an indication of only 0.3 kPa. A PCB gage subjected to the same experiment indicated 150 kPa.

The diffused silicone diaphragm used on the Endevco gage acts not only as a pressure sensor, but also (unfortunately) as a light sensor. A flash bulb set off in front of an Endevco gage will cause a full scale indication. A PCB gage subjected to the same experiment indicated less than 1% of full scale.

The photo sensitivity of the Endevco gage could be a problem in measurement locations near muzzle flash or the fireball of free air explosions. Normally, however, the gage is pointed perpendicular to the source of flash, and photo sensitivity is not a problem.

Although the Endevco gage produced usable records in the shock tube, no acceptable data were produced in field testing. The following experiment was conducted to demonstrate the effect of cable length.

3.2.4 (Cont'd)

The transducers were placed on a pencil-shaped ojive approximately 30-cm in front of a 10.16-cm (4-in.) diameter shock tube. A typical wave form from a PCB transducer is shown in figure 3.2-6. Note that a peaked wave is produced.

The response of the 100 kHz Endevco gage with short and long cables is shown in figures 3.2-7 and 3.2-8, respectively. Note that despite the ringing at resonant frequency in figure 3.2-7, it appears that a basically good peaked wave is present and the rise time is short. In figure 3.2-8, note the addition of long cable (152-m) causes a filtering effect that slows the rise time and suppresses resonant ringing.

Similar results for the 320 kHz Endevco gage are shown in figures 3.2-9 and 3.2-10. In figure 3.2-9, note that a fairly good peaked wave is produced with the short cable. The higher resonant frequency eliminates ringing, but the electrical noise level is increased. Remember that the maximum pressure shown is only 1% of the full scale pressure of this model.

Also note the strange shape of the peak. The reason for this shape is not known, but it is felt that part of this distortion is caused by the fact that the diaphragm is recessed approximately one diameter below the top of the gage, and part of the distortion is caused by the electrical noise that is present.

In figure 3.2-10, note that long cable length again has a filtering effect that increases the rise time. Experiments have shown that 150 meters of the standard four or eight conductor strain-gage cables used have a frequency response of 10 kHz and attenuate signals at 100 kHz by as much as 12 dB.

Unfortunately, this information was discovered after the field testing phase had been completed. It is felt that if special balanced line ("twinax" cable) were to be used on the signal lines of the strain bridge, acceptable frequency response could be obtained.

Even when short cable is used (i.e., when no frequency response problems are present), the ringing and waveform distortion of the Endevco gage are significant problems. Because of these problems, the Endevco gage was used primarily for assistance and verification of calibration techniques.

3.2.4 (Cont'd)

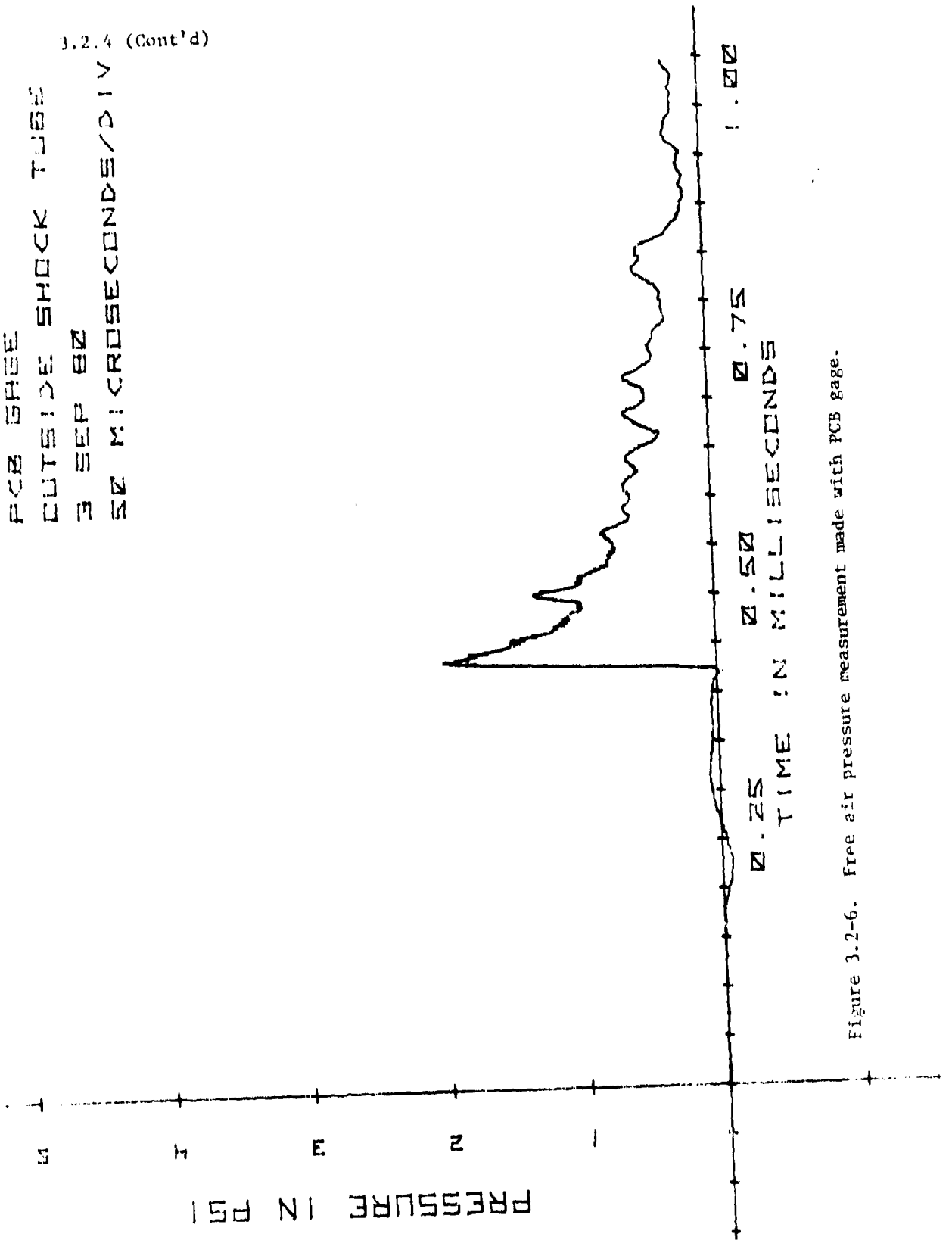

Figure 3.2-6. Free air pressure measurement made with PCB gage.

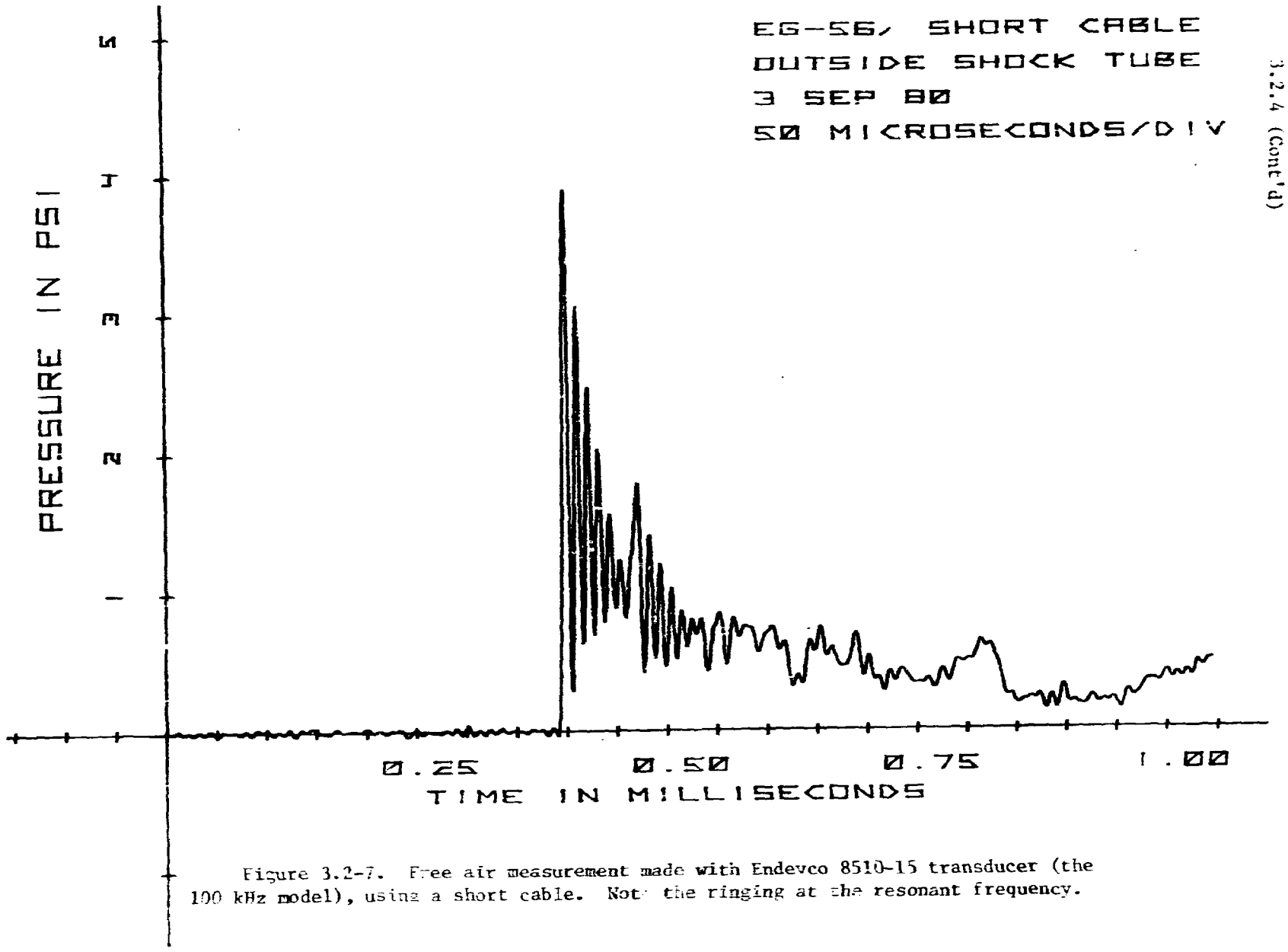

Figure 3.2-7. Free air measurement made with Endevco 8510-15 transducer (the 100 kHz model), using a short cable. Note the ringing at the resonant frequency.

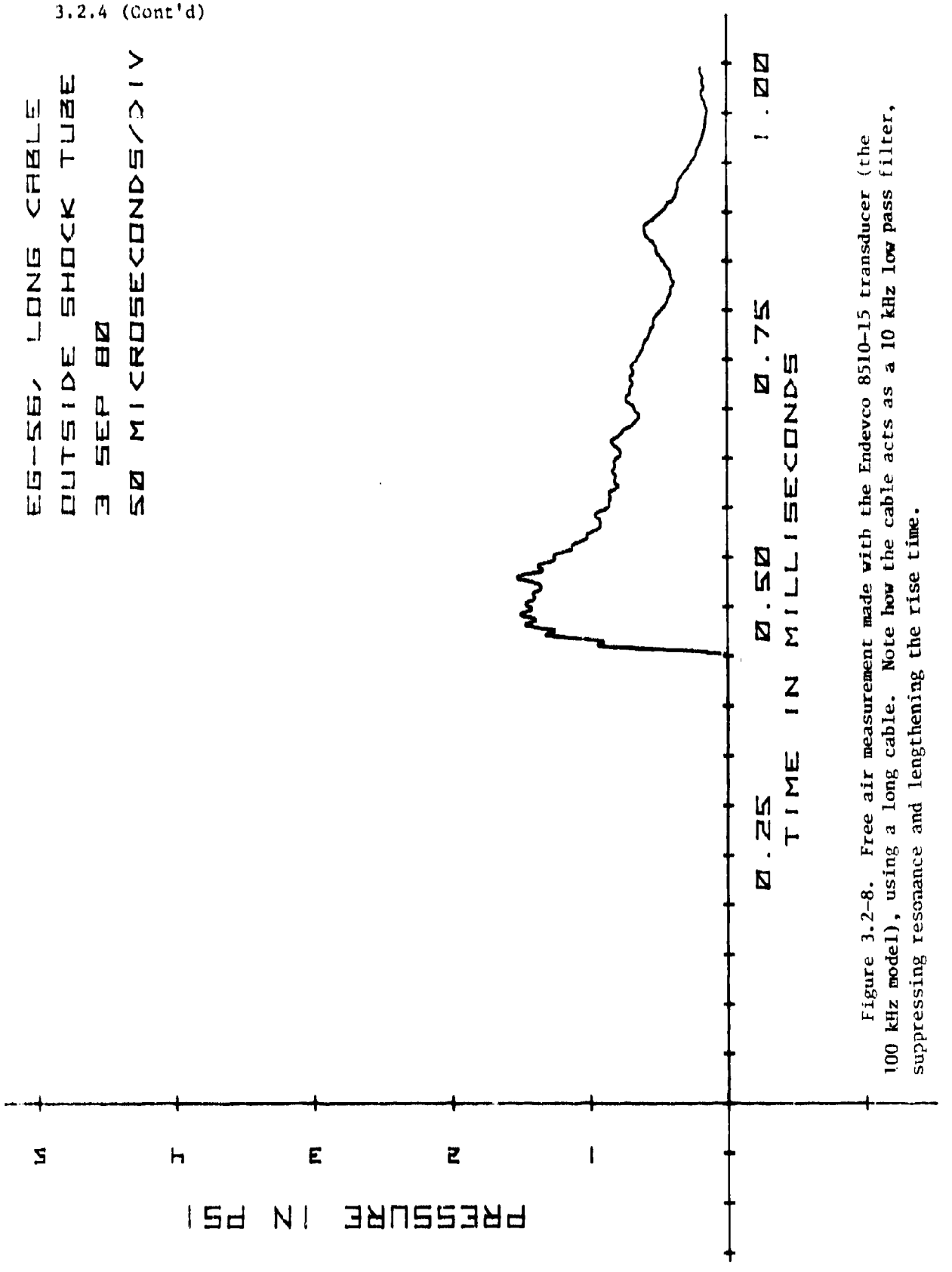

Figure 3.2-8. Free air measurement made with the Endevco 8510-15 transducer (the 100 kHz model), using a long cable. Note how the cable acts as a 10 kHz low pass filter, suppressing resonance and lengthening the rise time.

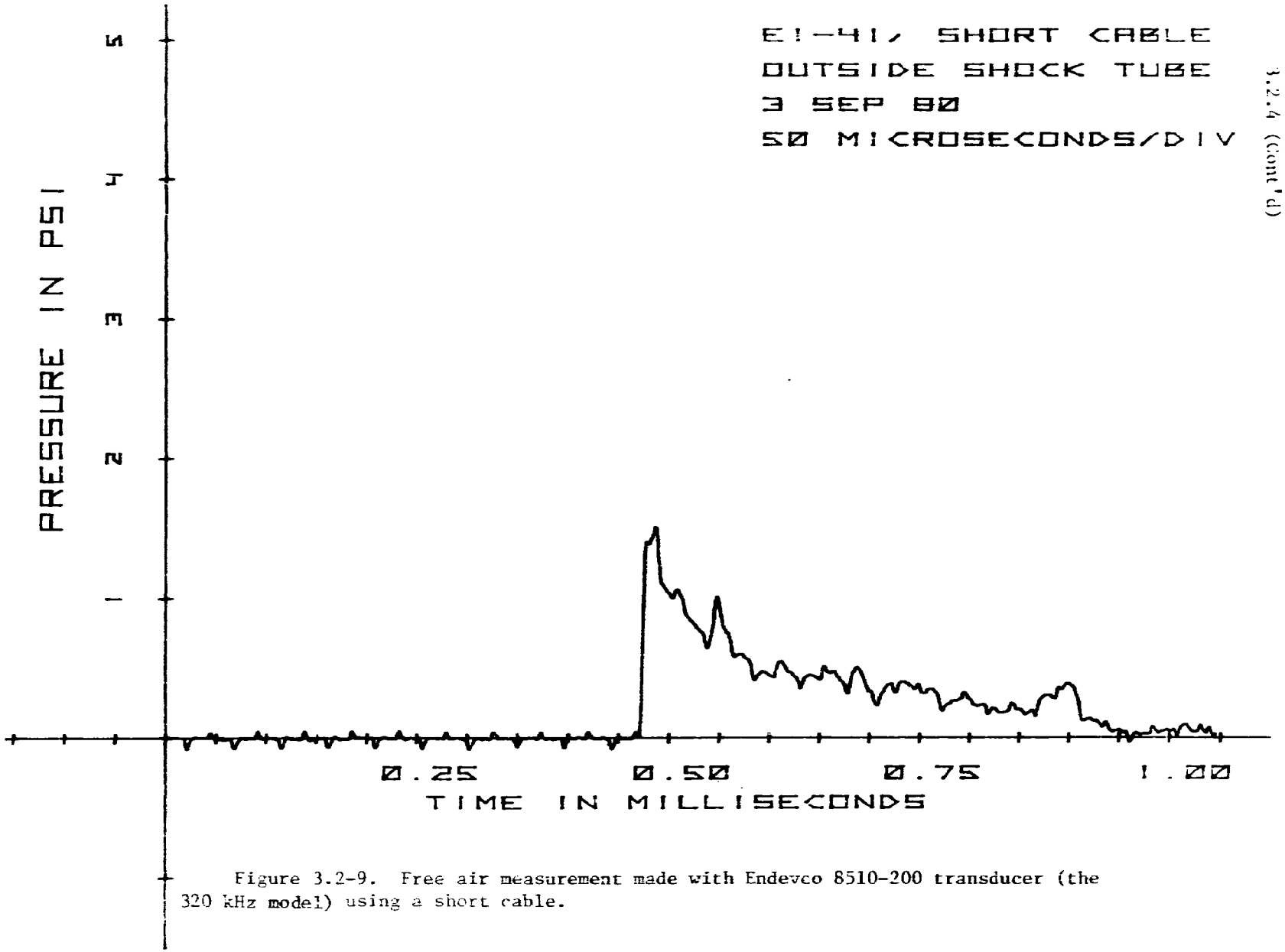

Figure 3.2-9. Free air measurement made with Endevco 8510-200 transducer (the 320 kHz model) using a short cable.

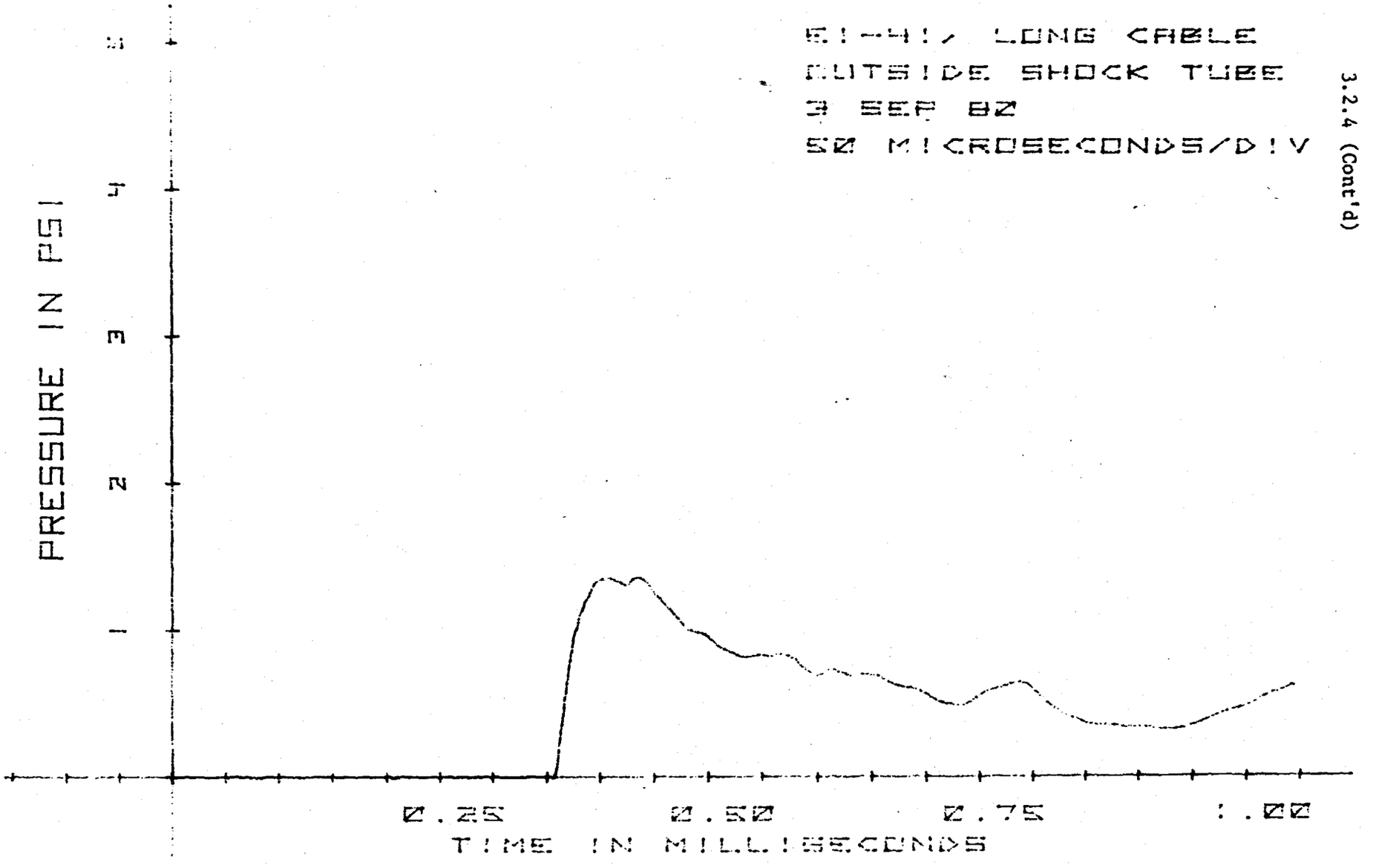

Figure 3.2-10. Free air measurement made with Endevco 8510-200 transducer (the 320 kHz model) using a long cable.

3.3 MOUNTING MINIATURE TRANSDUCERS

As shown in Figure 3.3-1, miniature gages can be placed in a variety of mounts. Several tests were conducted in the pentolite blast field to examine the differences between the various mounting techniques. Figures 3.3-2 through 3.3-4 show the dimensions of the various mounts.

Glon and Coulter of the USABRL are conducting a related study in the 58-cm shock tube (ref 6). Data from the USABRL shock tube study are presented in this section with the permission of the authors.

Figure 3.3-1. Mounts for miniature transducers. Clockwise from the left: blunt cylinder mount, pencil probe, skimmer plate, miniature transducer.

3.3 (Cont'd)

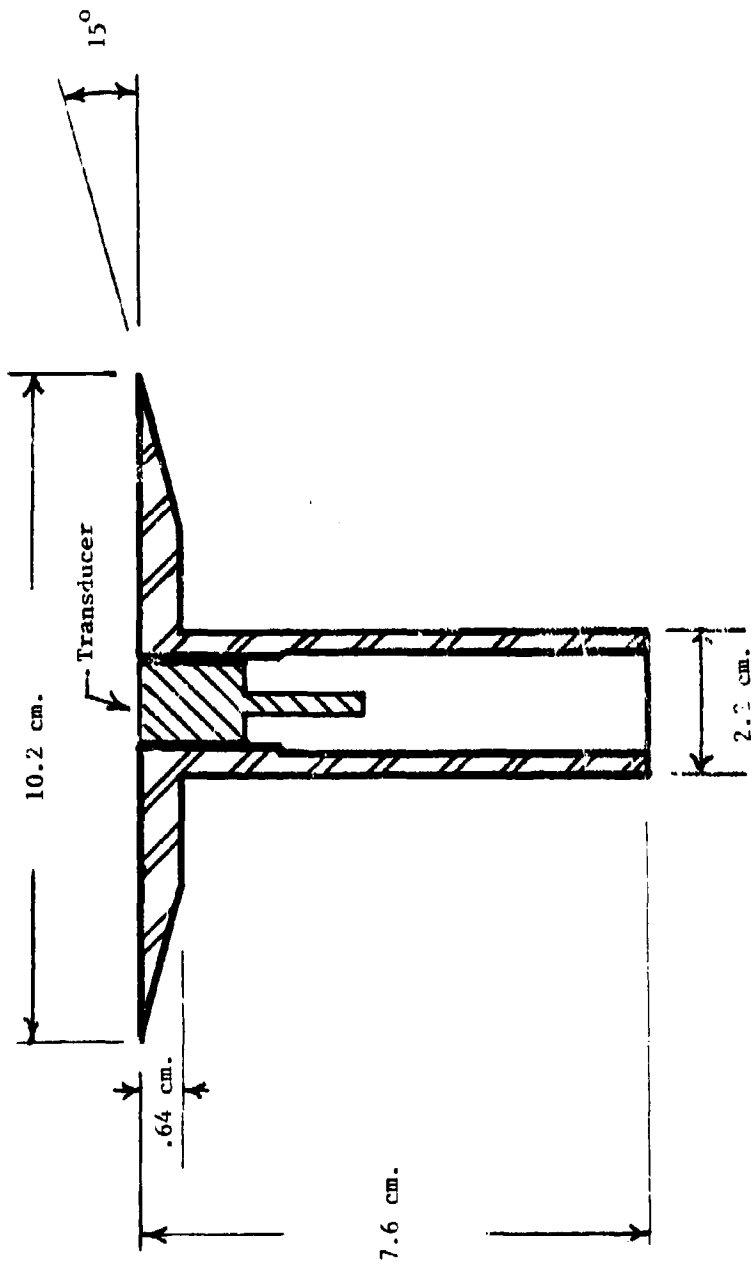

Figure 3.3-2. Dimensions of the skimmer plate designed by George Coulter of the USABRL.

3.3 (Cont'd)

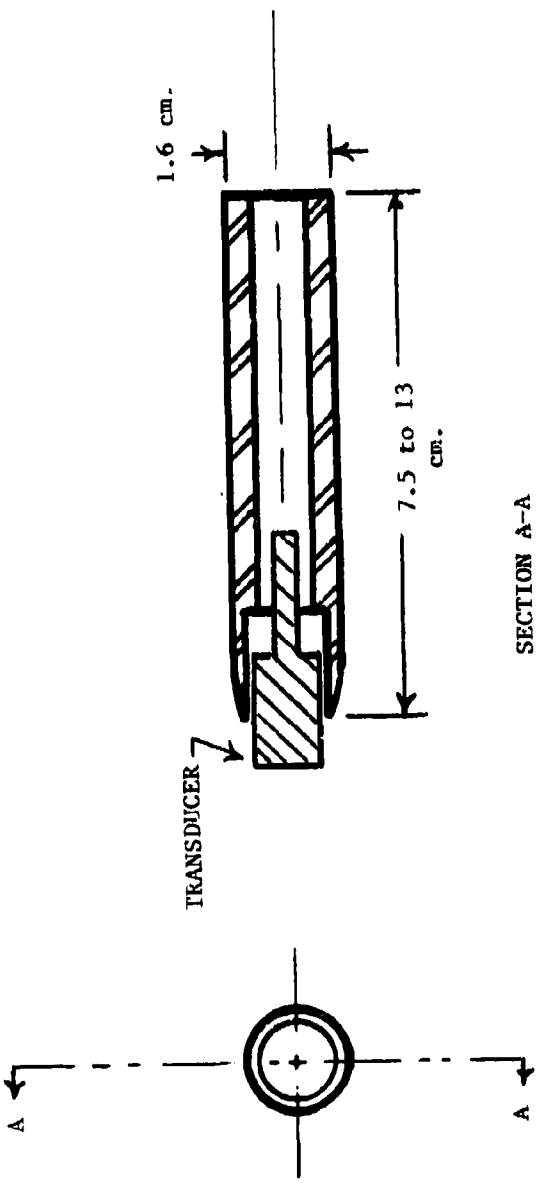

Figure 3.3-3. Dimensions of the blunt cylinder mount (courtesy of US Army Human Engineering Laboratory).

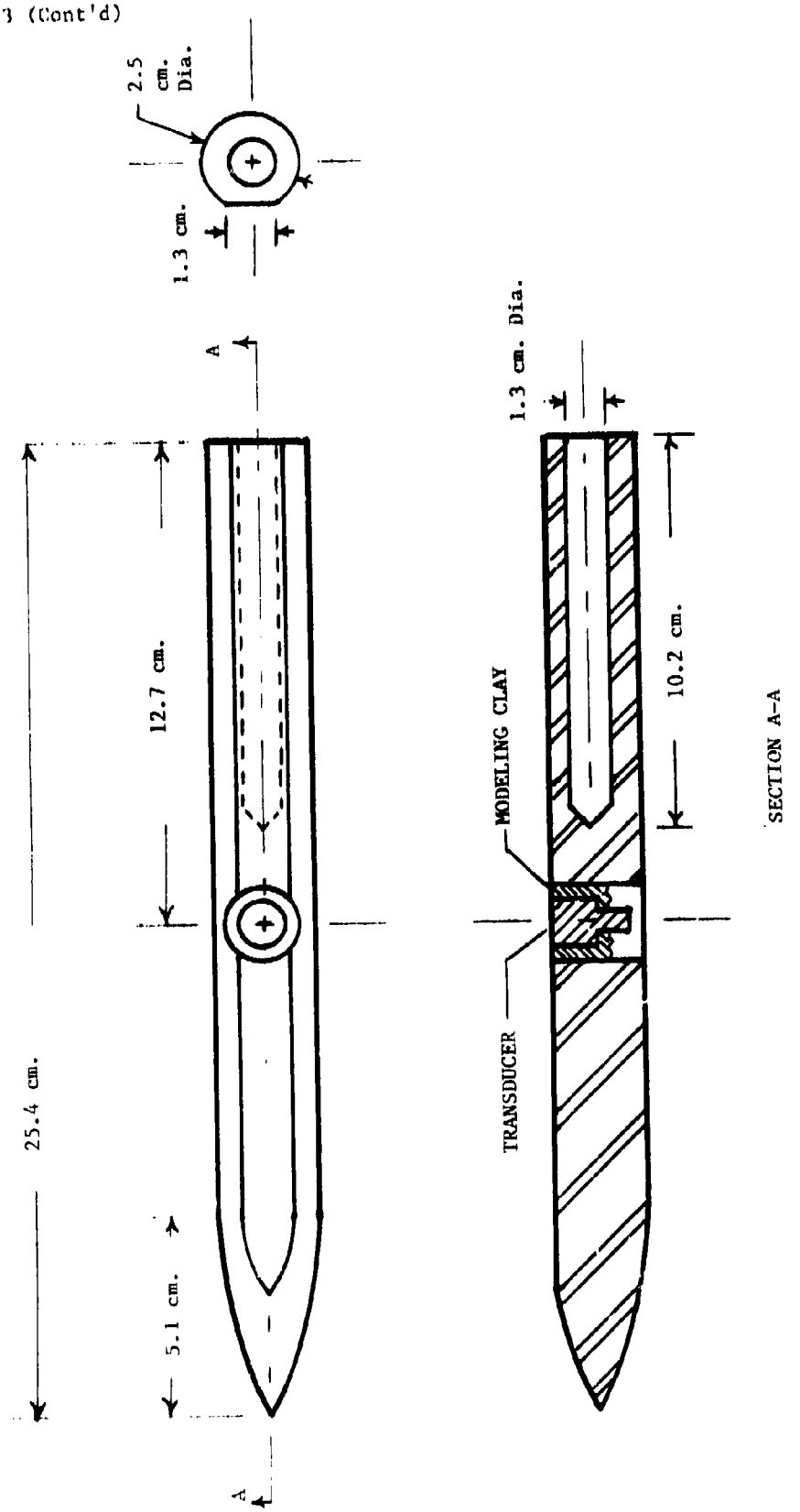

Figure 3.3-4. Dimensions of the pencil probe.

3.3.1 The Skimmer Plate

The skimmer plate used in this study was designed by George Coulter of the USABRL. Both Coulter's skimmer plate and a similar but slightly larger disk were used in the study by Gion and Coulter (ref 6).

Figure 3.3-5 is the face-on, shock tube response of a Kistler gage mounted in the larger disk. Face-on response of Coulter's skimmer plate was not measured in reference 6.

Note that face-on pressure is maintained for a relief time of roughly 170 microseconds. The pressure then drops down sharply to near stagnation pressure (at the pressure level used, stagnation pressure ≈ side-on pressure).

Figure 3.3-6 shows the shock tube response of the skimmer plate to small angle changes. Note that a change of 5 degrees in angle causes a 5 percent change in amplitude of the initial peak.

Figure 3.3-7 shows the skimmer plate designed by Coulter mounted on a lightweight stand in the field. Figure 3.3-8 shows the response of the skimmer plate to the peaked wave produced by free field pentolite blast. Note that when used face-on, the theoretical face-on pressure value is maintained for roughly 150 microseconds before decaying to stagnation (≈ side-on) pressure.

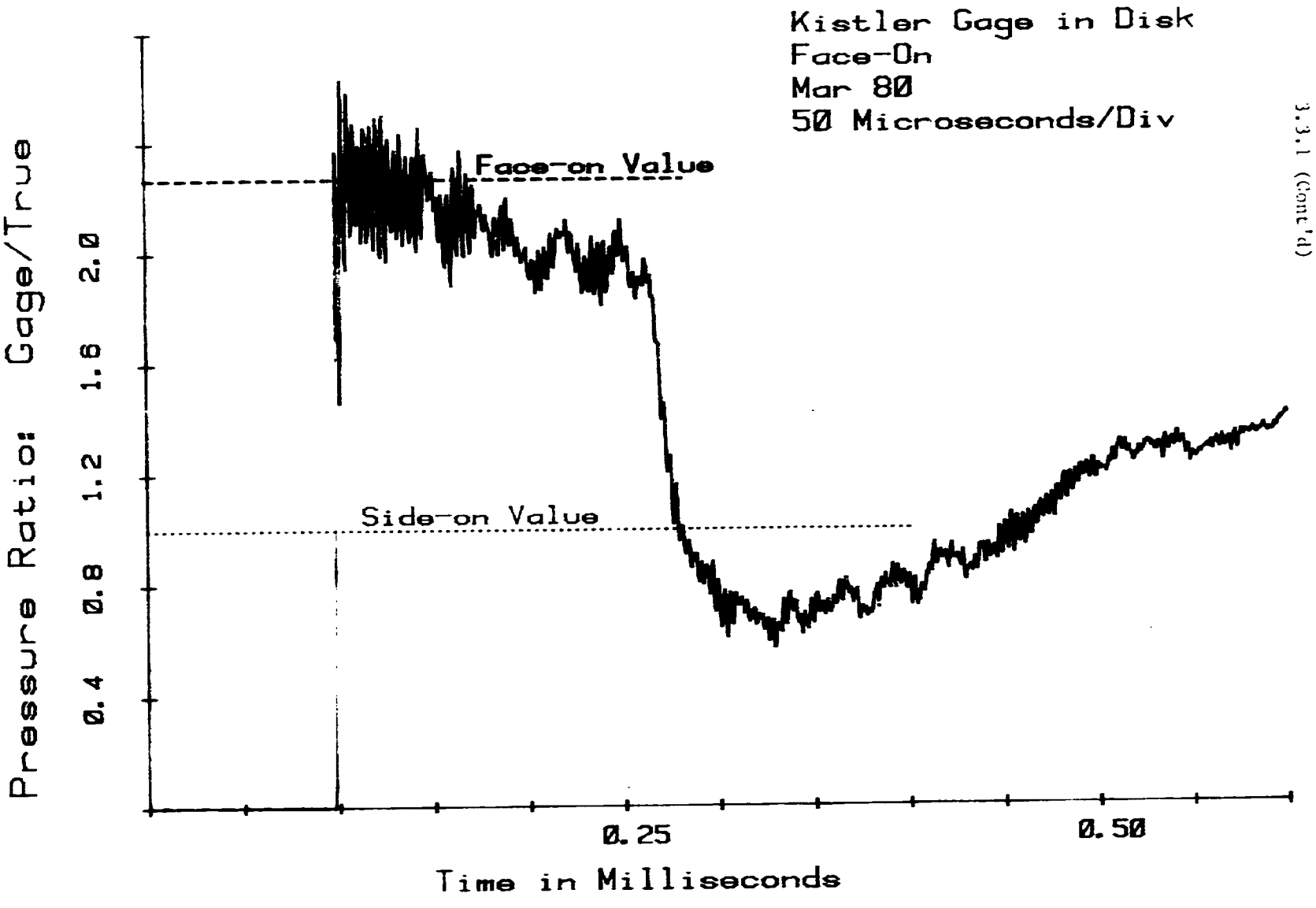

Figure 3.3-5. Face-on response of a disk in the USABRL shock tube. This signal was recorded on a digital transient recorder with no filter (data from ref 6).

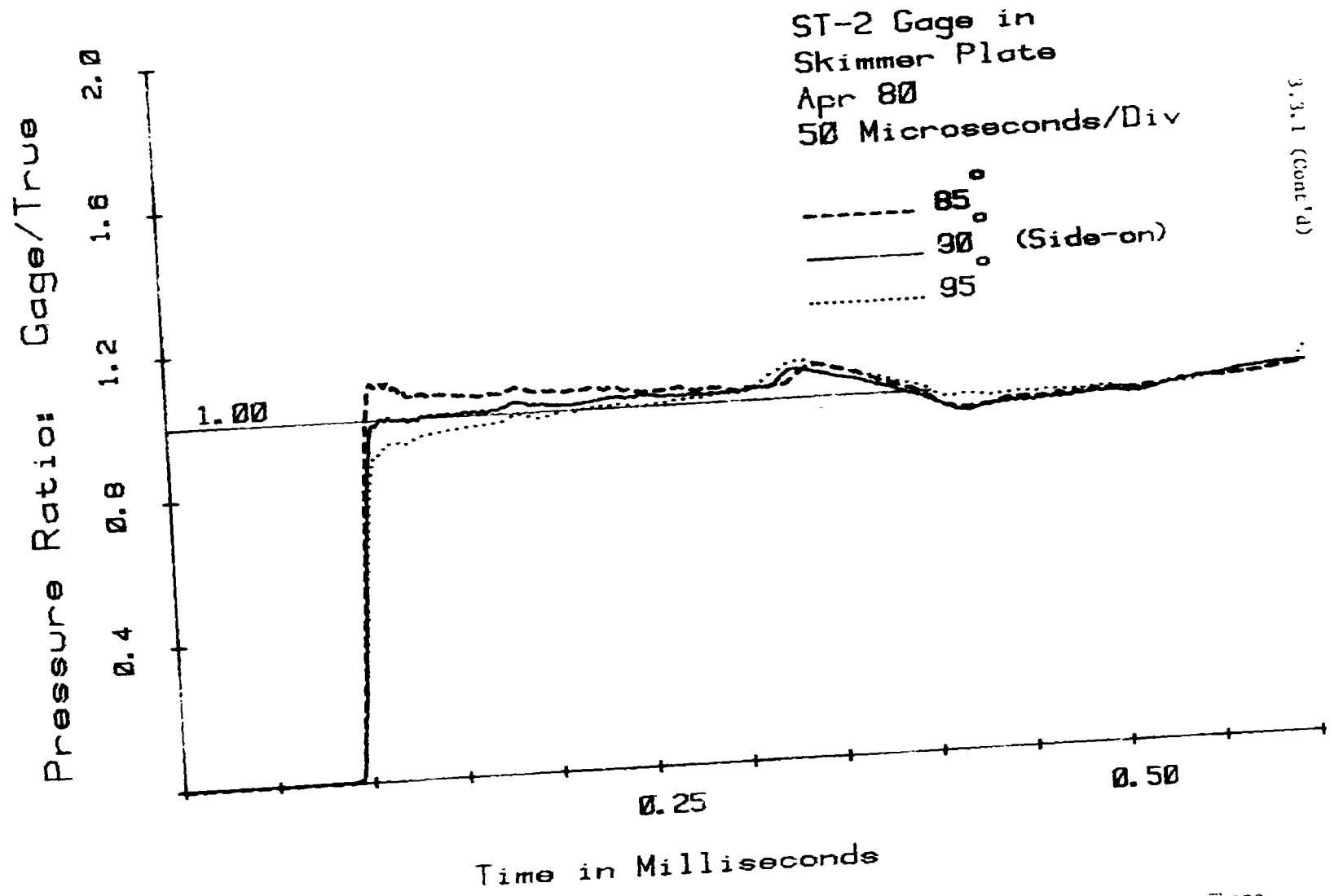

Figure 3.3-6. Response of skimmer plate to small angle misalignment in USABRL shock tube. These signals were recorded on a digital transient recorder with no filtering (data from ref 6).

3.3.1 (Cont'd)

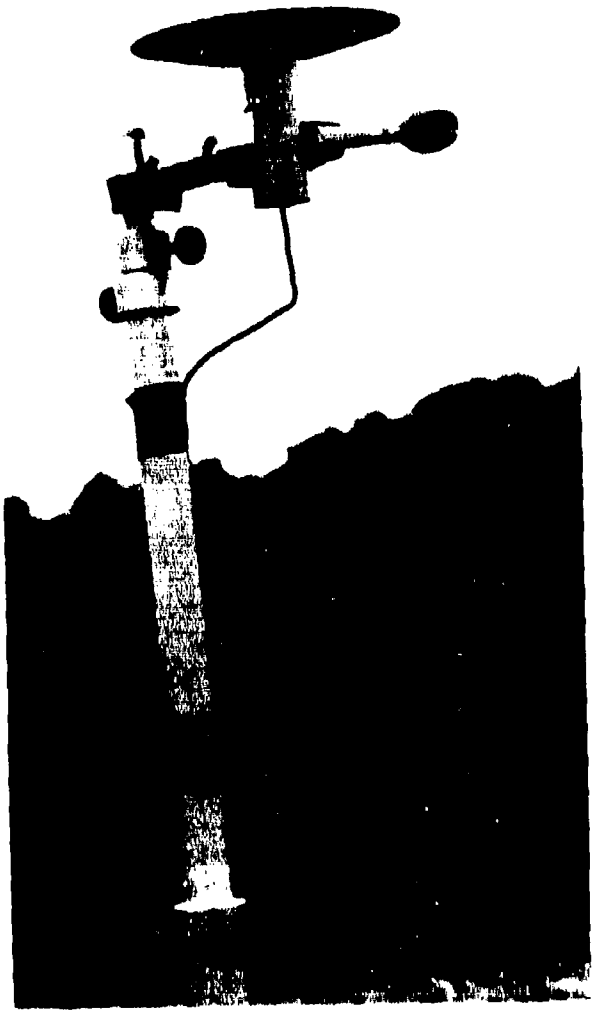

Figure 3.3.2. Photograph of skimmer plate mounted on lightweight stand.

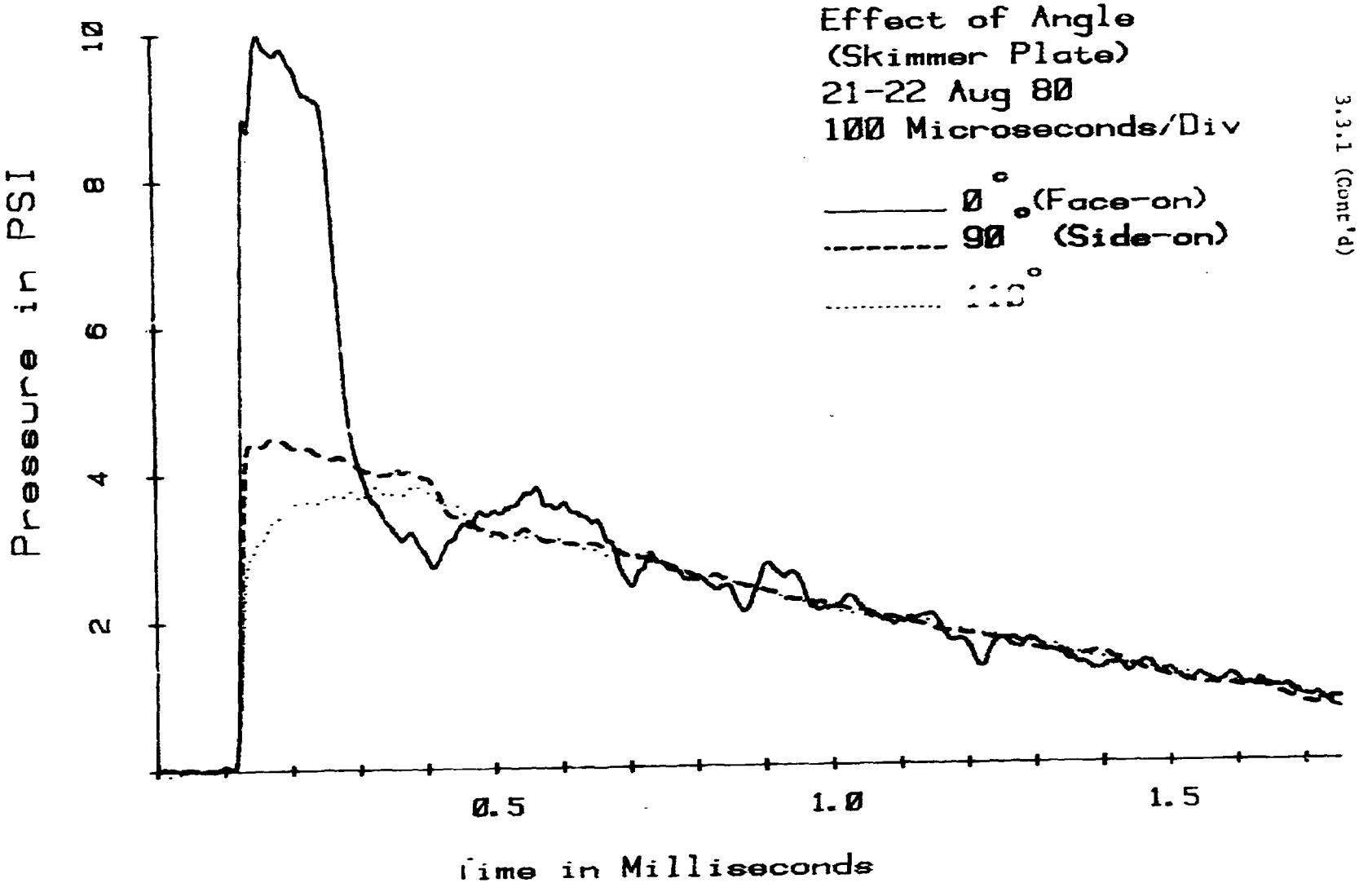

Figure 3.3-8. Response of skimmer plate to large angle misalignment in a pentolite free air explosion. These signals were recorded with an FM tape recorder using a 40 kHz, low pass filter.

3.3.2 The Blunt Cylinder Mount

Figure 3.3-9 shows the response of the blunt cylinder to shock tube blast waves of increasing pressure. Note that a peak of roughly 40 microseconds duration occurs. As pressure is increased, the peak becomes more pronounced. The value of the peak indicates side-on pressure.

Figure 3.3-10 shows the effect of incidence angle on the blunt cylinder mount in the shock tube. Note that in these unfiltered records, the theoretical face-on value of ~ 2.2 times the side-on pressure is reached when the transducer is oriented face-on.

Figure 3.3-11 is a photograph of the blunt cylinder mount attached to a lightweight blast stand in the field. Figure 3.3-12 shows the response of the blunt cylinder mount at various angles in a pentolite blast field. Note that the 40-microsecond peak is again present. Note also that the theoretical ratio (~ 2.2) of side-on to face-on pressure was not observed. It is felt that failure to reach the theoretical value is caused partially by the response of the blunt cylinder to a peaked wave and partially by the 40-kHz filter that was used in figure 3.3-12.

When the blunt cylinder mount is used, it is desirable to have a sighting plane longer than the outside diameter of the gage surface. Figure 3.3-13 shows a 13-cm-diameter removable plastic sighting disk that was used to align the blunt cylinder mount.

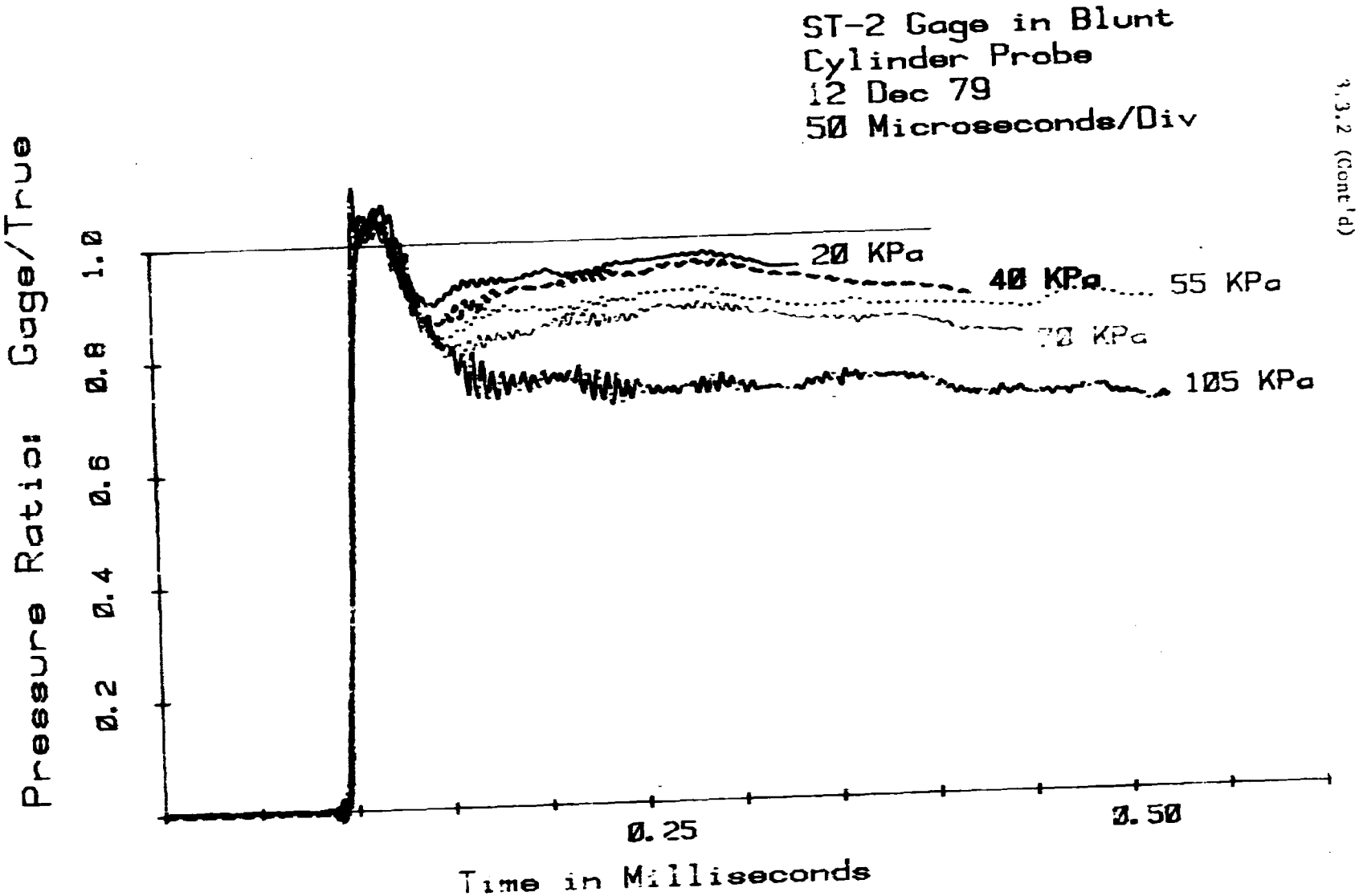

Figure 3.3-9. Shock tube response of blunt cylinder mount. Pressure ratio obtained by dividing transducer output by pressure level that corresponds to shock wave velocity. These signals were recorded with a digital transient recorder using no filtering (data from ref 6).

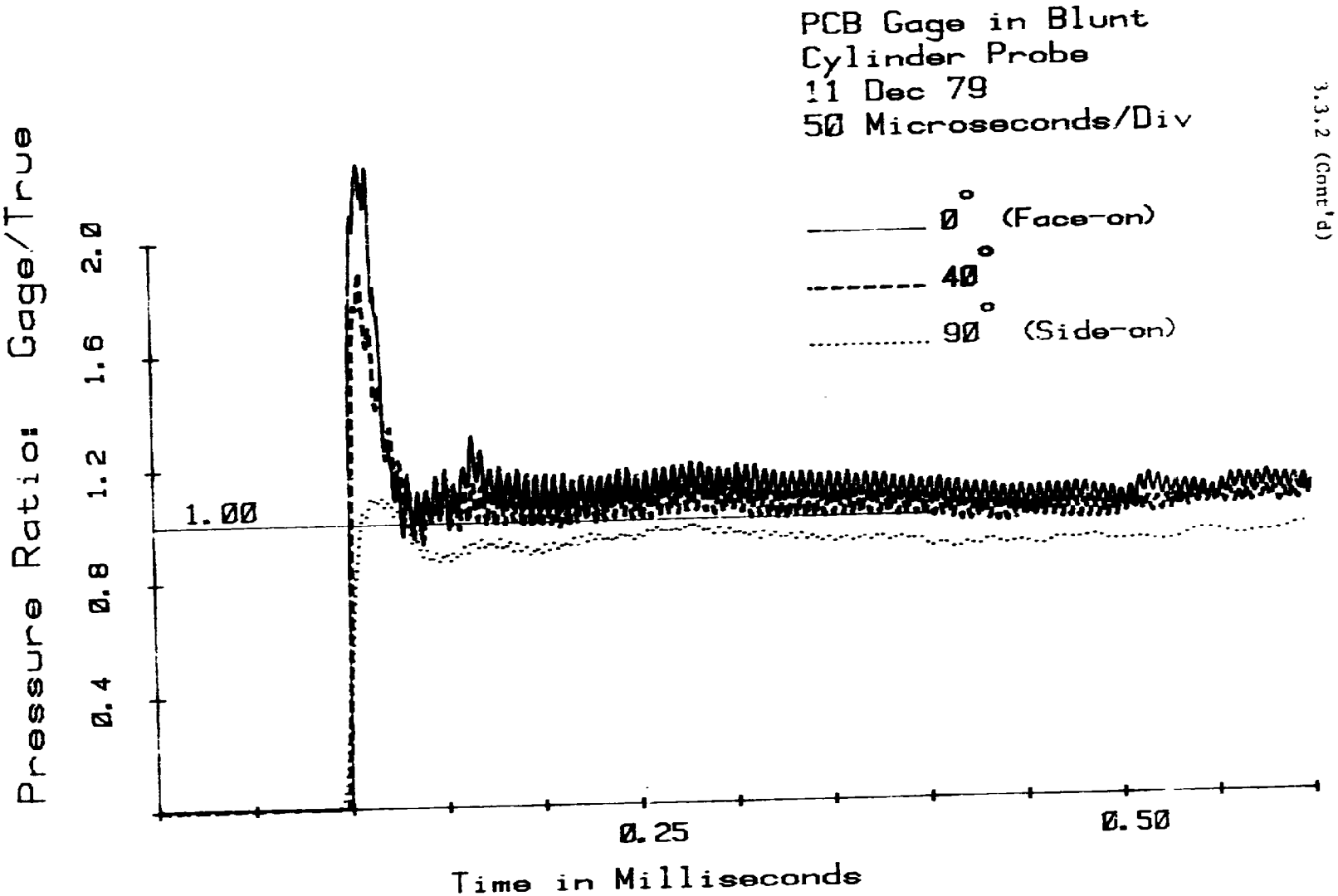

Figure 3.3-10. Effect of orientation measured in USABRL shock tube. These signals were recorded using a digital transient recorder with no filtering (data from ref 6).

3.3.2 (Cont'd)

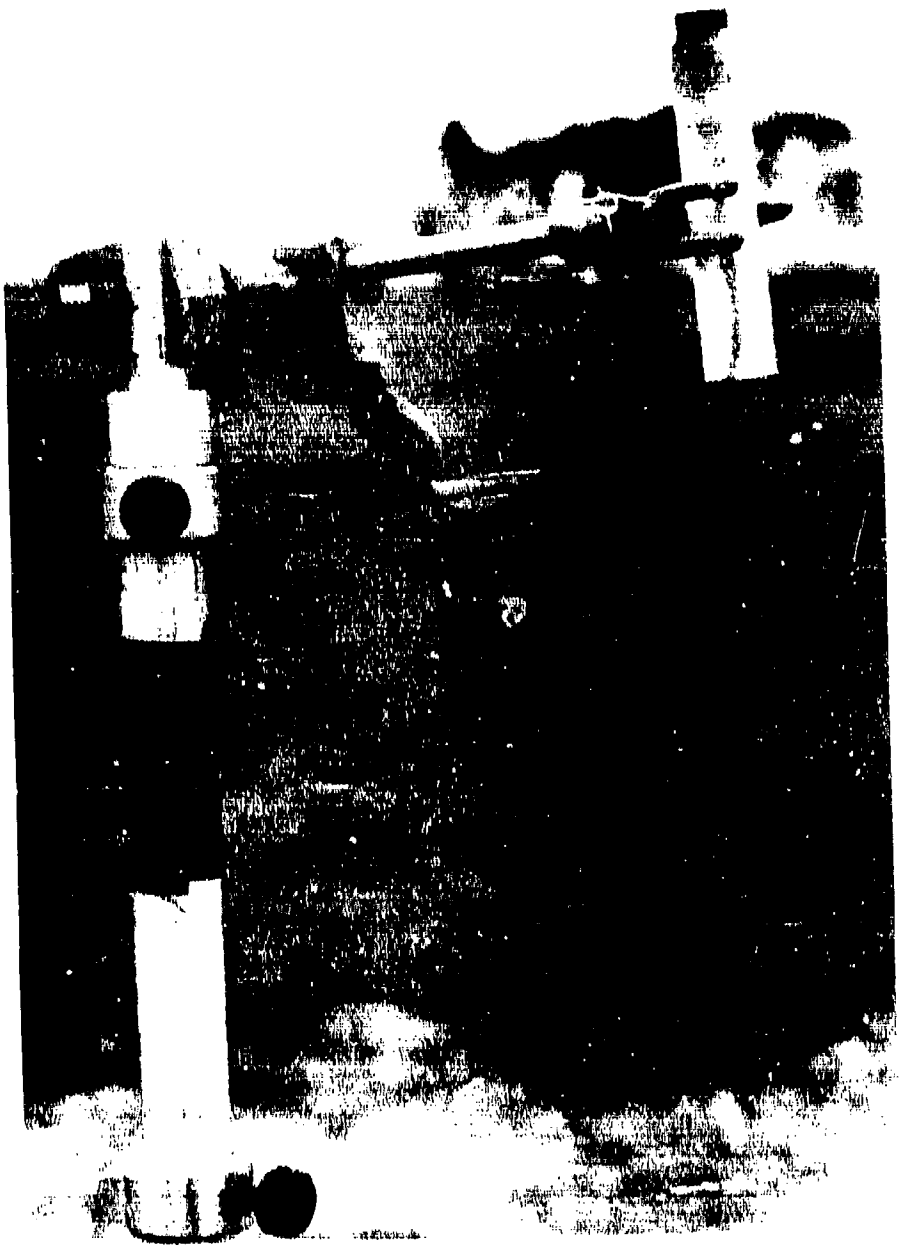

Figure 3.3.11. Pistol mount cylinder mount attached to stand.

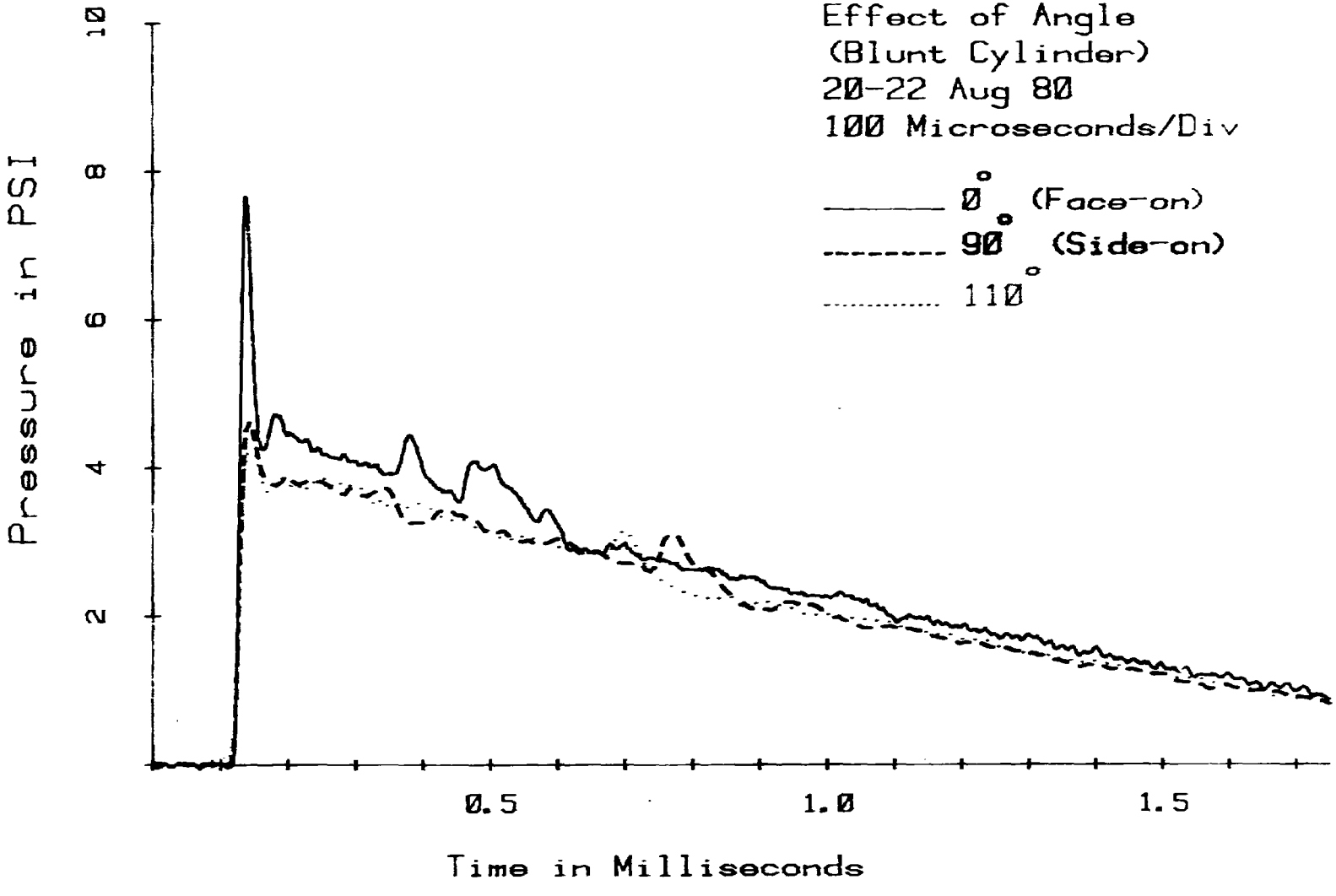

Figure 3.3-12. Response of blunt cylinder mount to changes in orientation. Measurements were made in pentolite free air explosions. These signals were recorded on an FM tape recorder. 40 kHz low-pass filtering was used.

3.3.3 The Pencil Probe

Figure 3.3-14 shows the pencil probe attached to a lightweight blast stand in the field. This probe is a plastic pencil-shaped ojive with a flat top. A miniature gage (ST-2 or PCB 113) is mounted in the ojive flush with the flat portion. Modeling clay is used to hold the miniature gage in place and also to provide isolation from acceleration.

Figure 3.3-14. Photograph of pencil probe attached to stand.

Figure 3.3-15 shows the response of the pencil probe at various angles in the pentolite blast field. Note that there is no sharp pressure drop from face-on to stagnation as was present with the skimmer plate. The relief time of the pencil probe is, however, significantly longer than the relief time of the blunt cylinder mount.

Note also that the ratio of side-on to face-on pressure is not quite up to the theoretical value. The pencil probe does, however, come closer to the theoretical ratio than the blunt cylinder. Once again, it is felt that the failure to reach the theoretical ratio is caused partially by the response of a pencil probe to a peaked wave and partially by the 40 kHz filter.

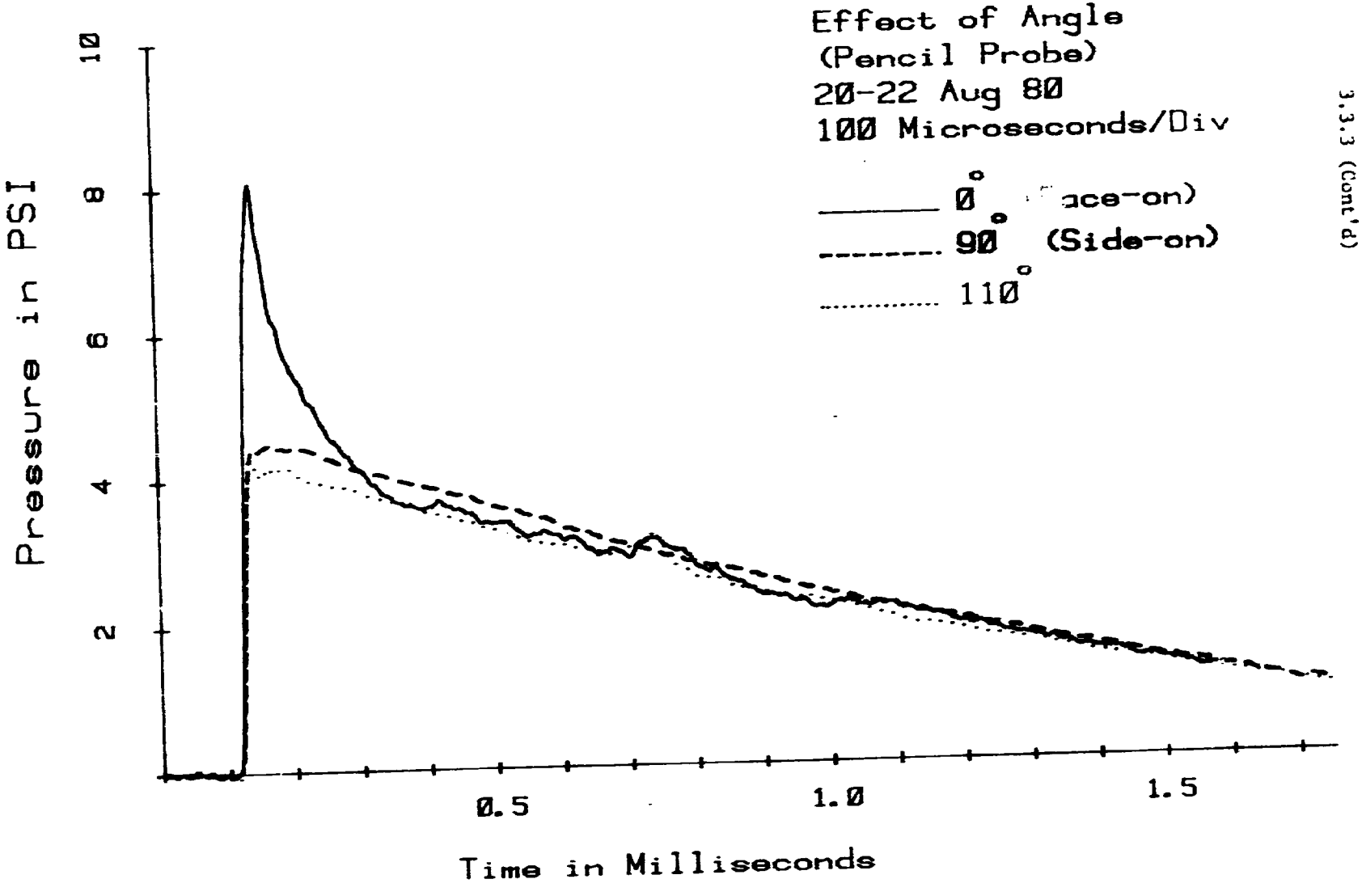

Figure 3.3-15. Response of pencil probe to changes in orientation. These measurements were made in pentolite free air explosions and recorded on an FM tape recorder. 40 kHz low-pass filtering was used.

3.3.4 Comparison of the Blunt Cylinder, the Skimmer Plate, and the Pencil Probe

Figure 3.3-16 shows the effect of small angle misalignment of the three methods of mounting miniature transducers. This chart was compiled by comparing the mean peak pressure of two shots obtained from pentolite using the stated configuration and misalignment angle to the mean peak pressure of five shots obtained with that configuration at grazing incidence (i.e., side-on orientation). All data were low pass filtered at 40 kHz.

Because of the small sample size and the variability of pentolite blast from shot to shot, the exact shape of the curves is not significant. The general trends indicated in the chart are, however, felt to be valid.

If one is attempting to measure side-on pressure, a reading of 100% on figure 3.3-16 could be considered zero "error." As the blast wave approaches face-on, either through improper alignment to the blast source or because a reflection if produced by an off-axis object, the "error" obtained will be a high reading. Positive misalignment angle indicated in figure 3.3-16 is toward face-on.

Note that the skimmer plate clearly indicates the highest "error" as it is rotated toward face-on. It is assumed that the short relief time of the blunt cylinder mount causes it to have the least "error" as it is rotated toward side-on.

As misalignment approaches a backwards orientation (negative misalignment angle), all configurations produce peak pressure readings below the side-on value. The pencil probe indicates slightly less "error" than the other two mounts in this configuration. Because of the small sample size, it is not certain that this difference is valid.

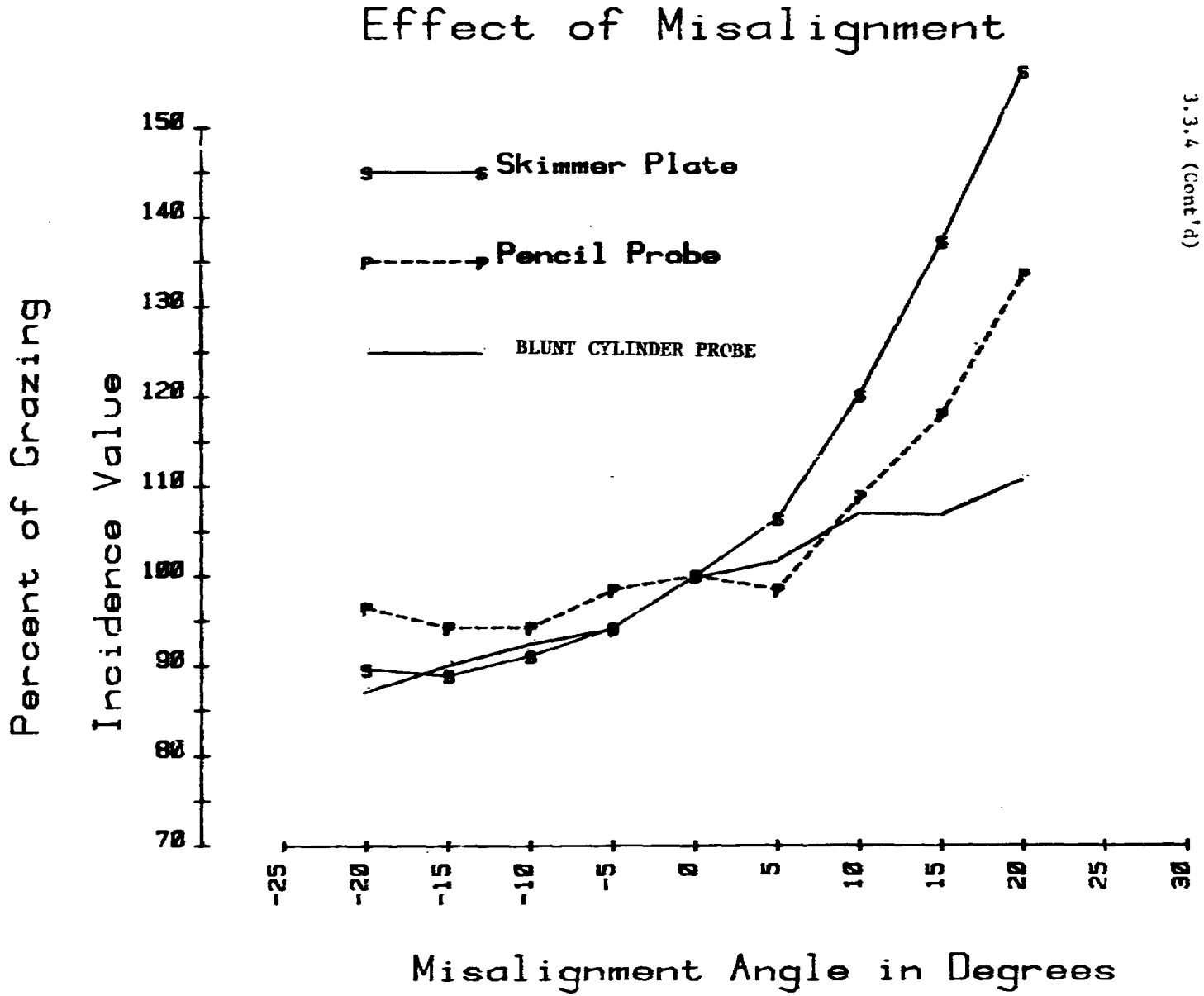

Figure 3.3-16. Small angle misalignment sensitivity of skimmer plate, pencil probe, and blunt cylinder. Each point represents mean of two pentolite free air explosions.

3.3.4 (Cont'd)

Figures 3.3-17 through 3.3-21 show the response of the three mounts to pentolite blast of varying pressure. Note that in figure 3.3-20 and 3.3-21, no skimmer plate data is provided.

Instead, a theoretical pressure versus time curve is presented. The peak pressure values for the theoretical curves were obtained from Goodman's equation (ref 7). The exponential equations for the decay of the positive peak were obtained from Brode (ref 8).

Note that the familiar 40-microsecond peak produced by the blunt cylinder mount becomes more pronounced as pressure level increases. This result is similar to what was observed in the shock tube shown previously in figure 3.3-9.

In general, it appears that the pencil probe and the skimmer plate produce similar curves. The 40-microsecond peak of the blunt cylinder mount distinguishes itself clearly at higher pressure values, and would produce a significant error if the pressure versus time curve were integrated to obtain impulse.

At low pressure values, the three mounting techniques produce little difference. The pencil probe appears to produce the smoothest waveform.

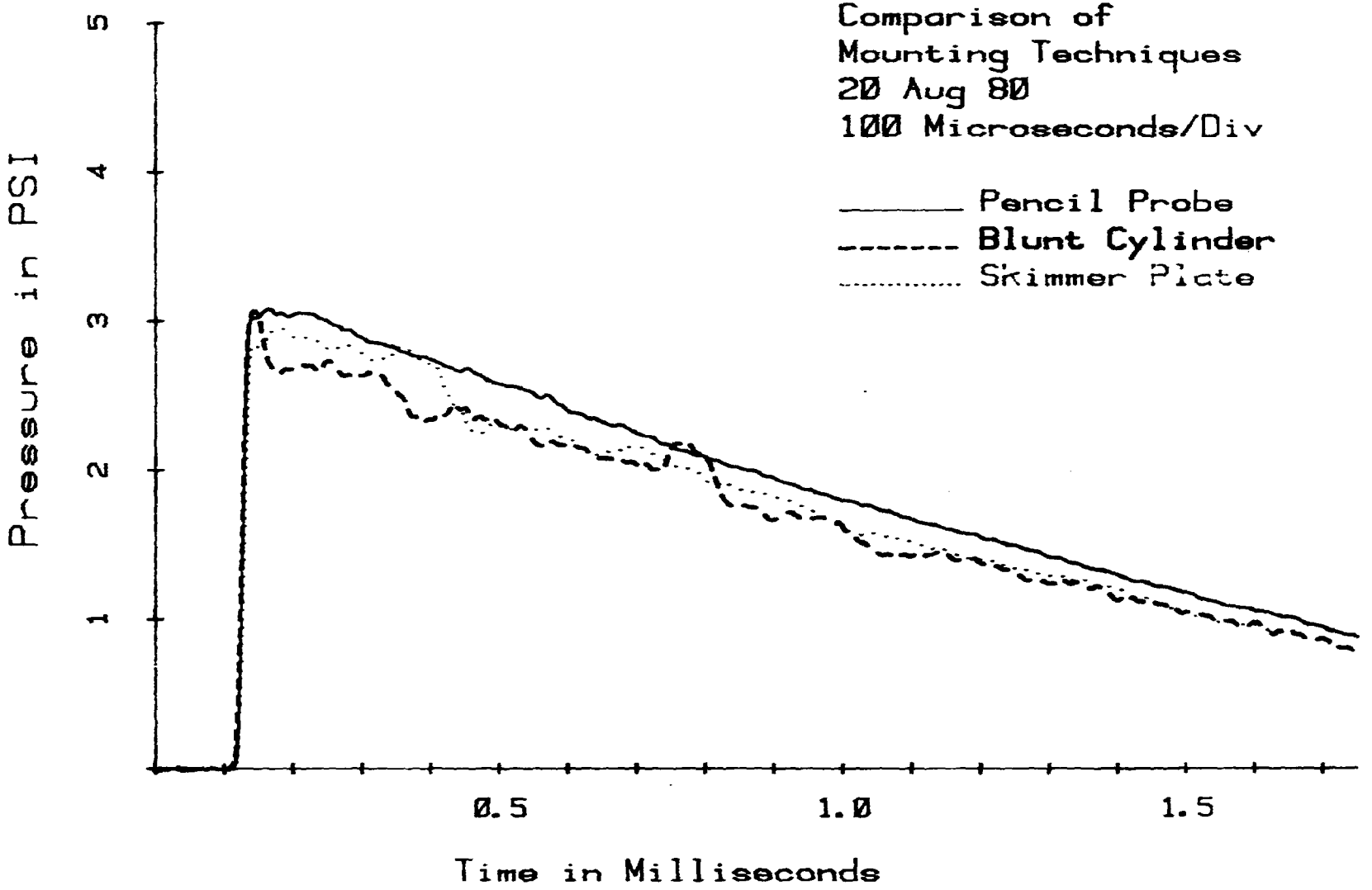

Figure 3.3-17. Comparison of response of different mounts to pentolite free air explosion at 20 kPa level.

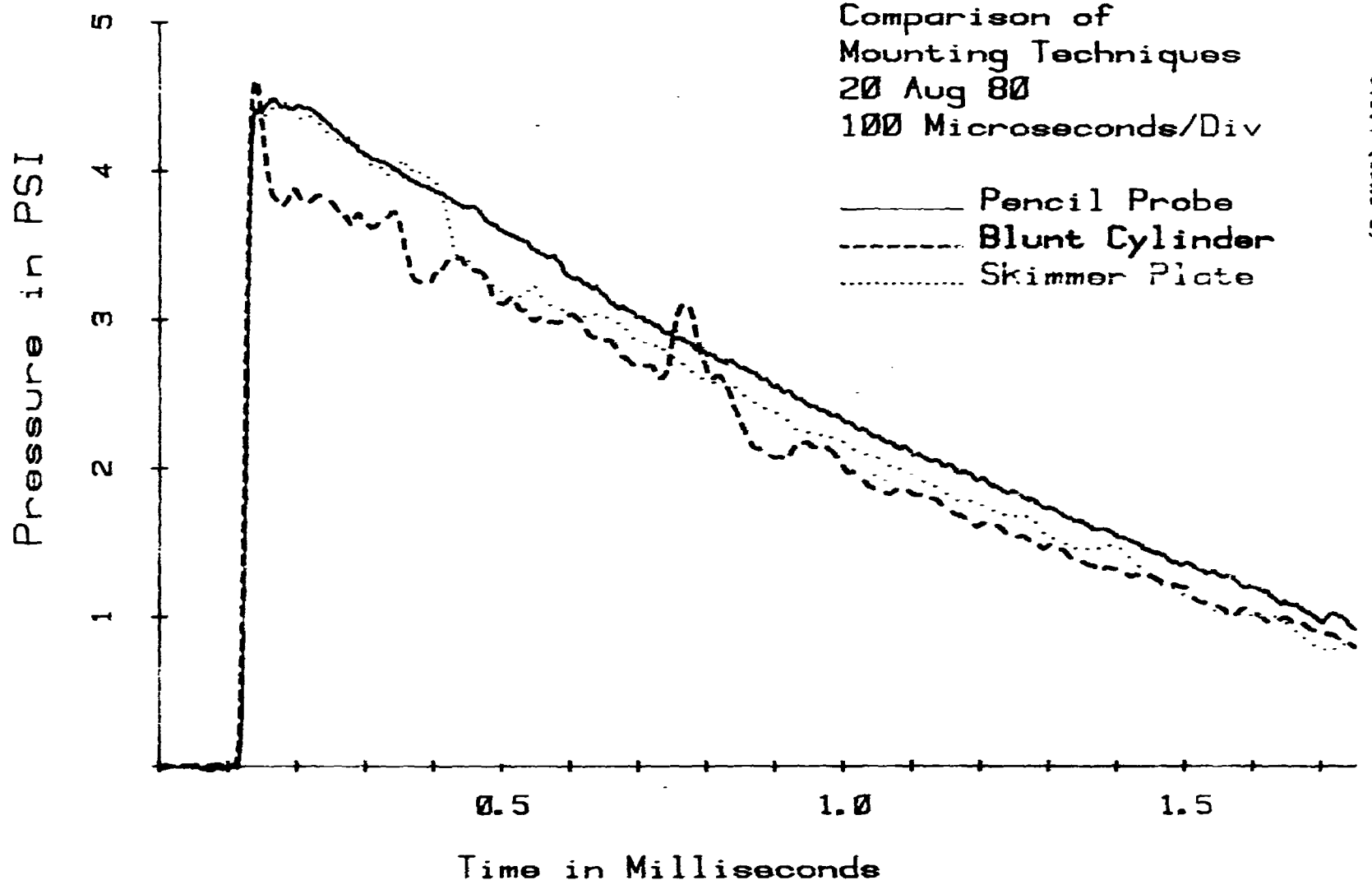

Figure 3.3-18. Comparison of response of different mounts to pentolite free air explosion at 30 kPa level.

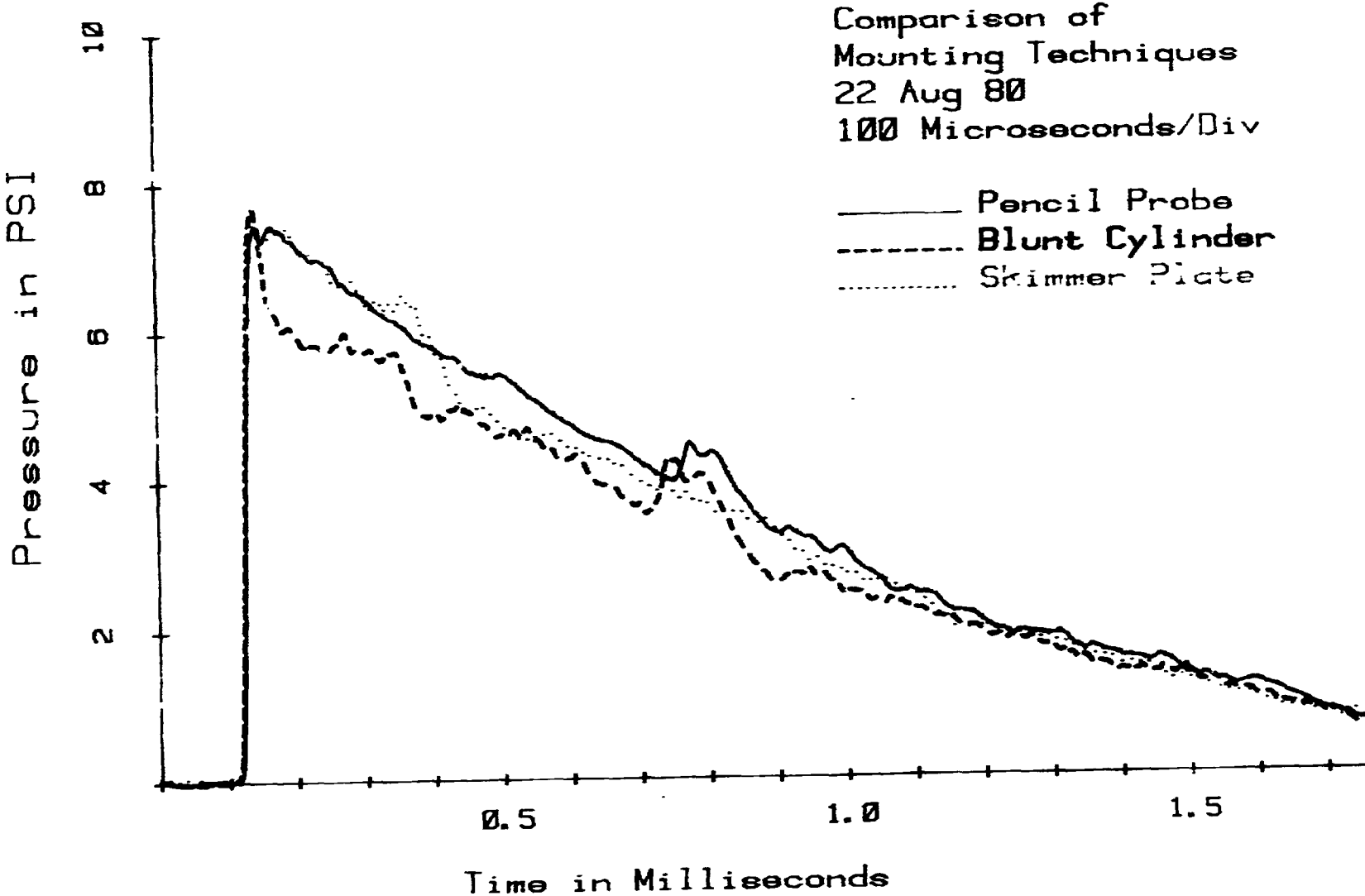

Figure 3.3-19. Comparison of response of different mounts to a pentolite free air explosion at 50 kPa level.

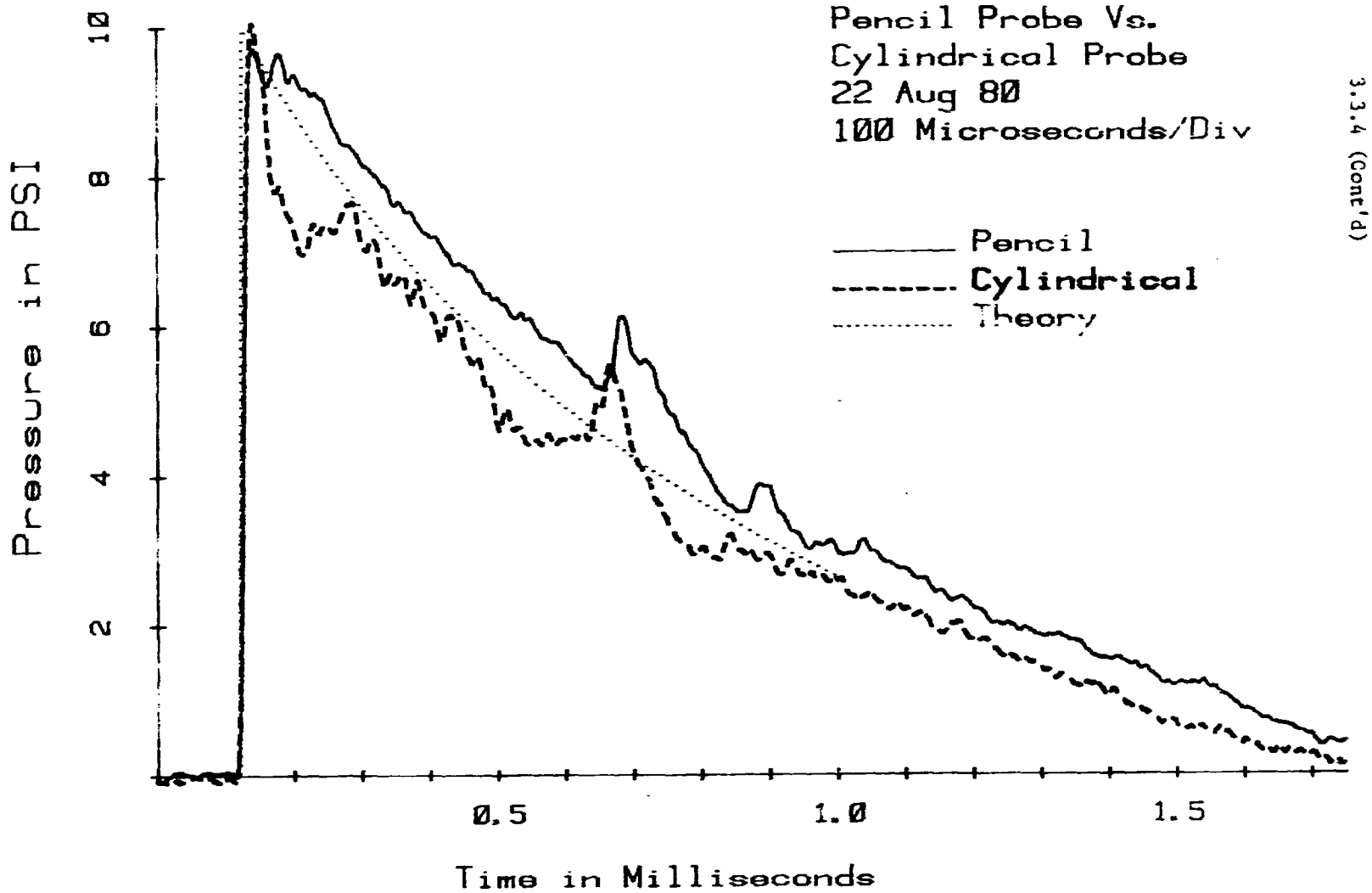

Figure 3.3-20. Comparison of blunt cylinder and pencil probe mount to theory for a pentolite free air explosion at 70 kPa level. The notation "cylindrical probe" refers to the blunt cylinder mount.

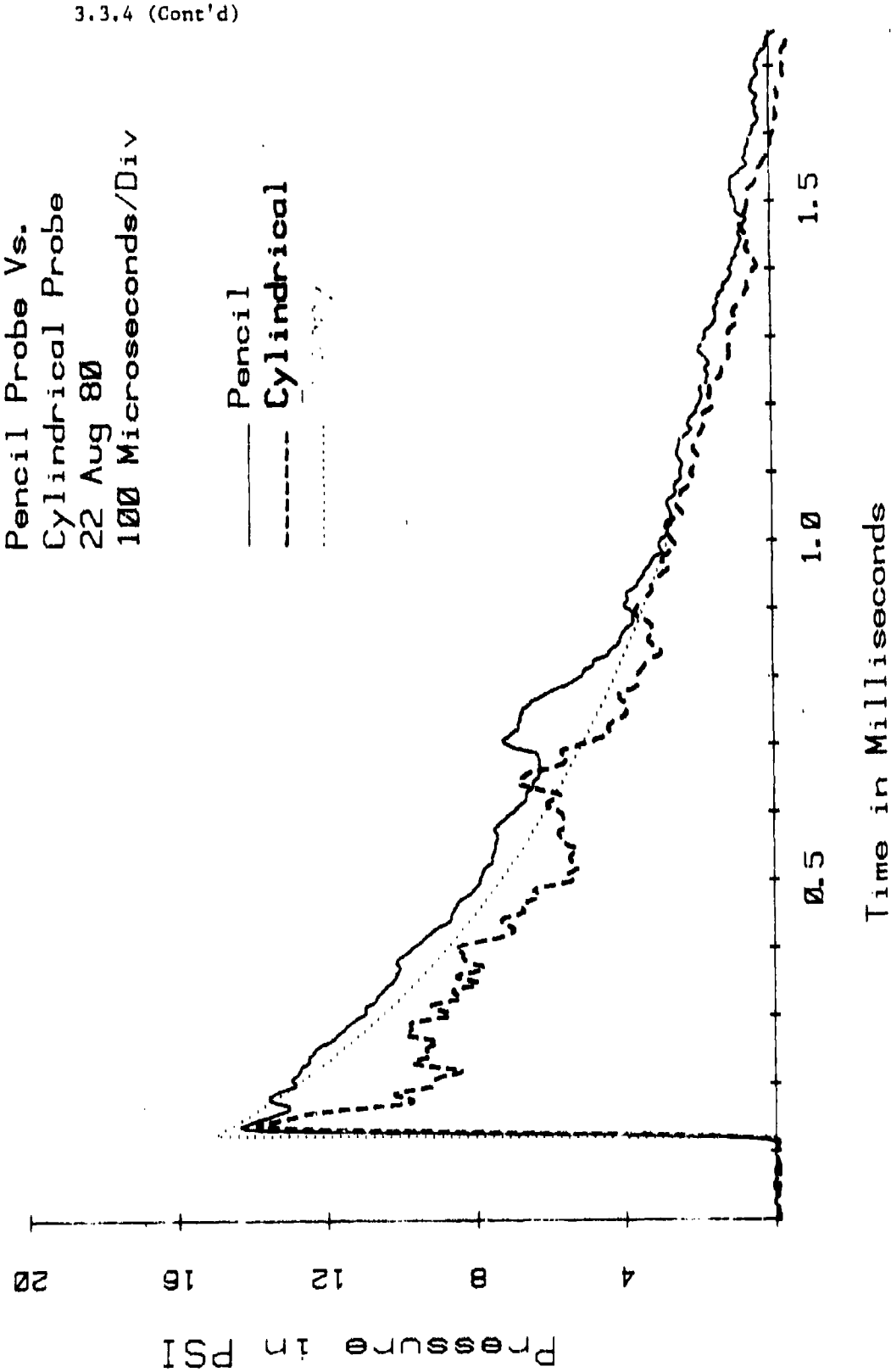

Figure 3.3-21. Comparison of blunt cylinder and pencil probe mount to theory for a pentolite free air explosion at 100 kPa level. The notation "cylindrical probe" refers to the blunt cylinder mount.

Each of the mounts described has a peculiar set of strengths and faults. The following application guide is based on the observations presented in this section:

a. Pencil probe. Best suited for applications where the exact shape of the waveform is critical and the blast source is well defined and presents an easy point for alignment.

b. Skimmer plate. Best suited for applications where exact shape of the waveform is still critical and an omnidirectional plane is needed (such as near the muzzle of a gun). The blast source must present some well defined line for alignment because misalignment of more than 5 degrees will cause significant error.

c. Blunt cylinder. Best suited for measurement in complicated blast fields where small errors in wave shape are preferable to large errors caused by unavoidable misalignment. Ideal for low pressure fields.

3.4 SIDE-ON PRESSURE TRANSDUCERS

The following transducers consist of a pressure sensing element and an integral aerodynamic ojive. The effect of the sensing element is combined with the flow effects of the ojive to produce the overall performance of the transducer. The intent of the ojive is to facilitate accurate measurement of side-on pressure.

3.4.1 Celesco Model LC-33 Pencil Gage

The LC-33 pencil gage shown in figure 3.4-1 was formerly manufactured by Atlantic Research and is now manufactured by Celesco. This transducer has been the standard for blast measurement by the Materiel Testing Directorate at APG for at least 20 years.

The low resonant frequency of this transducer makes it unacceptable by the standards presented in reference 4. Despite this fact, a number of experiments were conducted using the LC-33 transducer in this study. Because of the large historical data base that has been collected with this transducer, it is felt that understanding and analyzing its characteristics are important.

Figure 3.4-2 shows the side on response of the LC-33 in the USABRL shock tube. Note the long, slow rise time ($\sim$50 μs).

The LC-33 has a cylindrical sensing crystal that is only 0.635 cm (0.25 in.) long. It is estimated that the shock wave of figure 3.4-2 was traveling approximately 380 m/s. At this velocity, it would only take 17 microseconds to traverse the length of the crystal.

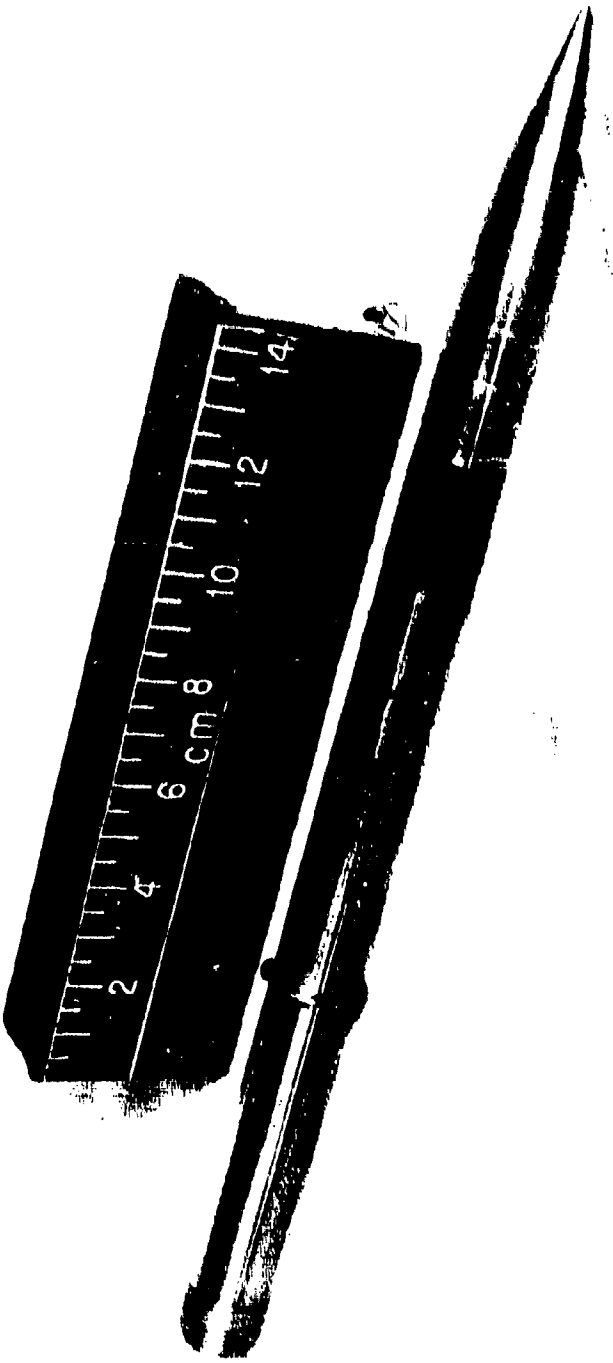

Figure 3.--1. The LC-33 pencil gage.

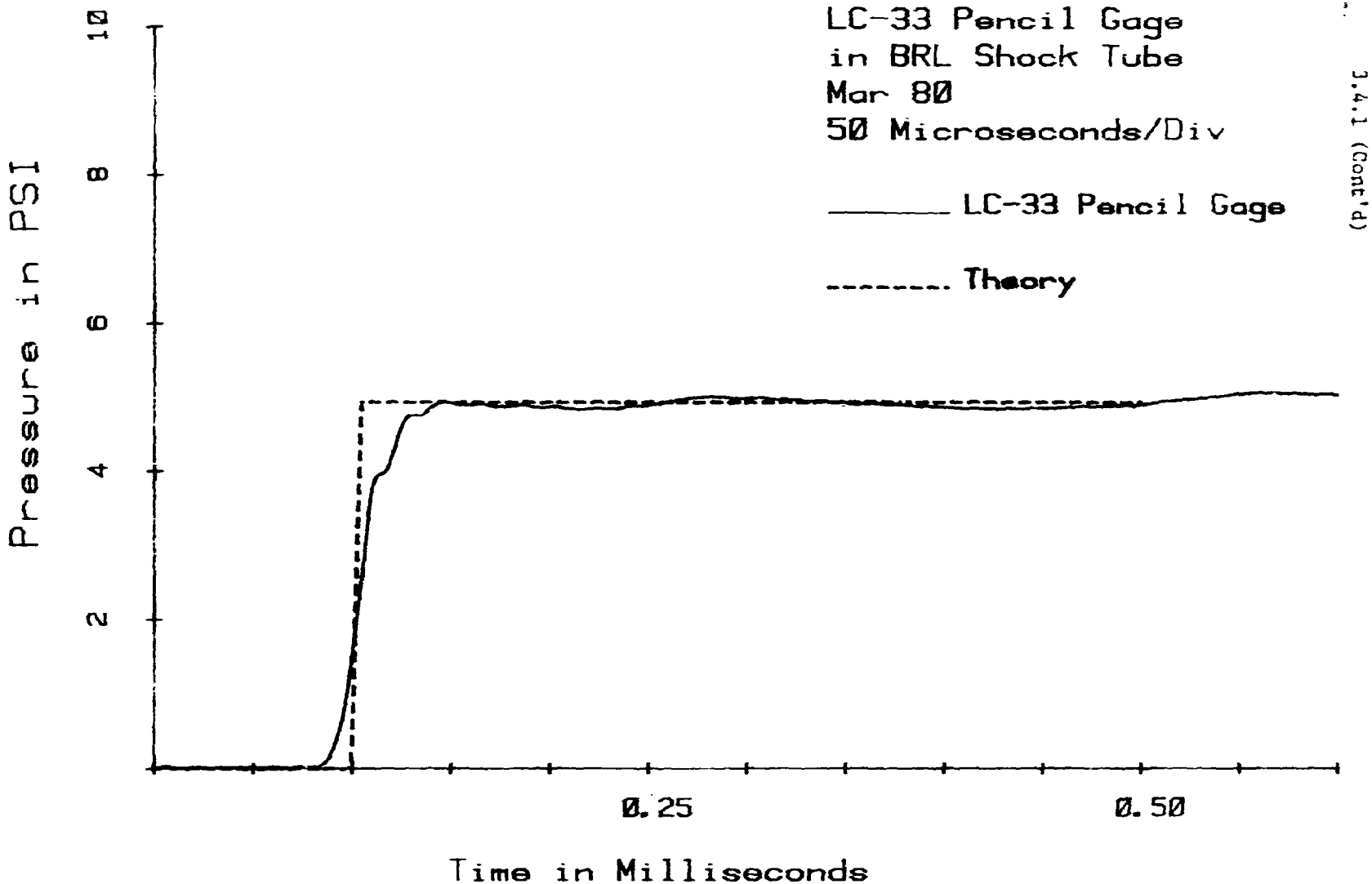

Figure 3.4-2. Side-on response of the LC-33 pencil gage in the USABRL shock tube. This signal was recorded on a digital transient recorder with no filtering. Note the long (50 us) rise time (data from ref 61).

The 50 microsecond rise time suggests that the transducer construction is such that the effective length of the crystal is approximately 1.0 cm. This characteristic would be a distinct disadvantage in measuring blast waves that begin a rapid decay immediately after peak pressure is reached, such as the blast produced by small arms. In this situation, the long slow rise time of the LC-33 would prevent measurement of the true peak pressure.

To measure side-on pressure, the LC-33 is pointed toward the blast source. The cylindrical sensing crystal of the LC-33 produces interesting directional characteristics. It produces a peak pressure indication of less than true side-on pressure as it is rotated away from side-on orientation. The LC-33 produces very little error for small angle misalignment.

The specifications of the LC-33 are listed below:

a. Electronics: Charge type.

b. Crystal: Lead zirconate Titanate.

c. Crystal length: 0.635 cm (0.25 in.)[a].

d. Time constant: Depends on charge amplifier, typically 2 seconds or longer.

e. Acceleration sensitivity: 0.07 kPa/g (0.01 psi/g) (measured)[b].

[a]Due to construction, the effective crystal length is approximately 2 cm long.
[b]This quantity was not available in the manufacturer's literature, so it was measured on one sample transducer.

3.4.2 PCB Model 113 Lollipop

The PCB lollipop consists of the acceleration compensated PCB 113 sensing element described earlier placed in a lollipop-shaped ojive. Detail of the ojive shape is shown in figure 3.4-3. A photograph of the PCB lollipop is shown in figure 3.4-4. The specifications of the PCB lollipop are presented below:

a. Electronics: Voltage mode.

b. Crystal: Quartz.

c. Resonant frequency: 500 kHz.

d. Crystal diameter: 5.54 mm.

e. Time constant: 10 seconds.

3.4.2 (Cont'd)

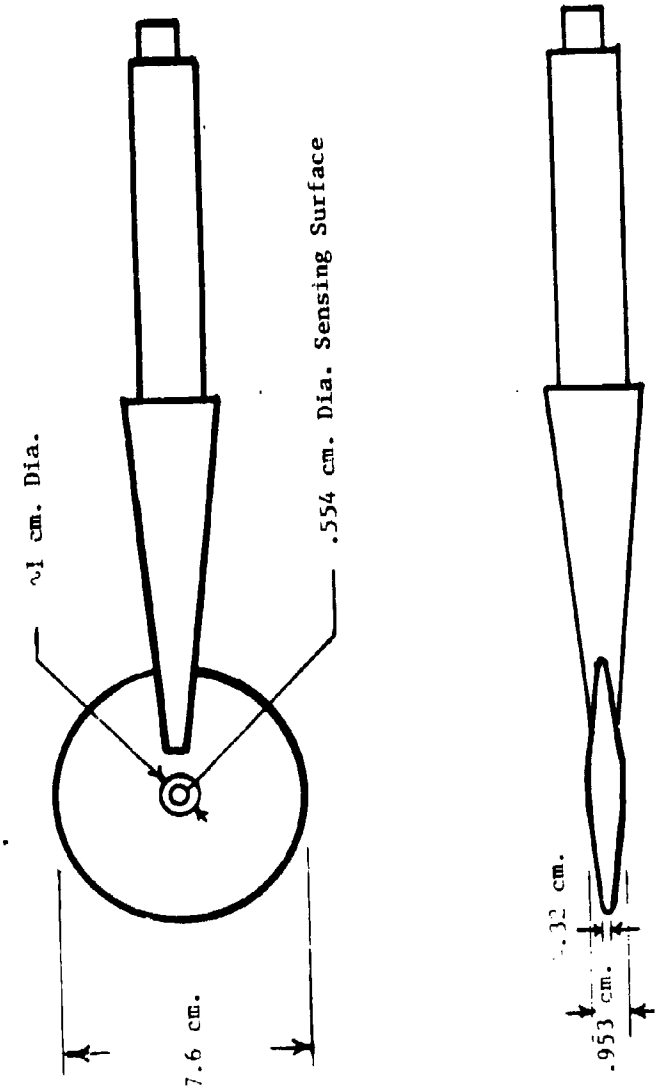

Figure 3.4-3. Detail of the ojive shape of the PCB lollipop.

3.4.2 (Cont'd)

Figure 3.4-4. Photograph of the PCB lollipop.

3.4.2 (Cont'd)

f. Acceleration sensitivity: 0.014 kPa/g (0.002 psi/g).

g. Change in scale factor with temperature: 0.054%/°C (0.03%/°F).

Figure 3.4-5 shows the side-on response of the PCB lollipop in the USABRL shock tube. Note the sharp peak which indicates the correct pressure value, followed by an indication of slightly below the correct value.

Figure 3.4-6 shows the PCB lollipop mounted in the field. Figure 3.4-7 shows the side-on response of the PCB lollipop to a pentolite blast wave. Note that the sharp peak is again present.

Like the the skimmer plate, the PCB lollipop is omnidirectional in one plane but is very sensitive to misalignment out of that plane. Figure 3.4-8 demonstrates the effect of misalignment on pressure versus time curves.

Figure 3.4-9 compares the effect of small angle misalignment of the PCB lollipop and the LC-33 pencil gage. This chart was compiled by comparing the mean of two pentolite shots in the misaligned configuration to the mean of five shots in the side-on orientation.

Because of the variability of pentolite and the small sample size, the exact shape of the curve is not significant. The general trends indicated in the chart are, however, felt to be valid.

Note that the LC-33 attenuates when misaligned, and is within 5% of the side-on value for more than ±10 degrees. The PCB lollipop is within 5% of the side-on value for only ±5 degrees and essentially duplicates the directional characteristics of the skimmer plate.

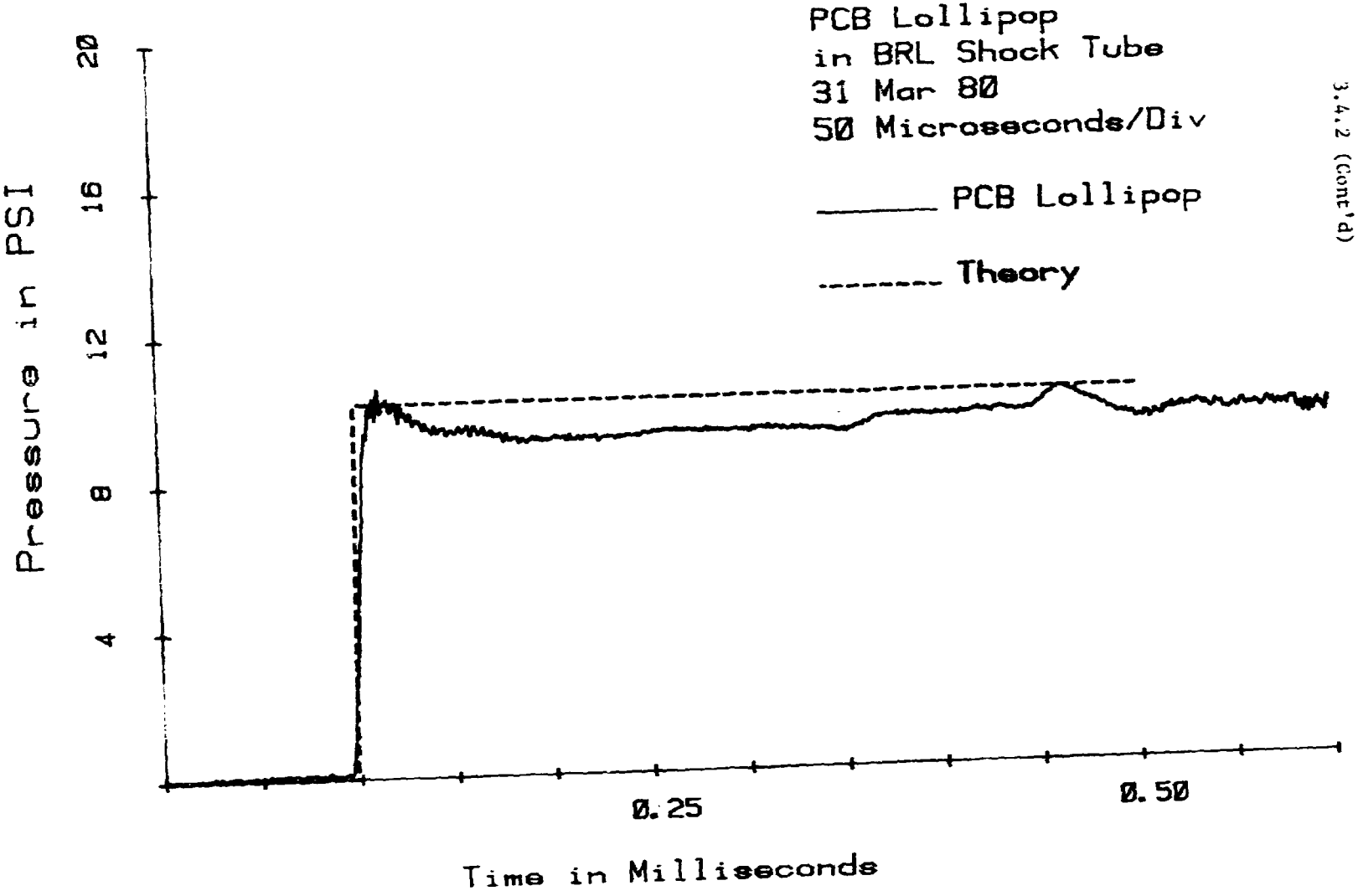

Figure 3.4-5. Side-on response of the PCB lollipop in the USABRL shock tube. This signal was recorded using a digital transient recorder with no filtering. Note peaking effect (data from ref 6).

3.4.2 (Cont'd)

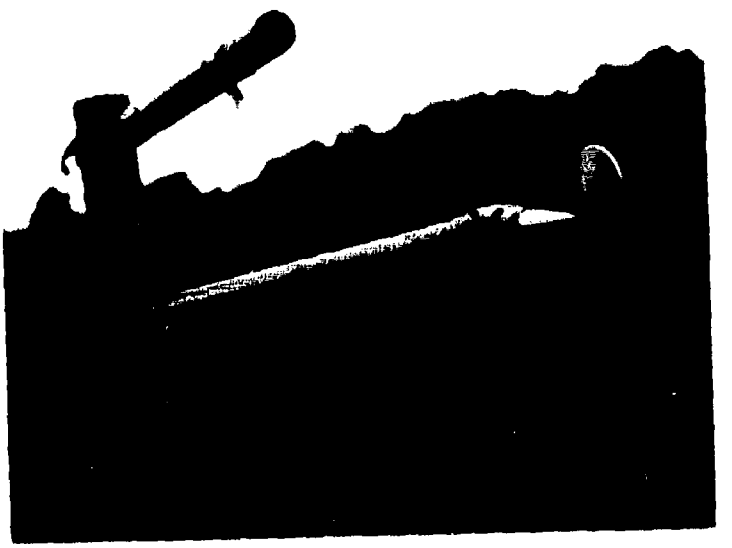

Figure 3.4-6. Photograph of PCB lollipop transducer mounted on heavy weight blast stand.

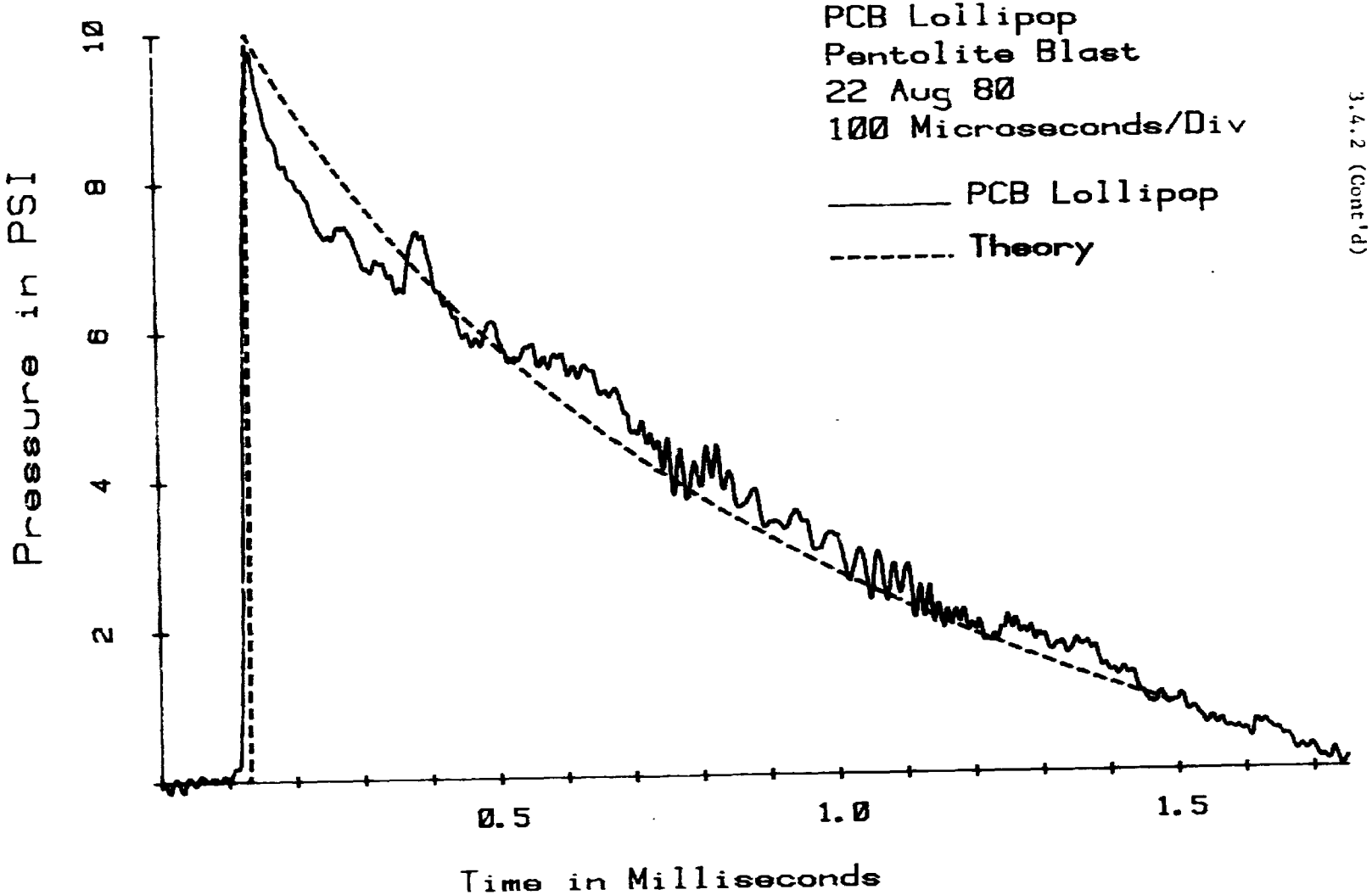

Figure 3.4-7. Side-on response of PCB lollipop in free air explosion. Note the peaking effect. This signal was recorded on an FM tape recorder. 40 kHz low pass filtering was used.

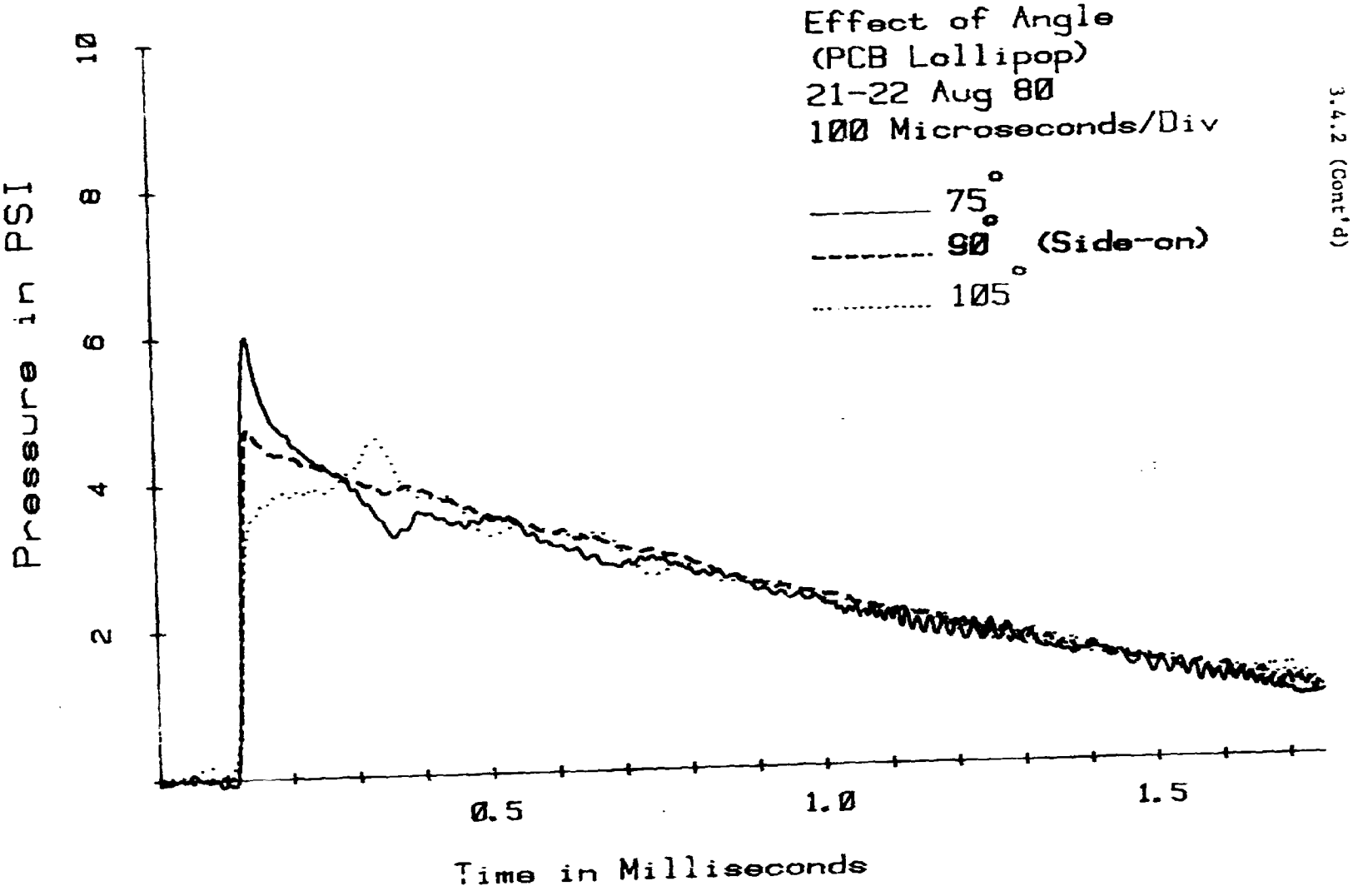

Figure 3.4-8. Plots of pressure versus time for various orientations of the PCB lollipop in pentolite free air explosions. These signals were recorded on an FM tape recorder. 40 kHz low pass filtering was used.

3.4.2 (Cont'd)

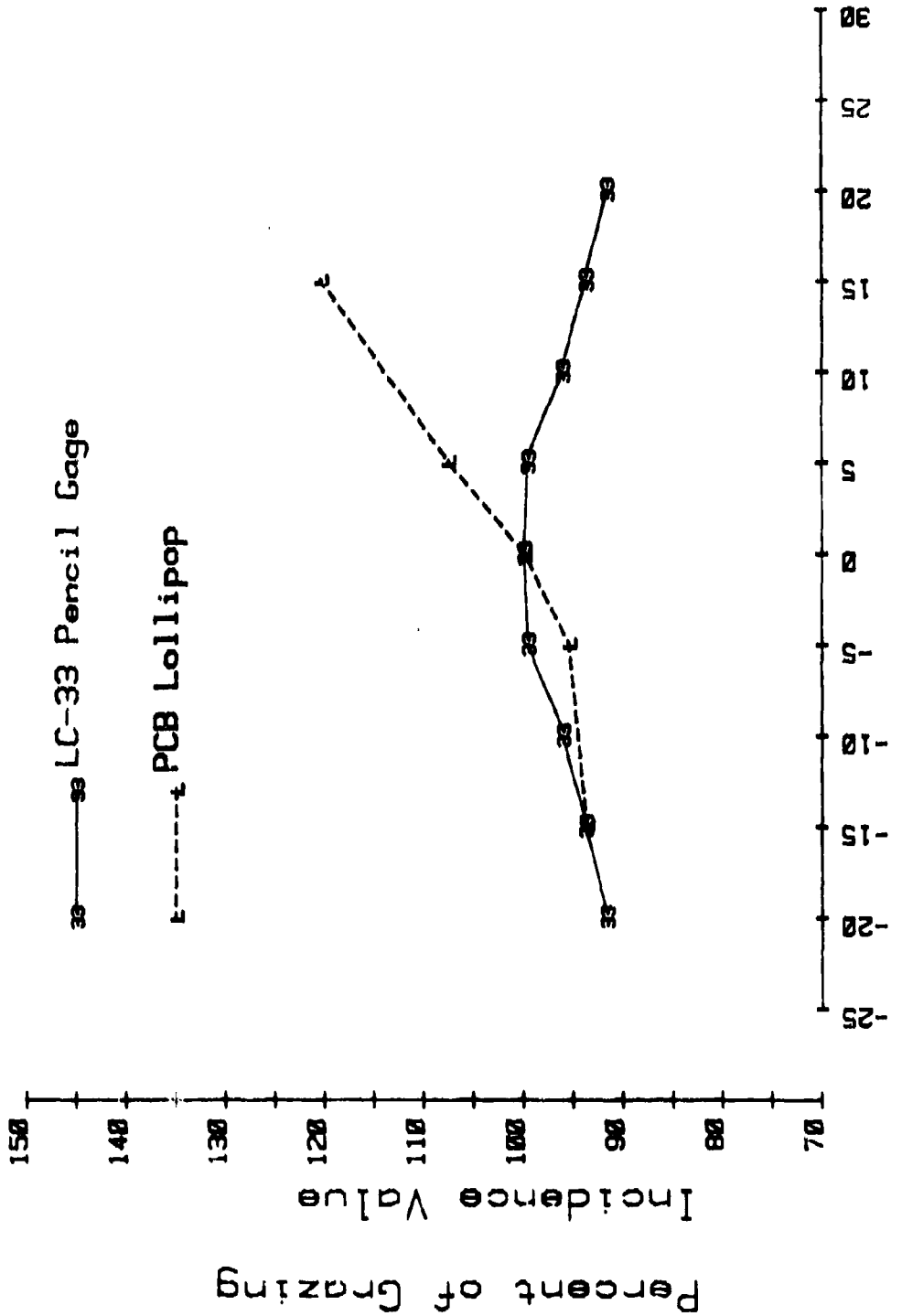

Figure 3.4-9. Sensitivity of LC-33 pencil gage and PCB lollipop to misalignment. Each point represents the mean of two measurements made in a pentolite free air explosion.

(Page 88 Blank)

SECTION 4. CALIBRATION TECHNIQUES

4.1 INTRODUCTION

It is rather straightforward to determine the sensitivity of an electrical pressure transducer which has DC response. Very accurate standards for generating or reading static pressure are available. Calibration is simply a matter of reading the electrical transducer's output at a given pressure.

Most blast transducers do not have DC response. Various techniques have been devised to calibrate these AC-coupled transducers. This section discusses four of those techniques.

4.2 THE SHOCK TUBE

The shock tube can be used for blast experimentation, to check for proper transducer operation, and to calibrate transducers. Figure 4.2-1 is a schematic diagram showing operation of a shock tube. Figure 4.2-2 is a photograph of a 10.2-cm (4-in.) inside-diameter shock tube. Figure 4.2-3 shows a typical plot of pressure versus time from that shock tube.

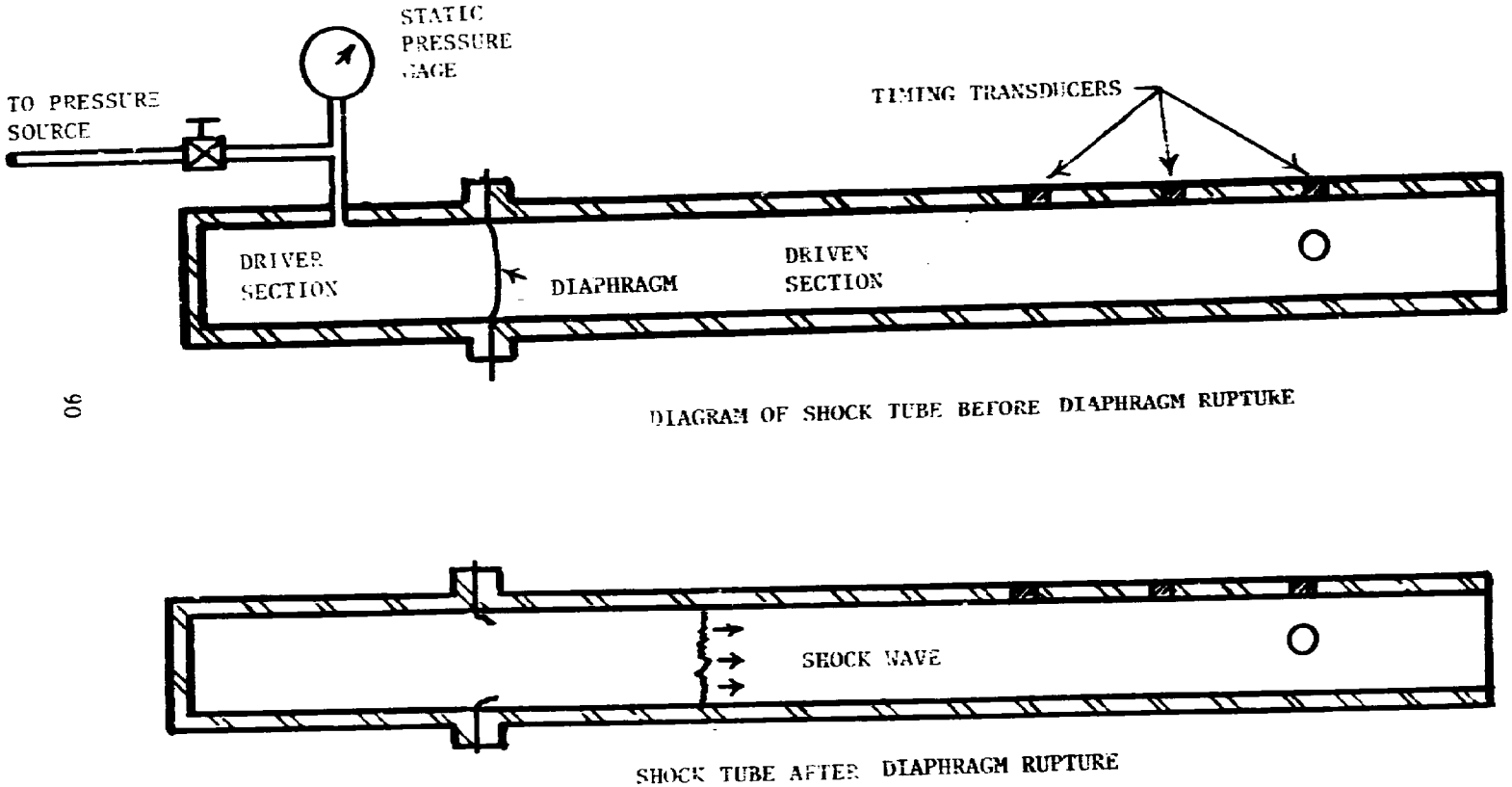

Figure 4.2-1. Schematic diagram of shock tube operation.

4.2 (Cont'd)

Figure 4.2-2. Photograph of a 10.2 cm (4 in.) shock tube.

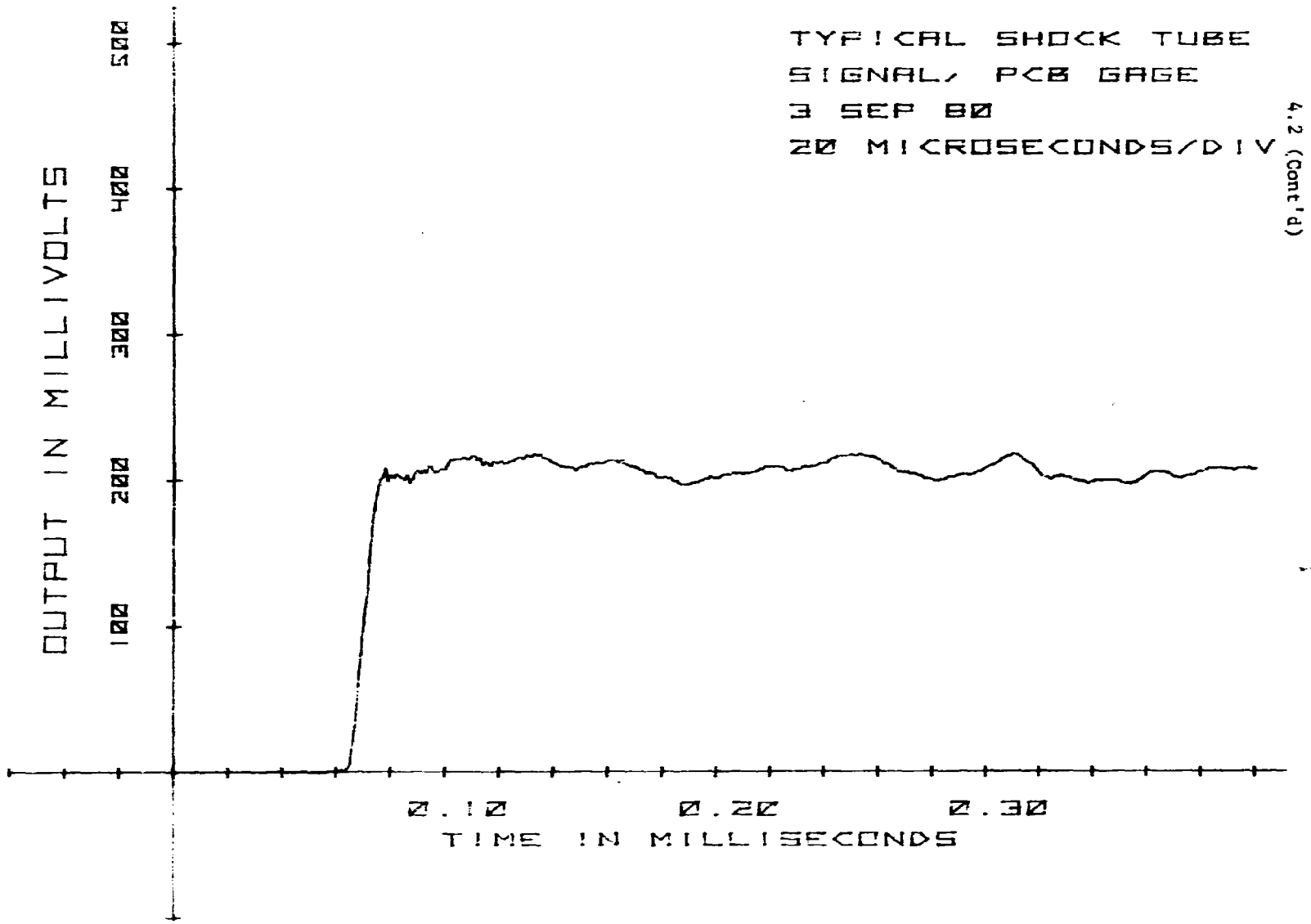

Figure 4.2-3. Typical plot of side-on pressure versus time from 10.2 cm shock tube.

4.2 (Cont'd)

Sensors placed a known distance apart are used to measure the velocity of the shock wave as it travels down the shock tube. In the shock tube shown in figure 4.2-2, the sensors are 30.48 cm and 60.96 cm apart. The Rankine-Hugoniot Equation introduced in section 2.1 is used to calculate the side-on pressure level of the shock wave:

$$P_s = P_o \frac{7}{6} (m^2-1)$$

where

P_s = Side-on pressure

P_o = Ambient pressure

m = Mach number

$$= \frac{v}{a}$$

where

v = Shock velocity

a = Speed of sound in air

$$= 20.09 \sqrt{T} \text{ meters/sec}$$

where

T = Temperature in degrees kelvin.

4.2 (Cont'd)

It should be pointed out that the Rankine-Hugoniot Equation becomes very sensitive to measurement errors at low pressures. Tables 4.2-1 and 4.2-2 illustrate this fact.

Table 4.2-1, Measurement errors that will cause a 1% error in calculated side-on pressure level. P_o = 101.35 kPa (14.7 psi), θ_o = 20° C (68° F), a = 343.979 m/s, velocity gage base length L = 30.48 cm (12 in.).

TABLE 4.2-1. MEASUREMENT ERRORS

Item	Pressure Level 15 kPa (2.18 psi)	35 kPa (5.08 psi)	70 kPa (10.15 psi)
Time T to cross baseline (microseconds)	834.7	778.4	702.3
ΔT for 1% error (microseconds)	0.5	0.9	1.3
ΔL for 1% error (mm)	0.17	0.35	0.57
Δθ for 1% error (°C)	0.33	0.67	1.09
ΔP_o for 1% error (kPa)	1.01	1.01	1.01

Table 4.2-2, Measurement errors that will cause a 1% error in calculated side-on pressure level. P_o = 101.35 kPa (14.7 psi), θ_o = 20° C (68° F), a = 343.979 m/s, velocity gage base length L = 60.96 cm (24 in.).

TABLE 4.2-2. MEASUREMENT ERRORS

Item	Pressure Level 15 kPa (2.18 psi)	35 kPa (5.08 psi)	70 kPa (10.15 psi)
Time T to cross baseline (microseconds)	1669.4	1556.8	1404.6
ΔT for 1% error (microseconds)	1.0	1.8	2.6
ΔL for 1% error (mm)	0.34	0.70	1.14
Δθ for 1% error (°C)	0.33	0.67	1.09
ΔP_o for 1% error (kPa)	1.01	1.01	1.01

Four measurements are required to calculate the side-on pressure of a shock wave: baseline length, transit time, ambient temperature, and ambient pressure. From the tables above, it is obvious that ambient pressure is the least critical of the four measurements. Precise length measurement is also rather straight-forward.

The critical measurements are air temperature and transit time. Low thermal mass thermocouples and elimination of thermal gradients are required to obtain accurate air temperature measurements.

Note that timing accuracies on the order of 1 microsecond are required. Counters are readily available which have 0.1 microsecond resolution. The critical matter is triggering the counter.

Most transducers have a 10-microsecond rise time. Both the start and the stop triggering circuits must be adjusted to function at the same point during their respective 10-microsecond rise times.

The shock tube provides an excellent means of testing dynamic response of a transducer. Flow problems and anomalies in the pressure versus time curve, such as overshoot and ringing, are immediately apparent.

Shock tube calibration of transducers has two disadvantages: first is the sensitivity to measurement errors presented in the tables above, and second is the difficulty of determining which point (to within 1%) on a signal such as figure 4.2-3 corresponds to the calculated pressure level.

4.3 THE STATIC PULSE CALIBRATOR

Figure 4.3-1 shows a simplified schematic describing the theory of the static pulse calibrator. Pressurized air is stored in a large tank. The air pressure level can be accurately measured with a static pressure gage.

The test transducer is connected to a 3-way, quick-acting valve that normally exposes the transducer to ambient atmospheric pressure. When the valve is actuated, the transducer is exposed to the pressure in the large tank. The valve is designed so that the volume change caused by exposing the transducer to tank pressure is negligible. Therefore, the transducer is exposed to a pressure step equal to the pressure level indicated by the tank static pressure gage.

Figure 4.3-2 is a photograph of a commercial static pulse calibrator. Unfortunately, the large tank is not visible in this photograph. The large tank is behind the wooden panel which holds the gages and controls. Figure 4.3-3 is a typical pressure versus time signal produced by the static pulse calibrator.

4.3 (Cont'd)

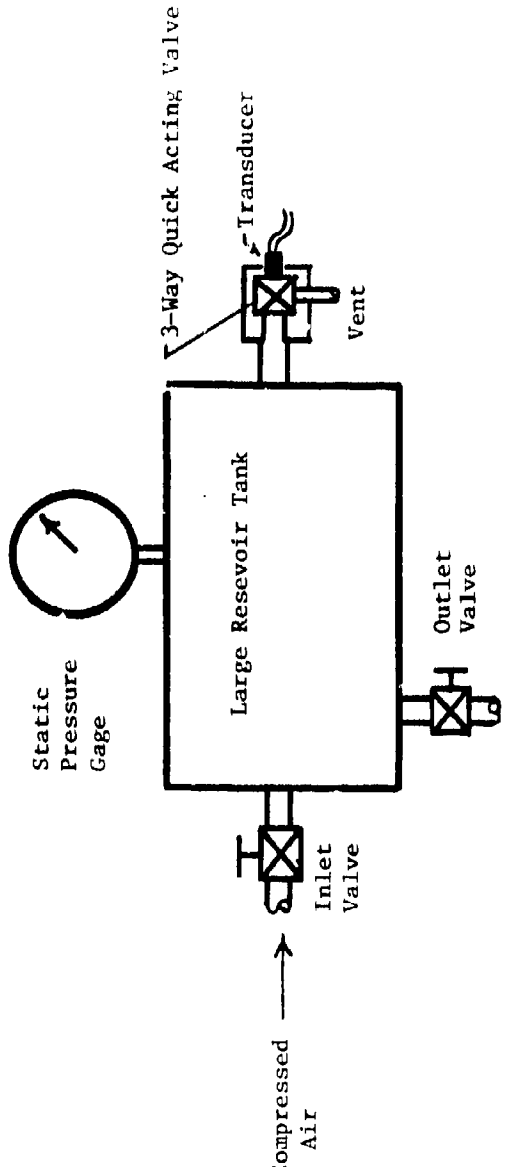

Figure 4.3-1. Simplified schematic diagram of static pulse calibrator.

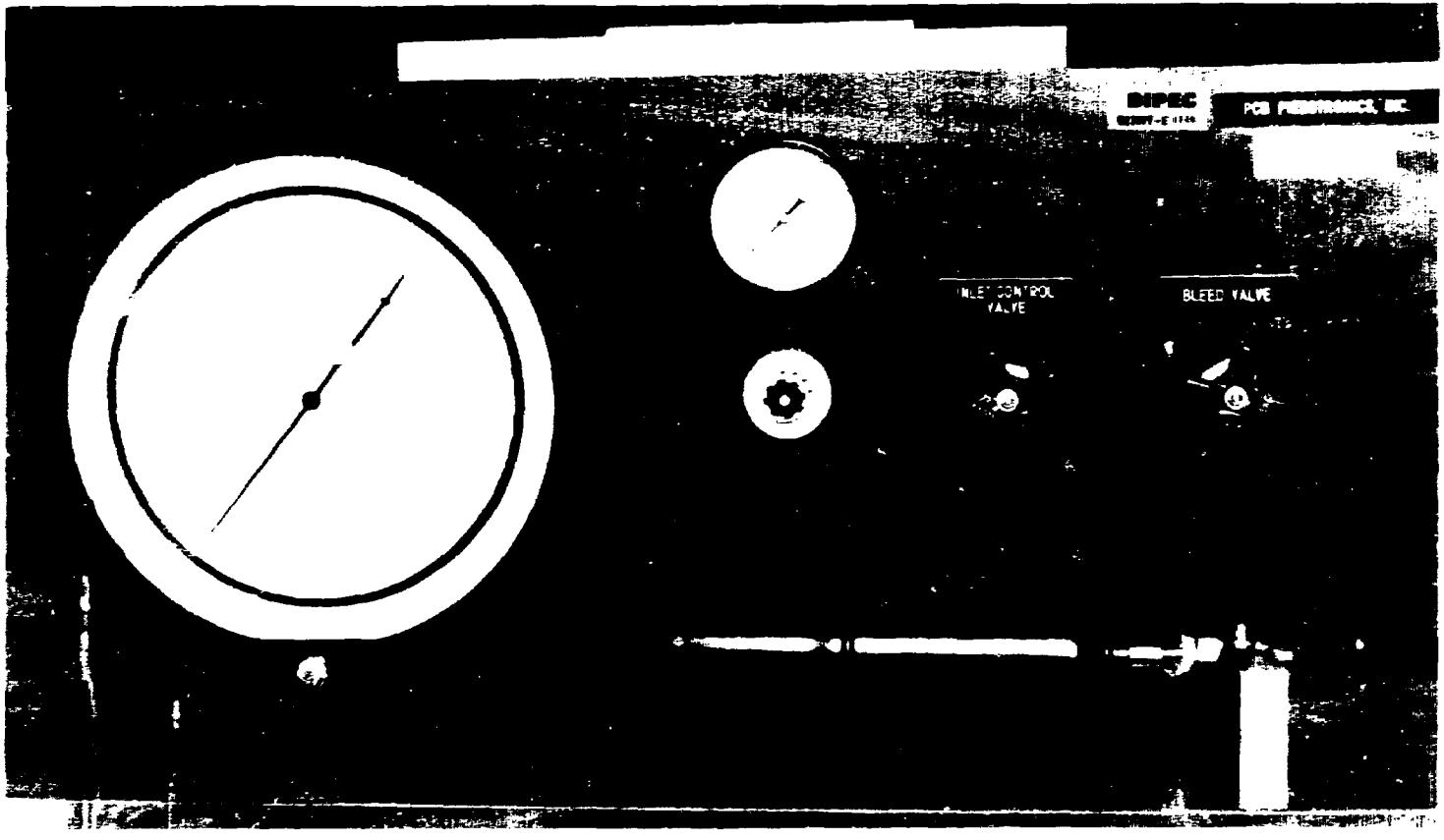
DIPEC
INLET CONTROL VALVE
BLEED VALVE

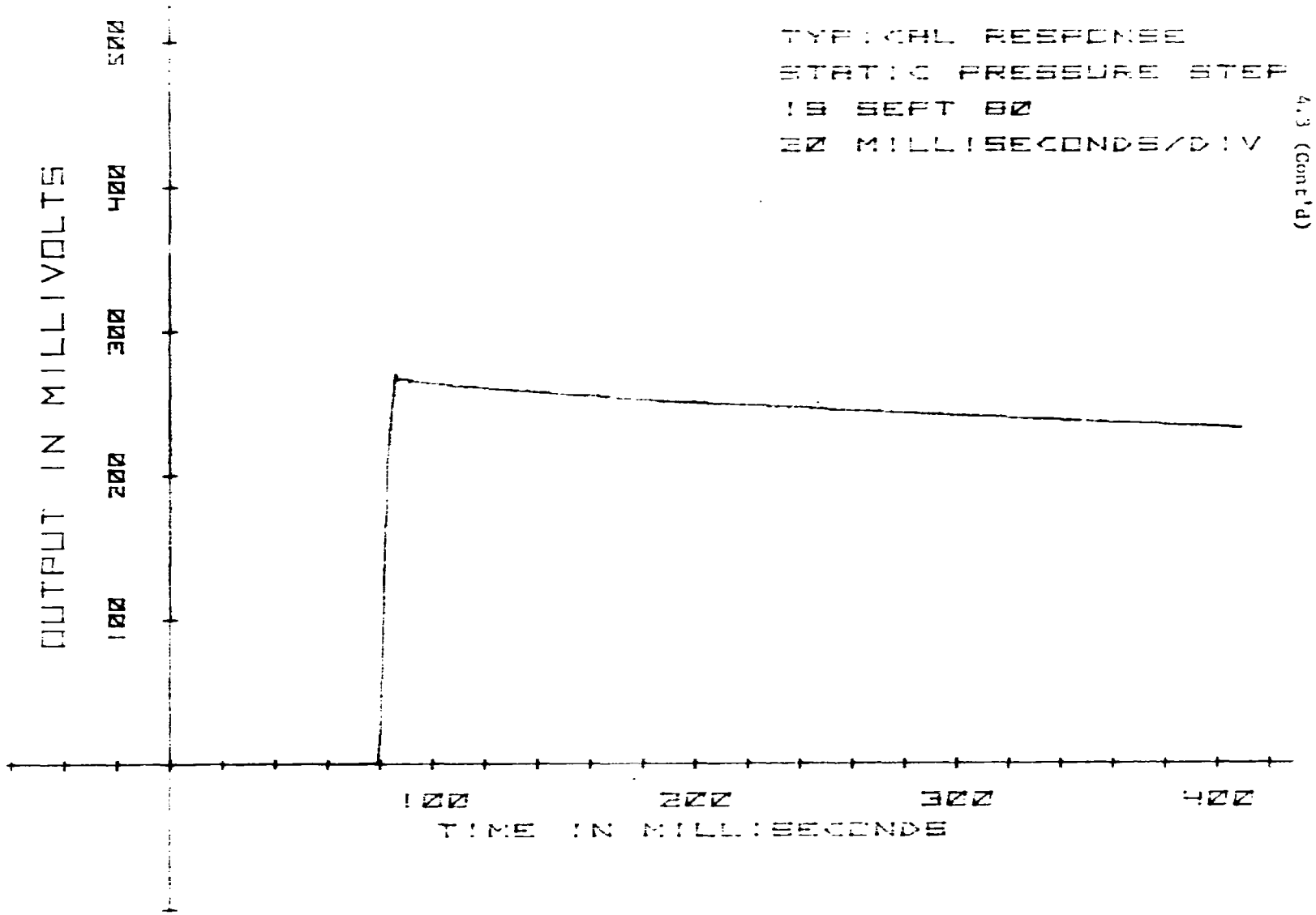

Figure 4.3-3. Typical plot of pressure versus time from the static pulse calibrator. Rise time is 76 milliseconds.

4.3 (Cont'd)

Measurement of the exact calibration pressure level is very accurate when using the static pulse calibrator. Unfortunately, acoustic resonance in the plumbing of the calibrator causes ringing in the transducer signal. This ringing makes it difficult to determine the exact output level of the transducer for a given pressure level.

The static pulse calibrator can be used to examine low frequency characteristics of transducers. Figure 4.3-4 shows the response of the Endevco gage to a static step. Because the Endevco gage has DC response, the correct step function is produced.

Note that the rise time shown in figure 4.3-4 is shorter than the rise time shown in figure 4.3-3. Rise times shorter than 5 milliseconds exhibit acoustic ringing in this particular static pulse calibrator. The speed with which the manually actuated 3-way valve is opened affects the rise time.

Figure 4.3-5 shows the response of the PCB gage to a static step. Note that because this gage is AC-coupled, the signal immediately begins an exponential decay. This exponential decay can be described by the period required to decay from peak value to 37% of that value. This period is known as the time constant of the gage.

The ST-2 gage has a much shorter time constant than the PCB gage. Figure 4.3-6 shows the response of the ST-2 gage to a static step. Note that the short time constant causes rapid decay. The rapid decay, combined with acoustic ringing, make accurate static pulse calibration of the ST-2 gage difficult.

Another problem introduced by the static pulse calibrator is the thermal effect of adiabatic compression. When the small volume of air in the quick-acting valve is compressed from ambient pressure to the calibration pressure level, the air is also heated. This same thermal effect is present when a shock wave compresses air; however, the duration of the compression caused by a shock wave is very short as opposed to the static calibration pulse, which is a steady state change.

The change in temperature caused by adiabatic compression is calculated as shown below:

$$\frac{T_1}{T_o} = \left(\frac{P_1}{P_o}\right)^{\frac{k-1}{k}}$$

4.3 (Cont'd)
where

T_o = Ambient temperature (absolute)

T_1 = Temperature after compression (absolute)

P_o = Ambient pressure (absolute)

P_1 = Pressure after compression (absolute)

k = 1.4 for air.

Air compressed from laboratory conditions of 1 atmosphere and 20° C to 1.5 atmospheres (an overpressure of 50.7 kPa = 7.35 psi) will experience a temperature increase of 36° C. Figure 4.3-7 shows how the thermal effect of adiabatic compression can be reduced by a layer of black electrical tape.

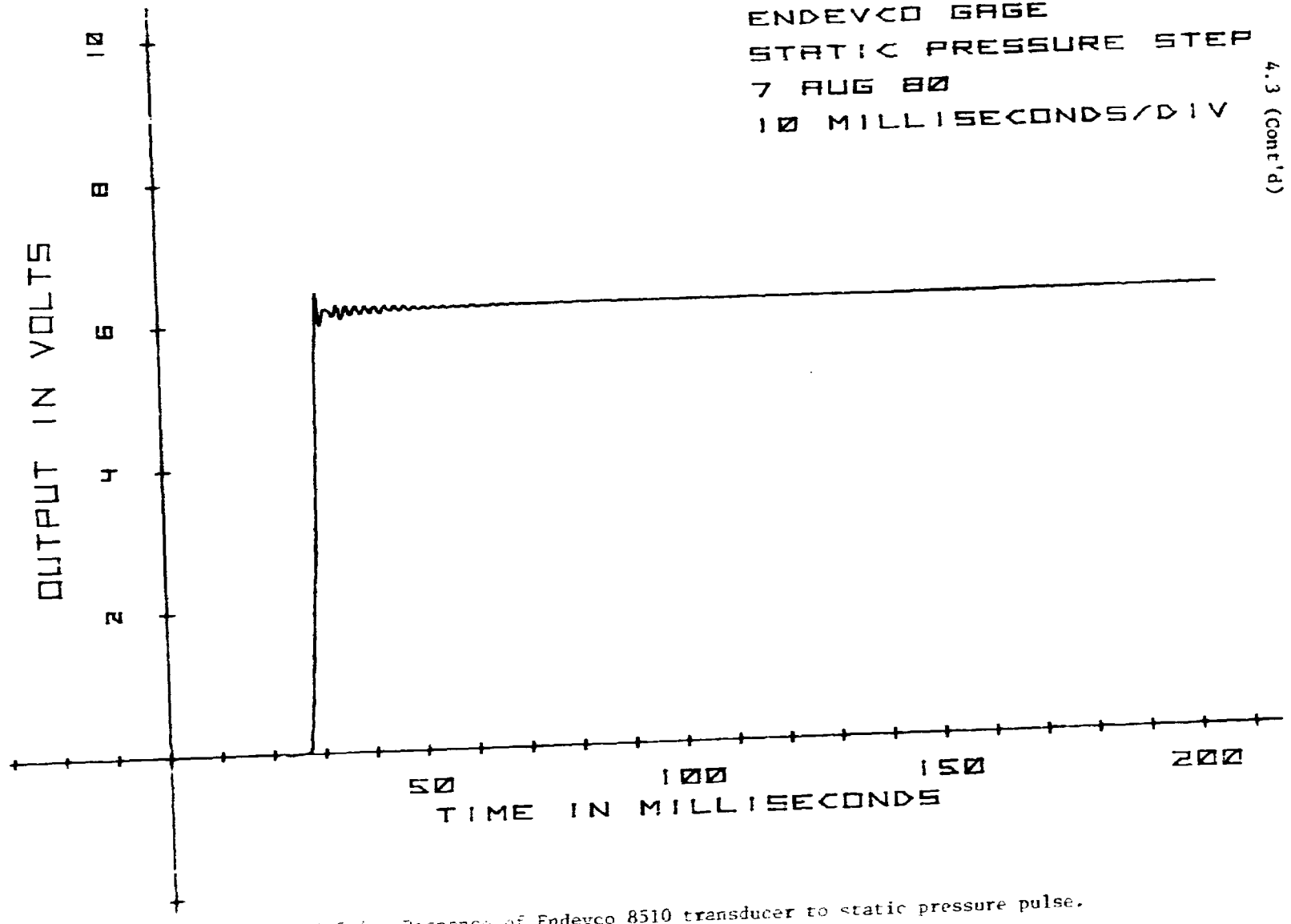

Figure 4.3-4. Response of Endevco 8510 transducer to static pressure pulse.

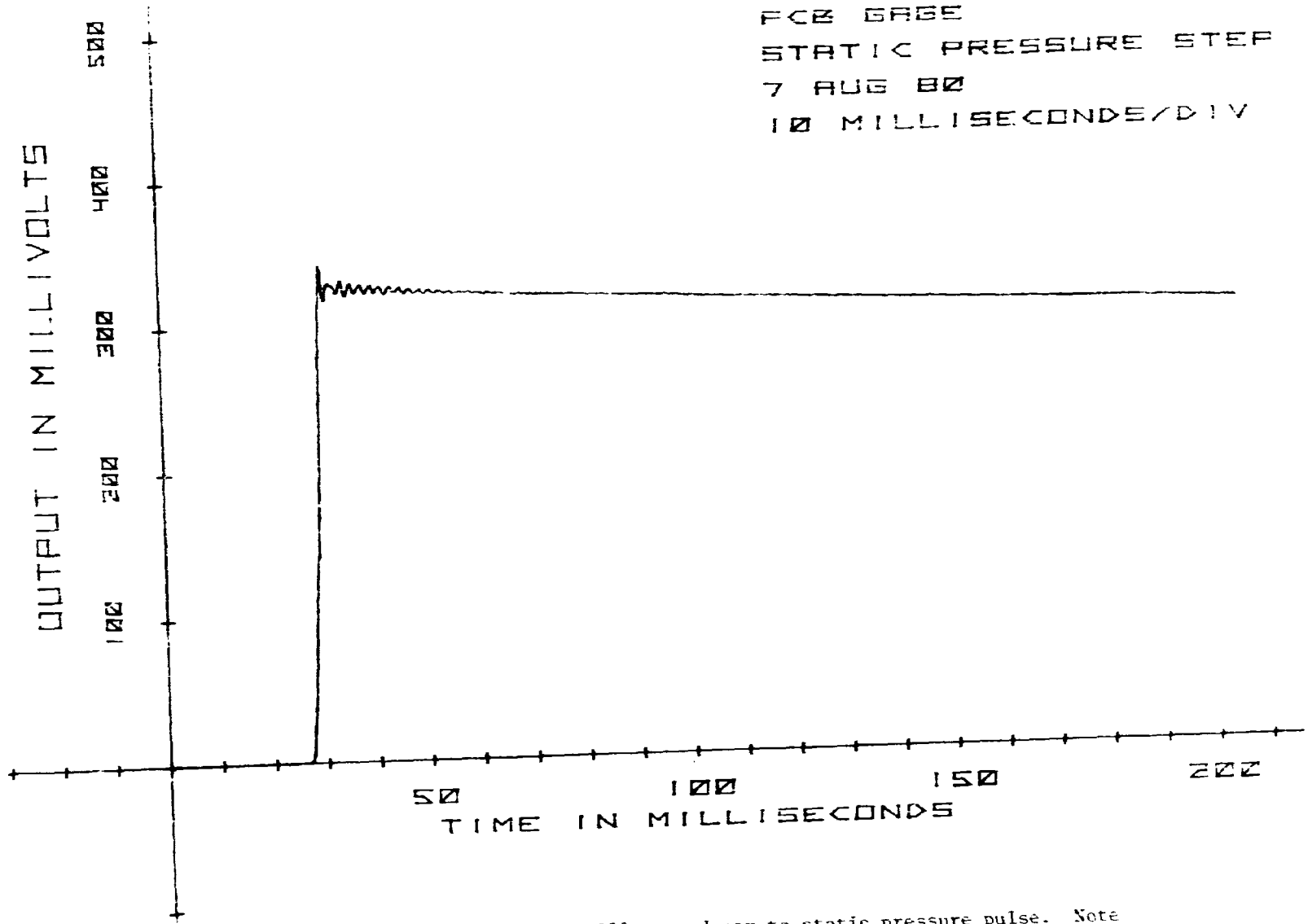

Figure 4.3-5. Response of PCB 113 transducer to static pressure pulse. Note slight decay caused by AC coupling.

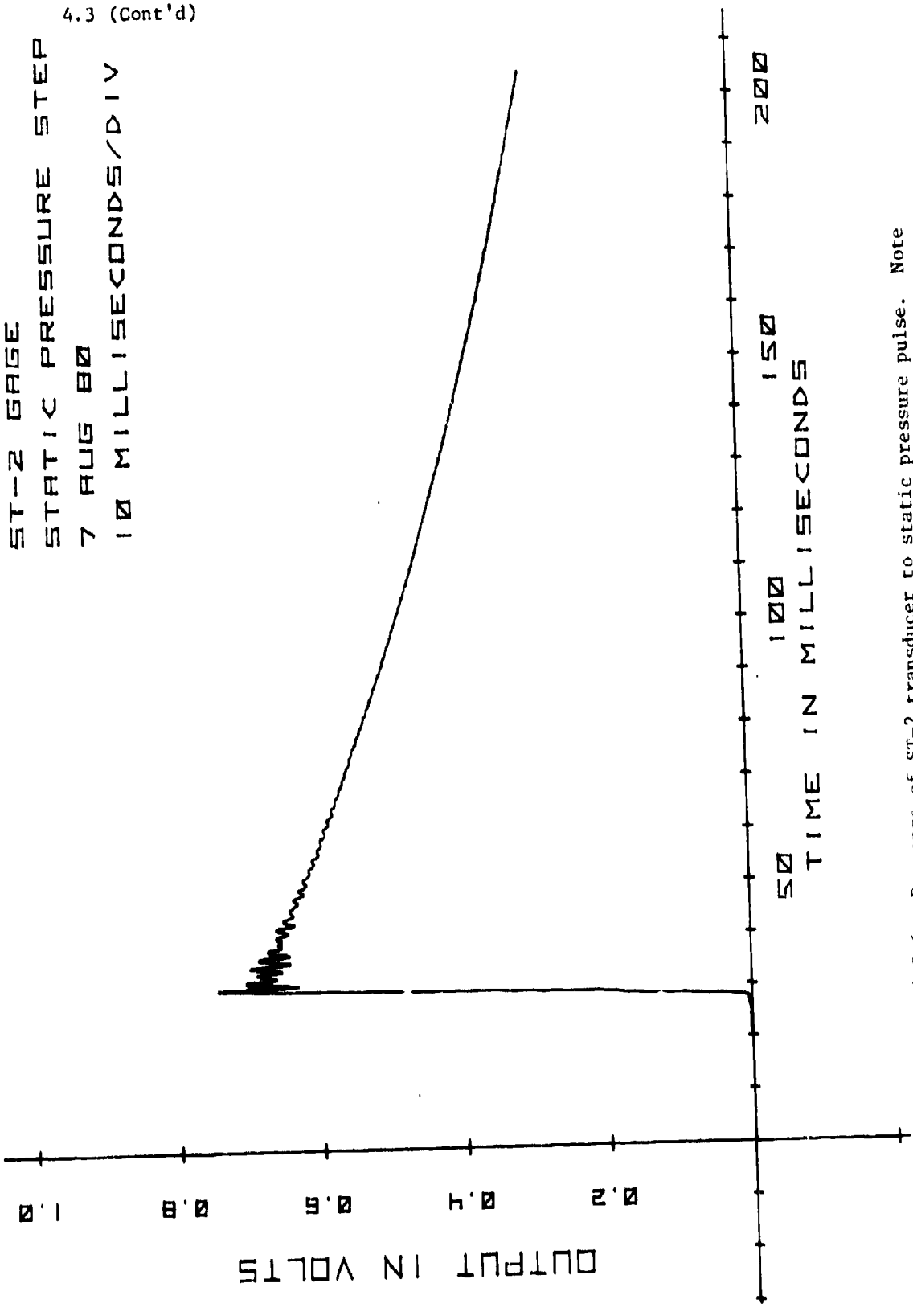

Figure 4.3-6. Response of ST-2 transducer to static pressure pulse. Note rapid decay caused by AC coupling with a short time constant.

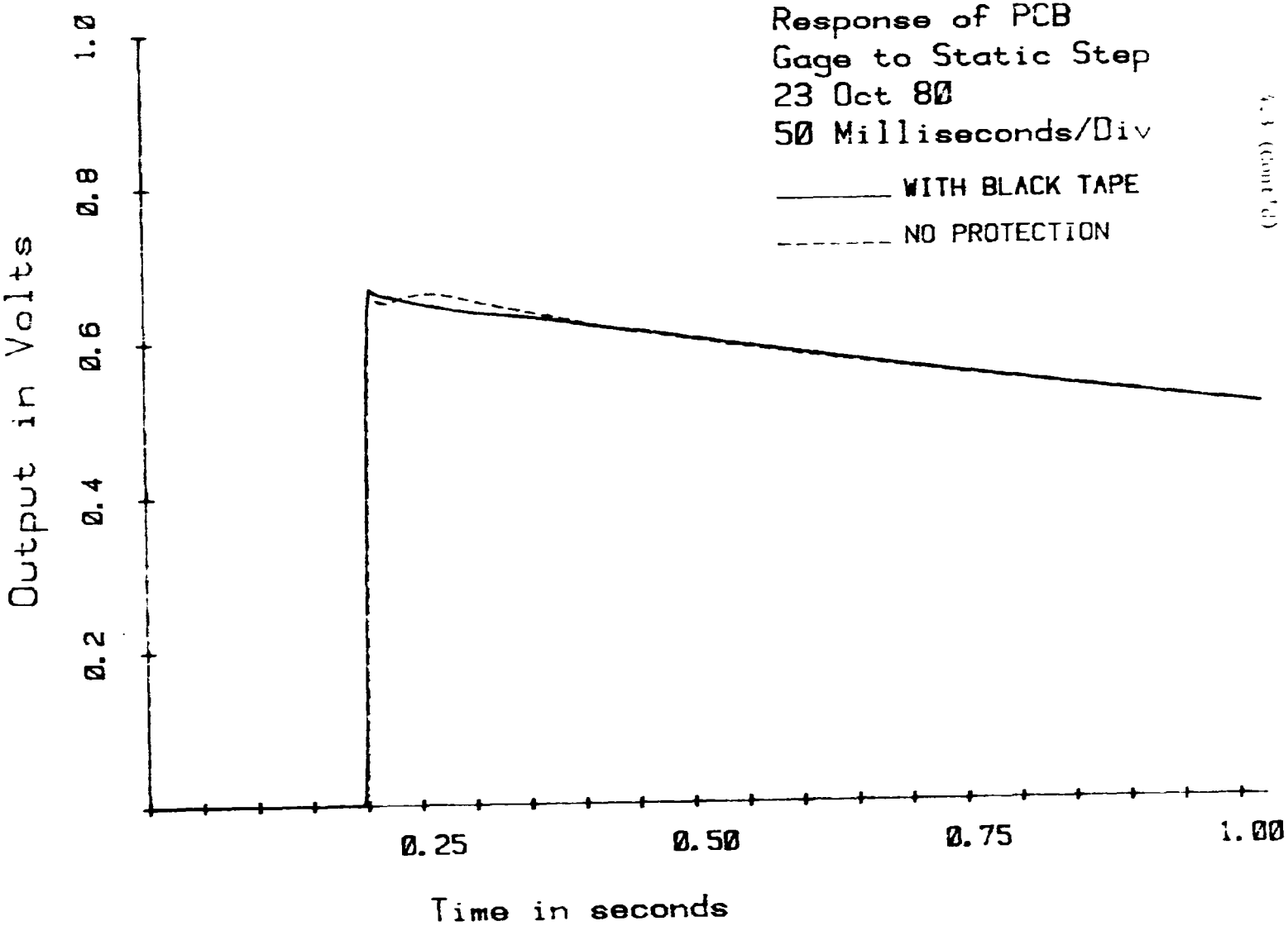

Figure 4.3-7. Reduction of thermal effects of adiabatic air compression by use of black electrical tape.

4.4 SINUSOIDAL PRESSURE CALIBRATION

Figure 4.4-1 is a simplified schematic diagram describing the operating principle of a commercial high-intensity microphone calibrator. This unit is essentially an enclosed loud speaker. An electrical sine wave input to the coil causes the piston to generate a sinusoidal pressure variation.

A calibrated resistor is used to monitor the input current to the coil and produces a calibrated electrical output that indicates the magnitude of the pressure that the transducers are sensing. Figure 4.4-2 is a photograph of the calibrator and a locally fabricated power unit. Figure 4.4-3 is a typical transducer output signal produced by the calibrator at 100 Hz.

Figure 4.4-4 shows the electrical schematic diagram of a power unit that was built to drive the calibrator. Its operation is described below. The letters in parentheses refer to the large capital letters in the diagram.

The power unit has three modes of operation:

I. Manual Mode: The signal from a 100 Hz oscillator (A) is adjusted by the "manual gain adjust" potentiometer and drives the power amplifier (B), which provides up to 1.5 amps required to drive the calibrator.

II. External Mode: The signal from an external oscillator drives a variable gain amplifier (C), which drives the power amplifier (B).

III. Self Adjust Mode: The calibrator provides an accurate monitor voltage at the "voltmeter jack" which is proportional to pressure (20 Pa = 1 mV). The power unit shown in Figure 4.4-2 has been adjusted to maintain 121.9 mV RMS at the "voltmeter" jack which corresponds to 2.44 kPa RMS or 1 psi peak-to-peak.

The AC signal from the "voltmeter" jack is converted to a DC voltage (D). This voltage is compared to the desired reference level by a servo amplifier. Any resulting error signal drives an integrator (E). The integrator controls the gain of a 100 Hz sine wave by use of a multiplier (F), which in turn, drives the power amplifier (B).

When used in the "Self Adjust Mode," the proportional feedback servo system is underdamped (i.e., it has overshoot). The output settles to within 1% tolerance of the desired value in 1 cycle, which is approximately 4 seconds long.

4.4 (Cont'd)

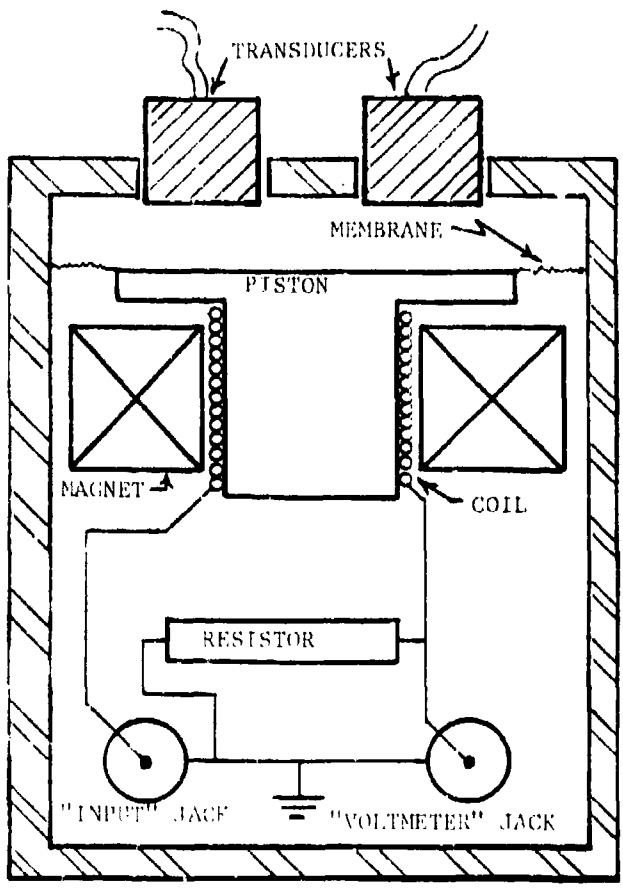

Figure 4.4-1. Simplified schematic of sine wave calibrator.

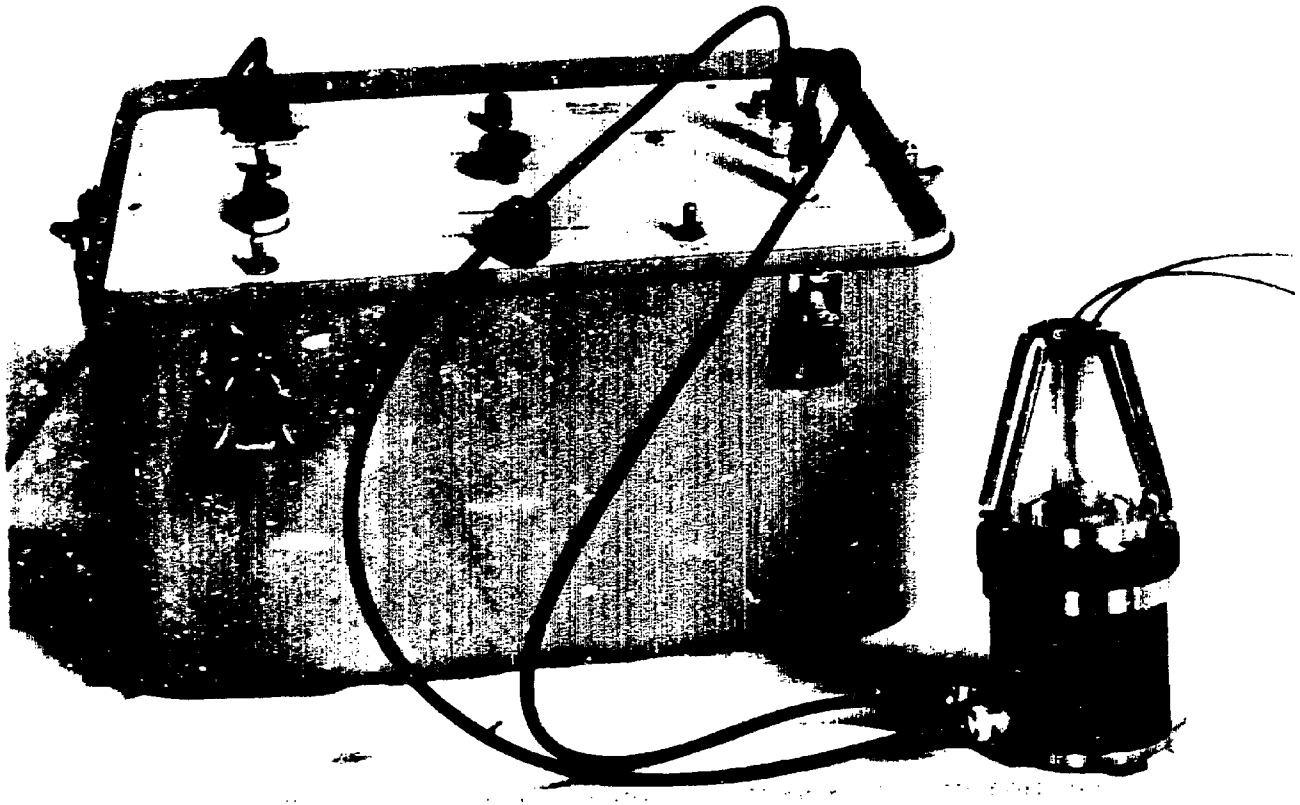

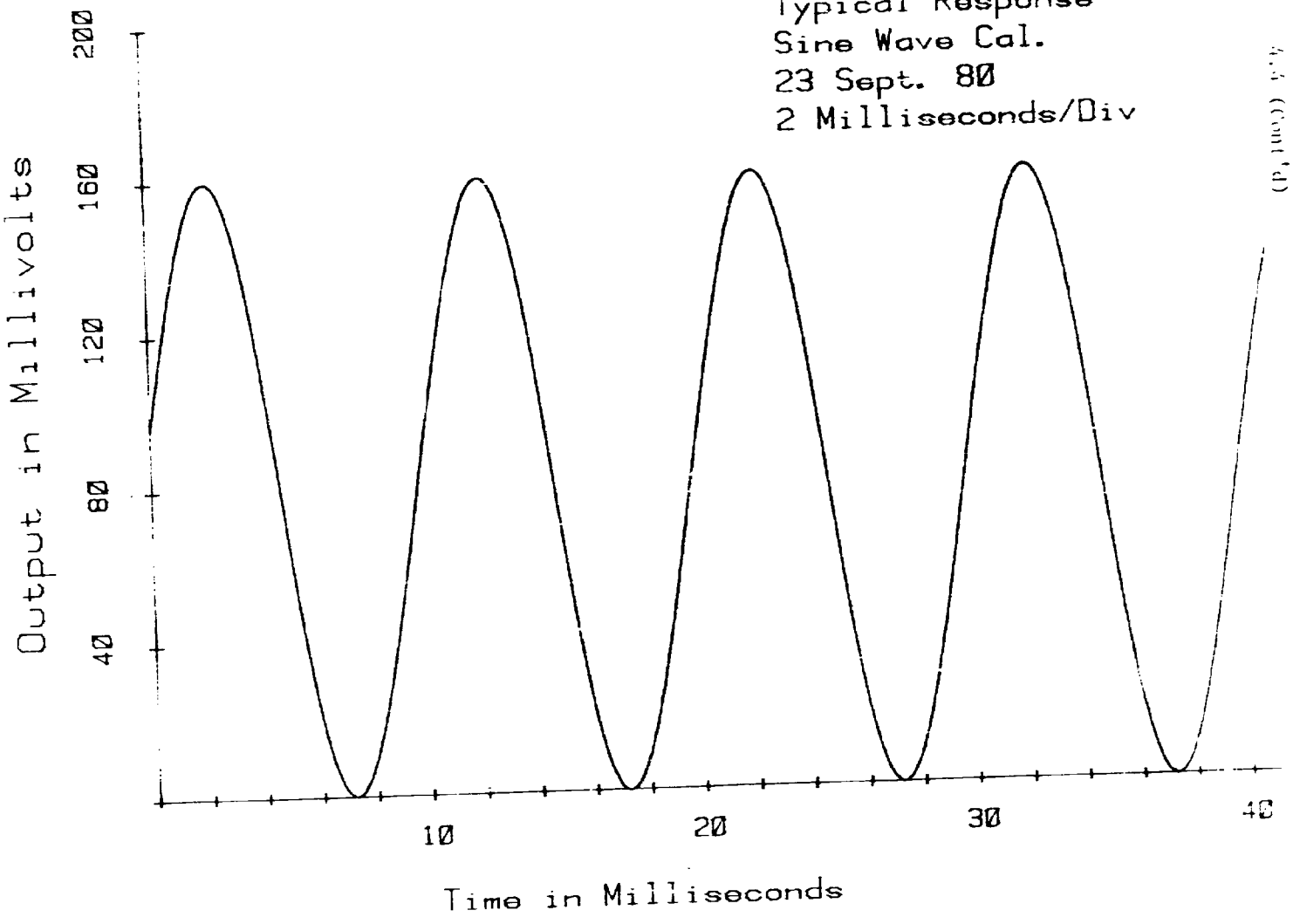

Figure 4.4-3. Typical output signal of a transducer in the sine wave calibrator.

4.4 (Cont'd)

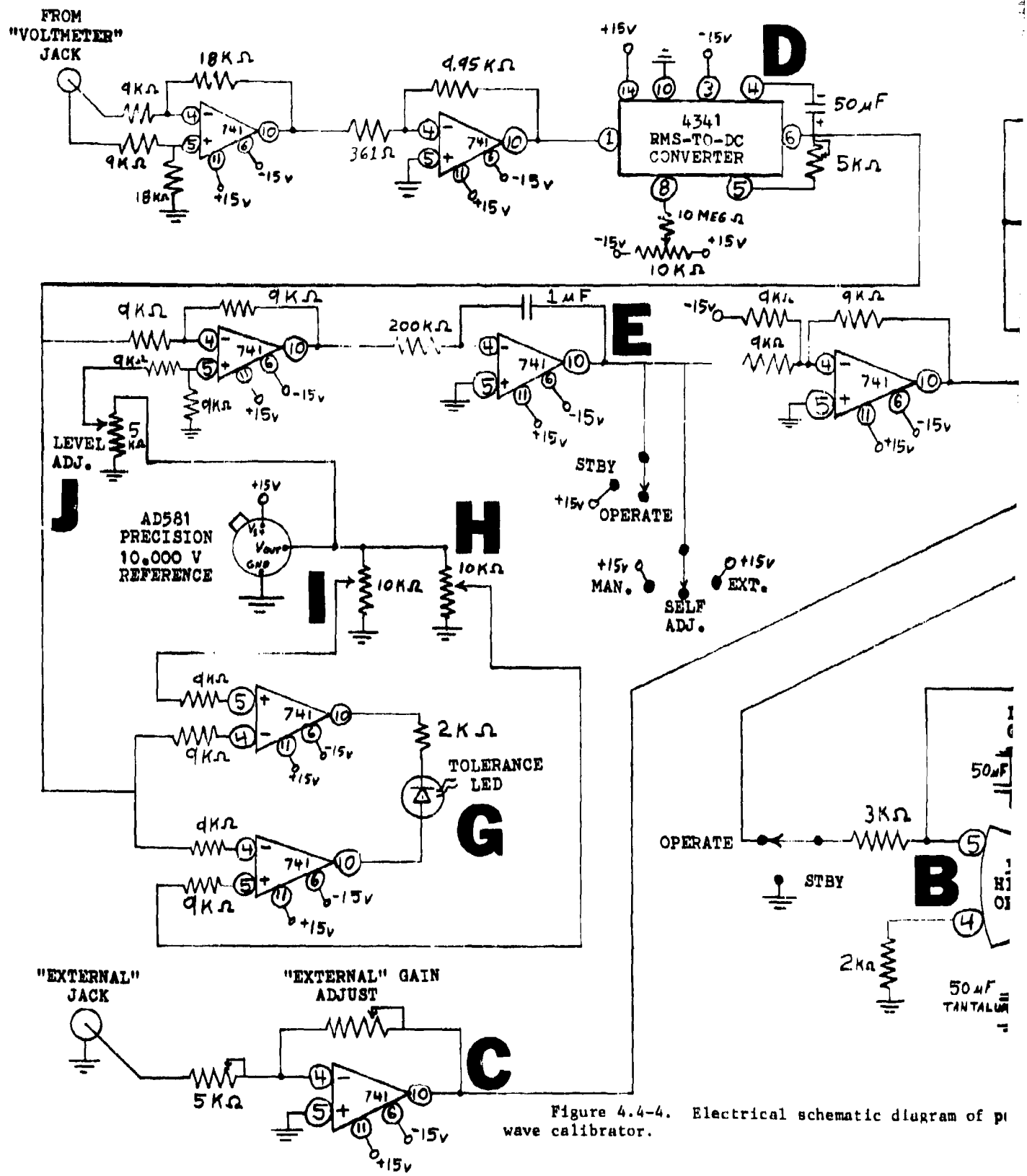

Figure 4.4-4. Electrical schematic diagram of pu
wave calibrator.

(Page 110 Blank)

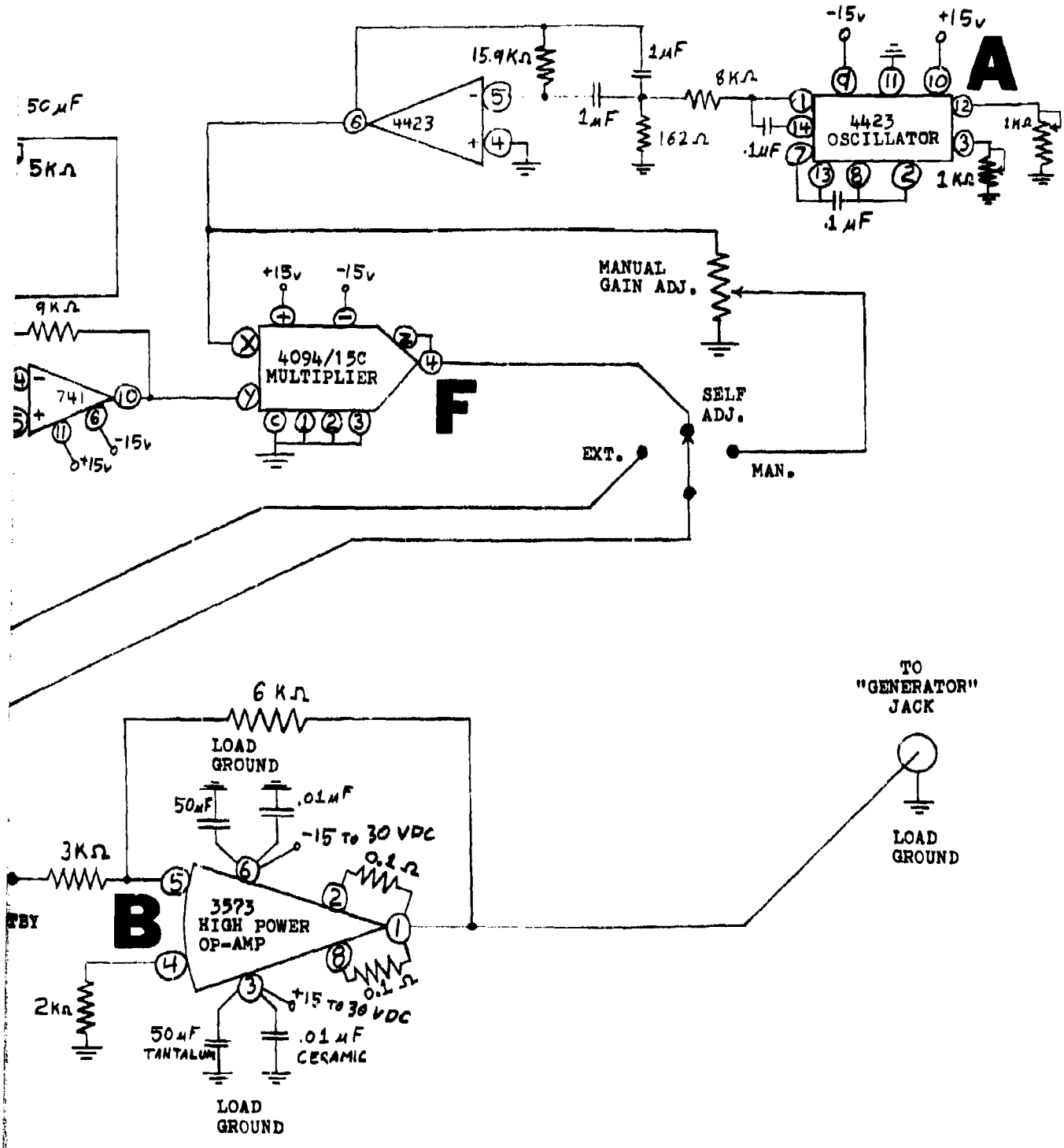

hematic diagram of power unit for sine

A tolerance LED (G) is illuminated when the "voltmeter" signal is within 1% of the desired level. The upper tolerance potentiometer (H) and lower tolerance potentiometer (I) must be periodically checked and adjusted to perform this function. The level adjust potentiometer (J) should be adjusted if the desired pressure level is not being maintained.

Any time it is necessary to monitor the signal at the "voltmeter" jack, a voltmeter completely isolated from ground must be used. Otherwise, ground loops will cause a variation in the pressure level generated, and the relationship between pressure and voltage (20 Pa = 1 mV) will no longer be valid.

The transducer signal produced during sine wave calibration can be accurately read with a voltmeter or digital transient recorder. The calibrator is portable, so on-site calibration can be performed. Because calibration is performed well above the low-frequency rolloff point, the time constant of AC-coupled transducers does not affect calibration.

The fact that sine wave calibration is conducted at a relatively low level (2.4 kPa RMS) introduces several problems. This level is often at or below the low amplitude limit of the transducer's pressure range, which means the signal to noise ratio may be small.

Transducer nonlinearity becomes a problem at low pressure levels. A transducer with a full scale range of 500 kPa for example, could have a linearity error of 2.5 kPa at its low range. This error represents an error of only 0.5% of full scale, but represents an error of 50% to 100% of the reading at the low range used in sine wave calibration.

It has also been discovered that the small piece of electrical tape used for thermal protection of the transducer can cause errors in low level sine wave calibration. This is particularly true if the tape is old and not sticking well.

4.5 PENTOLITE CALIBRATION

Figure 4.5-1 shows a 454-gram (1-lb) bare spherical charge of pentolite being prepared for detonation. Goodman has presented (in ref 7) an empirically fit equation to predict the peak pressure level produced by a given charge of pentolite at a given distance. Figure 4.5-2 shows the variation of peak pressure and the author's conversion of Goodman's equation into SI units.

Figure 4.5-3 shows a typical plot of pressure versus time from a pentolite explosion. On very rare occasions, strange waveforms, such as the signal shown in figure 4.5-4 are produced. In almost 400 observations, strange waveforms like the one shown were observed three times.

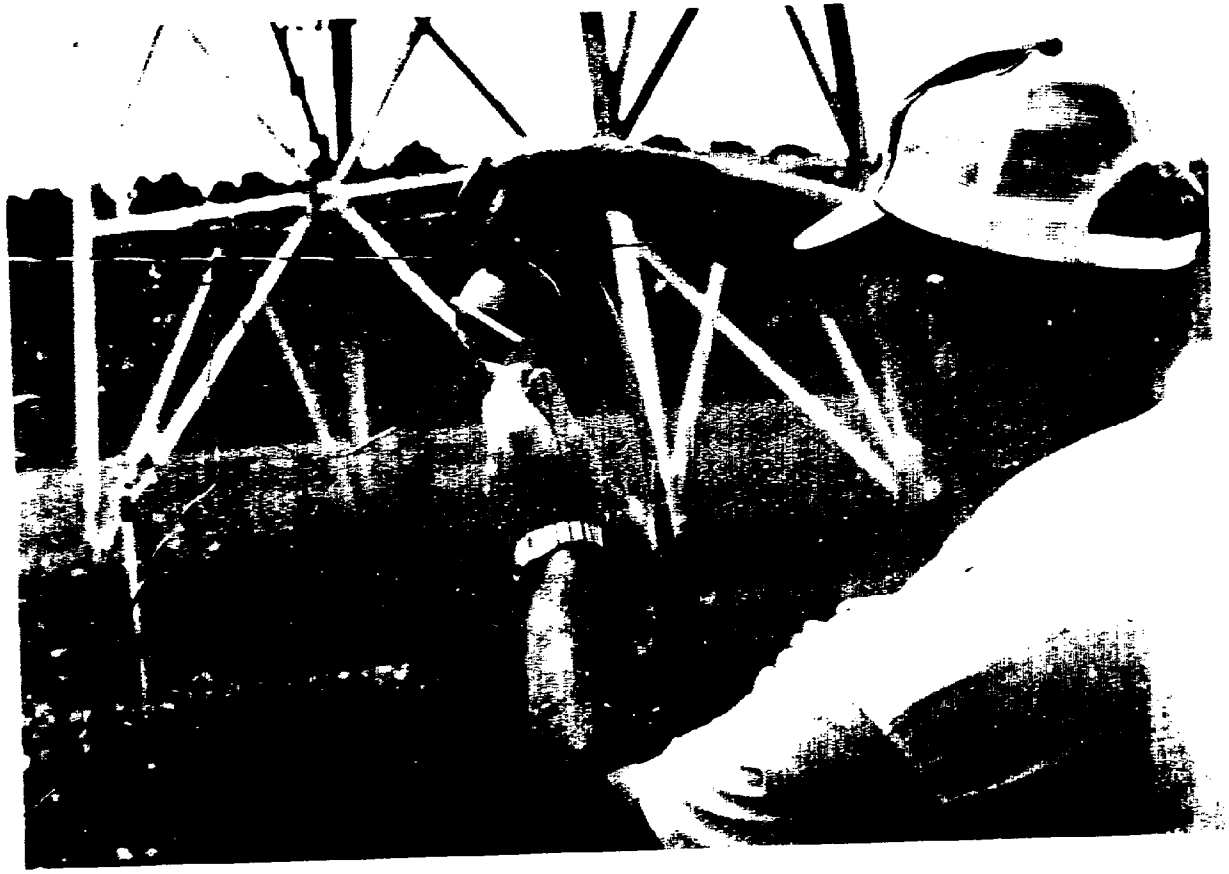

Figure 4.5-1. Bare spherical charge of pentolite (454 gram = 1 lb) being prepared for detonation by explosives technician.

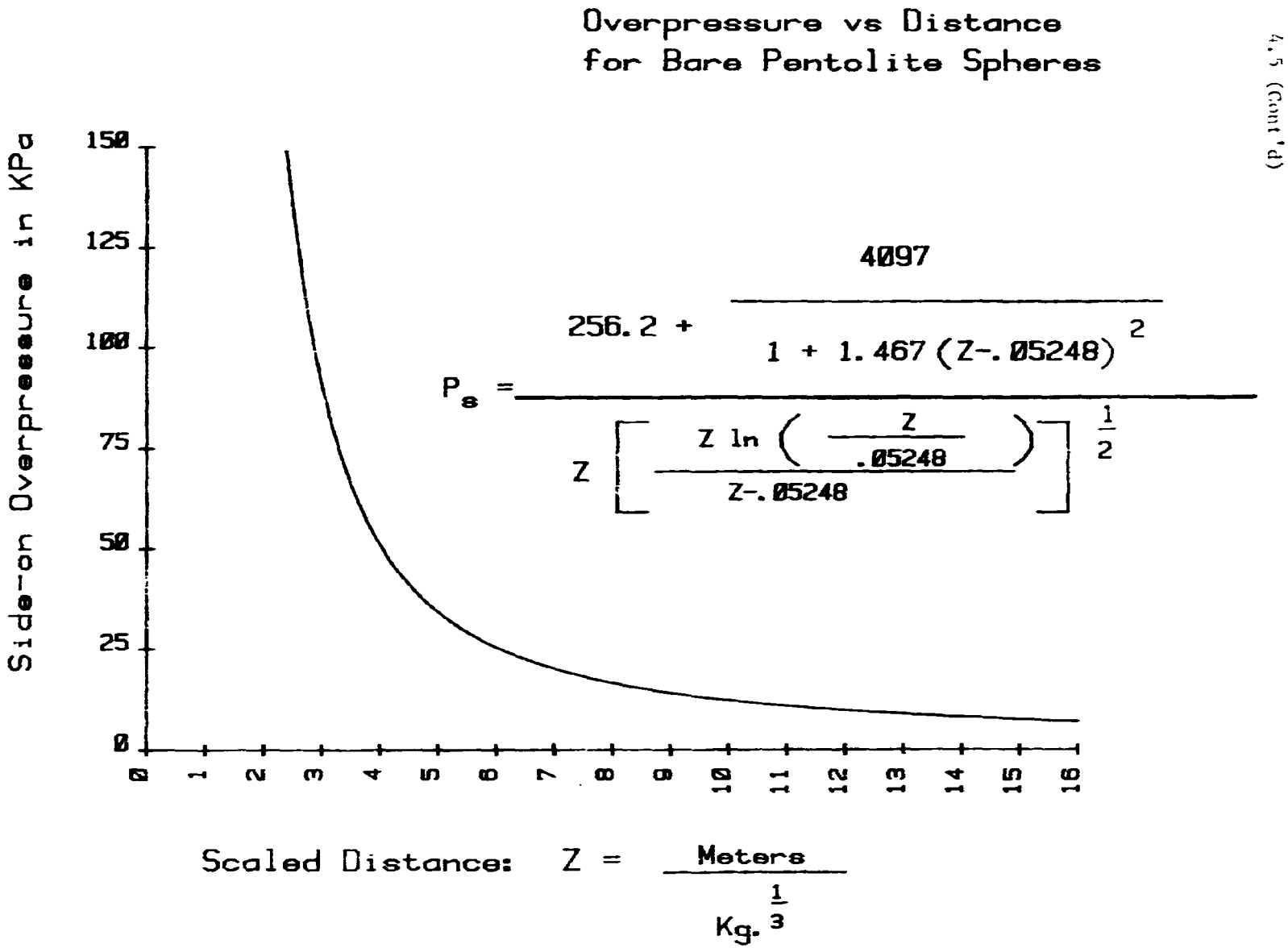

Figure 4.5-2. Relationship for peak side-on pressure generated by pentolite from Goodman (ref 7), converted to SI units by author.

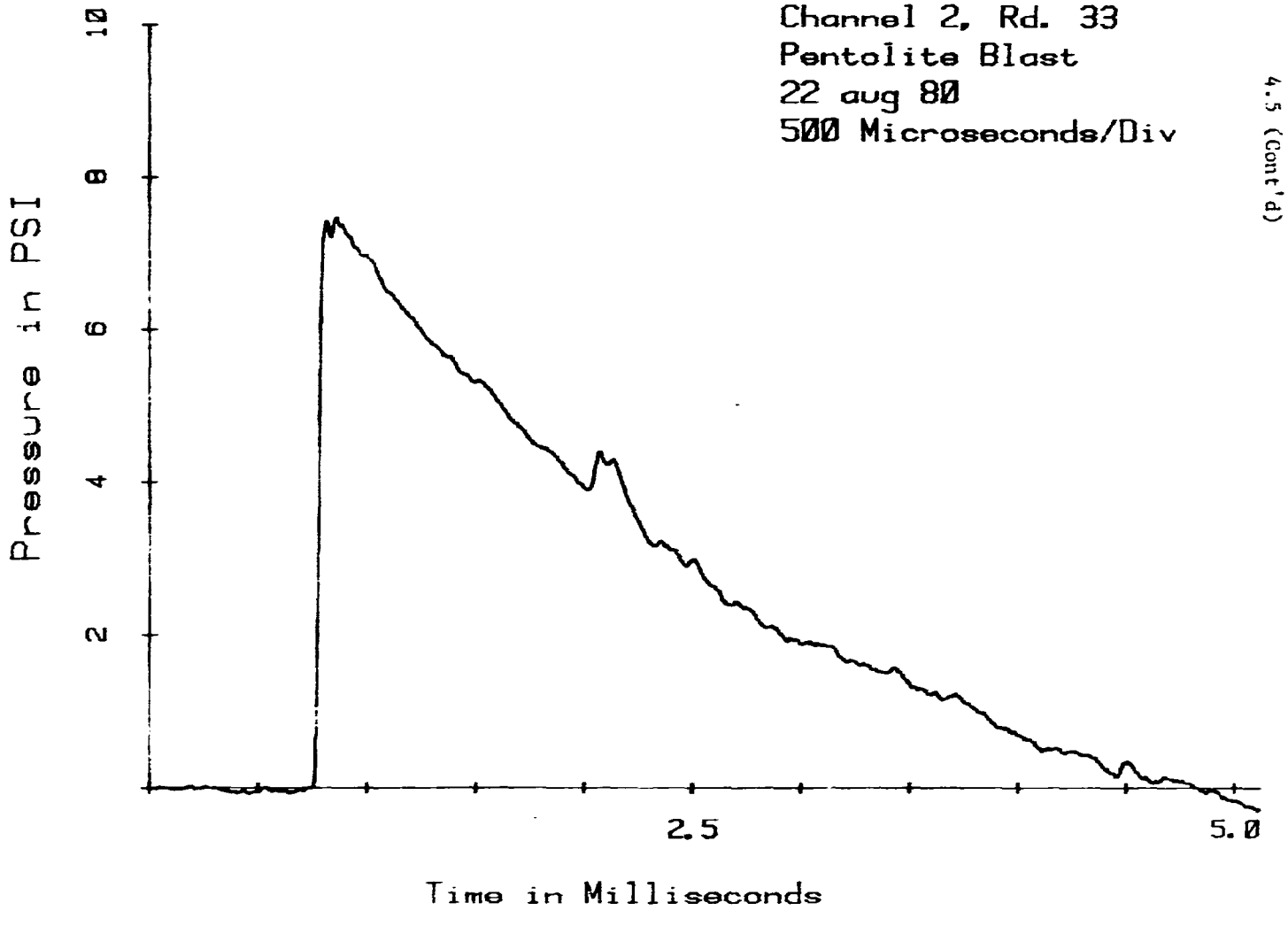

Figure 4.5-3. Typical plot pressure versus time produced from pentolite free air explosion on more occasions.

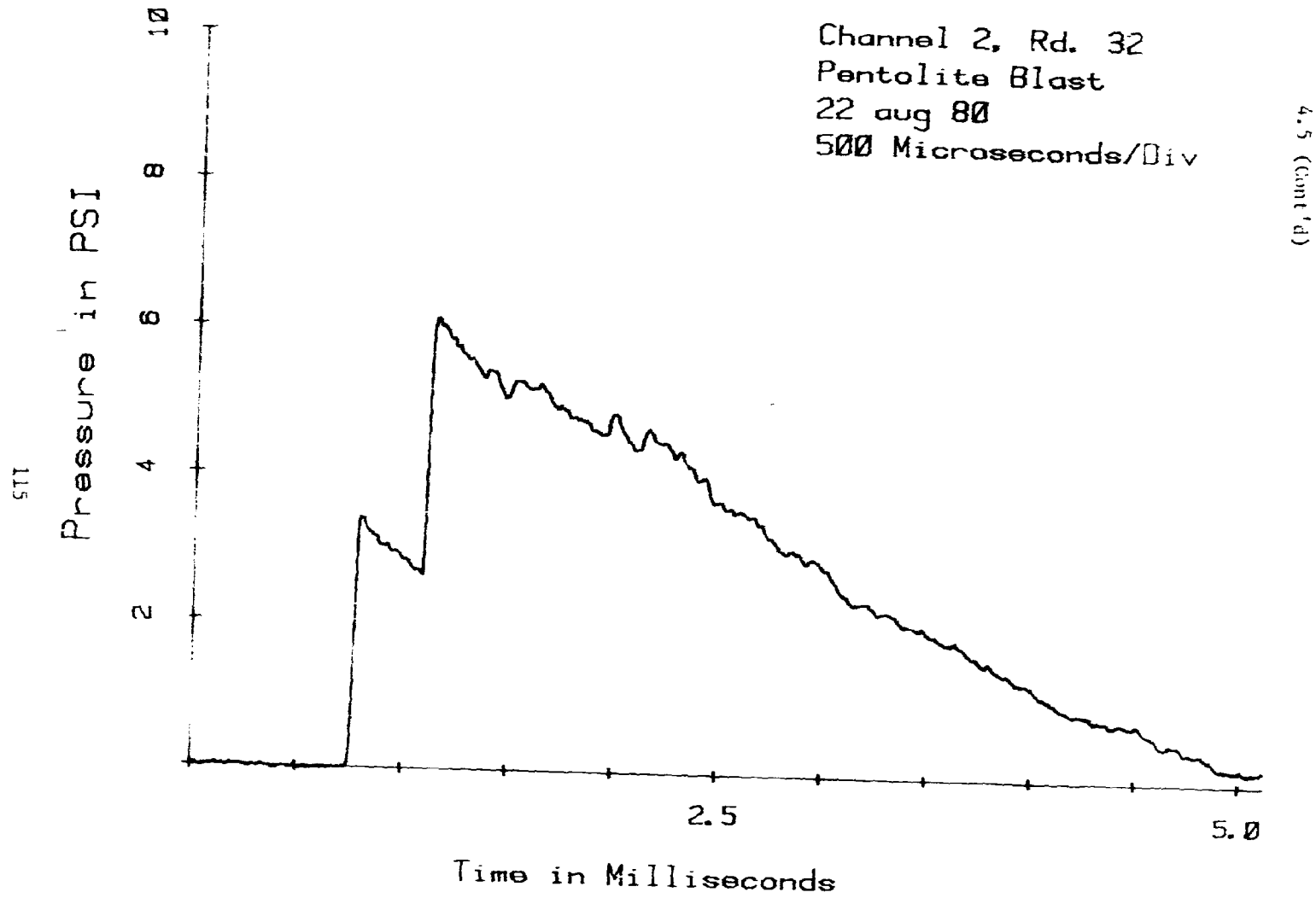

Figure 4.5-4. Nontypical plot pressure versus time produced from pentolite free air explosion.

4.5 (Cont'd)

Table 4.5-1 shows typical shot-to-shot variation obtained with pentolite. Note that at low pressure levels, the variation of arrival times correlates well with the variation of indicated pressure. At higher pressure levels, however, variations in arrival time do not correlate with variations in indicated pressure. Section 4.7 will address discrepancies between the indicated pressure levels and those calculated from Goodman's equation.

TABLE 4.5-1. PEAK PRESSURES AND ARRIVAL TIMES OBSERVED FROM DETONATION OF 479 GRAM PENTOLITE SPHERES

Distance (m)	Peak Pressure (kPa)	Arrival Time (ms)
5.42	22.1	10.55
5.42	21.7	10.61
5.42	21.2	10.69
5.42	22.1	10.46
4.39	29.3	7.900
4.39	29.9	7.906
4.39	29.9	7.931
4.39	30.7	7.769
3.19	48.5	4.906
3.19	49.4	4.806
3.19	48.2	4.900
3.19	49.2	4.763
2.64	68.6	3.500
2.64	67.2	3.575
2.64	67.1	3.531
2.64	63.7	3.481
2.17	97.2	2.416
2.17	98.6	2.581
2.17	99.3	2.556
2.17	104.8	2.556

4.6 COMPARISON OF LABORATORY CALIBRATION TECHNIQUES

Three of the calibration techniques previously discussed can be performed in the laboratory: Shock Tube, Sine Wave, and Static Pulse. Table 4.6-1 shows the results of these three different techniques on 10 ST-2 gages.

Since any one of these techniques could be used alone to calibrate a transducer, it is disappointing to see such large discrepancies between the various techniques. Although three of the gages produced quite consistent readings, the mean extreme spread observed was 4.8%.

Table 4.6-2 shows before fire and after fire calibration data from seven PCB gages and eight other transducers. The mean extreme spread observed was 4.5%.

These two tables lead one to the disappointing conclusion that laboratory tests are seldom more accurate than 5%. Hand-picking transducers can improve this accuracy.

Laboratory tests are conducted in much more favorable conditions than field tests. Ambient temperature change, long cables, acceleration of stands, rain, mud, etc., can all be expected to cause errors that are added to the 5% calibration error.

TABLE 4.6-1. COMPARISON OF VARIOUS LABORATORY CALIBRATIONS OF 10 DIFFERENT ST-2 GAGES. SENSITIVITY OF TRANSDUCERS EXPRESSED IN MV/KPA

GAGE SERIAL NO.	STATIC PULSE	SINE WAVE	SHOCK TUBE	MEAN	EXTREME SPREAD (%)
1481	20.7	20.5	20.7	20.6	1.0%
2104	16.4	15.8	16.7	16.3	5.5%
2262	17.4	16.9	17.1	17.1	2.9%
1262	25.8	23.6	25.3	24.9	8.8%
2267	20.7	20.3	21.8	20.9	7.2%
2106	15.3	15.0	16.1	15.5	7.1%
2103	21.3	21.0	21.1	21.1	1.4%
2093	15.1	14.9	16.3	15.4	9.1%
2094	16.6	16.2	16.7	16.5	3.0%
2091	16.1	15.8	15.8	15.9	1.9%

TABLE 4.6-2. COMPARISON OF BEFORE AND AFTER FIRE CALIBRATION DATA FOR A VARIETY OF TRANSDUCERS. SENSITIVITY OF TRANSDUCERS EXPRESSED IN MV/KPA

GAGE TYPE & SERIAL #	BEFORE FIRE CALIBRATION 13-19 AUG STATIC PULSE	SINE WAVE	SHOCK TUBE	AFTER FIRE CALIBRATION 25-29AUG STATIC PULSE	SINE WAVE	SHOCK TUBE	MEAN	EXTREME SPREAD (%)
PCB # 2174	9.51	9.54	-	9.46	9.70	9.53	9.55	2.5
PCB # 2178	10.08	9.96	-	10.05	10.21	9.86	10.03	3.5
PCB # 2179	7.41	7.51	7.69	7.30	7.09	7.30	7.38	8.1
PCB # 2180	8.57	8.67	8.61	8.60	8.50	8.54	8.58	2.0
PCB # 2181	8.64	8.66	8.48	8.47	8.64	8.92	8.64	5.2
PCB # 2182	8.03	8.18	8.03	7.88	7.92	7.96	8.00	3.8
PCB # 2184	7.11	7.22	7.11	6.95	7.22	6.90	7.09	4.5
ST-2 # 1481	19.9	20.0	19.7	20.7	20.0	19.4	20.0	6.5
ST-2 # 1482	19.7	20.2	18.6	20.0	19.4	18.6	19.4	8.2
LC-33 # 99	400	-	387	-	-	-	394	3.3
LC-33 # 104	435	-	420	-	-	-	428	3.5
LC-33 # 667	417	-	407	-	-	-	412	2.4
LC-70 # 737	15.8	15.8	14.5	-	-	-	15.4	8.4
LC-70 # 719	15.5	16.2	15.5	-	-	-	15.7	4.5
Endevco # EG-56	57.4	58.0	-	-	-	-	57.7	1.0

4.7 COMPARISON OF PENTOLITE CALIBRATION WITH LABORATORY CALIBRATION

Many different transducers were calibrated in the laboratory, using the shock tube, sine wave calibration, and static pulse calibration. These transducers were then placed in a pentolite blast field to measure peak pressure.

Blast wave velocity was also measured, as well as ambient temperature and pressure. The velocity measurements and the Rankine-Hugoniot Equation were used to calculate peak pressure levels.

Two types of probes were used to make velocity measurements. One probe had three PCB transducers with 30.48-cm (1-ft) spacings. The other probe used two LC-70 transducers 45.72 cm (18 in.) apart. Figures 4.7-1 and 4.7-2 show the probe which used LC-70 transducers.

Table 4.7-1 presents the results, comparing the transducer measurements, velocity measurements, and calculation of peak pressure from Goodman's equation (ref 7). Note that at low pressure levels (20 kPa), the transducer measurements indicate peak pressures roughly 10% higher than the calculated peak pressures. The velocity measurements also indicate higher peak pressure levels than the equation predicts. At higher pressure levels (70 kPa and 100 kPa), agreement is much better.

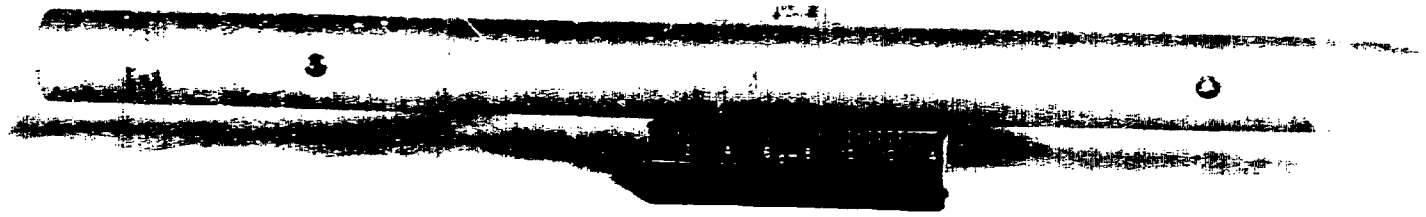

Figure 4.7-1. Probe used for making velocity measurements. Two L5-70 transducers spaced 47.72 cm (18.9 in.) apart.

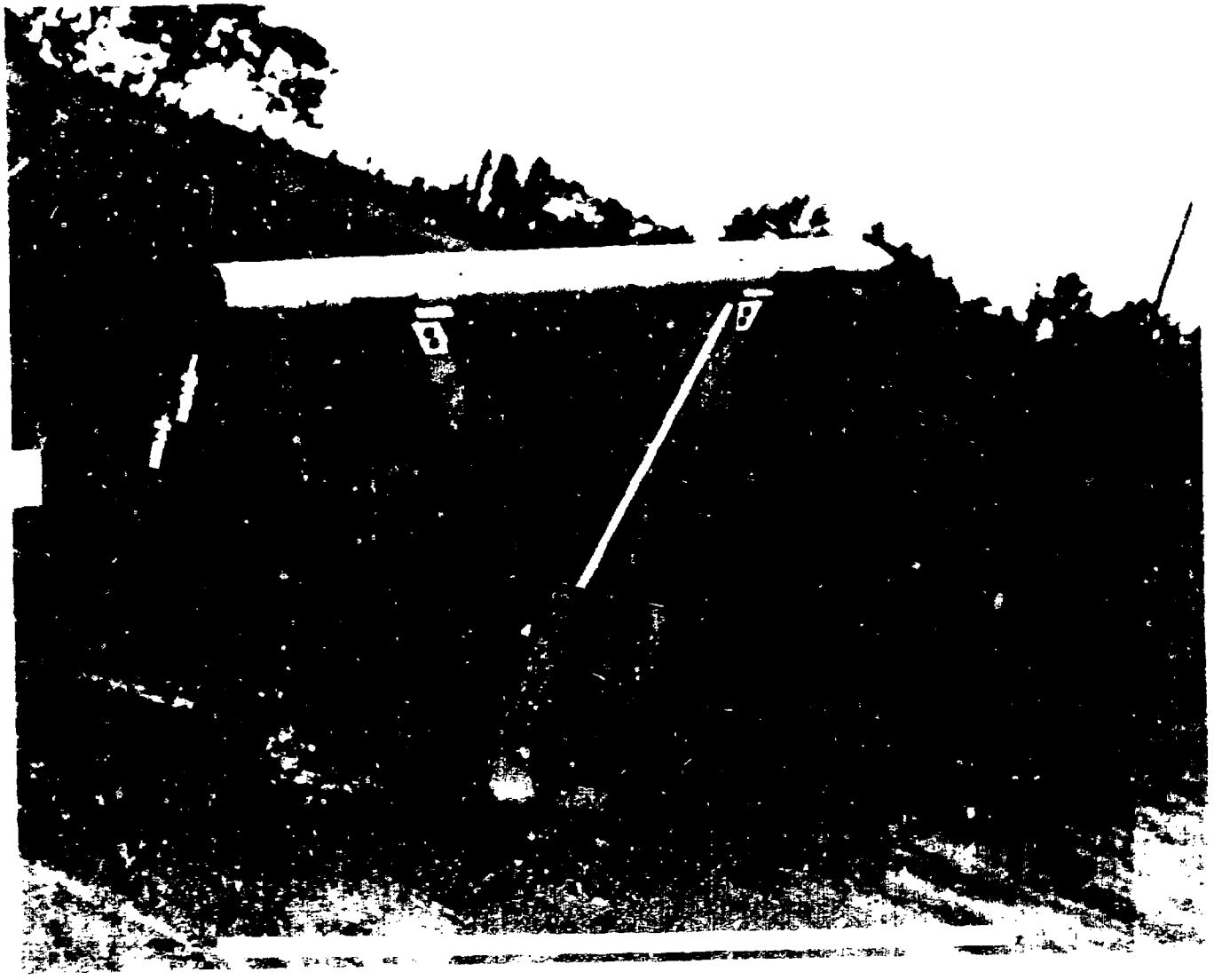

TABLE 4.7-1. COMPARISON OF PRESSURE AND VELOCITY MEASUREMENTS WITH PREDICTIONS FROM GOODMAN'S EQUATION FOR PENTOLITE EXPLOSIONS. BARE SPHERICAL CHARGES WEIGHING 479 GRAMS WERE USED.

MEASUREMENTS MADE AT A NOMINAL 20 KPa LEVEL

N	CH	SCALED DISTANCE (M/Kg 1/3)	THEO PK (KPa)	MEAS MEAN PK PRESS (KPa)	% ERROR	
4	ST-2 1	7.23	19.2	23.4	21.9	DIRECT PRESSURE MEASUREMENTS
5	ST-2 2	7.23	19.2	21.3	10.9	
5	PCB 3	7.05	19.9	21.7	9.0	
5	PCB 4	7.03	20.0	20.1	.5	
5	LC-33 5	7.09	19.8	20.8	5.1	$\bar{X}$ = 10.8
5	PCB 6	6.56	22.2	25.0	12.6	
4	PCB 6'	6.96	20.3	24.5	20.7	
4	PCB 7'	6.94	20.4	21.7	6.4	
5	PCB 8	7.34	18.8	20.0	6.4	
5	LC-6 9	6.90	20.6	22.8	10.7	
5	LC-6 10	7.48	18.3	20.1	9.8	
4	PCB Lollipop 11'	7.13	19.6	22.7	15.8	

N	START DISTANCE (METERS)	STOP DISTANCE (METERS)	MID PT THEO PK (KPa)	VEL MEAN PK PRESS (KPa)	% ERROR	
5	5.14	5.44	21.2	21.4	.9	VELOCITY MEASUREMENTS
5	5.44	5.75	19.6	21.8	11.2	$\bar{X}$ = 7.1
5	5.14	5.75	20.4	21.7	6.4	
5	5.39	5.85	19.4	21.3	9.8	

MEASUREMENTS MADE AT A NOMINAL 30 KPa LEVEL

N	CH	SCALED DISTANCE (M/Kg 1/3)	THEO PK (KPa)	MEAS MEAN PK PRESS (KPa)	% ERROR	
5	1	5.67	27.8	32.9	18.3	DIRECT PRESSURE MEASUREMENTS
5	2	5.53	29.0	30.2	4.1	
5	3	5.61	28.3	32.7	15.5	
5	4	5.49	29.3	30.5	4.1	
5	5	5.55	28.8	29.9	3.8	$\bar{X}$ = 8.9
5	6	5.14	32.7	37.5	14.7	
4	6'	5.61	28.3	31.5	11.3	
4	7'	5.61	28.3	30.0	6.0	
5	8	5.92	26.0	27.7	6	
5	9	5.57	28.6	29.1	1.7	
5	10	6.15	24.5	26.5	8.2	
4	11'	5.66	27.9	31.4	12.5	

N	START DISTANCE (METERS)	STOP DISTANCE (METERS)	MID PT THEO PK (KPa)	VEL MEAN PK PRESS (KPa)	% ERROR	
5	4.02	4.33	30.7	30.5	-.7	VELOCITY MEASUREMENTS
5	4.33	4.63	27.4	29.8	8.8	
5	4.02	4.63	29.0	30.4	4.8	$\bar{X}$ = 5.3
5	4.36	4.82	26.4	27.8	5.3	
2	4.33	4.79	26.7	28.9	8.2	

(Page 122 Blank)

MEASUREMENTS MADE AT A NOMINAL 50 KPa LEVEL

N	CH	SCALED DISTANCE (M/Kg 1/3)	THEO PK (KPa)	MEAS MEAN PK PRESS (KPa)	% ERROR	
6	1	4.05	49.9	56.1	12.4	DIRECT PRESSURE MEASUREMENTS
5	2	"	"	51.2	2.6	
6	3	"	"	53.9	8.0	
5	4	"	"	51.4	3.0	$\bar{X}$ = 4.1
5	5	"	"	53.2	6.6	
4	6'	4.07	49.4	50.6	2.4	
4	7'	"	"	48.8	-1.2	
2	11'	4.06	49.6	49.2	-.8	

N	START DISTANCE (METERS)	STOP DISTANCE (METERS)	MID PT THEO PK (KPa)	VEL MEAN PK PRESS (KPa)	% ERROR
3	3.08	3.54	46.1	50.8	10.2

MEASUREMENTS MADE AT A NOMINAL 70 KPa LEVEL

N	CH	SCALED DISTANCE (M/Kg 1/3)	THEO PK (KPa)	MEAS MEAN PK PRESS (KPa)	% ERROR	
4	6'	3.37	71.5	71.6	.1	DIRECT PRESSURE MEASUREMENTS
4	7'	3.37	71.5	66.7	-6.7	
3	11'	3.49	66.6	69.6	4.5	$\bar{X}$ = -.7

MEASUREMENTS MADE AT A NOMINAL 105 KPa LEVEL

N	CH	SCALED DISTANCE (M/Kg 1/3)	THEO PK (KPa)	MEAS MEAN PK PRESS (KPa)	% ERROR	
4	6'	2.78	107.3	98.3	-8.4	DIRECT PRESSURE MEASUREMENTS
4	7'	2.78	"	100.0	-6.8	$\bar{X}$ = -8.9
2	11'	2.77	108.2	95.8	-11.5	

LEGEND: N= Number of shots at stated location. CH= Channel number.

SCALED DISTANCE = Distance from charge/(Mass of charge) $\frac{1}{3}$ = Distance from charge/0.7824

THEO PK= Peak side-on overpressure calculated from Goodman's equation.

MEAS MEAN PK PRESS = Mean of N peak side-on pressure measurements made at stated location.

START DISTANCE = Distance from charge at which the blast wave starts a timer.

STOP DISTANCE = Distance from charge at which the blast wave stops a timer.

MID PT THEO PK = Peak side-on overpressure calculated from Goodman's equation at a point midway between stop and start distance.

VEL MEAN PK PRESS = Peak side-on overpressure obtained using velocity from timer and the Rankine-Hugoniot equation. Mean of N shots.

4.7 (Cont'd)

The reason for discrepancy at the low pressures is not fully understood. There are several possible causes. Differences between field testing conditions and laboratory conditions, such as ambient temperature, acceleration of the transducer stands, etc., may be responsible for the difference.

The particular lot of pentolite used may have been unusual. The explosives technician who cast the spheres noted that this lot required twice as long to melt as brand new pentolite normally requires.

This characteristic is not thought to be irregular. It occurs any time pentolite is "recycled" (i.e., cast, shredded, and recast). The explosives technician did not feel that "recycling" affects the explosive properties of pentolite.

Goodman's equation has been the foundation for much of the blast work in the last 20 years. Many investigators have confirmed his work. It would be unwise to conclude that Goodman's equation is in error by 10%, based on one set of observations. It would seem equally unwise, however, to continue to use pentolite as a calibration technique until the observed discrepancies have been resolved.

(Page 124 Blank)

SECTION 5. EXTRANEOUS EFFECTS

Blast overpressure transducers often measure events not related to pressure, such as acceleration and thermal transients. Testing conditions, such as ambient temperature, transducer mounting, and choice of test site also affect the measurements. This section describes various observations and experiments conducted to investigate these extraneous effects.

5.1 ACCELERATION ERROR USING A MINIATURE TRANSDUCER

Figure 5.1-1 shows a PCB transducer mounted on a lightweight stand and covered with a metal cap. The cap is sealed with a teflon-coated nut to prevent pressure from reaching the transducer.

Figure 5.1-2 shows the output of an accelerometer mounted to the stand when it is struck by a pentolite blast wave. Note the low frequency oscillation at about 40 Hz that occurs after the stand has been struck by the blast wave. It is assumed that this oscillation is caused by stand whip.

Figure 5.1-3 shows the output of the transducer when it is not covered. Note that the peak pressure level is approximately 30 kPa.

Figure 5.1-4 shows the output of the covered transducer. Note that if there is any 40 Hz signal caused by stand whip, it is below the ambient electrical noise level. The peak "apparent pressure" is 3 kPa or 10% of the actual pressure level present.

Figure 5.1-5 is an expanded view of the signal from the transducer when it is not covered. Note the two distinct peaks caused by the incident wave and the ground reflection.

Figure 5.1-6 is an expanded view of the accelerometer mounted to the stand. Note the two distinct envelopes corresponding to the incident wave and the ground reflection striking the stand. Oscillation in the first envelope is approximately 30 g at 11,000 Hz.

Figure 5.1-7 is an expanded view of the output of the covered transducer. Once again, two distinct envelopes are present. Note the oscillations are now at 16,000 Hz rather than 11,000 Hz. This shot was fired without the mass of the accelerometer and its clamping hardware attached to the stand. It is assumed that this reduction of mass caused the higher resonant frequency.

5.1 (Cont'd)

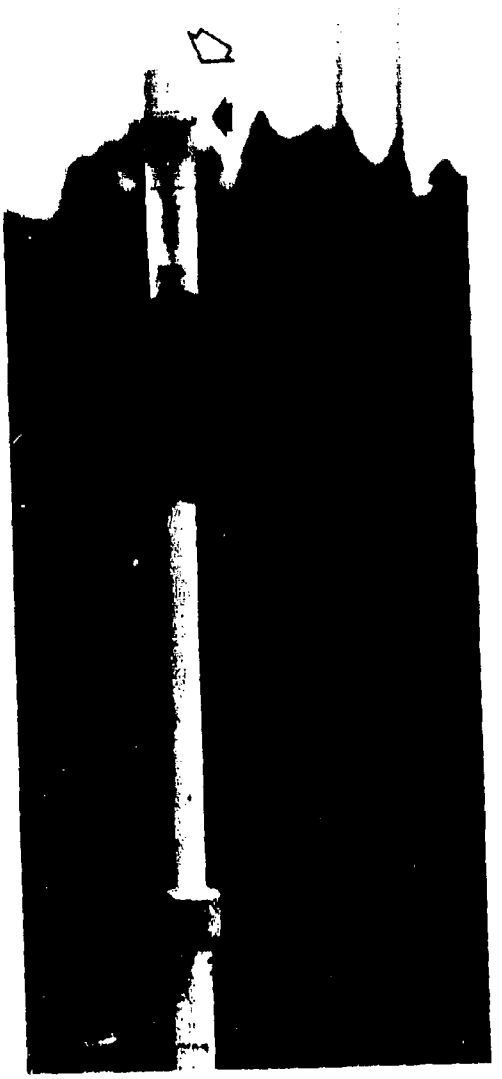

Figure 5.1 1. PCR transducer covered with a metal cap (outline arrow). Solid arrow points to Teflon coated nut for sealing out pressure.

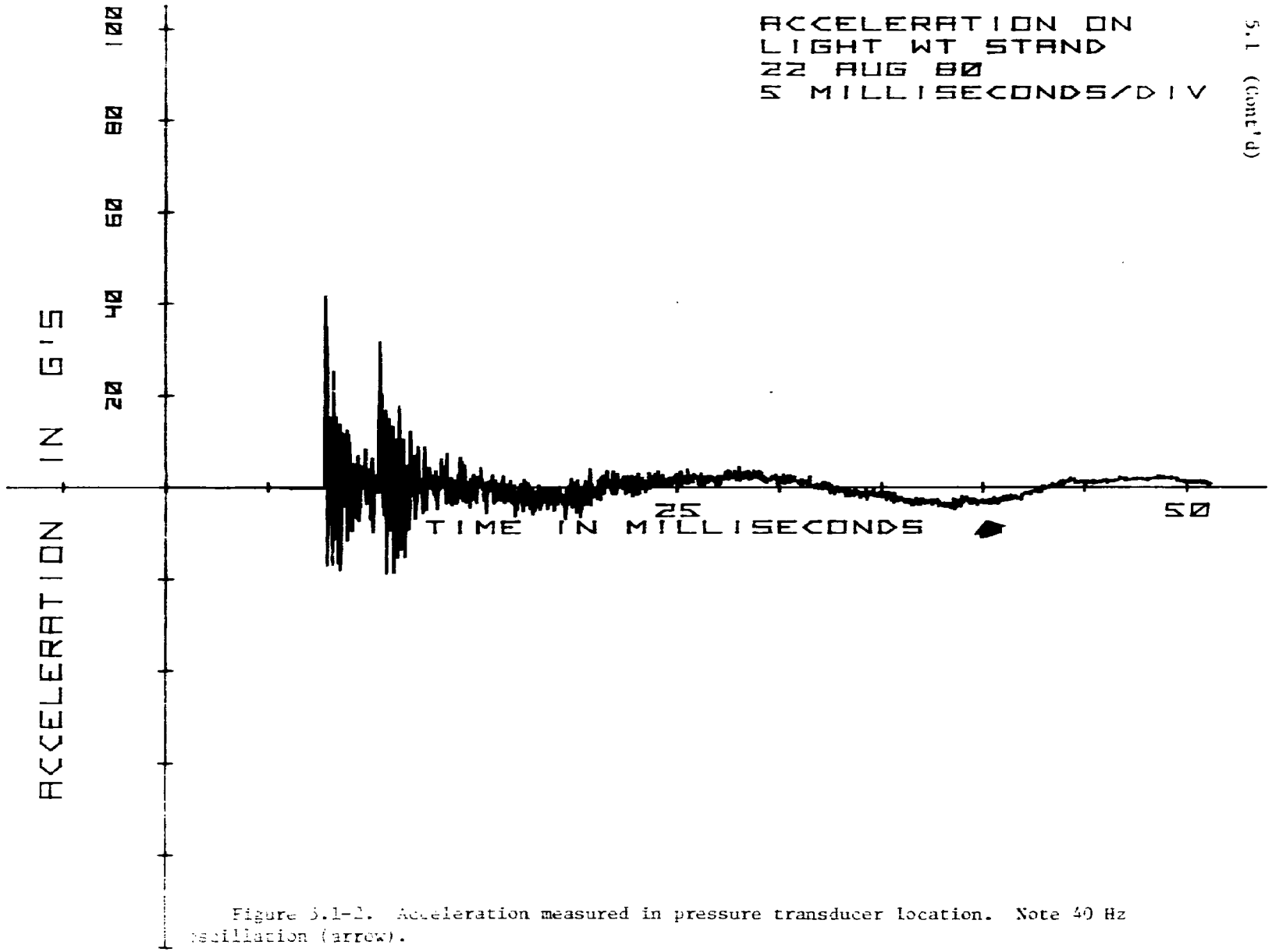

Figure 5.1-2. Acceleration measured in pressure transducer location. Note 40 Hz oscillation (arrow).

5.1 (Cont'd)

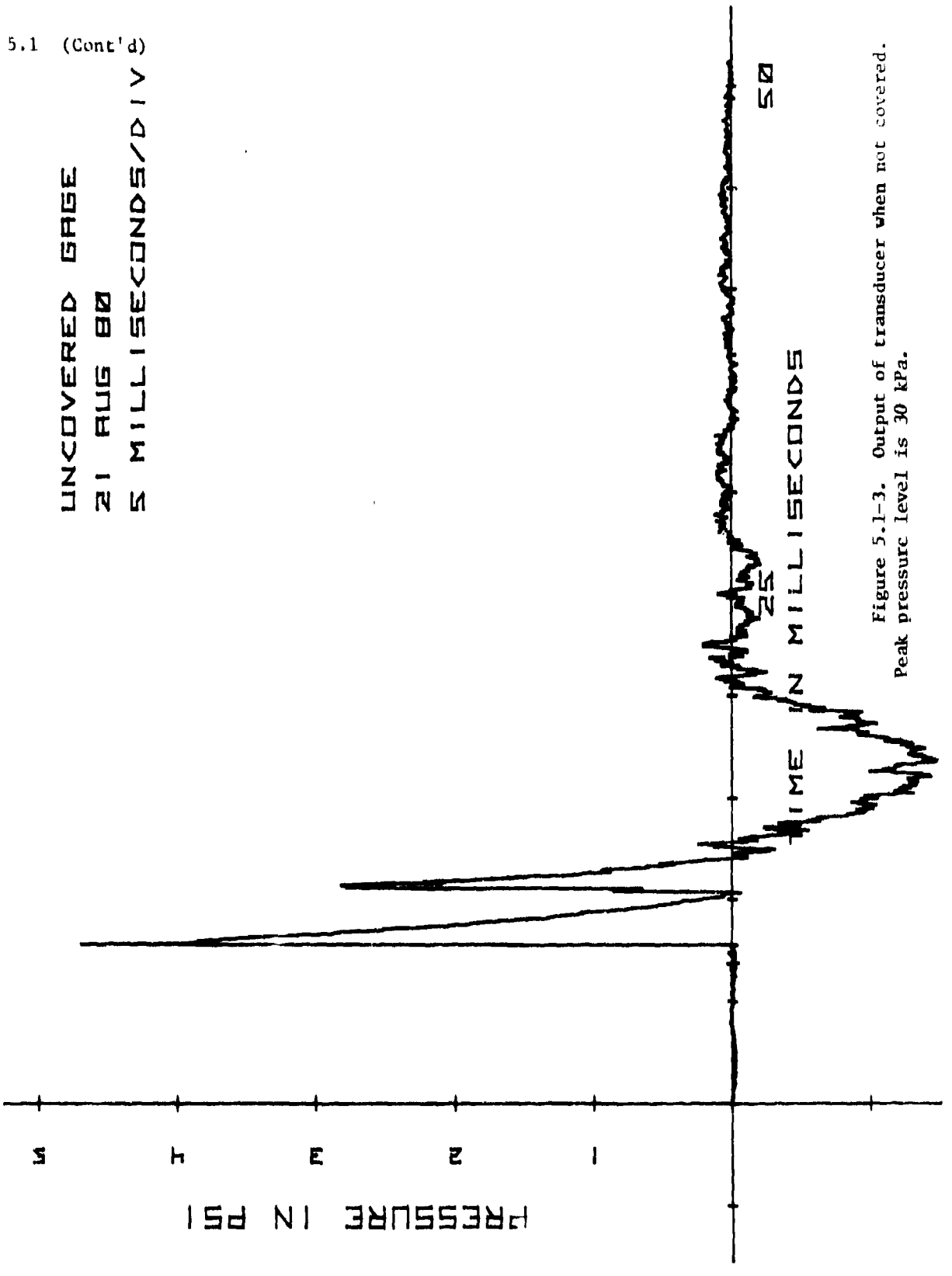

Figure 5.1-3. Output of transducer when not covered. Peak pressure level is 30 kPa.

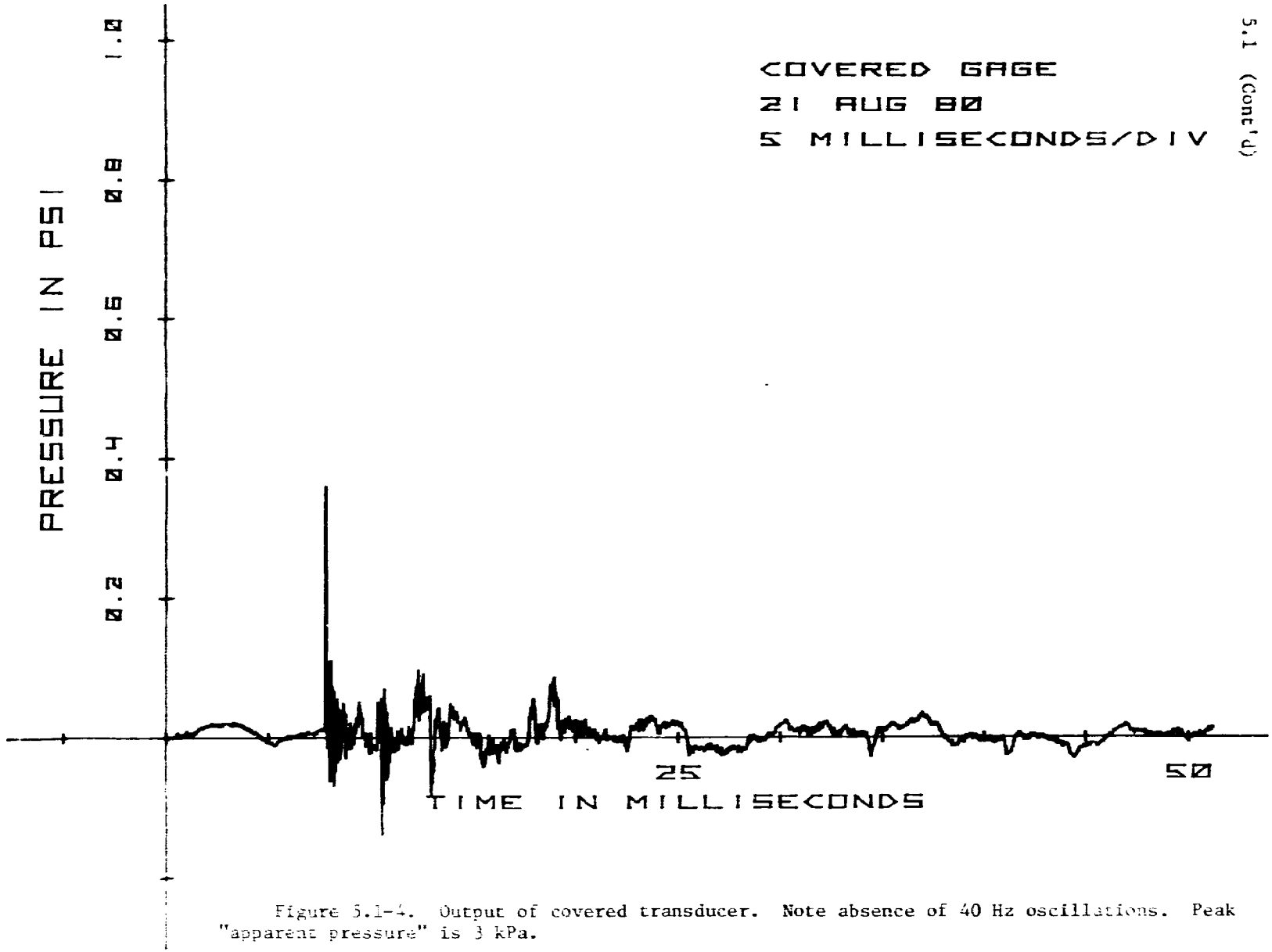

Figure 5.1-4. Output of covered transducer. Note absence of 40 Hz oscillations. Peak "apparent pressure" is 3 kPa.

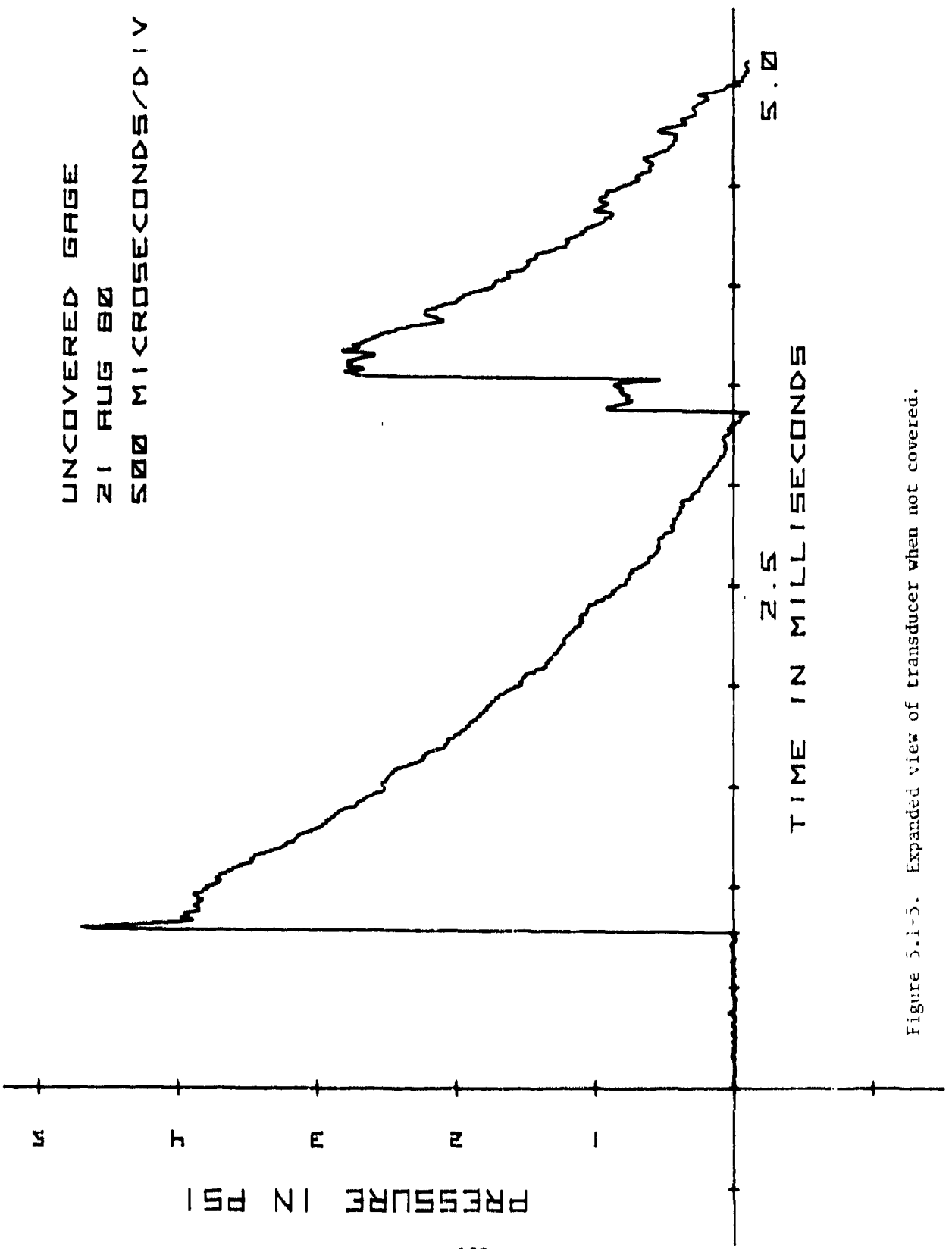

Figure 5.1-5. Expanded view of transducer when not covered.

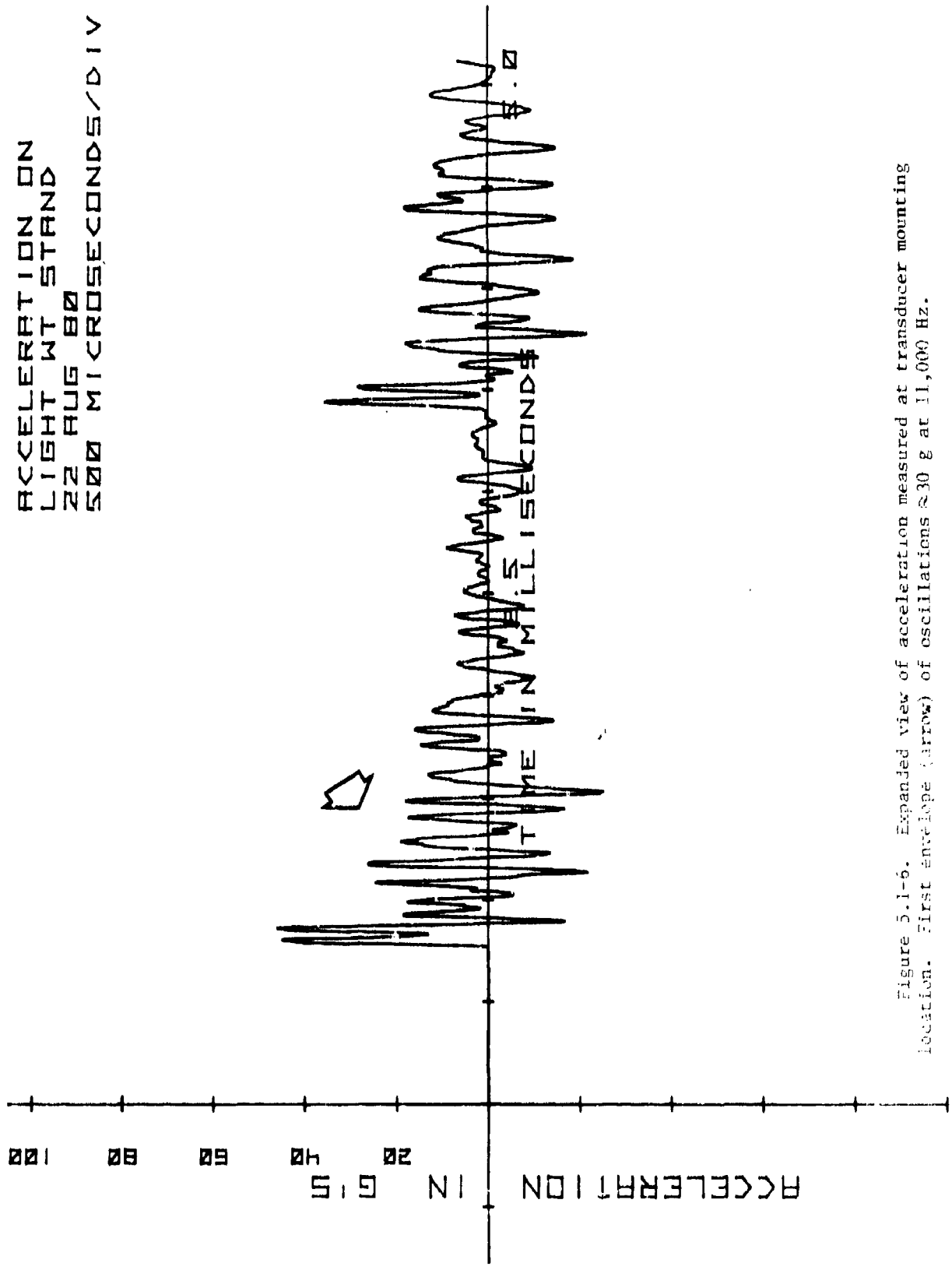

Figure 5.1-6. Expanded view of acceleration measured at transducer mounting location. First envelope (arrow) of oscillations ≈30 g at 11,000 Hz.

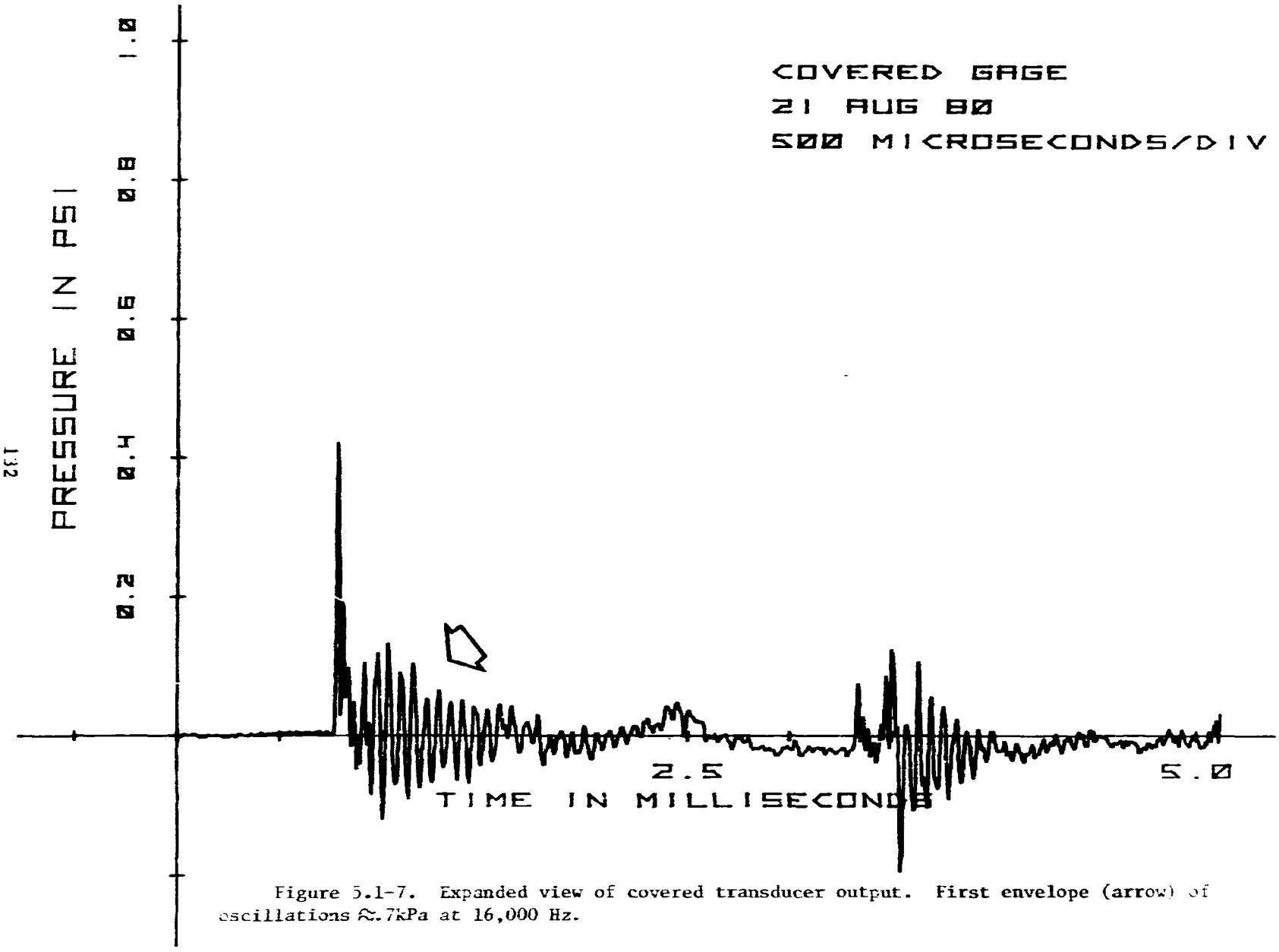

Figure 5.1-7. Expanded view of covered transducer output. First envelope (arrow) of oscillations ≈.7kPa at 16,000 Hz.

Just as removal of the accelerometer and clamping hardware increased the resonant frequency, it is assumed that the acceleration level was also increased. A crude method of estimating the increased acceleration level is to multiply by the ratio of the frequencies:

$$\text{Estimated Acceleration Level} = 30\ g\ \left(\frac{16,000}{11,000}\right) = 44\ g$$

In figure 5.1-7, oscillation in the first envelope is approximately 0.7 kPa. The acceleration sensitivity, therefore, is:

$$\frac{0.7\ \text{kPa}}{44\ g} = 0.016\ \text{kPa/g}$$

The manufacturer advertises an acceleration sensitivity of 0.014 kPa/g for this transducer.

It should be noted that the covered gage produced a signal that was approximately 9% of the level measured by the uncovered gage. This result emphasizes that acceleration can cause significant error, and that careful attention should be given to isolating the transducer from acceleration.

5.2 ACCELERATION ERROR USING THE LC-33 PENCIL GAGE

Figures 5.2-1 through 5.2-4 show the steps of preparing and installing the LC-33 pencil gage in heavyweight blast stands. Note particularly the two rolls of rubber tape used to support the transducer in the stand.

These pieces of rubber support the gage in the blast stand. They also isolate the transducer from high frequency vibration. As described below, these pieces of rubber can also cause problems.

Figure 5.2-5 shows the response of a properly mounted LC-33 gage to a pentolite blast wave. Contrast that signal with the signal shown in figure 5.2-6 which is the response of an improperly mounted LC-33 gage.

Figure 5.2-7 is the response of the same improperly mounted transducer when its sensing element was covered. Note the oscillation at approximately 240 Hz. The amplitude of these oscillations is almost 10% of the actual pressure level. This transducer was found to be loose in the blast stand, and would vibrate if tapped by hand.

Figure 5.2-8 shows acceleration measured on a heavyweight blast stand. Note that high frequency acceleration is present. None of this high frequency acceleration appears on the signal from the transducer, indicating that the rubber did effectively isolate the transducer from high frequency acceleration.

Note also that no low frequency acceleration (stand whip) is present. The heavyweight stand is apparently rigid enough that stand whip is eliminated.

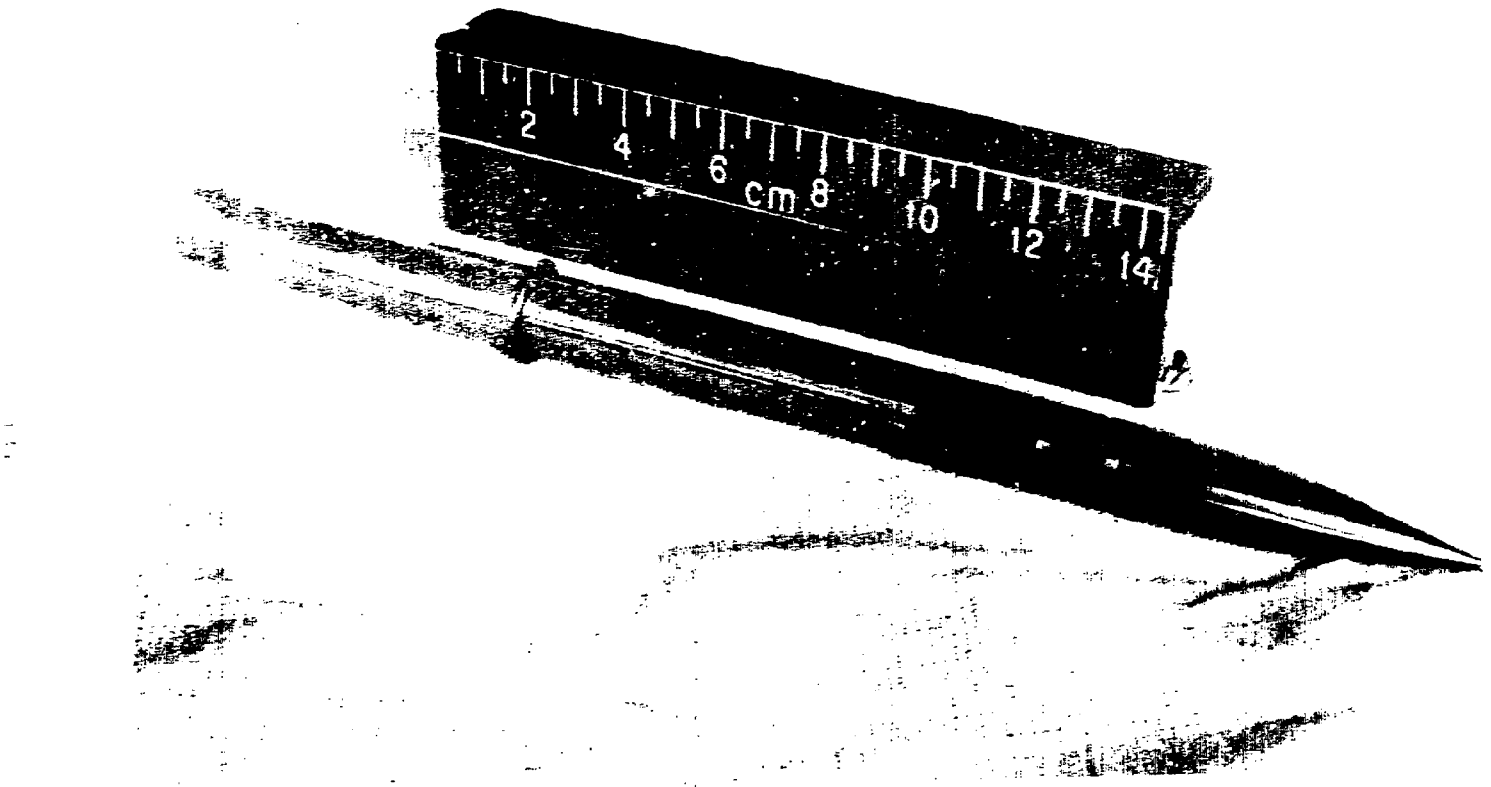

Figure 5.2-1. LC-33 pencil gage unmounted.

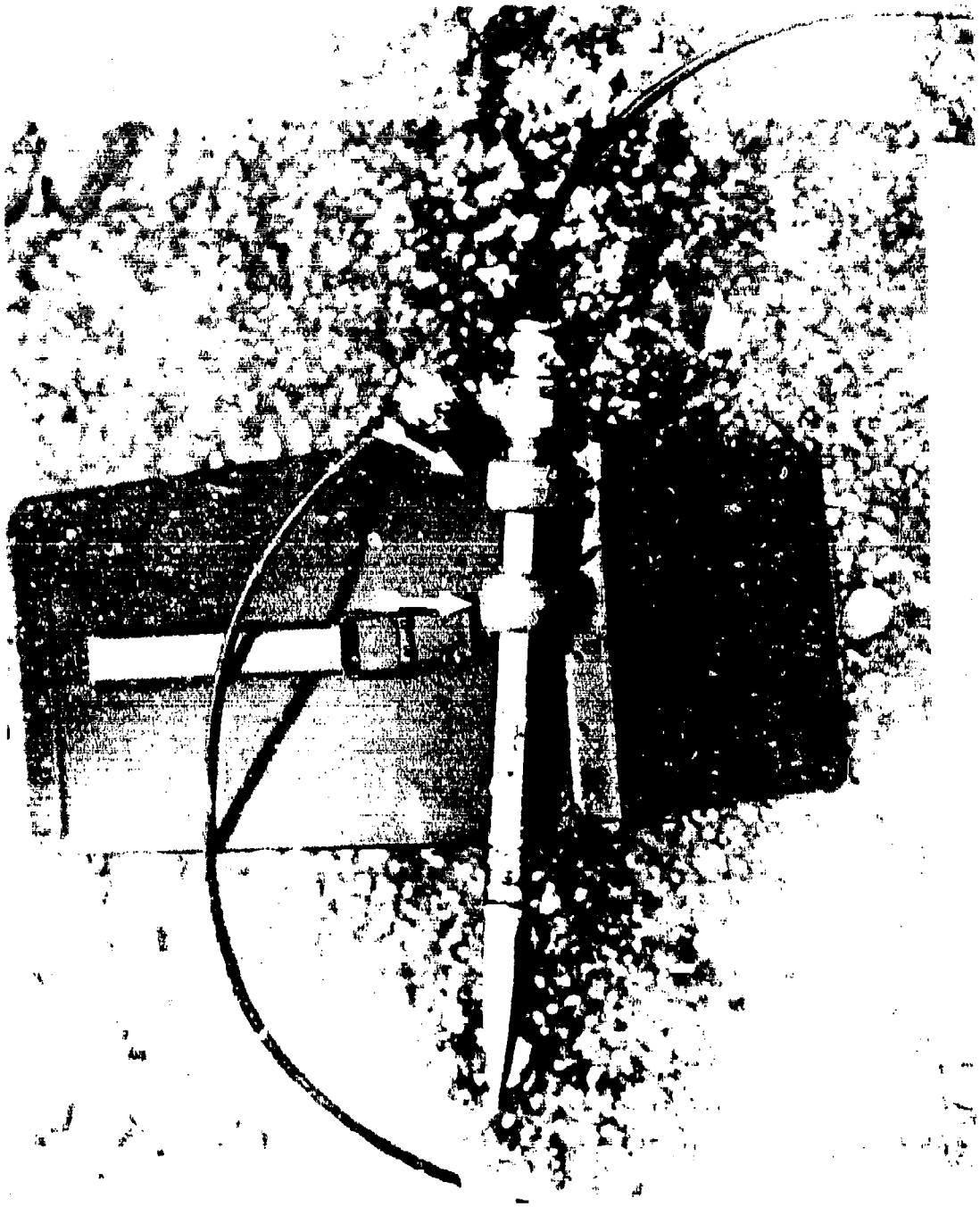

Figure 5.2-4. Detail of LC-33 pencil gage mounted in blast stand.
Note use of rubber tape to form smooth transition between stand and transducer.

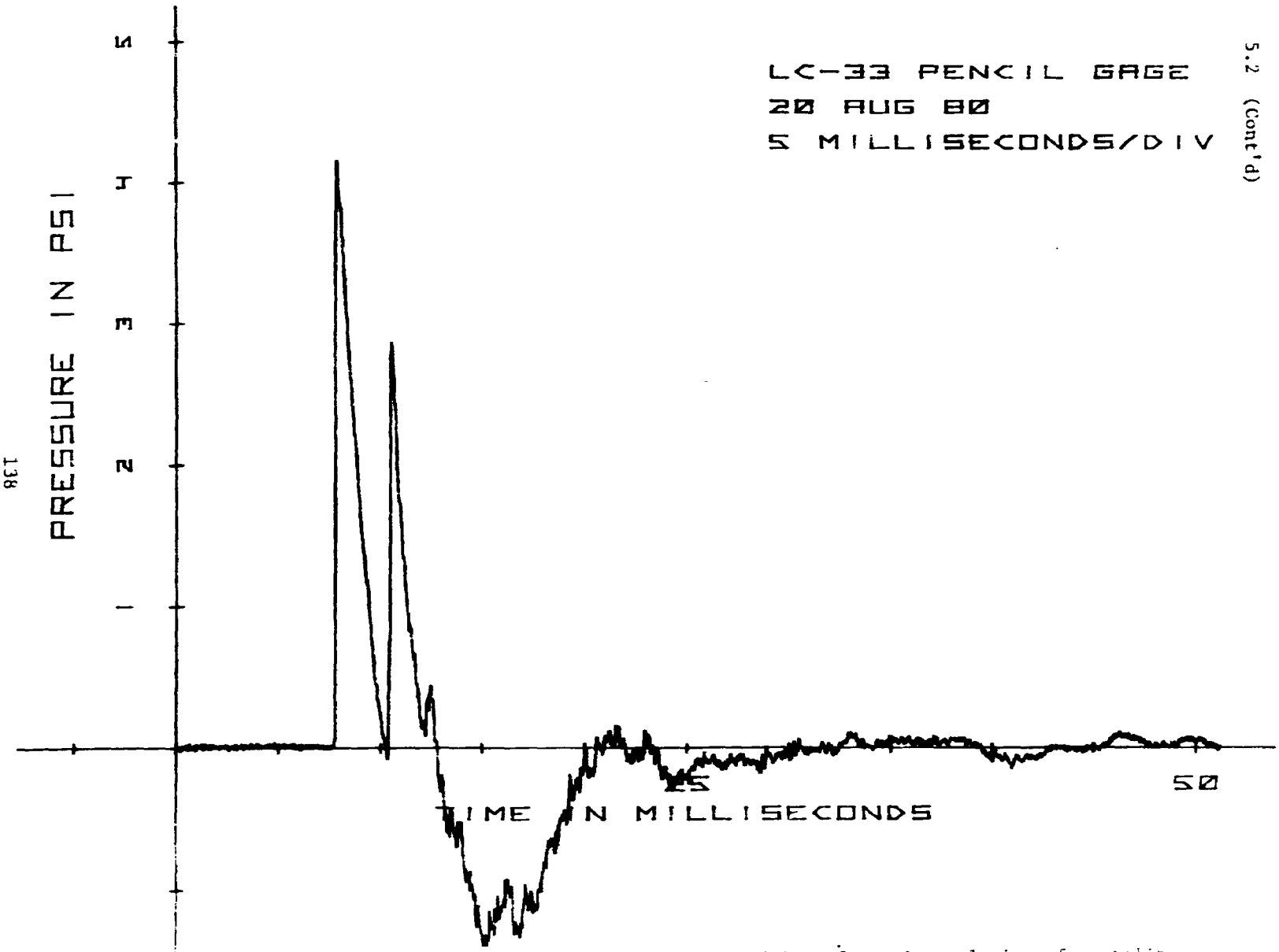

Figure 5.2-5. Pressure versus time measured in a free air explosion of pentolite with a properly mounted LC-33 pencil gage.

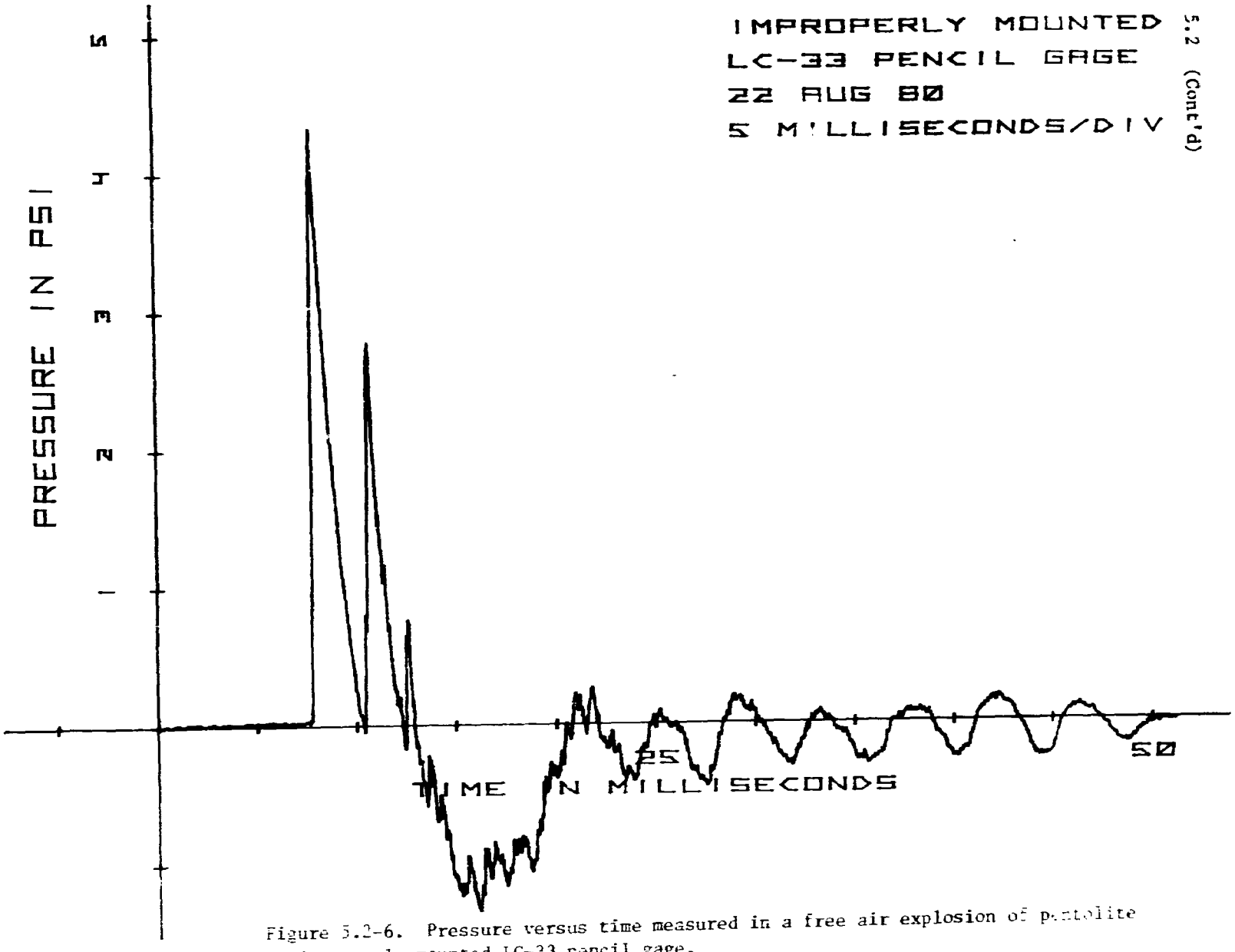

Figure 5.2-6. Pressure versus time measured in a free air explosion of pentolite with an improperly mounted LC-33 pencil gage.

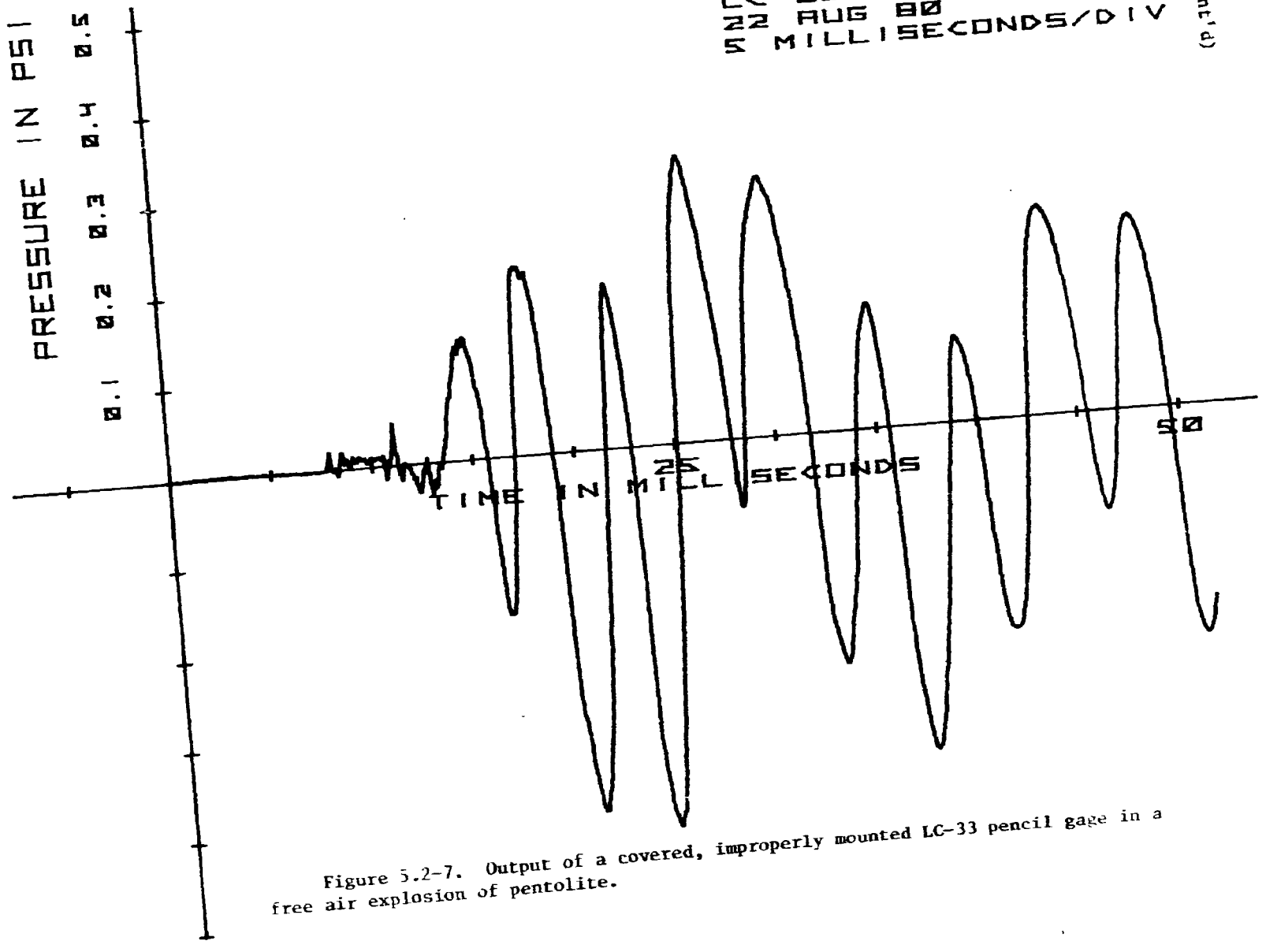

Figure 5.2-7. Output of a covered, improperly mounted LC-33 pencil gage in a free air explosion of pentolite.

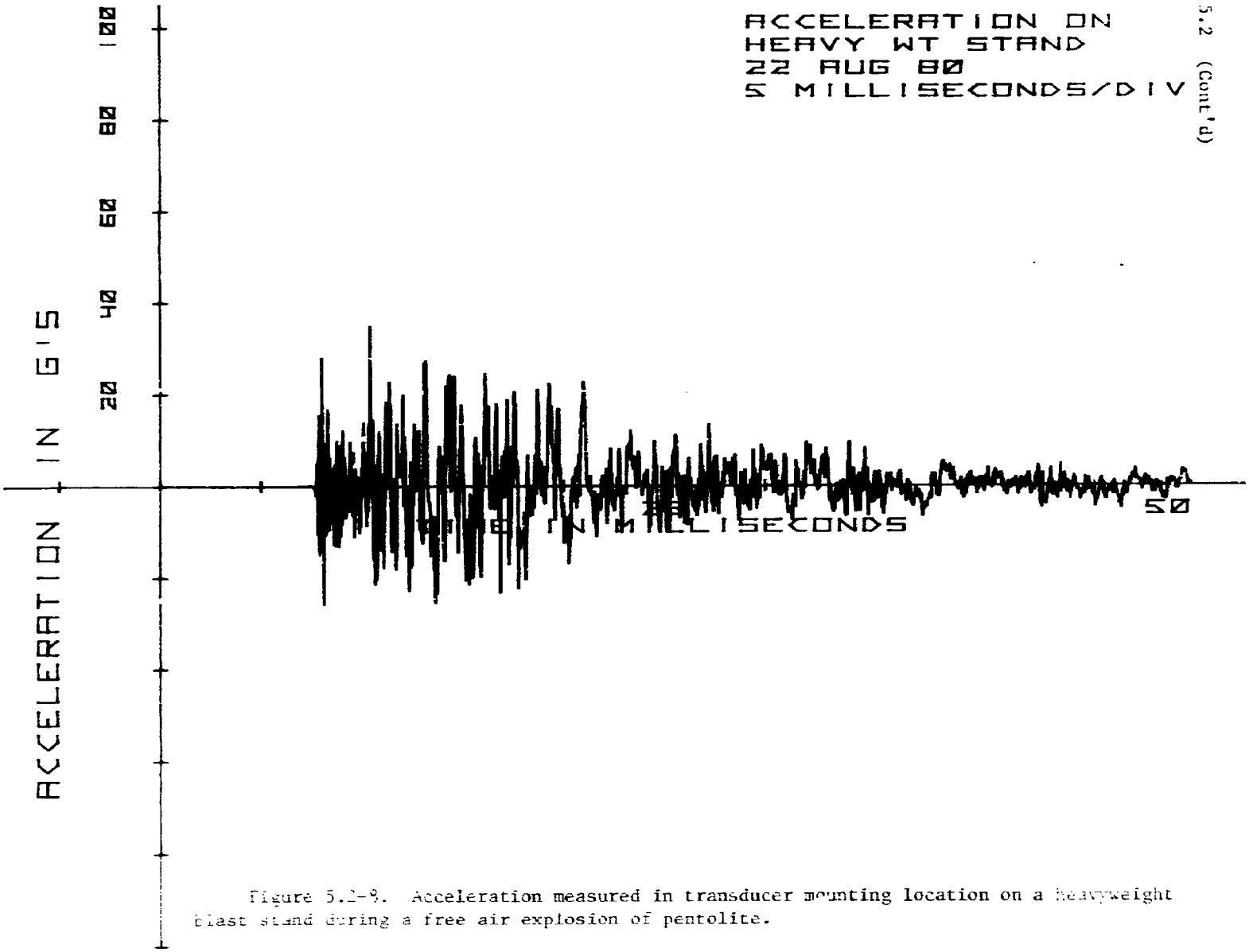

Figure 5.2-9. Acceleration measured in transducer mounting location on a heavyweight blast stand during a free air explosion of pentolite.

5.3 ACCELERATION ERROR IN VEHICLES

Figure 5.3-1 shows an example of a field measurement that was ruined by acceleration. This measurement was made with an ST-2 gage mounted on a stand which was attached to an armored personnel carrier.

Arrival of the first blast wave is indicated by a high amplitude pressure with a short rise time. Note that apparent deviations from ambient pressure begin before the first blast wave arrives.

These signals are assumed to be caused by acceleration of the mortar transmitted through the frame of the armored personnel carrier to the transducer. Because the acceleration waves travel through metal much faster than blast waves travel through air, the acceleration reaches the transducer before the blast wave. Note that additional acceleration-induced signals are produced at the end of the record.

Figures 5.3-2 and 5.3-3 show an "A" frame structure that was built to support the transducers. This structure permits accurate placement of the transducers without any contact between the vehicle and the transducer support system.

Figure 5.3-4 shows a blast measurement made using the "A" frame structure. Note that no extraneous acceleration signals are present.

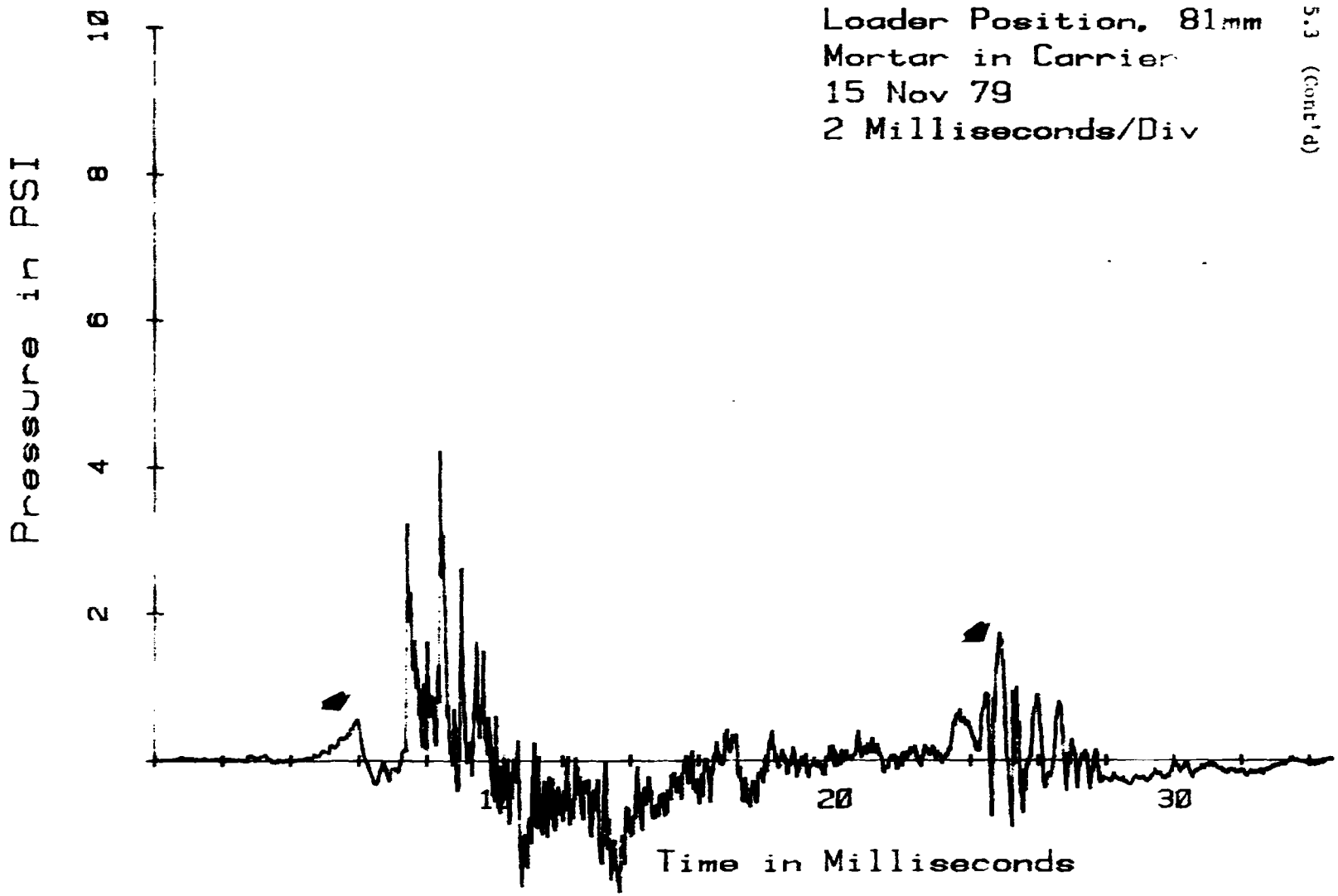

Figure 5.3-1. Blast measurement made in an armored personnel carrier. Acceleration from firing shock reached transducer before blast wave (arrow). Acceleration induced signal also observed after pressure decays back to ambient level (arrow).

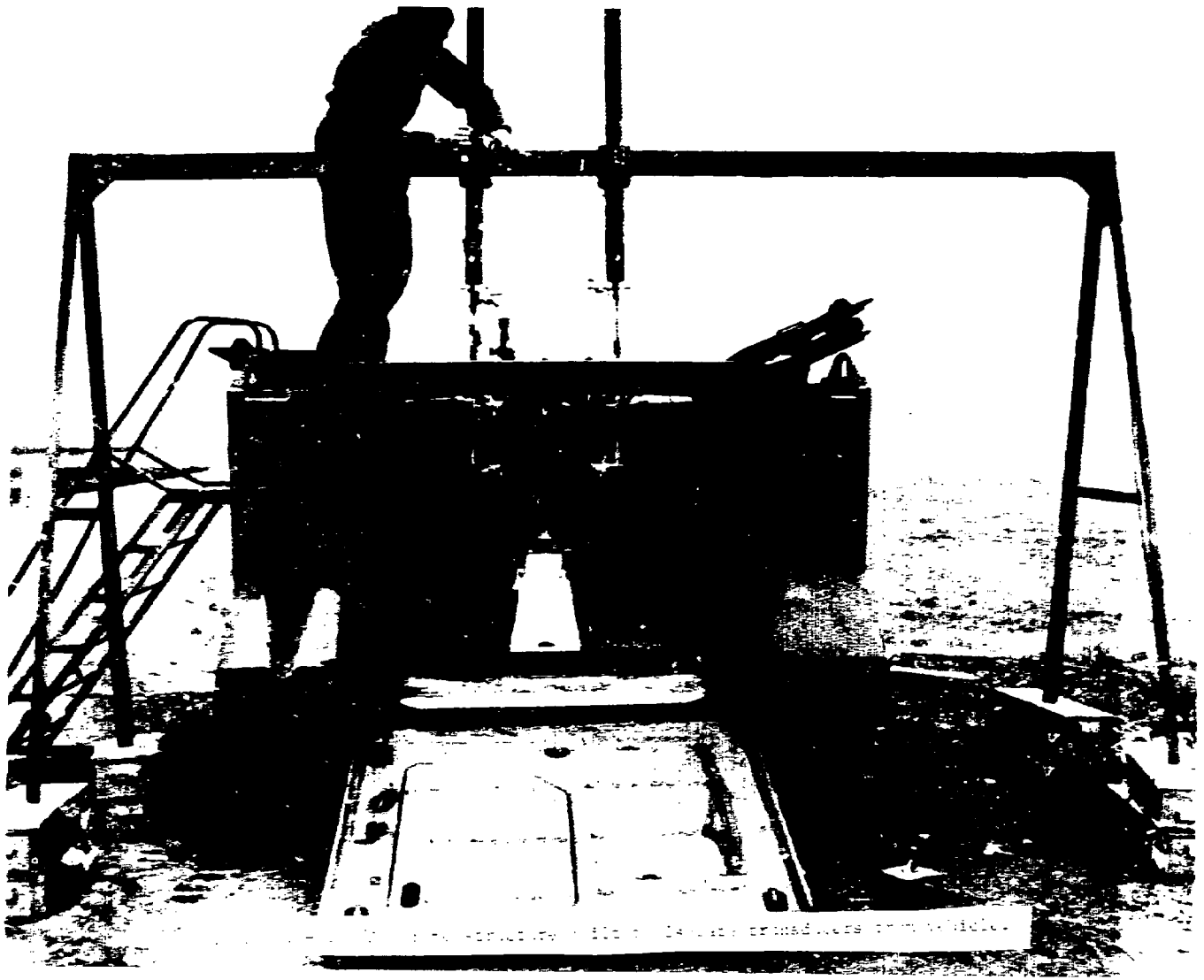

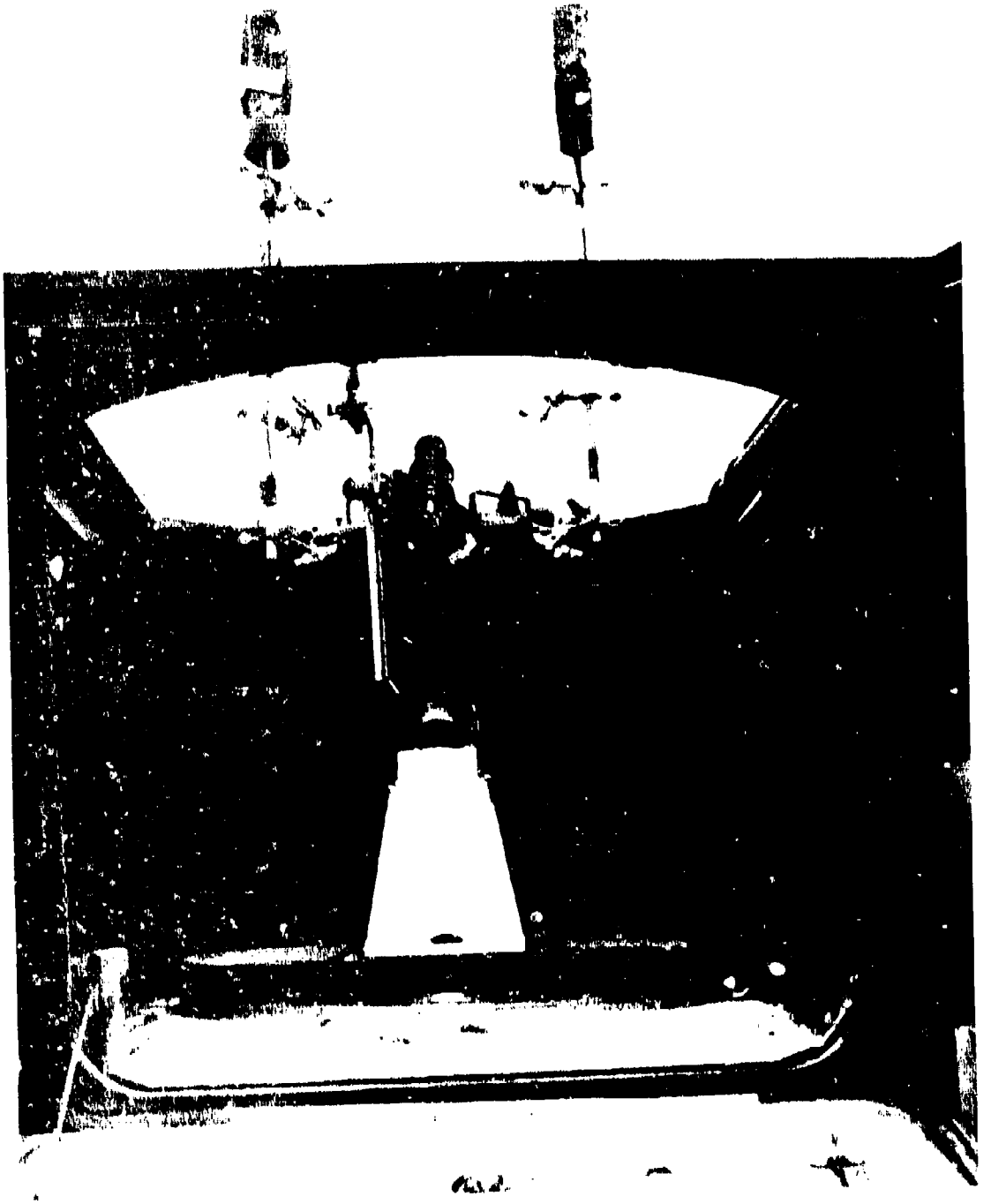

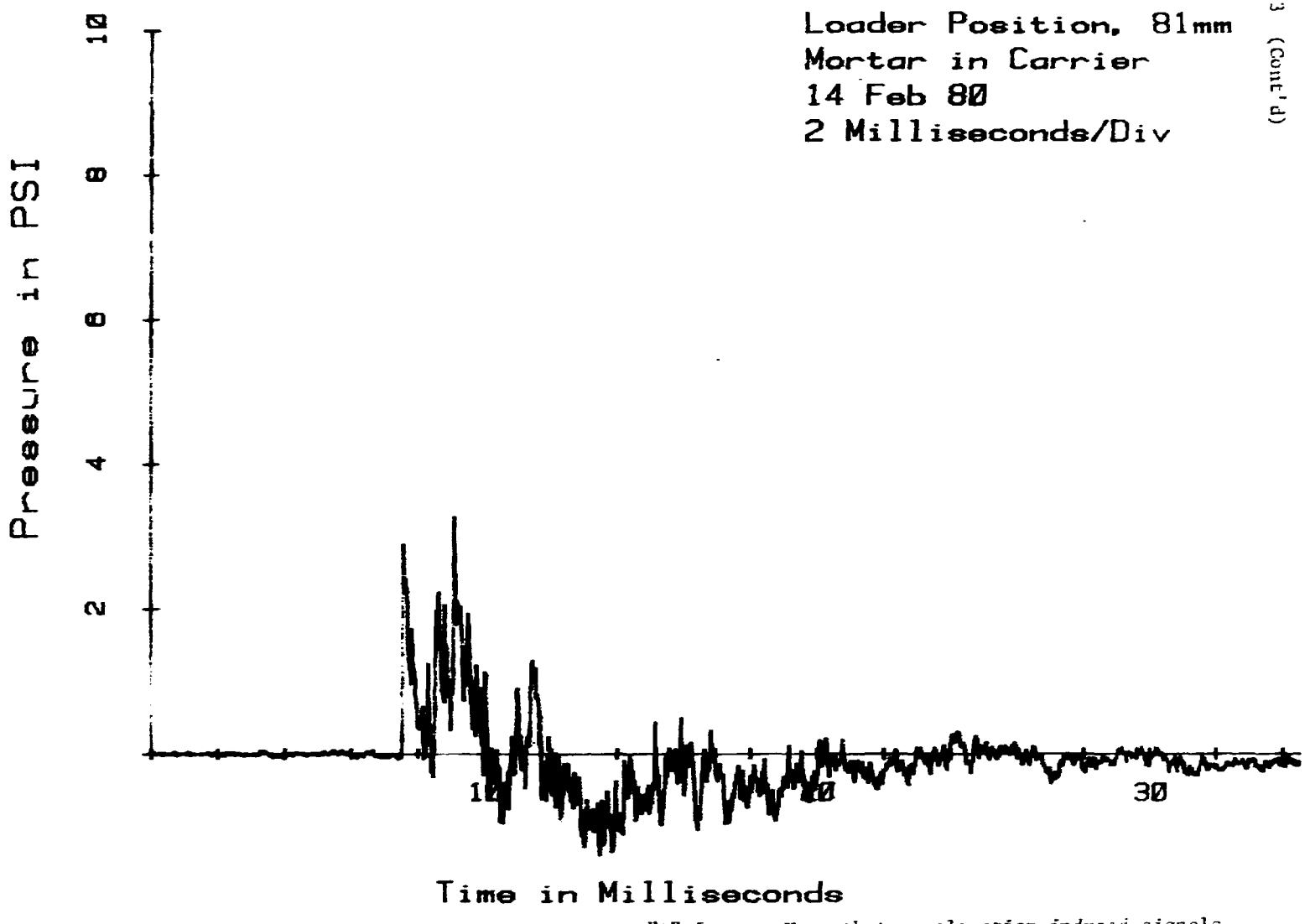

Figure 5.3-4. Blast measurement made using "A" frame. Note that acceleration induced signals are no longer present.

5.4 EFFECTS OF AMBIENT TEMPERATURE

Variations in ambient temperature occur in field measurements during the test day. During winter and summer testing, there is a dramatic difference between the field measurement temperature and the laboratory temperature where calibration of transducers is performed.

A laboratory experiment was conducted to determine the effect of ambient temperature on sensitivity (output/unit pressure) of various transducers. The transducers were placed in the static pressure pulse calibrator and heated or cooled to various temperatures. Figure 5.4-1 shows the results of this experiment.

It was necessary to complete the testing of each transducer in one 8-hour day. The transducers were not permitted to remain at one temperature long enough to eliminate all thermal gradients. A special fixture had to be constructed to use the LC-33 pencil gage in the pulse calibrator. It is assumed that thermal gradients in this fixture caused the very strange shape of the LC-33 curve in figure 5.4-1.

Because of the thermal gradients present, it is felt that the exact shape of any of the curves in figure 5.4-1 is not meaningful. The general trends of the different curves are, however, felt to be valid.

The temperature-compensated strain gages in the Endevco gage were far less sensitive to temperature change than the various crystals. The man-made crystals (lead metaniobate in the ST-2 and lead zirconate titanate in the LC-33) were more sensitive to temperature change than the natural crystal (quartz in the PCB gage).

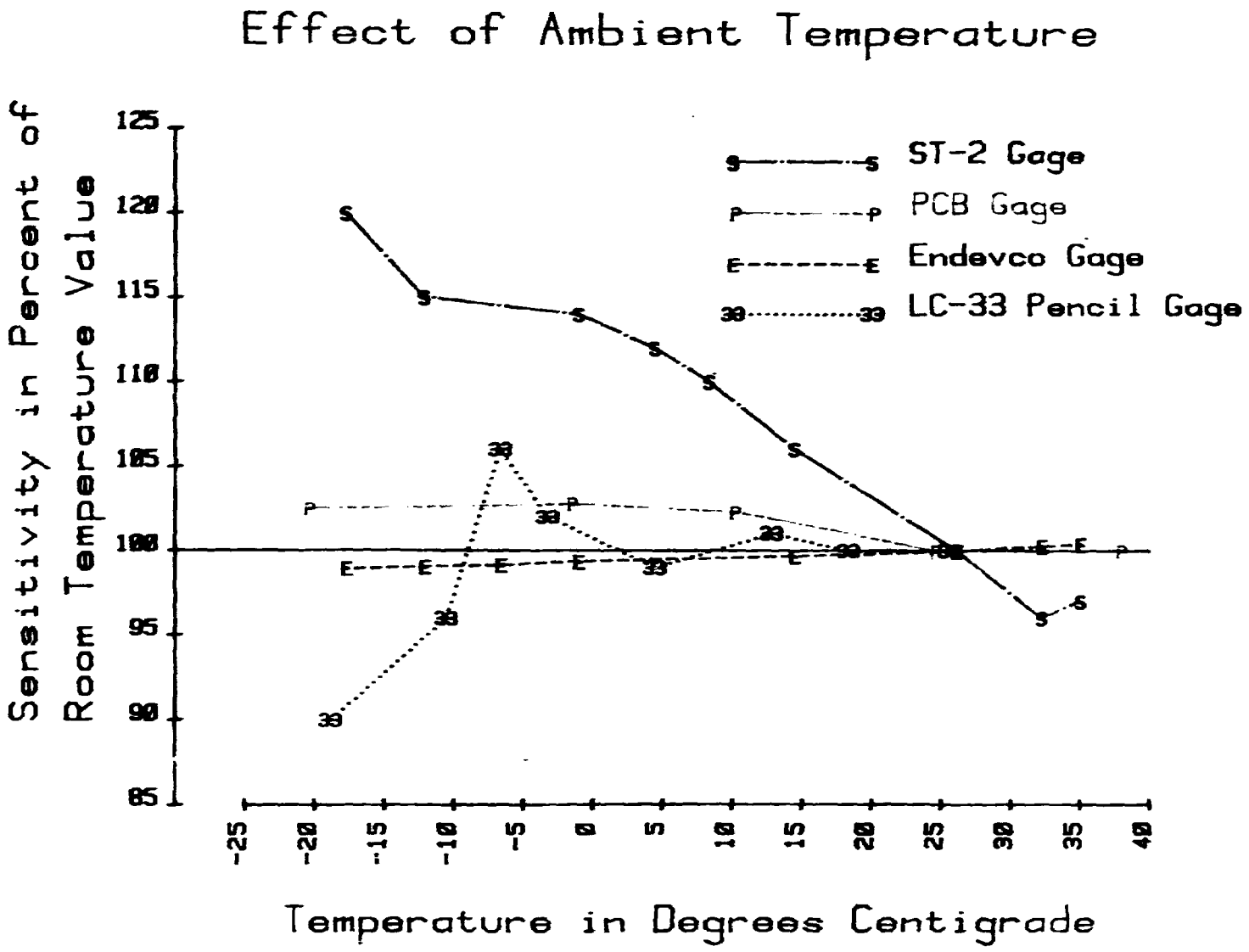

Figure 5.4-1. Change in sensitivity caused by changing ambient temperature for several transducers.

5.5 EFFECTS OF THERMAL TRANSIENTS

Figure 5.5-1 shows a blast measurement made in a crew location during firing of a TOW missile. Figure 5.5-2 shows a measurement made in the same location with the launcher slightly rotated.

In this second case, exhaust gages from the rocket caused a thermal transient large enough to affect the pressure measurement. Locations close to the muzzle of a large caliber artillery piece have produced similar thermal transient problems.

To further illustrate the sensitivity of pressure transducers to thermal transients, a technique suggested by the National Bureau of Standards (ref 9) was used. Figures 5.5-3 and 5.5-4 show the response of a silicon photo-diode placed 22 cm in front of an electronic flash and a Sylvania No. 2 flashbulb (equivalent to the GE No. 22 flashbulb discussed in ref 9).

Note that the integral, which is proportional to energy, of the flashbulb curve is roughly 10 times larger than the integral of the electronic flash curve. This indicates that in the near infrared spectrum to which the silicon photo-diode responds, the flashbulb produces 10 times as much energy.

Figures 5.5-5 and 5.5-6 show the response of the PCB gage and the ST-2 gage to the electronic flash, 22 cm from the transducer. Note that placing a layer of black electrical tape and a layer of aluminum-coated mylar tape over the transducer reduced the thermal transient response of both transducers dramatically.

Figures 5.5-7 and 5.5-8 show the response of the PCB gage and the ST-2 gage to the No. 2 flashbulb. Note that the response of both transducers is roughly an order of magnitude greater than their response to the electronic flash.

The quartz crystal in the PCB transducer is surrounded by stainless steel. When the end of the transducer is heated by the thermal transient it expands, pulling on the crystal. This tension on the crystal is electrically interpreted as a pressure rarefaction or "negative" pressure.

The lead metaniobate crystal in the ST-2 gage is mounted in stainless steel but covered with a nylon cap. The thermal coefficient of expansion of nylon is roughly five times larger than that of stainless steel.

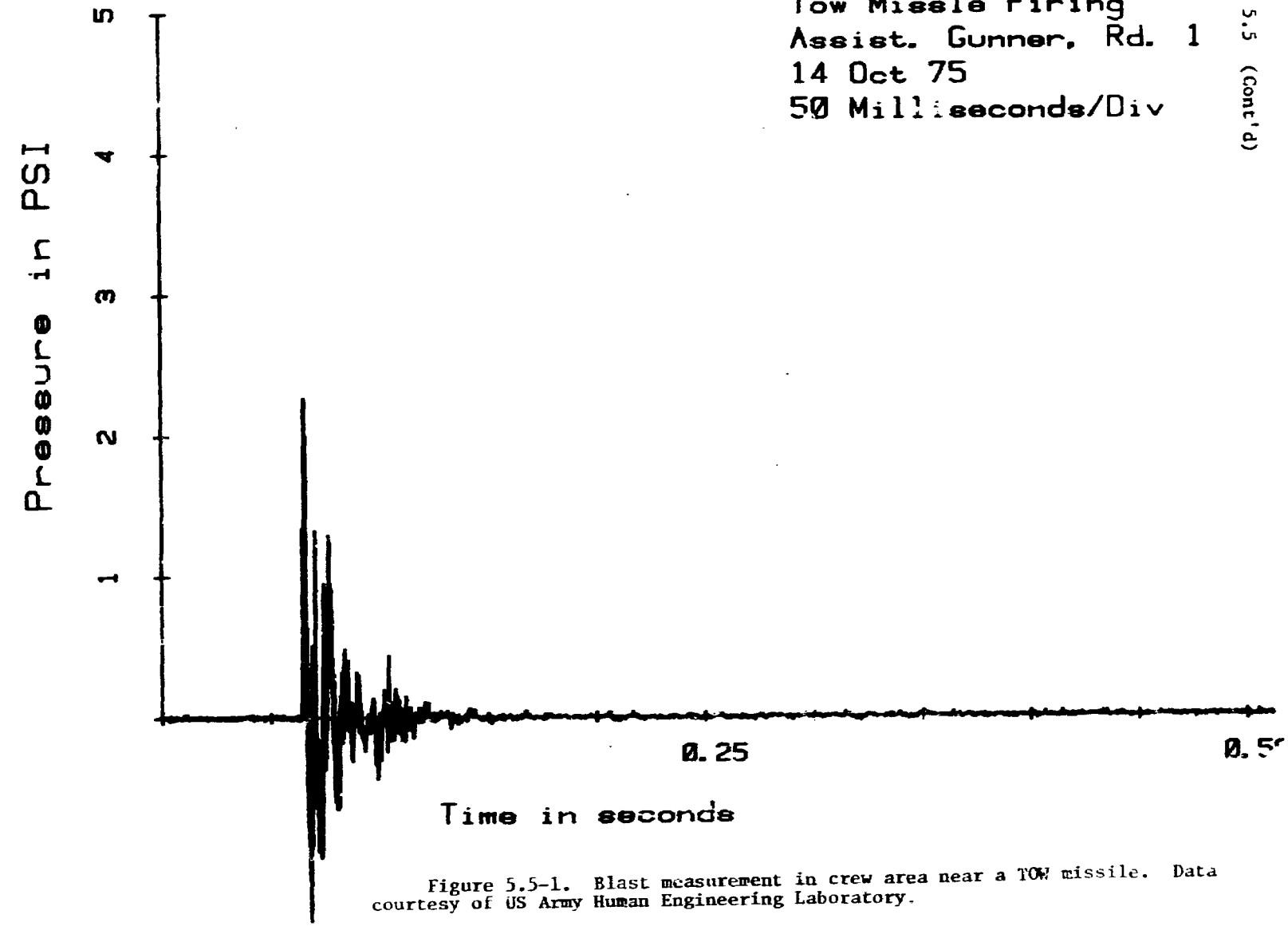

Figure 5.5-1. Blast measurement in crew area near a TOW missile. Data courtesy of US Army Human Engineering Laboratory.

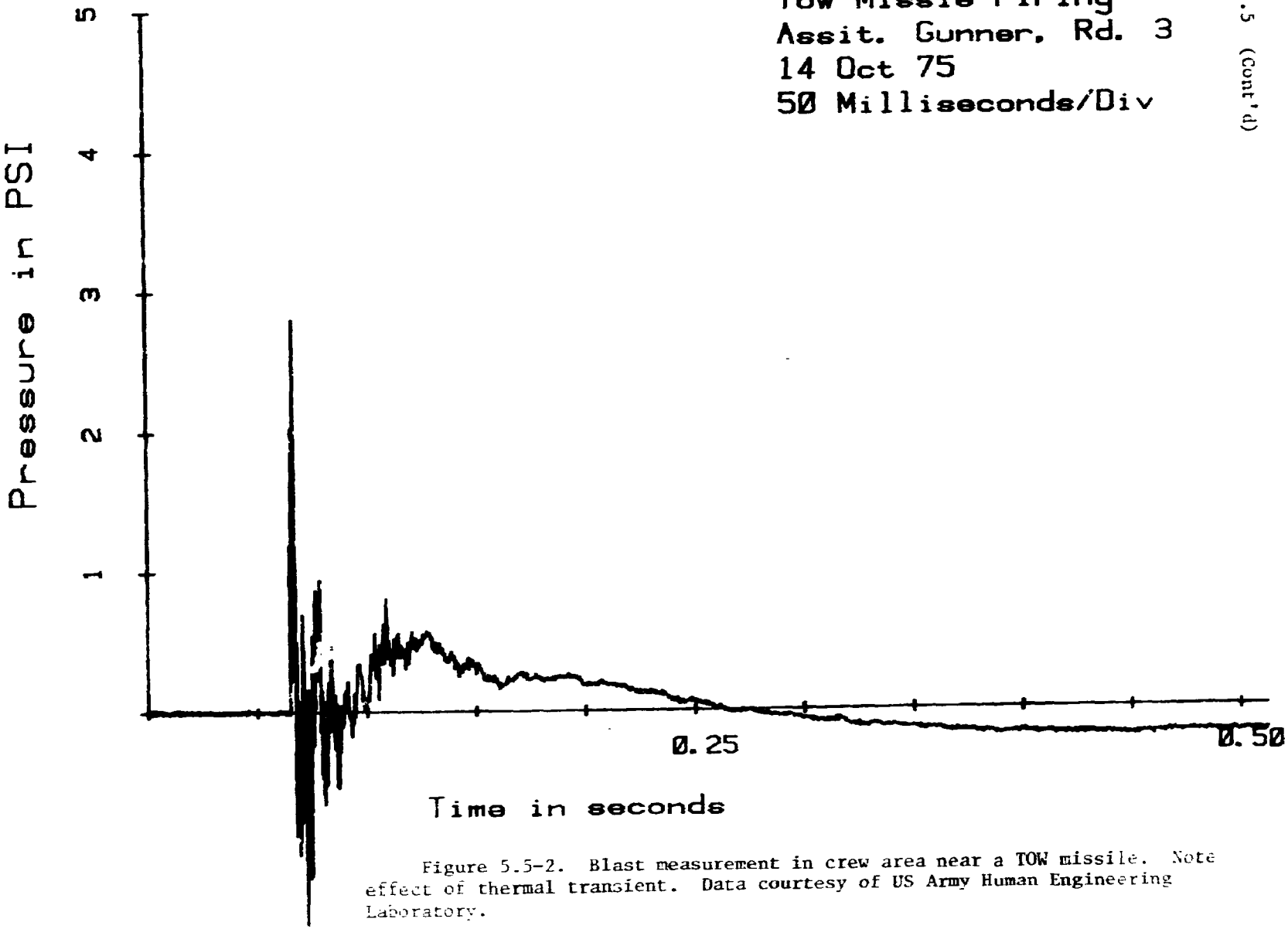

Figure 5.5-2. Blast measurement in crew area near a TOW missile. Note effect of thermal transient. Data courtesy of US Army Human Engineering Laboratory.

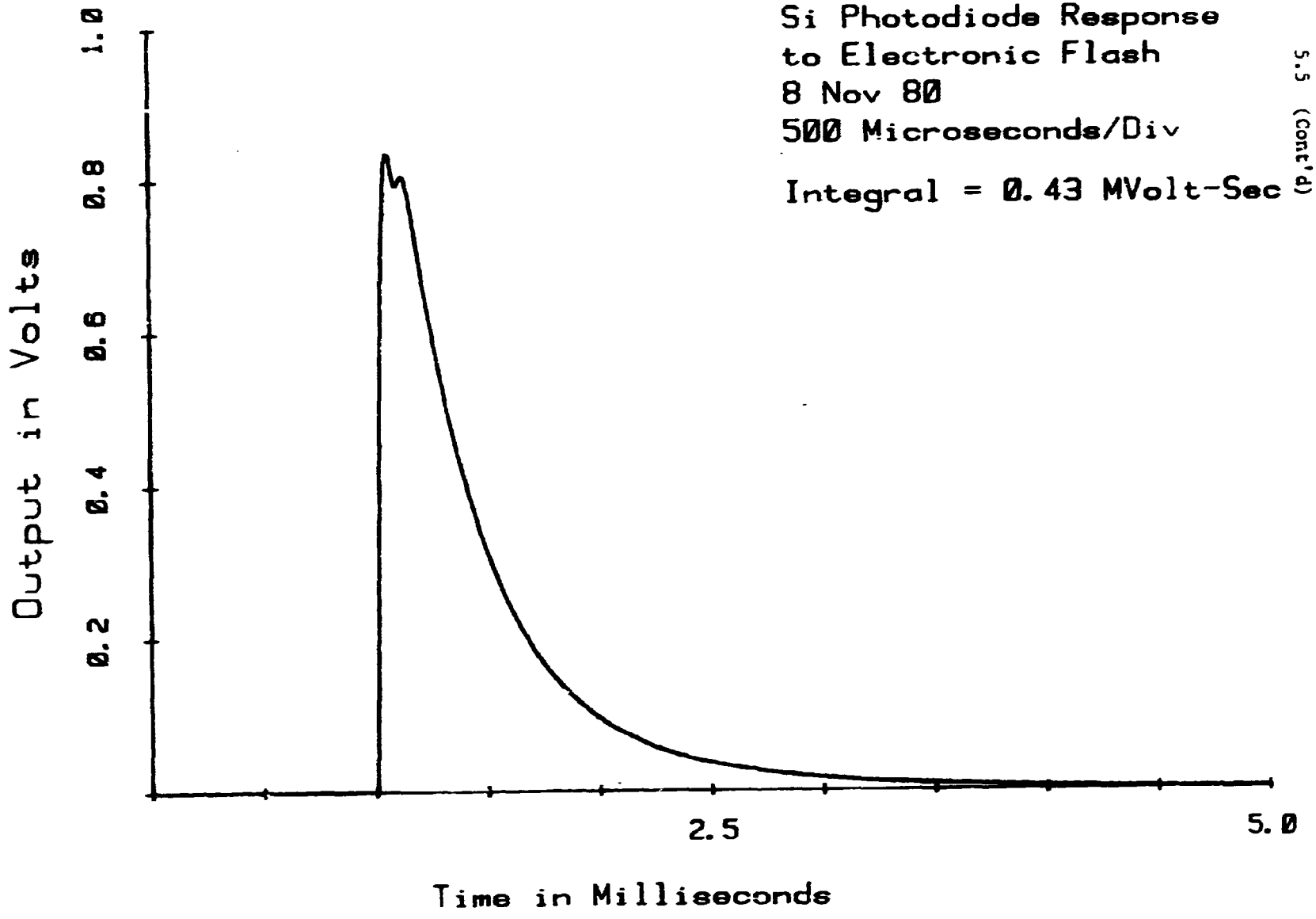

Figure 5.5-3. Silicon photodiode response measured 22 cm from an electronic flash.

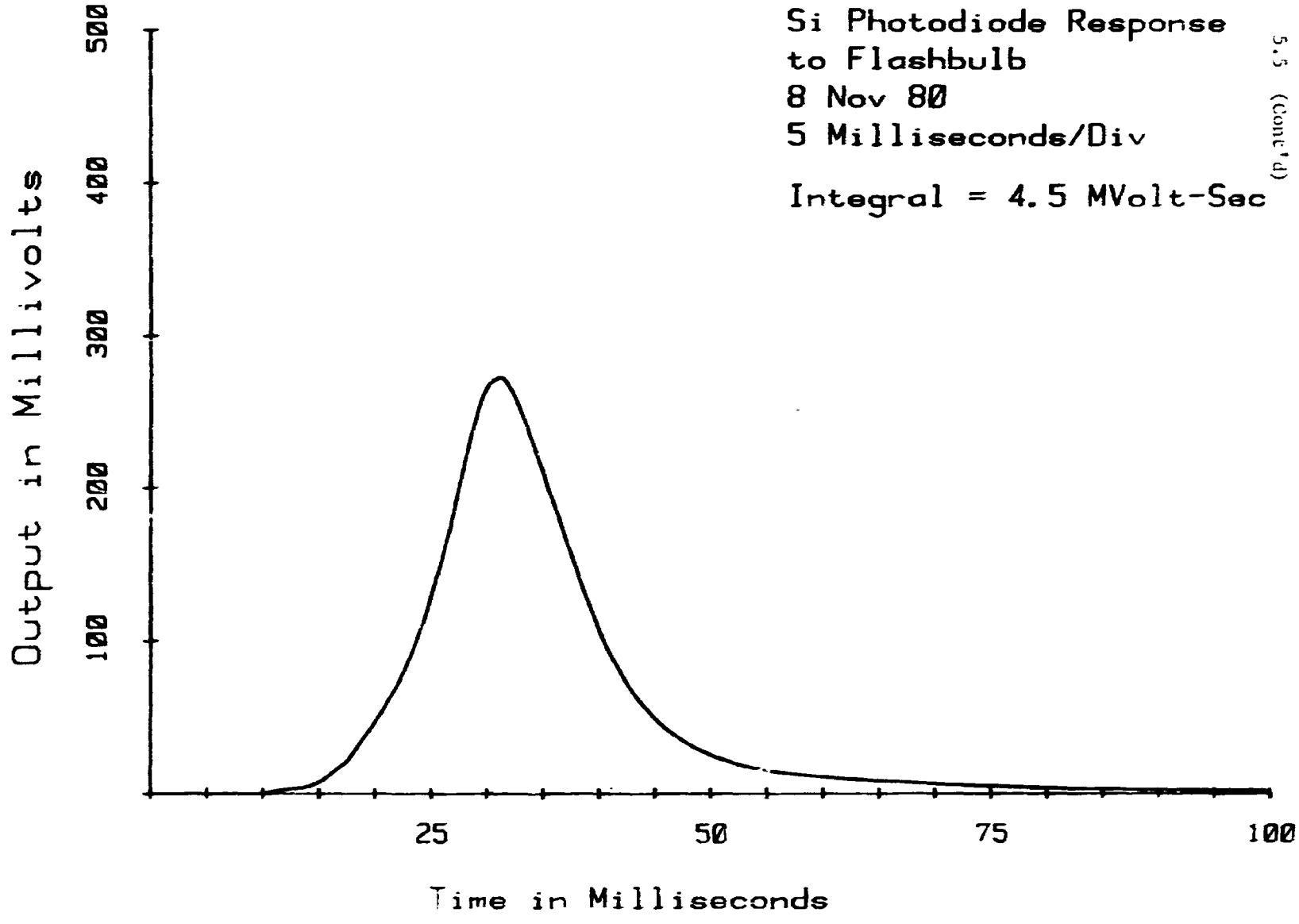

Figure 5.5-4. Silicon photodiode response measured 22 cm from a Sylvania No. 2 flashbulb.

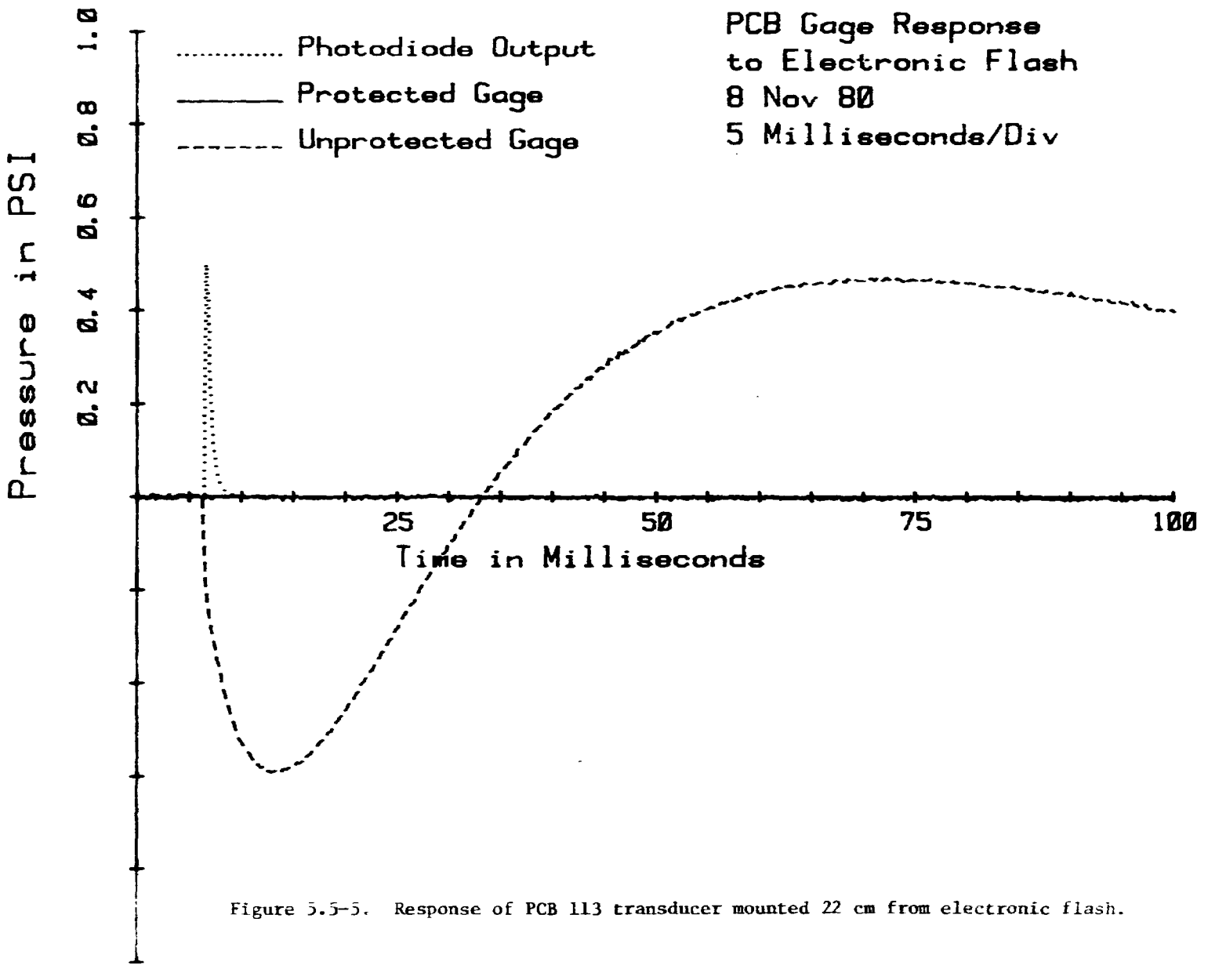

Figure 5.5-5. Response of PCB 113 transducer mounted 22 cm from electronic flash.

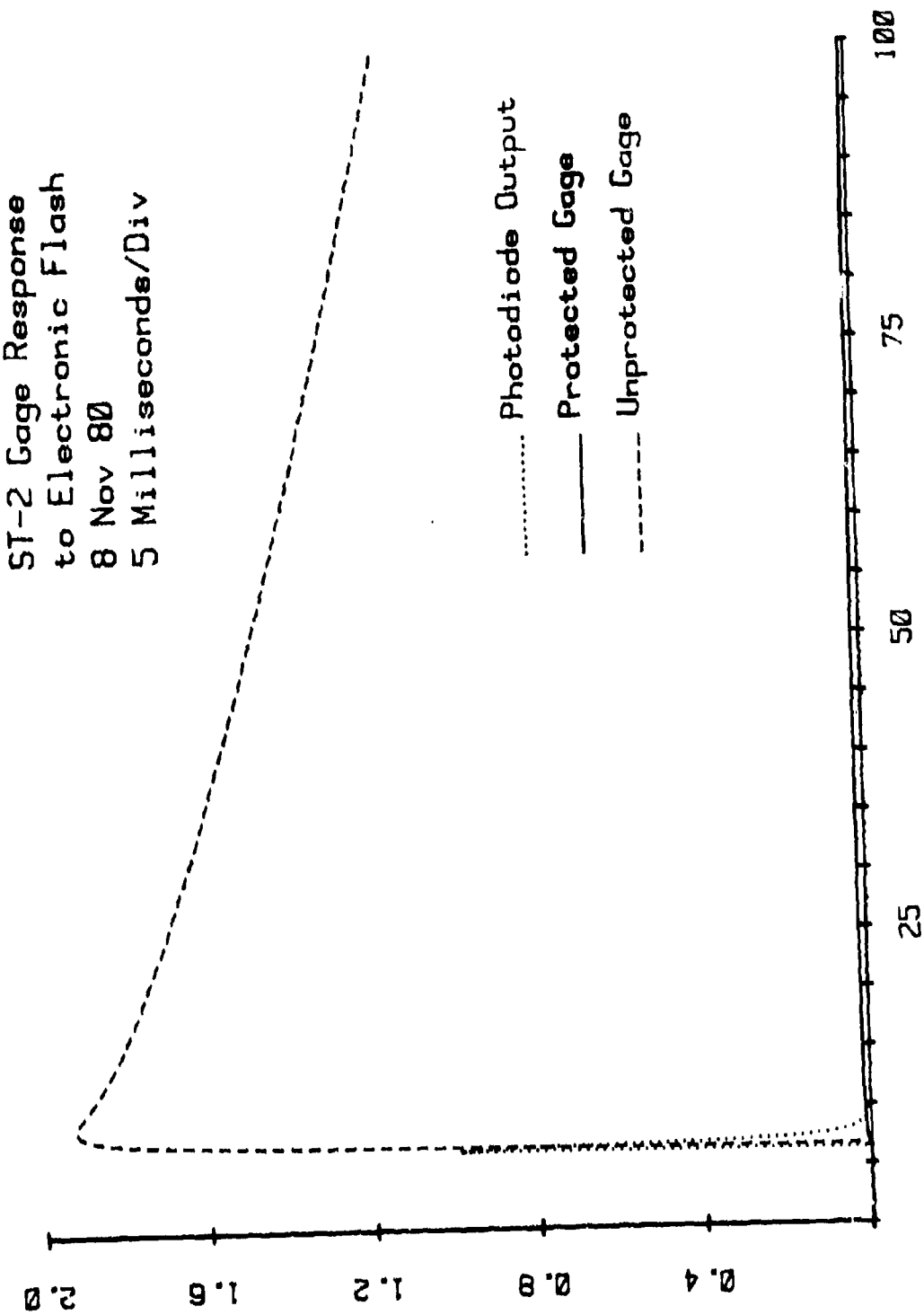

Figure 5.5-6. Response of ST-2 transducer mounted 22 cm from electronic flash.

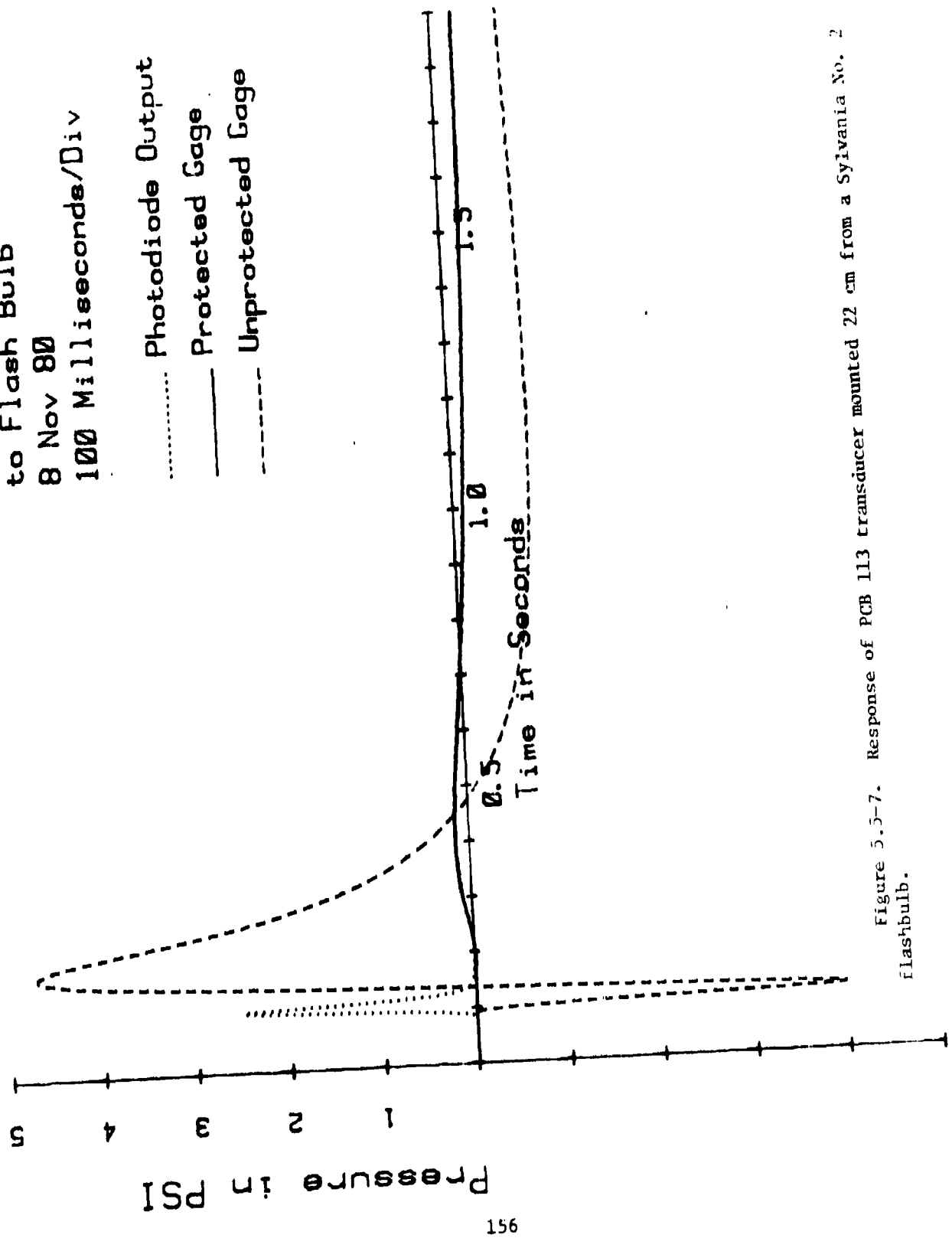

Figure 5.5-7. Response of PCB 113 transducer mounted 22 cm from a Sylvania No. 2 flashbulb.

5.5 (Cont'd)

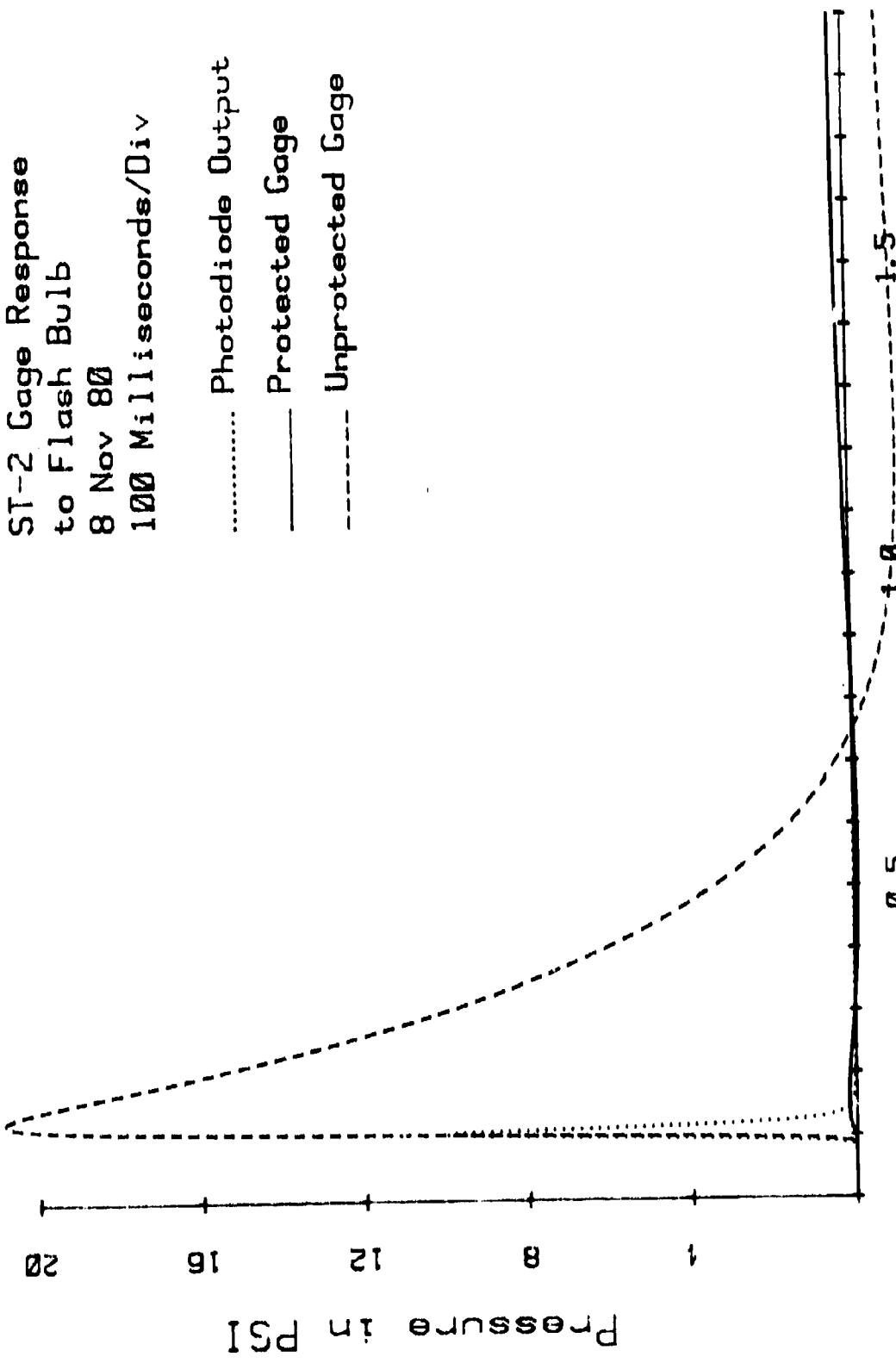

Figure 5.5-8. Response of ST-2 transducer mounted 22 cm from a Sylvania No. 2 flashbulb.

Heating the nylon cap caused it to expand more than the surrounding stainless steel. This differential expansion pushes on the crystal. Compression of the crystal is electrically interpreted as positive pressure.

Note that the unprotected ST-2 gage has roughly five times the thermal transient response of the PCB gage. When both transducers are protected, their thermal transient response is about the same.

The flashbulb produces a rather intense thermal transient, much more severe than would normally be encountered in testing. Certain test situations, such as shaped charge penetration of an armored vehicle, do, however, produce very large thermal transients.

It should also be mentioned that preliminary experiments with the Endevco gage produced immediate full scale deflection when it was subjected to any kind of flash. This result is caused by the fact that the diffused silicon diaphragm in the Endevco gage is photosensitive.

Because the Endevco gage is so sensitive to light, the technique described above could not be used to test its sensitivity to thermal transient. Other experiments, such as immersing the transducer in water at different temperatures, indicated that the Endevco gage had very little response to thermal transients that did not produce light.

An informative discussion of thermal sensitivity of transducers and ways to reduce thermal sensitivity can be found in a study conducted at the National Bureau of Standards (ref 10). Additional information can be found in a study conducted by Coulter at the US Army Ballistic Research Laboratory (ref 11).

5.6 THERMAL DRIFT IN FIELD MEASUREMENTS

When the transducers discussed in this report were used to measure very small pressures ($\sim$ 2 kPa), very small thermal gradients can cause problems. Changes in temperature caused by a small breeze cooling the transducer, or the sun going behind a cloud cause very minor contraction and expansion of the transducer housing.

If the instrumentation time constant is long and the pressure level is small, measurements such as the example shown in figure 5.6-1 can result. The fact that any measurement at all was obtained tends to understate the situation that day.

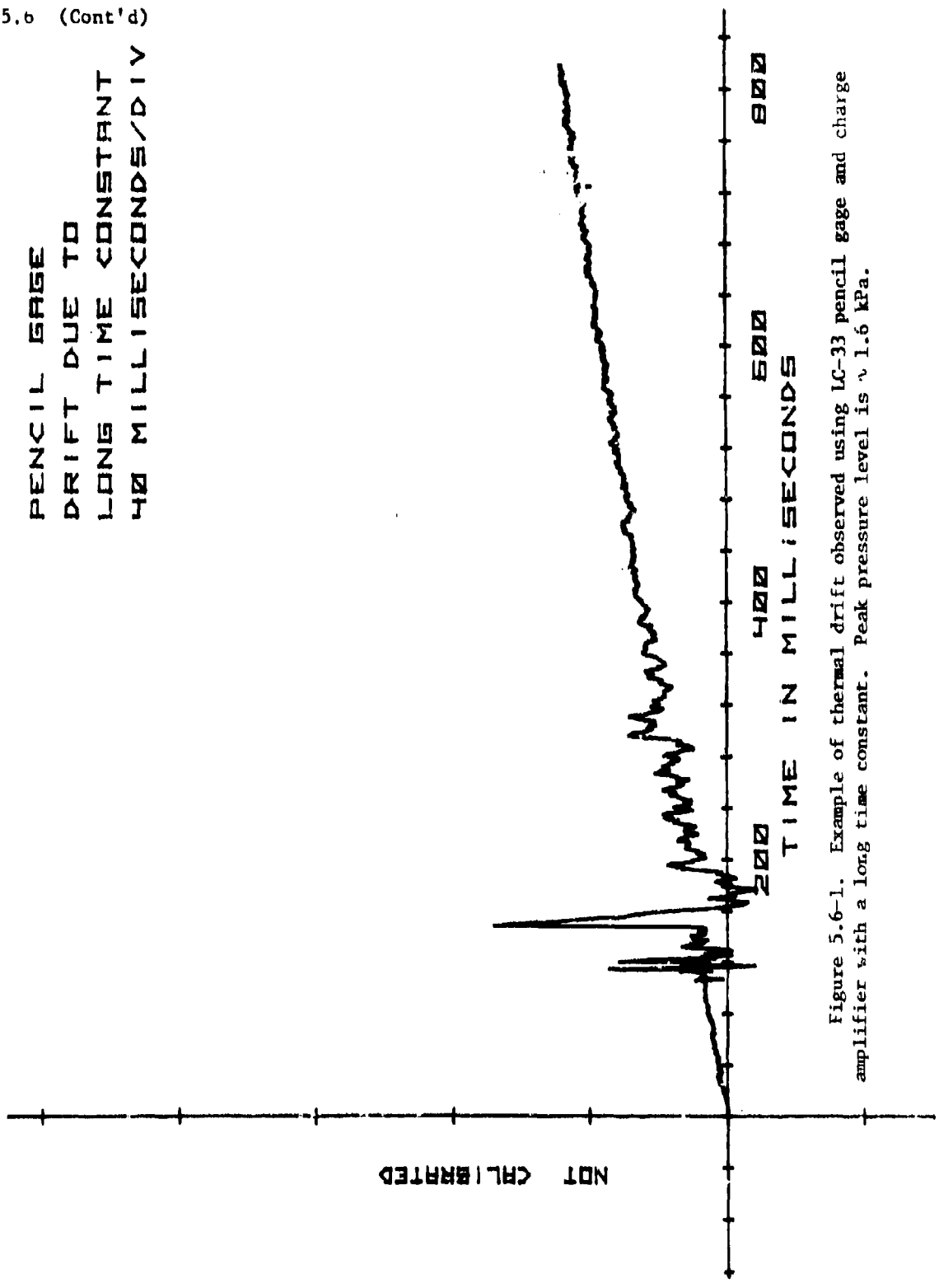

Figure 5.6-1. Example of thermal drift observed using LC-33 pencil gage and charge amplifier with a long time constant. Peak pressure level is ~ 1.6 kPa.

5.6 (Cont'd)

The charge amplifier output would drift first in one direction, and then in the opposite direction, sometimes slowly, sometimes rapidly. At the time the round was fired, the charge amplifier was being reset to zero every 1/2 second. The fact that the pressure wave did not arrive while the amplifier was being reset was purely chance.

The signal conditioning for all crystal type transducers is AC-coupled. By changing the low-frequency rolloff characteristics of the signal conditioning, thermal drift can be filtered out. There is a danger, however, that this filtering will also distort the pressure measurement.

An experiment was conducted by artificially changing the low-frequency rolloff characteristics of several transducers. The relationship between time constant and low-frequency rolloff is:

$$f_o = \frac{0.16}{TC}$$

where

f_o = rolloff frequency (-3 db down point) in Hz.
TC = time constant in seconds.

Transducers with different time constants were used to measure muzzle blast 100 meters from a 105-mm tank gun. The results are shown in figures 5.6-2 through 5.6-6 and summarized in table 5.6-1.

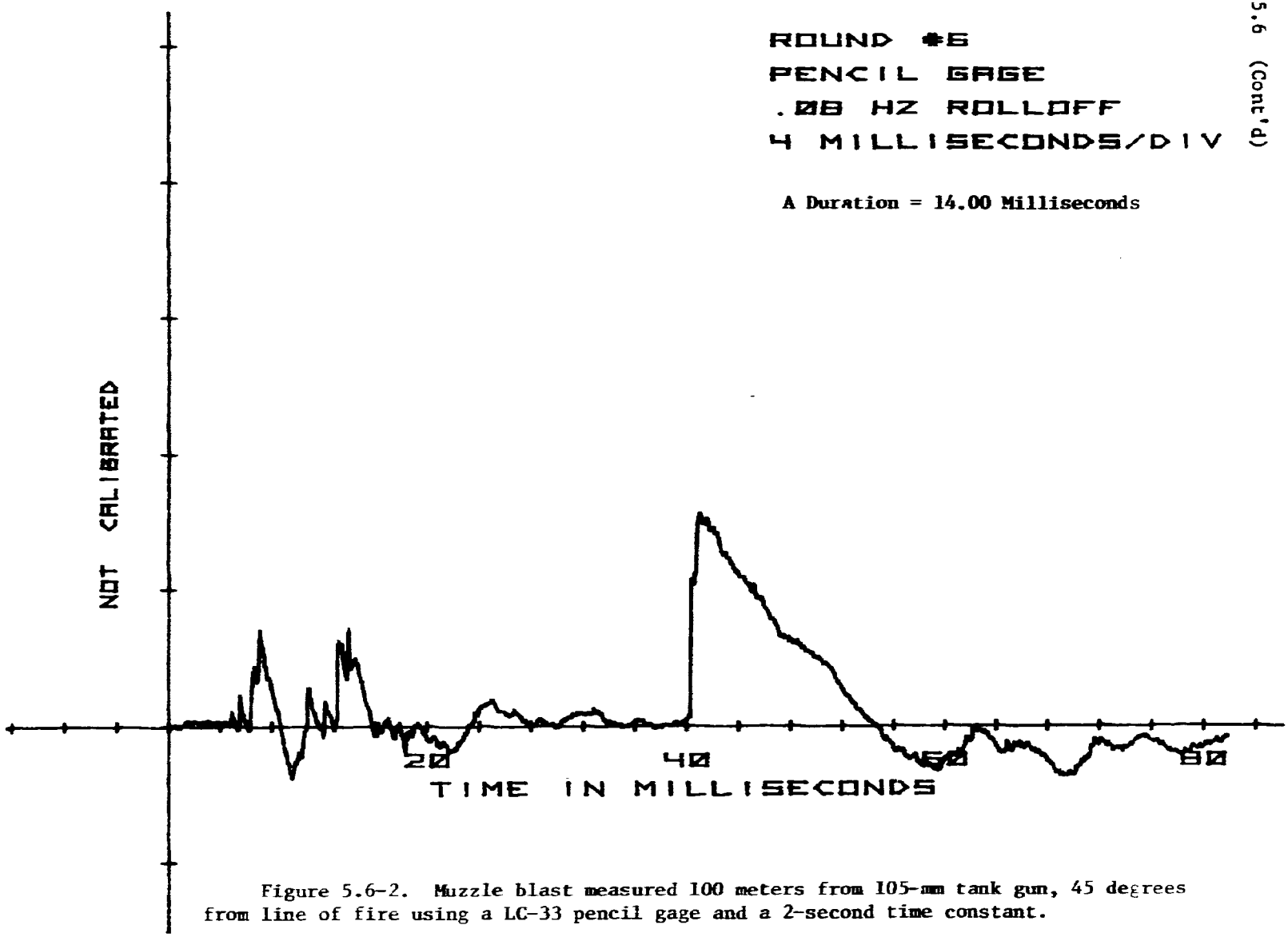

Figure 5.6-2. Muzzle blast measured 100 meters from 105-mm tank gun, 45 degrees from line of fire using a LC-33 pencil gage and a 2-second time constant.

5.6 (Cont'd)

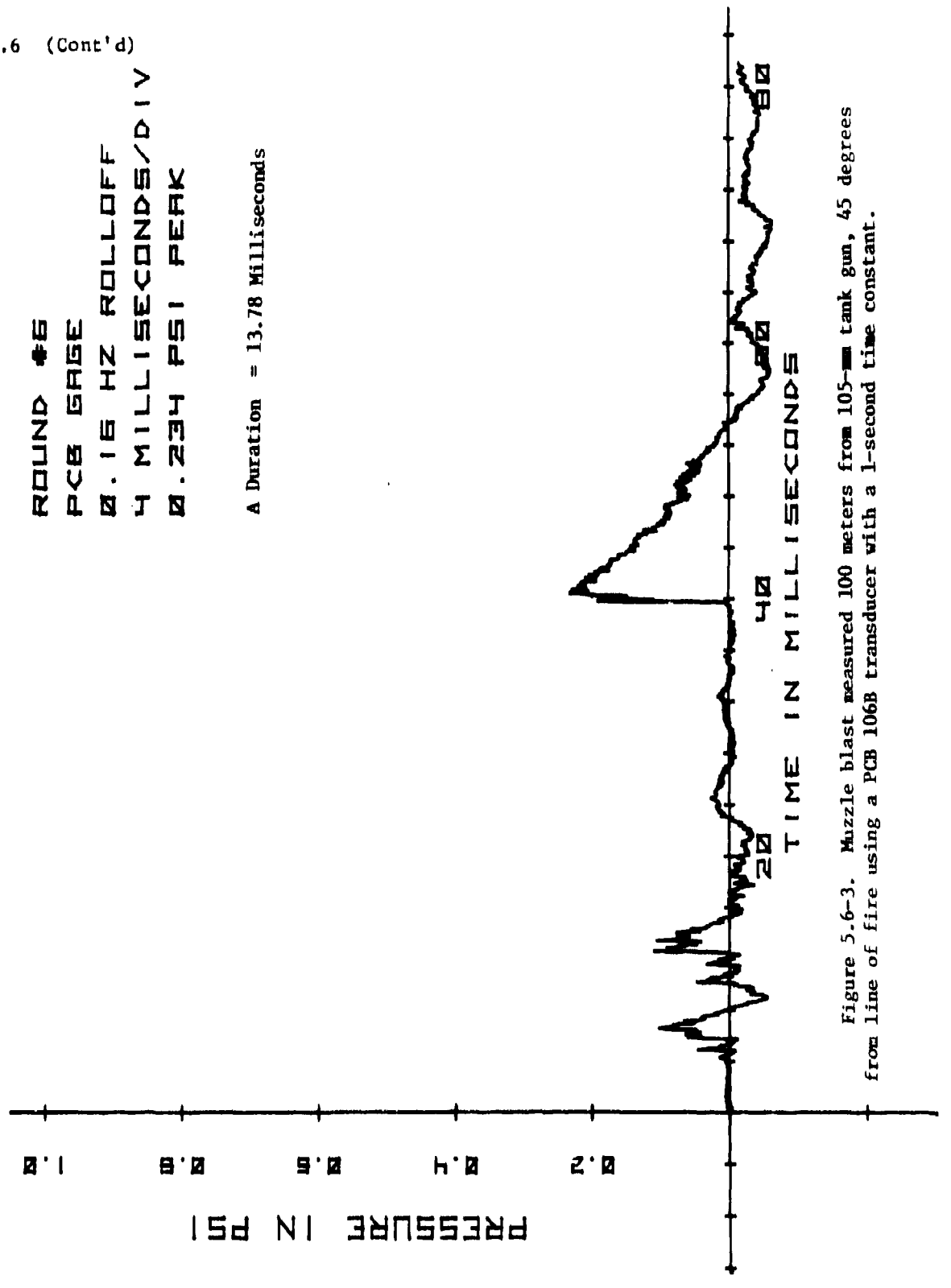

Figure 5.6-3. Muzzle blast measured 100 meters from 105-mm tank gun, 45 degrees from line of fire using a PCB 106B transducer with a 1-second time constant.

5.6 (Cont'd)

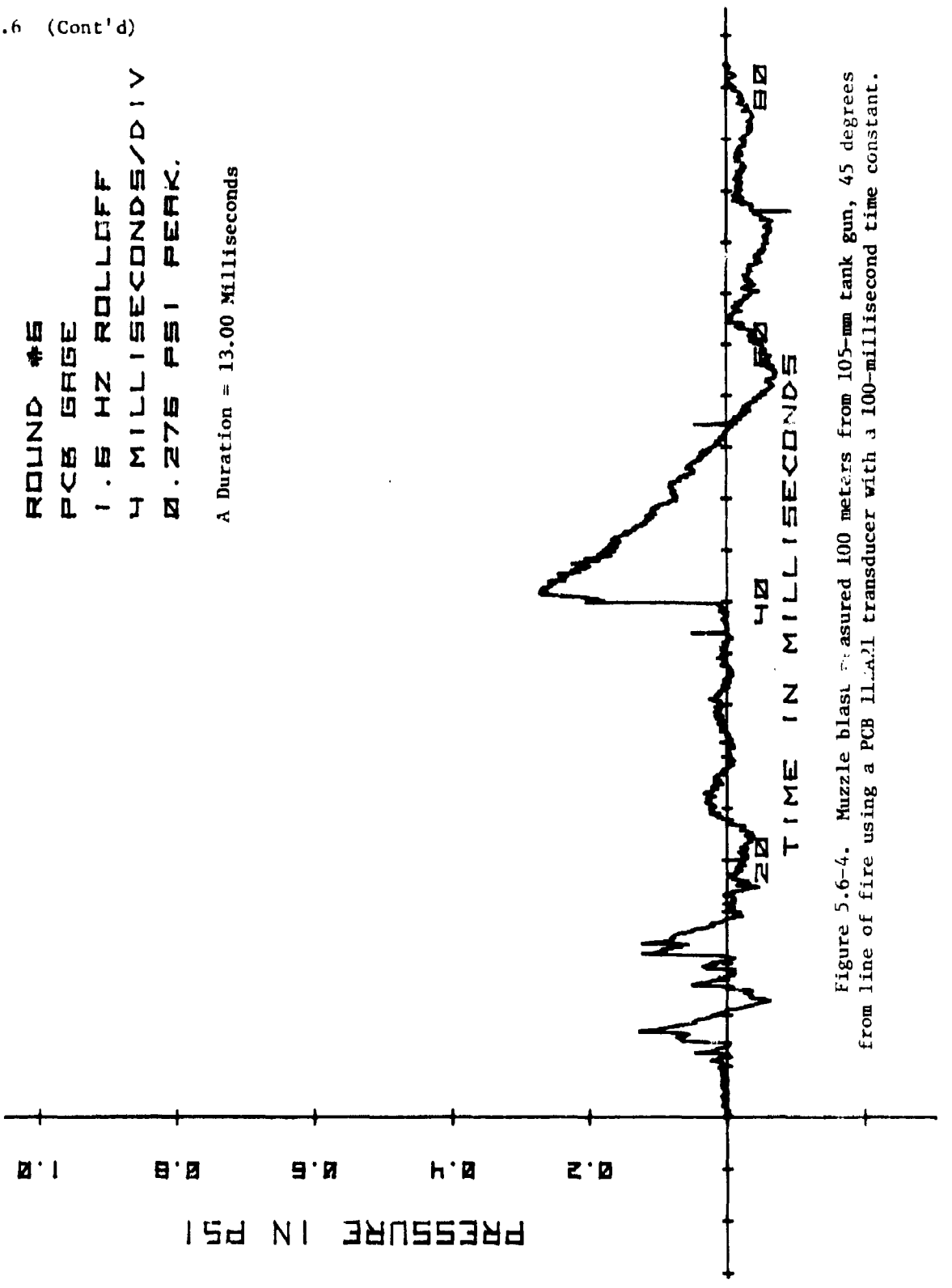

Figure 5.6-4. Muzzle blast measured 100 meters from 105-mm tank gun, 45 degrees from line of fire using a PCB 113A21 transducer with a 100-millisecond time constant.

5.6 (Cont'd)

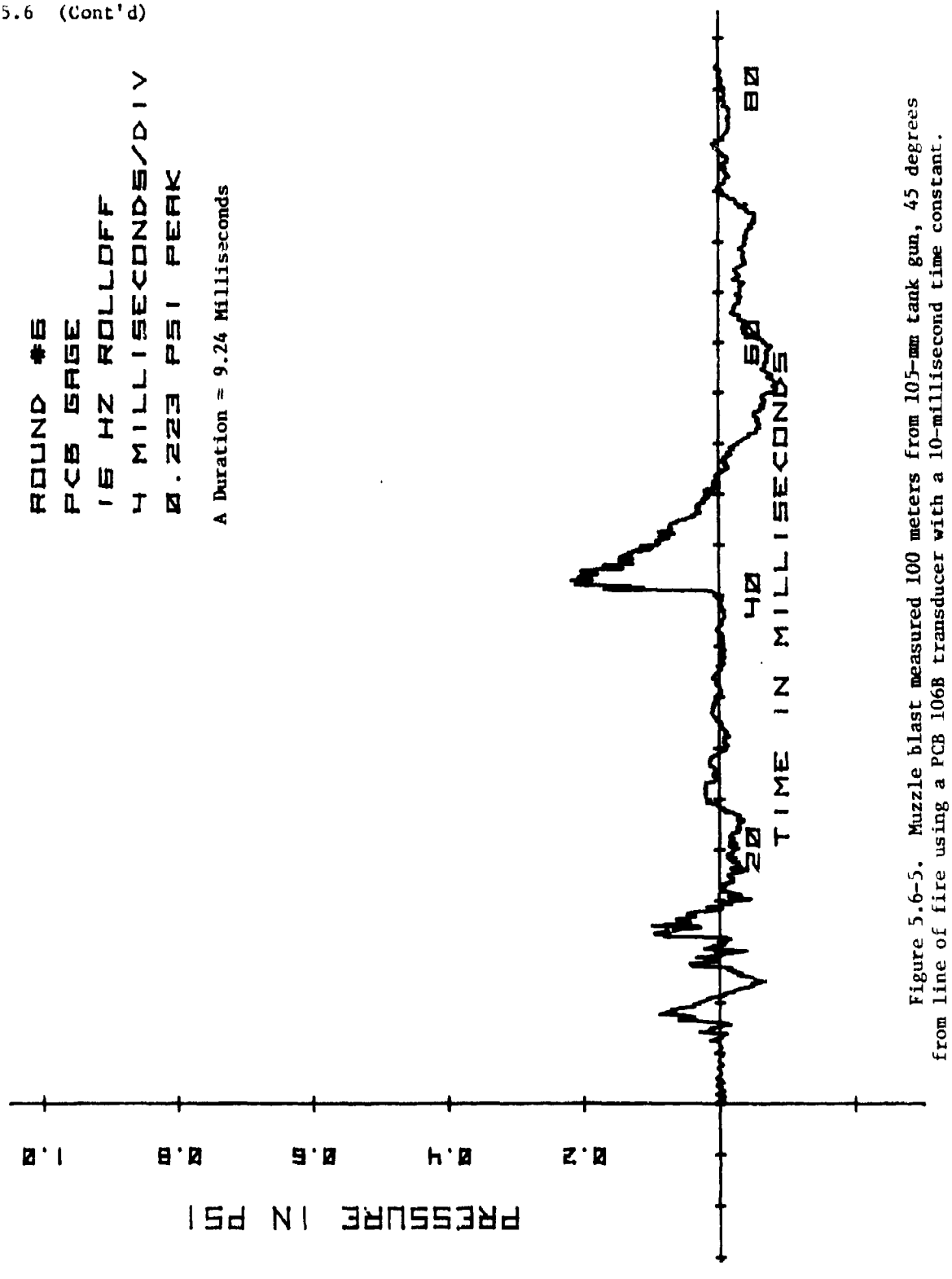

Figure 5.6-5. Muzzle blast measured 100 meters from 105-mm tank gun, 45 degrees from line of fire using a PCB 106B transducer with a 10-millisecond time constant.

5.6 (Cont'd)

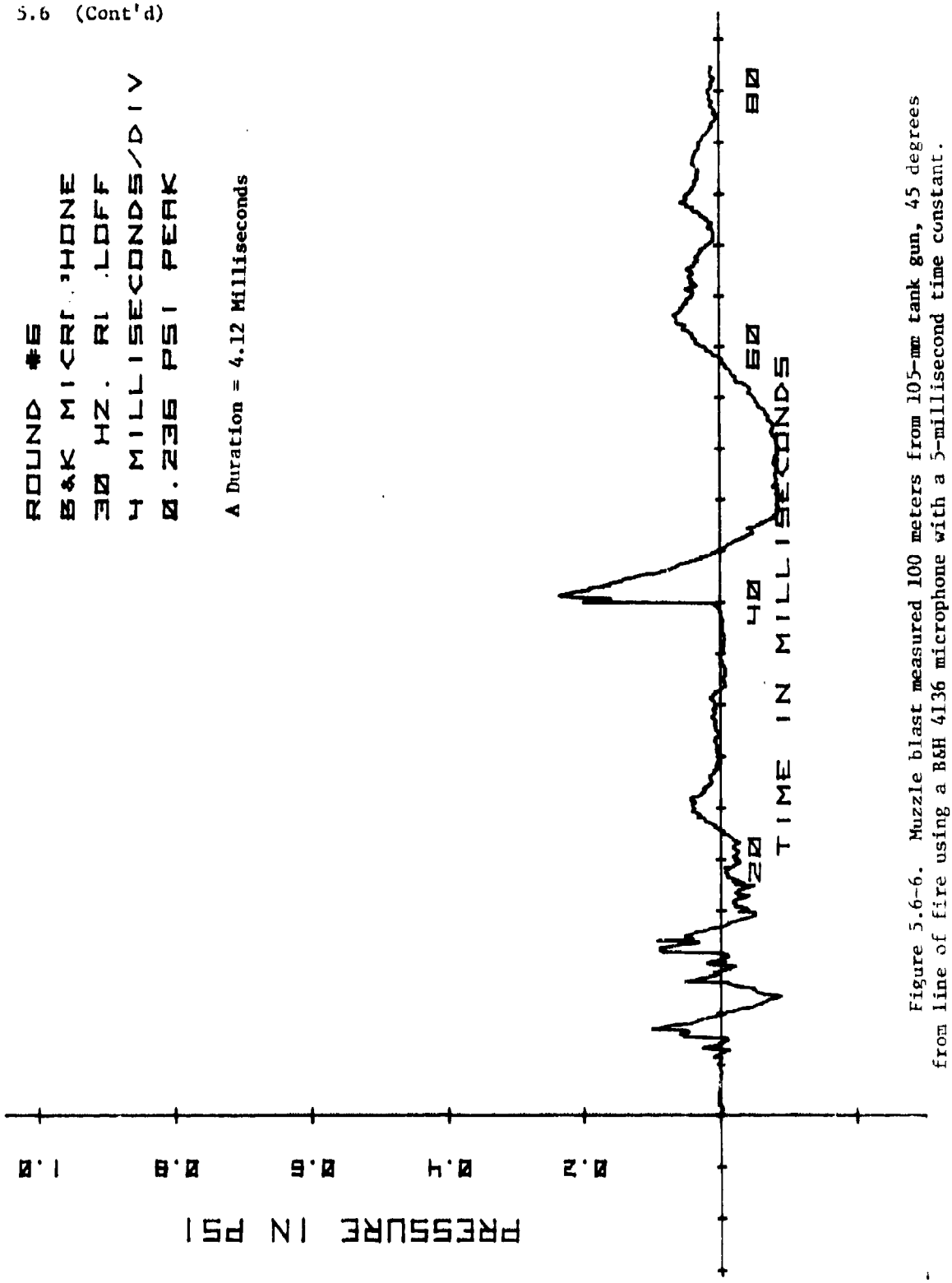

Figure 5.6-6. Muzzle blast measured 100 meters from 105-mm tank gun, 45 degrees from line of fire using a B&H 4136 microphone with a 5-millisecond time constant.

5.6 (Cont'd)

TABLE 5.6-1. SUMMARY OF THE RESULTS OF ROUND 6, 5 JULY 1979

Channel	Transducer	Low Frequency Rolloff (Hz)	Time Constant (sec)	Peak Pressure (kPa)	A-Duration (ms)
6	LC-33 pencil gage	0.08	2	-	14.00
7	PCB 106B	0.16	1	1.61	13.78
9	PCB 112A21	1.6	0.1	1.90	13.00
8	PCB 106B	16	0.01	1.61	9.24
1	B&K microphone	30	0.005	1.63	4.12

A mathematical model of an RC high-pass filter with a 6 dB/octave rolloff rate was constructed. A waveform similar to a blast wave was mathematically generated. This simulated blast wave was used as in input to high-pass filters with various rolloff frequencies.

The results of this mathematical exercise are shown in figure 5.6-7. These mathematical results agree quite well with the experimental results from round 6. Note the large discrepancy between the original waveform and the response of a circuit with a 30 Hz rolloff frequency.

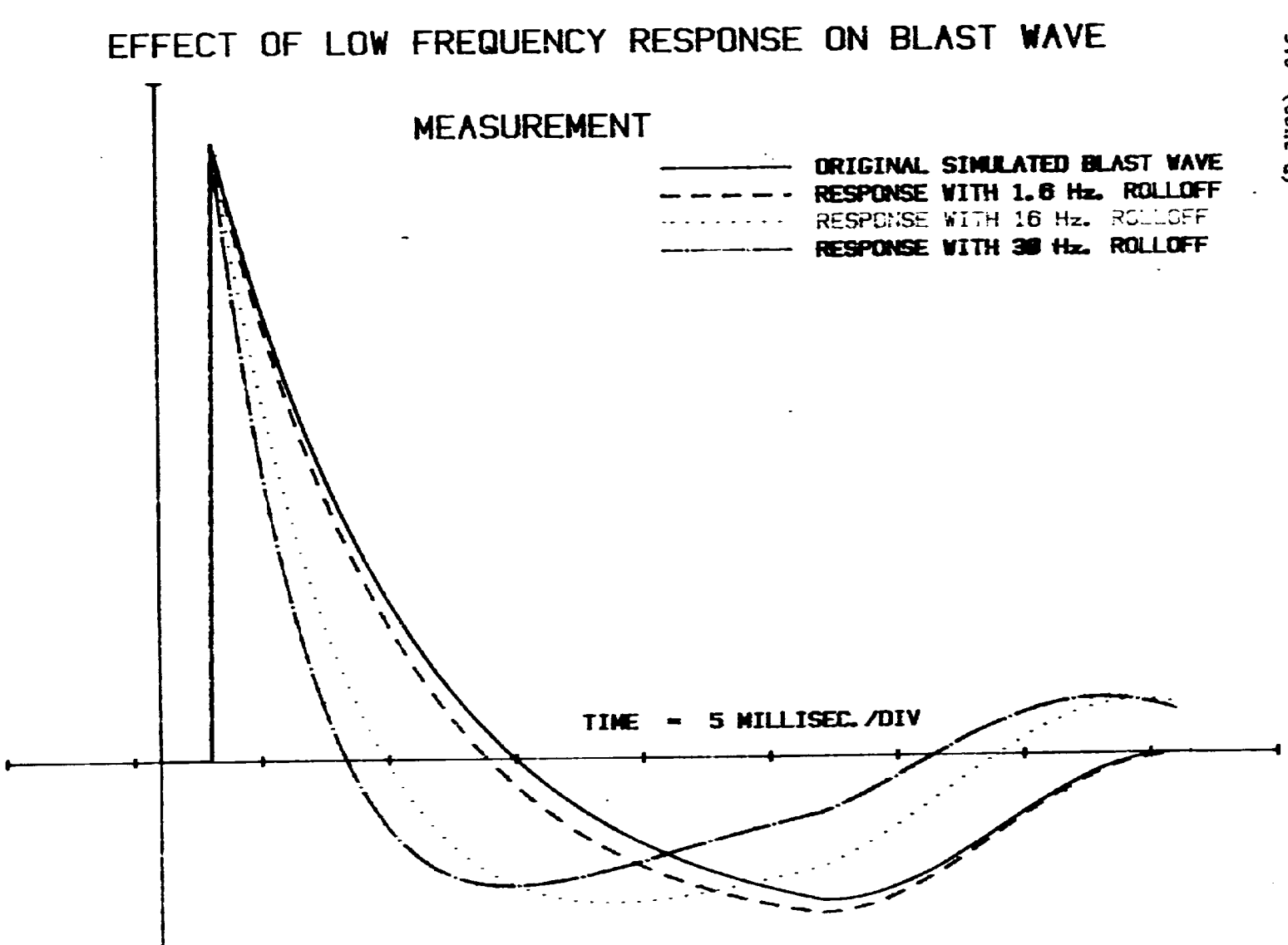

Figure 5.6-7. Mathematically calculated response of different high-pass RC filters with 6 dB/octave rolloff.

5.7 EFFECTS OF TEST SITE LAYOUT

The test site should be an open, flat area, clear of obstacles. Exactly how far the nearest obstacle can be to the transducers depends on the blast source. The following example illustrates how test site layout can affect blast measurements.

Figure 5.7-1 is a scale drawing of a layout that was used to make some measurements of the muzzle blast of the M198 howitzer. Note the proximity of the bombproofs (for test crew protection) to the weapon. Figures 5.7-2 through 5.7-4 are photographs of the test site.

Figures 5.7-5 through 5.7-8 show the outputs of the four transducers. This test produced two interesting observations:

a. Reflections from the bombproofs were occasionally greater than 10% of the peak pressure and therefore affected "B" duration.

b. In some cases, the peak pressure measured by the LC-33 pencil gage was caused by the ground reflection, whereas the peak pressure measured by the ST-2 gage was always caused by the initial blast wave.

In reference to observation No. 1, note the pressure pulse that appears 84 milliseconds after the primary wave on channels 1 and 2, and appears 88 milliseconds after the primary wave on channels 3 and 4. This pulse seems to be caused by reflection from bombproofs 2 and 3, as shown in figure 5.7-1. The following calculations confirm that suspicion:

Distance from muzzle to bombproof 2 and 3 and back to CH 1 and 2	123.6 feet
Distance from muzzle to CH 1 and 2	- 21.5 feet
	102.1 feet
Time for an acoustic wave traveling at speed of sound to go 102.1 feet	91 milliseconds
Distance from muzzle to bombproof 2 and 3 and back to CH 3 and 4	129.5 feet
Distance from muzzle to CH 3 and 4	- 22.3 feet
	107.2 feet
Time for an acoustic wave traveling at speed of sound to go 107.2 feet	96 milliseconds

5.7 (Cont'd)

TEST SITE FOR M198 BLAST TEST

23 April 1980

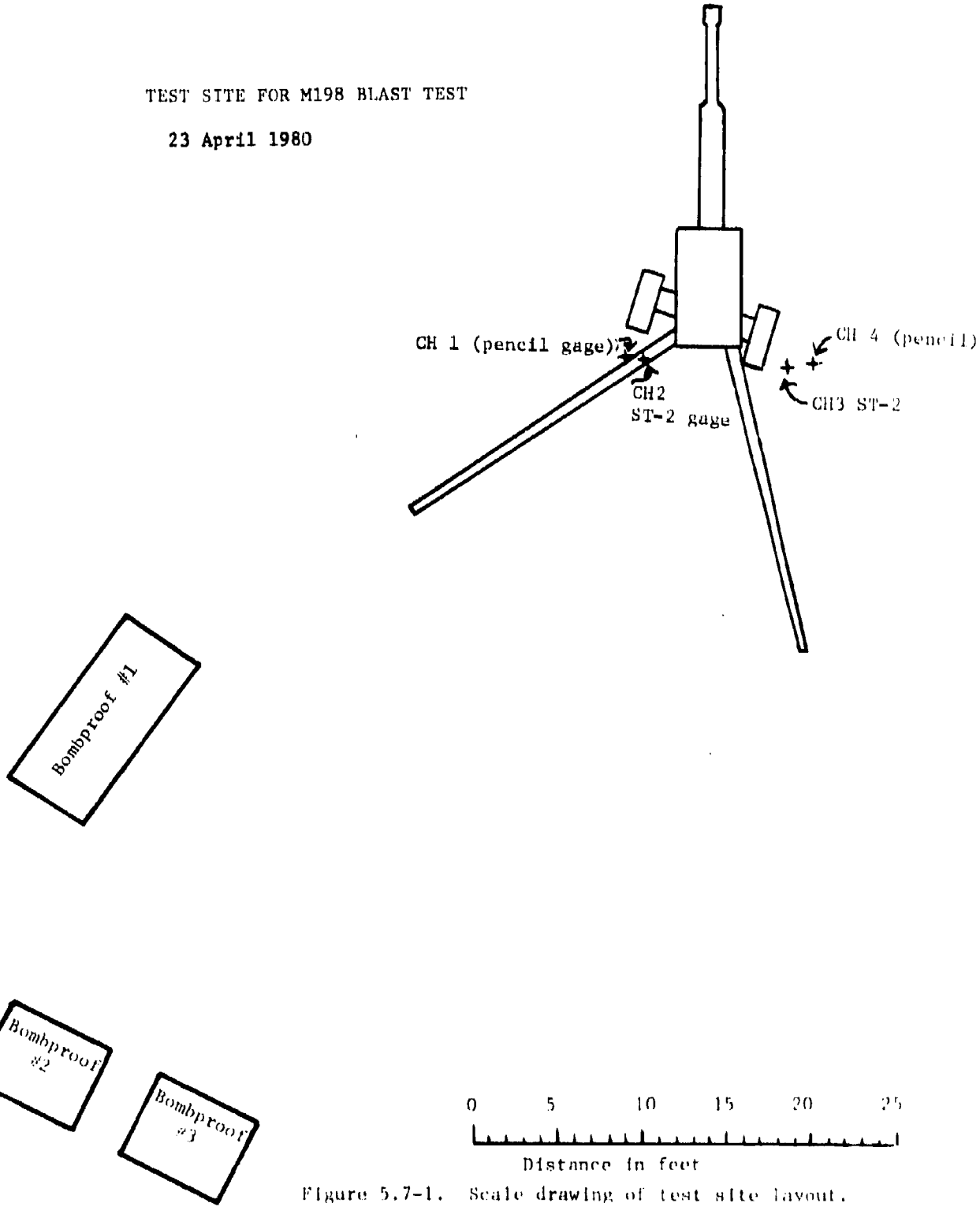

Figure 5.7-1. Scale drawing of test site layout.

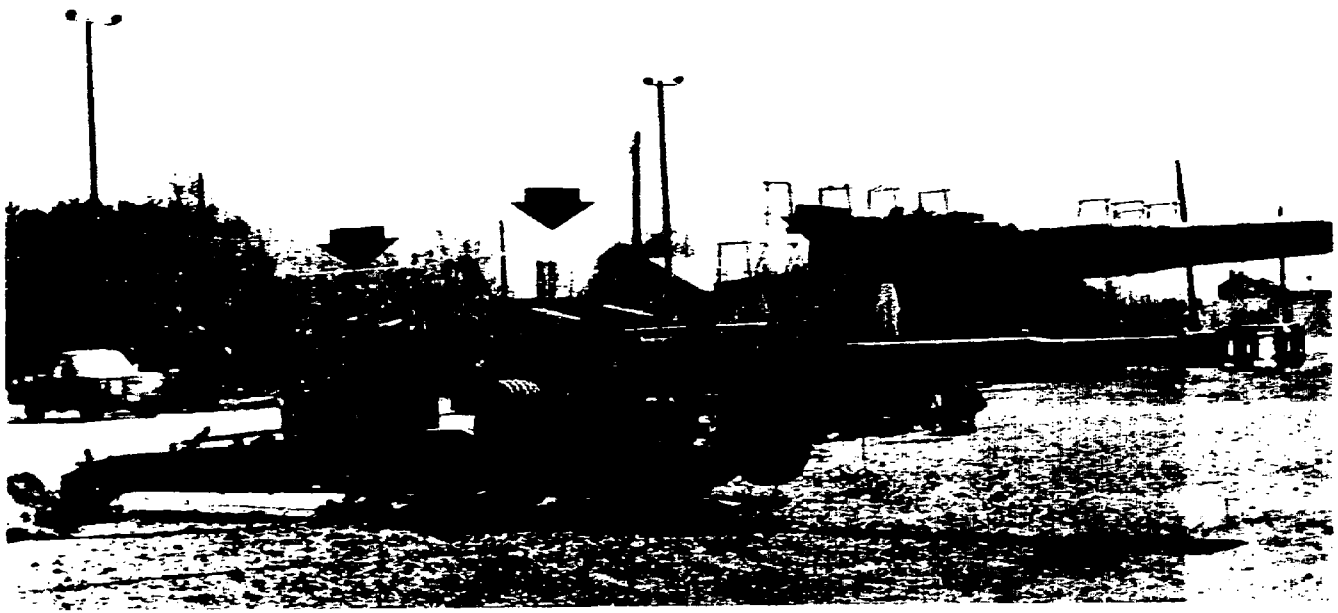

Figure 5.7-2. Photograph of test site. Large arrows point to bombproofs.

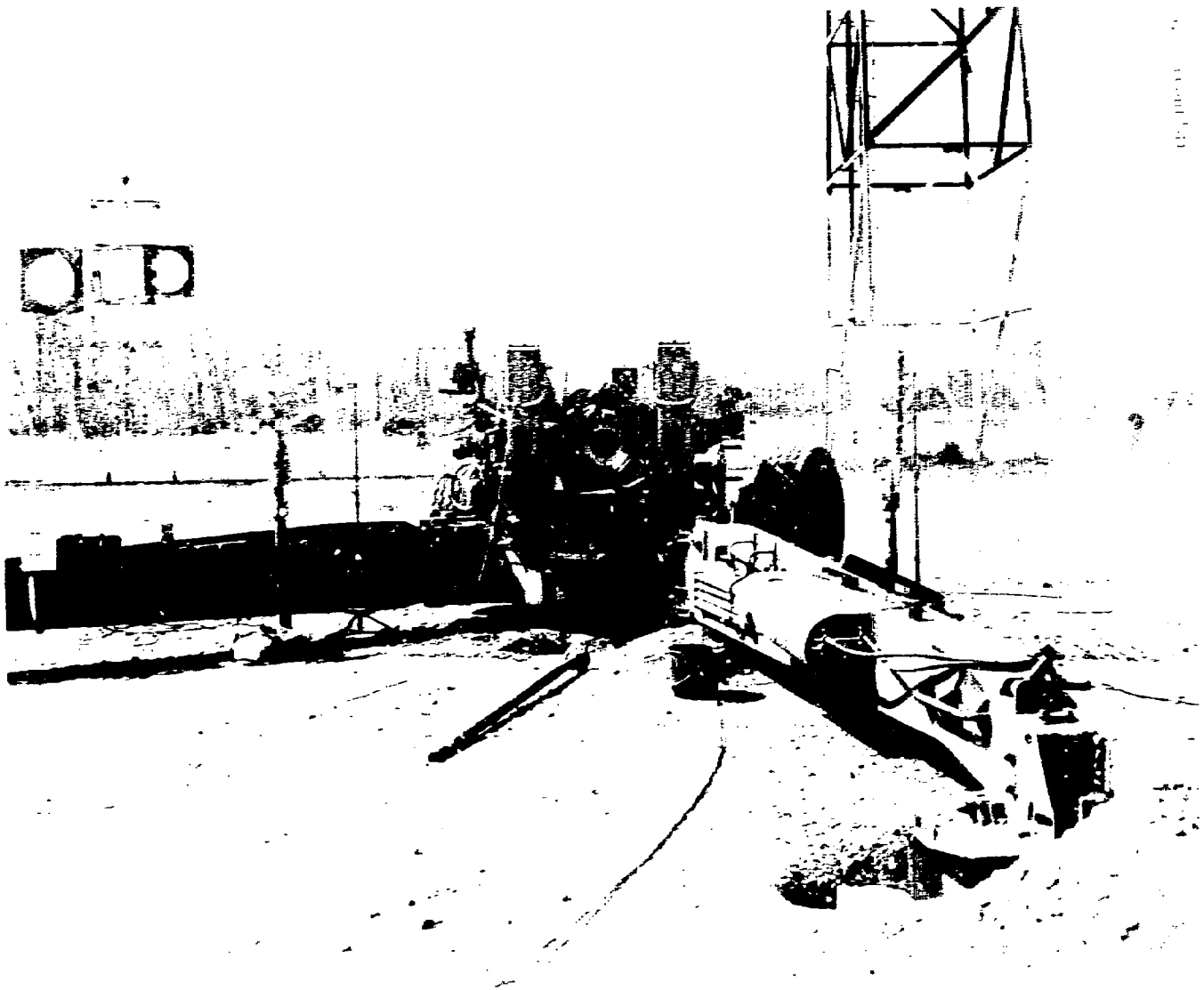

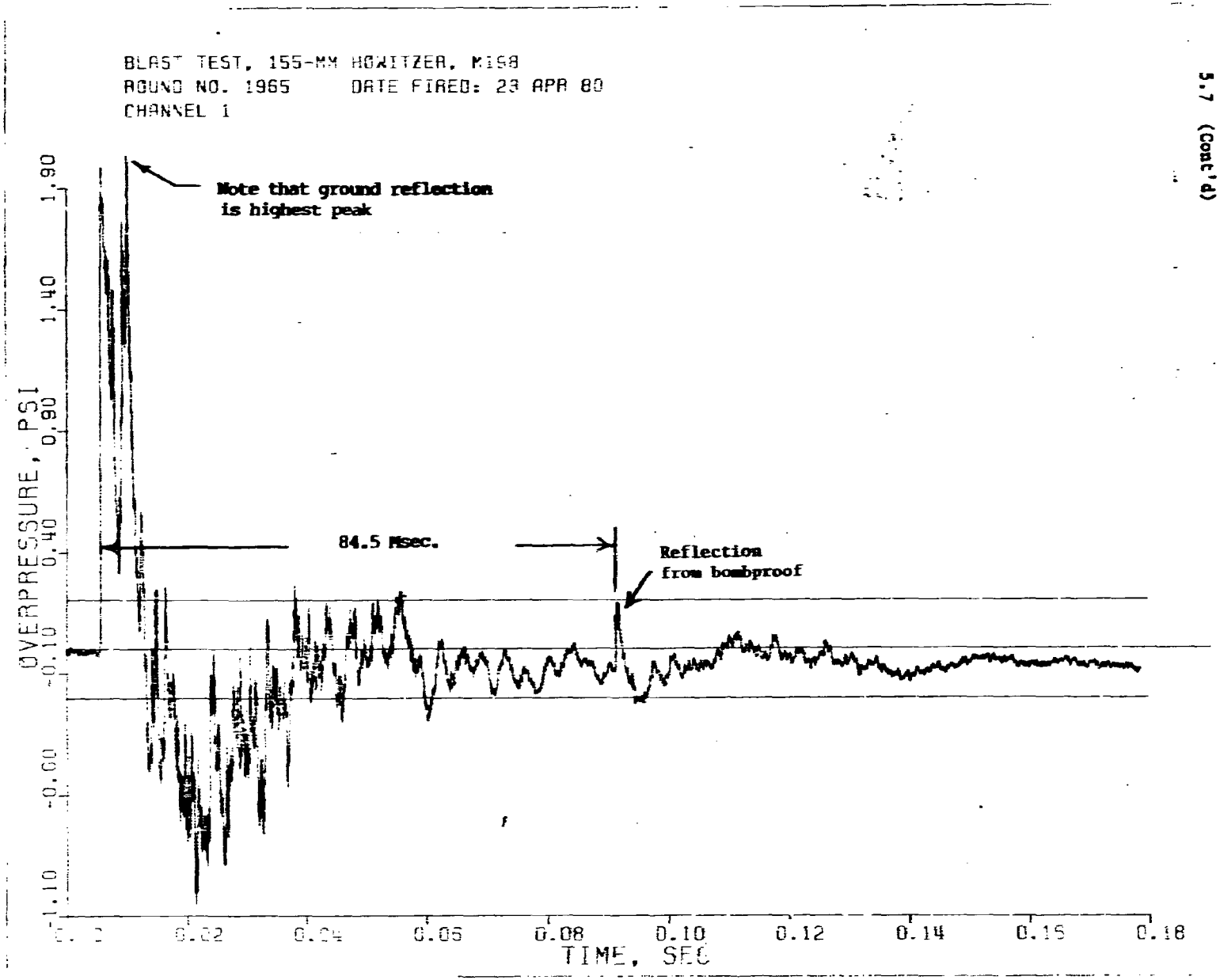

Figure 5.7-5. Output of LC-33 pencil gage in crew location (channel 1).

5.7 (Cont'd)

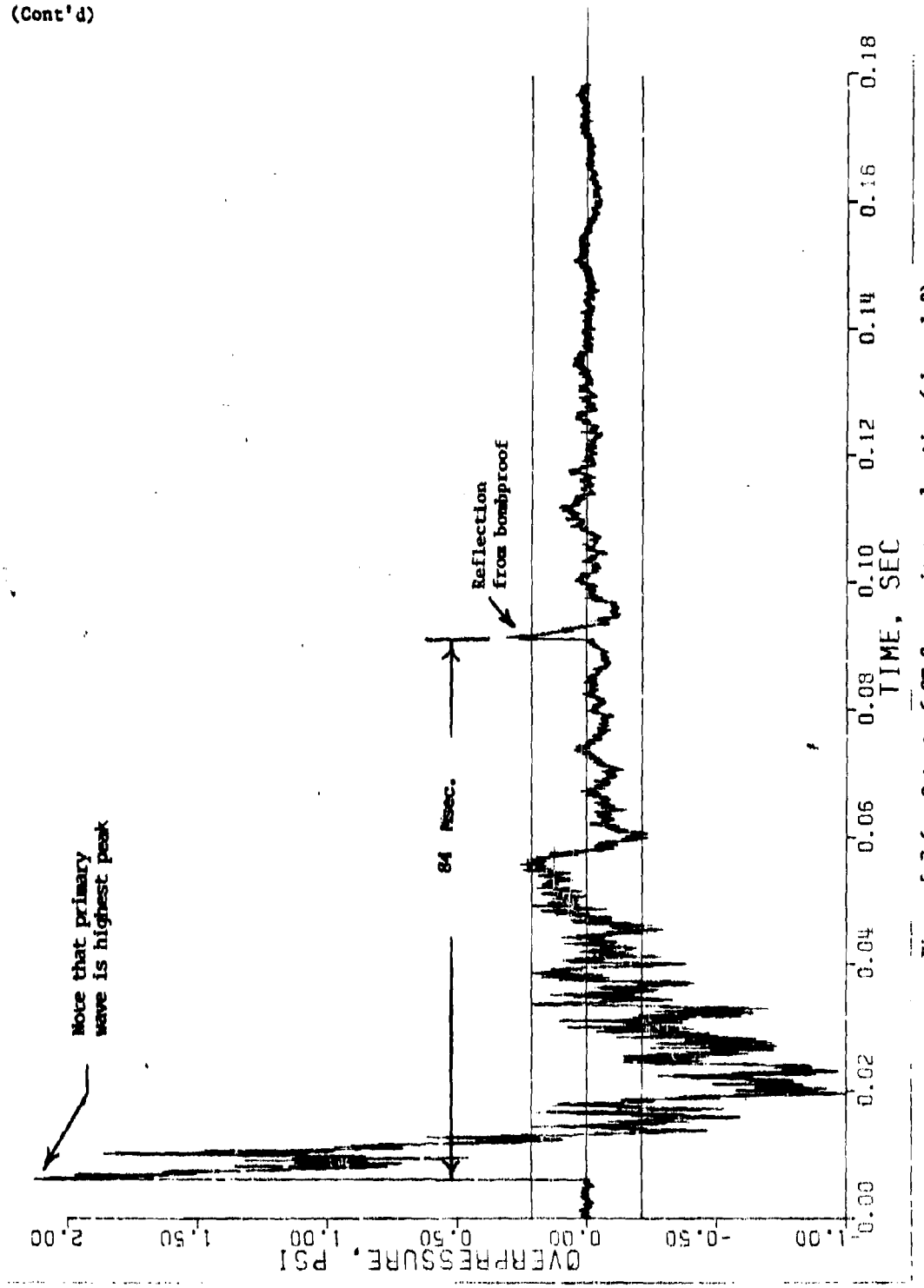

Figure 5.7-6. Output of ST-2 gage in crew location (channel 2).

5.7 (Cont'd)

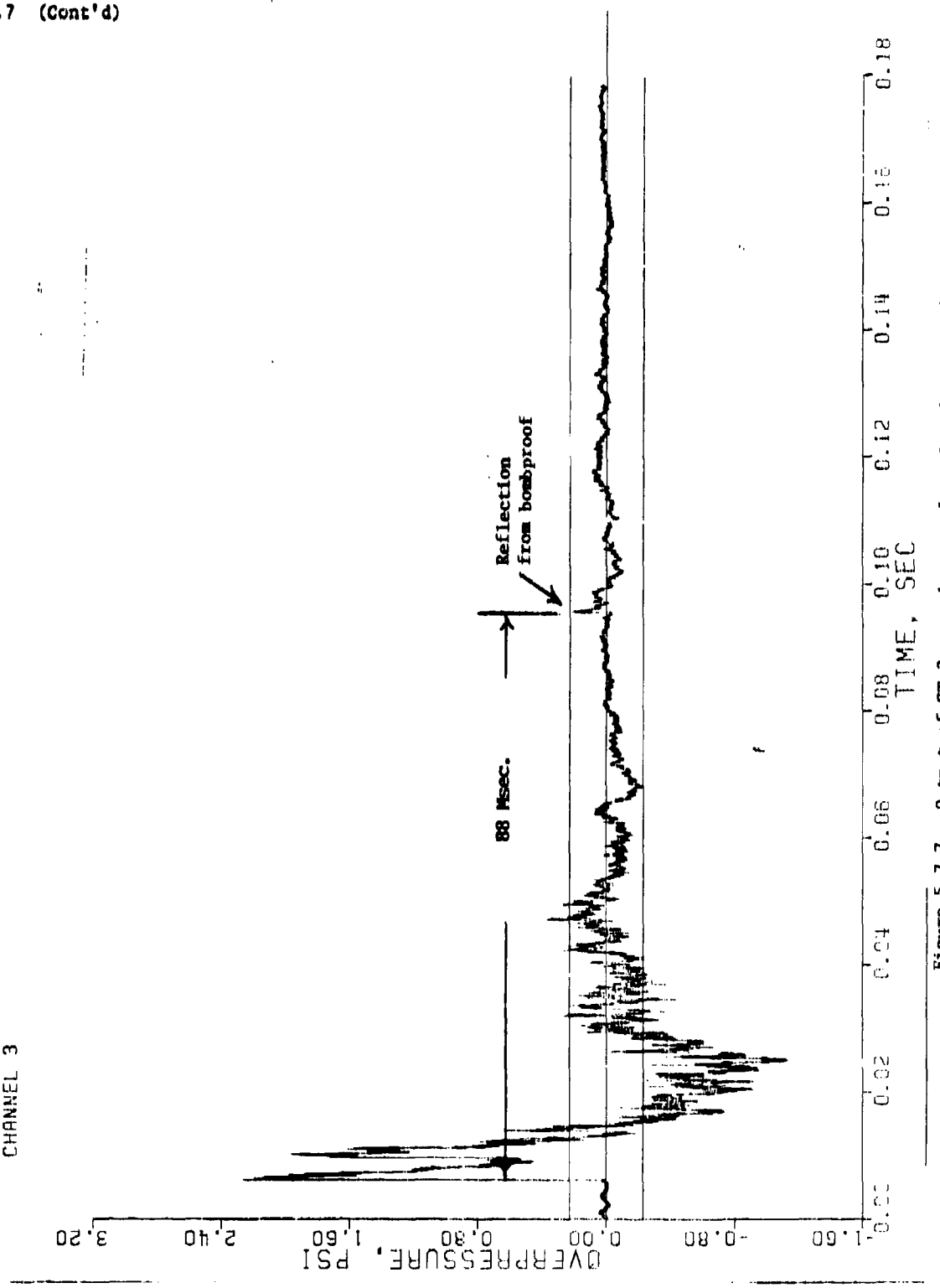

Figure 5.7-7. Output of ST-2 gage in crew location (channel 3).

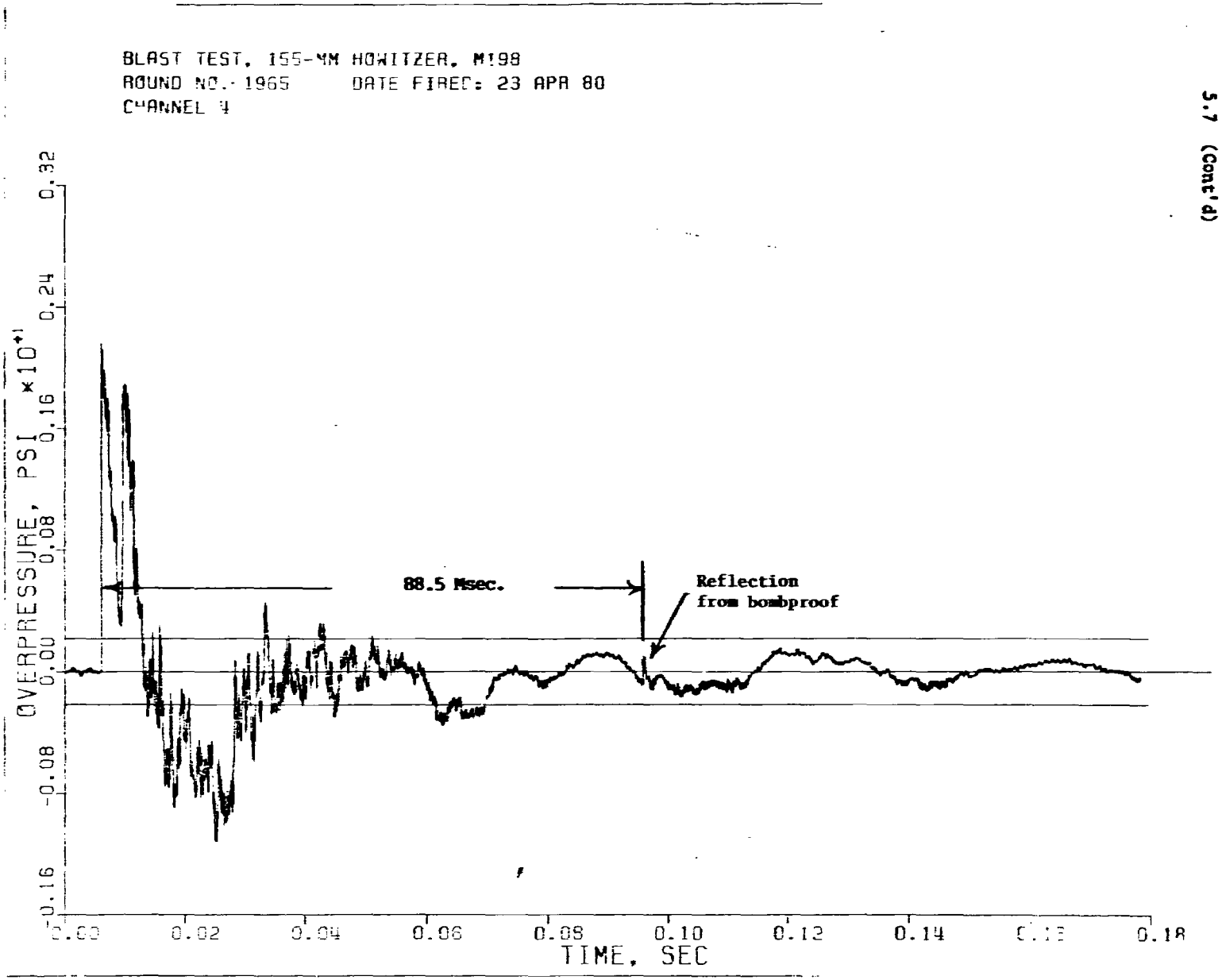

Figure 5.7-8. Output of LC-33 pencil gage in crew location (channel 4).

5.7 (Cont'd)

Since a blast wave travels faster than the speed of sound, a careful calculation of the transit times using the actual velocities (which are a function of blast pressure) would produce shorter transit times. The above rough calculations are so close to the observed transit times that a more sophisticated calculation is unnecessary.

The effect of bombproof No. 2 and 3 on the pressure time curve is clear. The effect (if any) of bombproof No. 1 is not clear. It does seem advantageous to insure that flat surfaces do not face directly toward the source of blast.

In reference to observation No. 2, the directional sensitivity of the LC-33 pencil gage and the blunt cylinder mount explains this observation. As shown in figure 5.7-9, note that at negative misalignment angles, the blunt cylinder mount attenuates more than the LC-33. It is estimated that a ground reflection would strike the transducer at an angle that corresponds to approximately -30 degrees on figure 5.7-1.

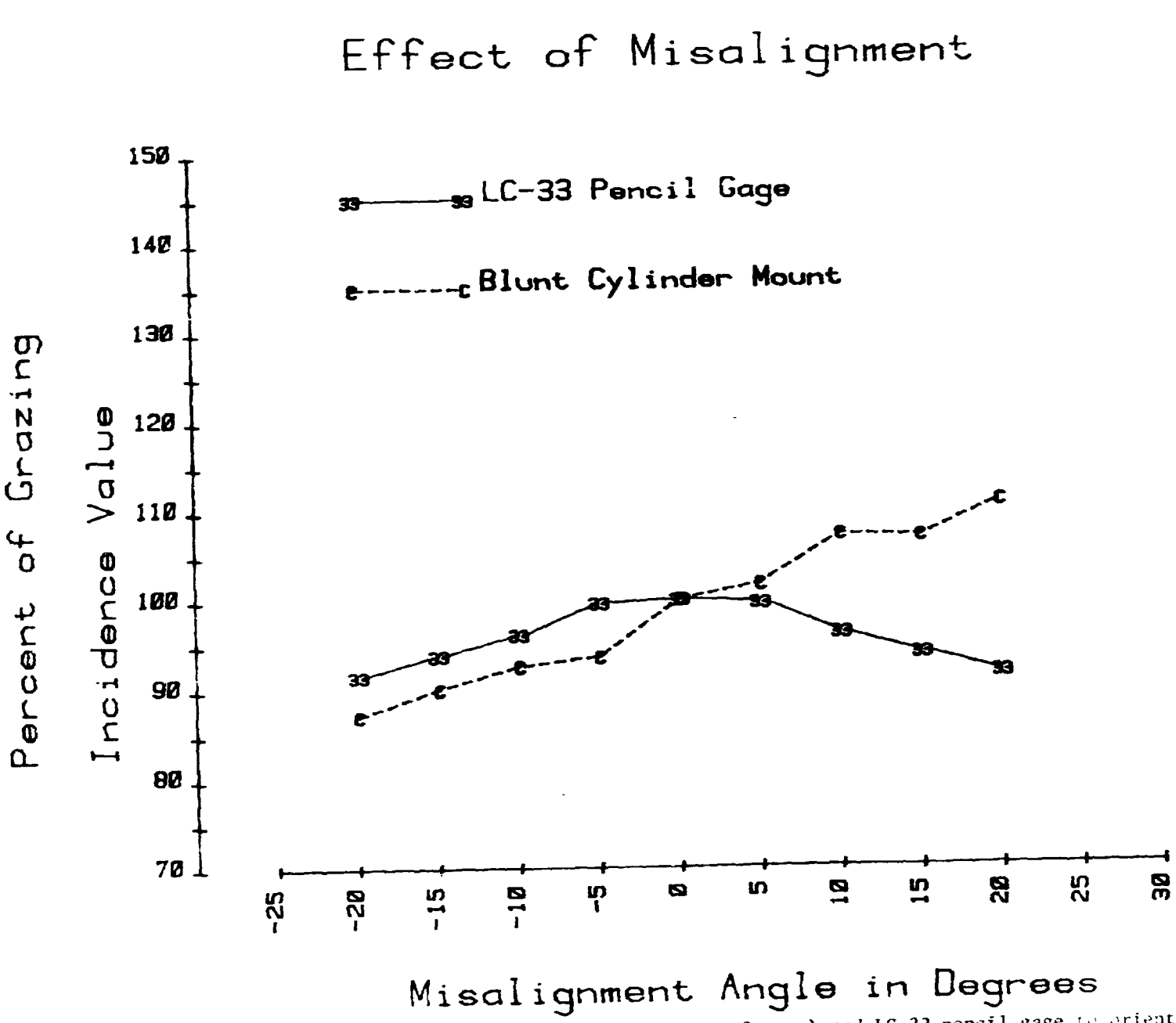

Figure 5.7-9. Sensitivity of blunt cylinder mount (as used with ST-2 gage) and LC-33 pencil gage to orientation.

5.8 EFFECTS OF AERODYNAMIC CLEANLINESS

Every object in the flow field of a shock wave generates a signature. It is desirable to have transducers that are as aerodynamically clean as possible. The following example illustrates this point.

Figure 5.8-1 shows the standard clamping arrangement used to secure the blunt cylinder mount. These clamps provide several rotational degrees of freedom to facilitate accurate alignment.

Figure 5.8-2 is a pressure-time history obtained with the standard clamp. Note the bump that occurs roughly 600 microseconds after the blast wave passes the transducer. This bump is assumed to be caused by a reflection from the clamping mechanism.

Figure 5.8-3 shows an aerodynamically clean method of holding the blunt cylinder mount. Alignment was accomplished by raising or lowering the stand until grazing incidence was achieved.

Figure 5.8-4 shows a pressure measurement made with the aerodynamically clean mount. Note that the pressure decay is smooth, indicating no reflections are present.

This experiment confirmed the suspicion that the bump during the decay portion of the standard mount measurement was caused by reflection from the clamping mechanism. The next step was to create an intentionally dirty clamping arrangement and see if doing so accentuates the reflection problem.

Figure 5.8-5 shows the aerodynamically dirty clamping arrangement. Note that the transducer is placed close to the supporting mechanism and the thumbscrews are turned so that they are flat, reflecting surfaces, perpendicular to the direction of flow.

Figure 5.8-6 is a pressure versus time history obtained with the dirty mount. Note that the reflection has been dramatically accentuated. In fact, the peak pressure in this measurement is caused by the reflection from the clamping mechanism, not from the incident pressure wave!

It is important to avoid situations where peak pressure depends more on the measurement system than the incident pressure wave. As illustrated in this example, attention to aerodynamic cleanliness is required to avoid such a situation.

5.8 (Cont'd)

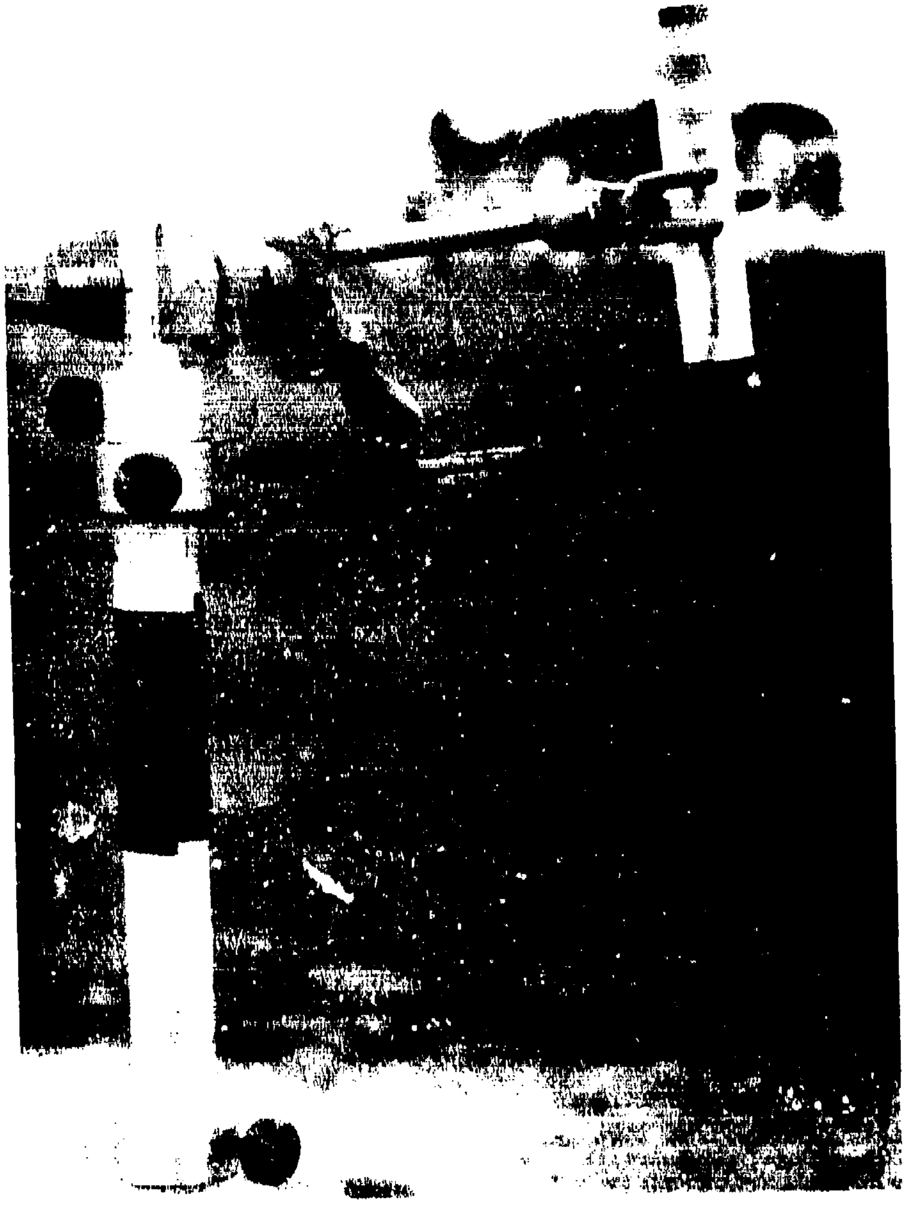

[illegible] arrangement used to hold [illegible]

5.8 (Cont'd)

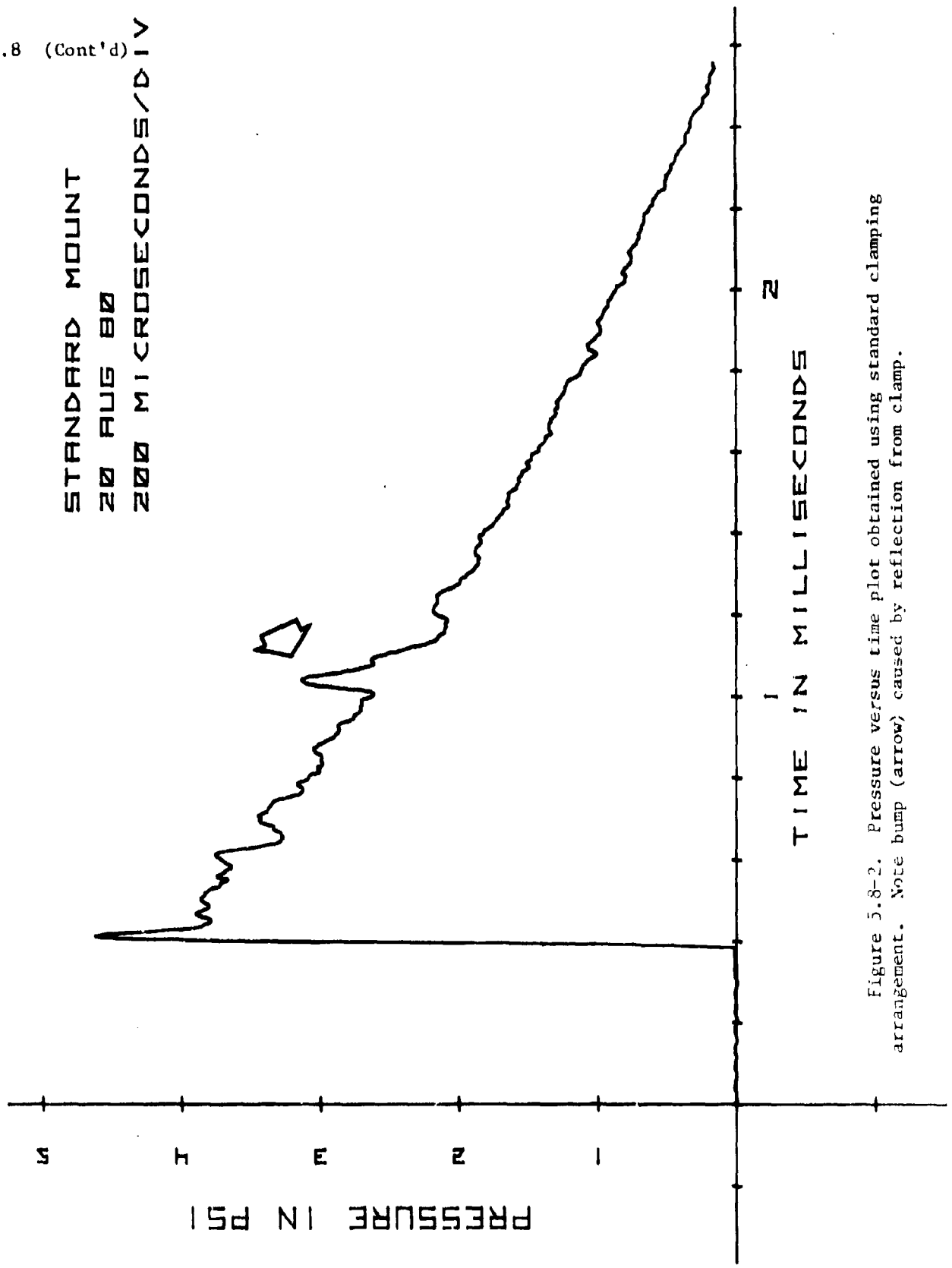

Figure 5.8-2. Pressure versus time plot obtained using standard clamping arrangement. Note bump (arrow) caused by reflection from clamp.

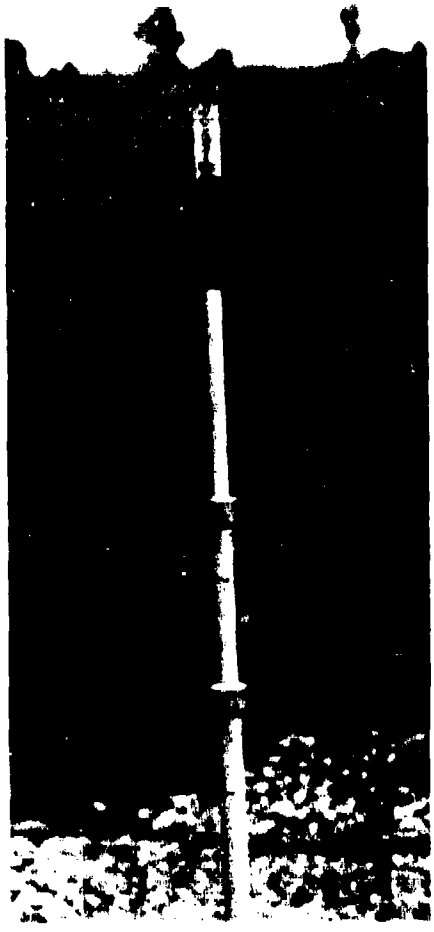

Figure 5.8-3. Photograph of aerodynamically clean method of supporting blunt cylinder model.

5.8 (Cont'd)

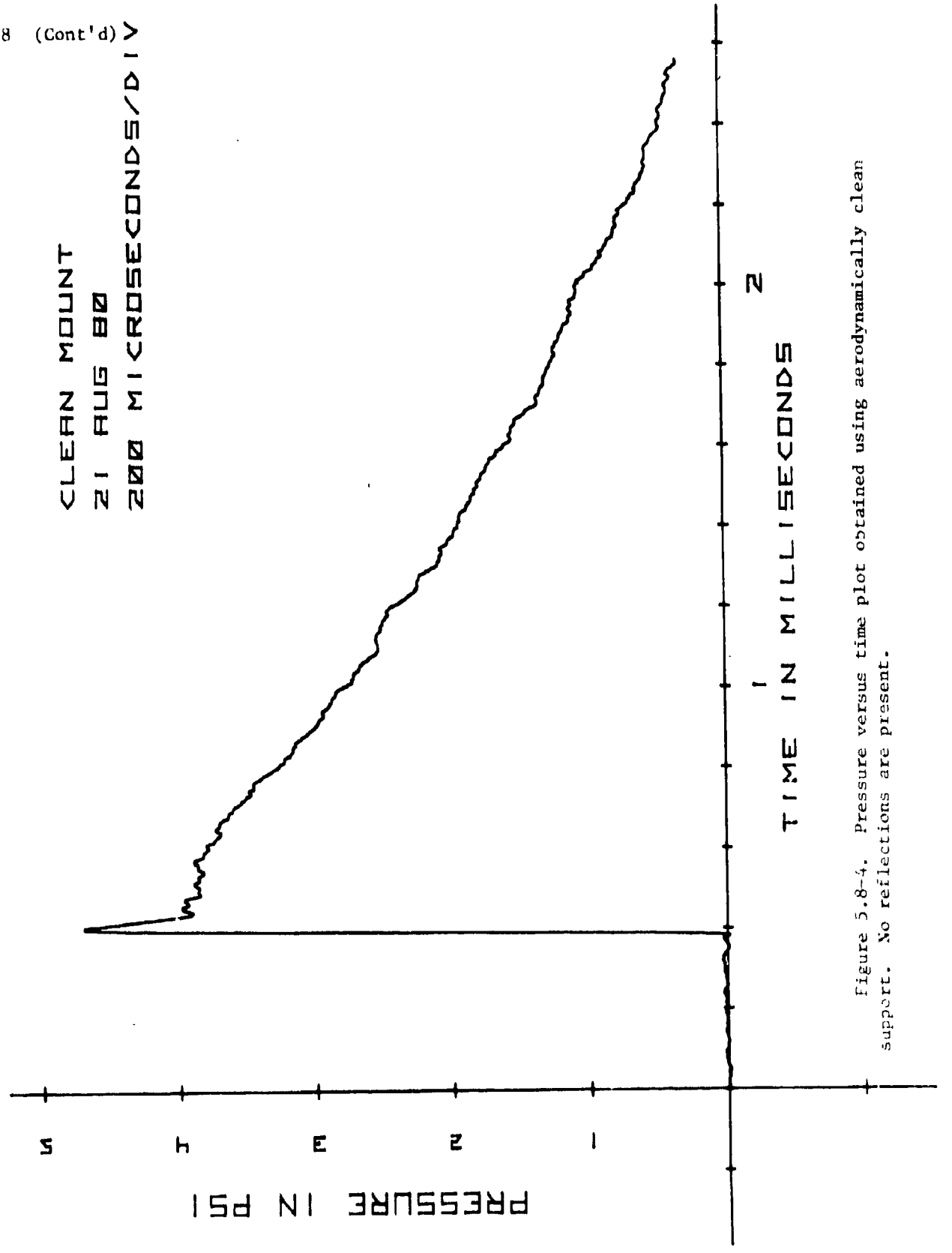

Figure 5.8-4. Pressure versus time plot obtained using aerodynamically clean support. No reflections are present.

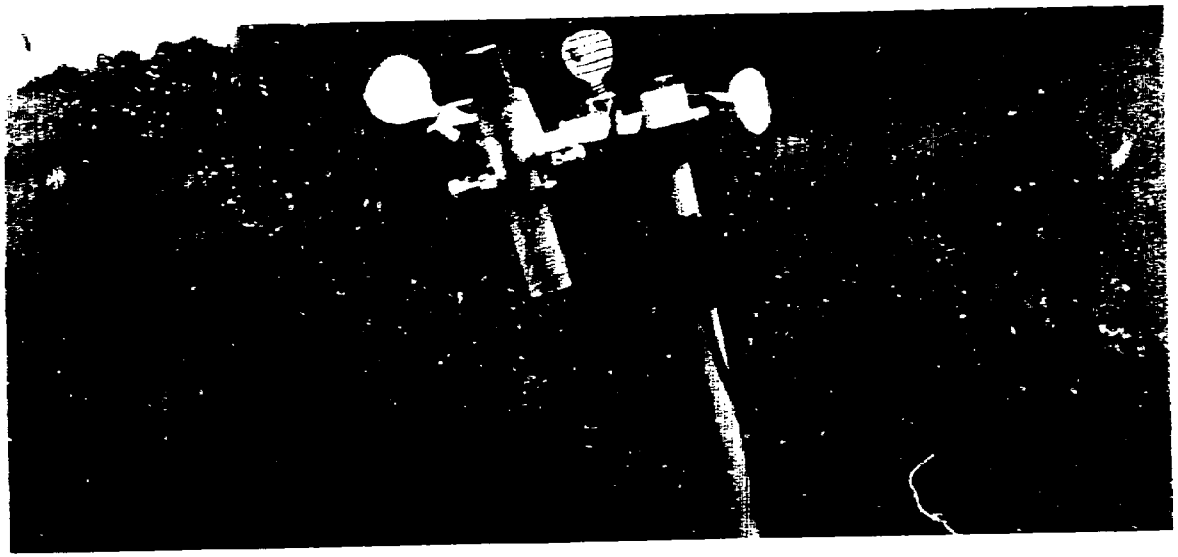

Figure 5.8-5. Photograph of aerodynamically dirty support.

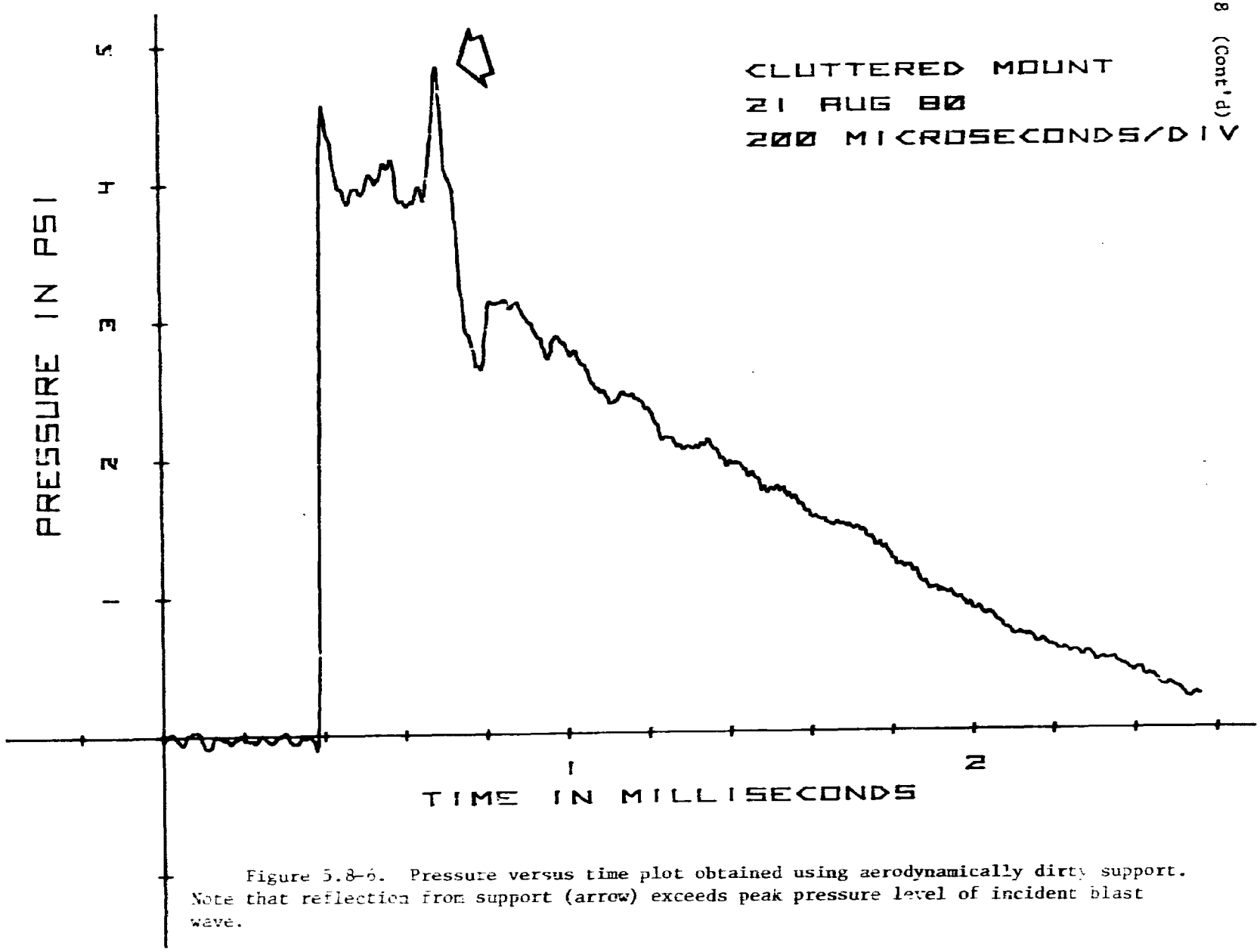

Figure 5.8-6. Pressure versus time plot obtained using aerodynamically dirty support. Note that reflection from support (arrow) exceeds peak pressure level of incident blast wave.

(Page 186 Blank)

SECTION 6. RECORDING, PLAYBACK, AND ANALYSIS OF DATA

6.1 INTRODUCTION

The choice of equipment used to record and analyze blast measurements can have a significant effect on the results obtained. Figure 6.1-1 shows a typical block diagram for data acquisition and data analysis instrumentation. Figure 6.1-2 shows a data-acquisition trailer in the field.

Figure 6.1-3 shows the interior of an FM tape recorder trailer. This kind of data-acquisition instrumentation has been standard at APG for many years. Analysis of the data is accomplished by subsequent digitizing of the FM magnetic tape.

Figure 6.1-4 shows the interior of one of the new digital data-acquisition trailers. In this facility, the analog signal from the transducer is immediately converted into digital form and stored in digital memory. A mini-computer in the trailer controls transfer of the data and can perform on the spot analysis if necessary.

Figure 6.1-5 shows a digital transient recorder that has been interfaced to a digital calculator and plotter. Because of its small memory (4000 words), only a portion of the blast record can be faithfully recorded and stored.

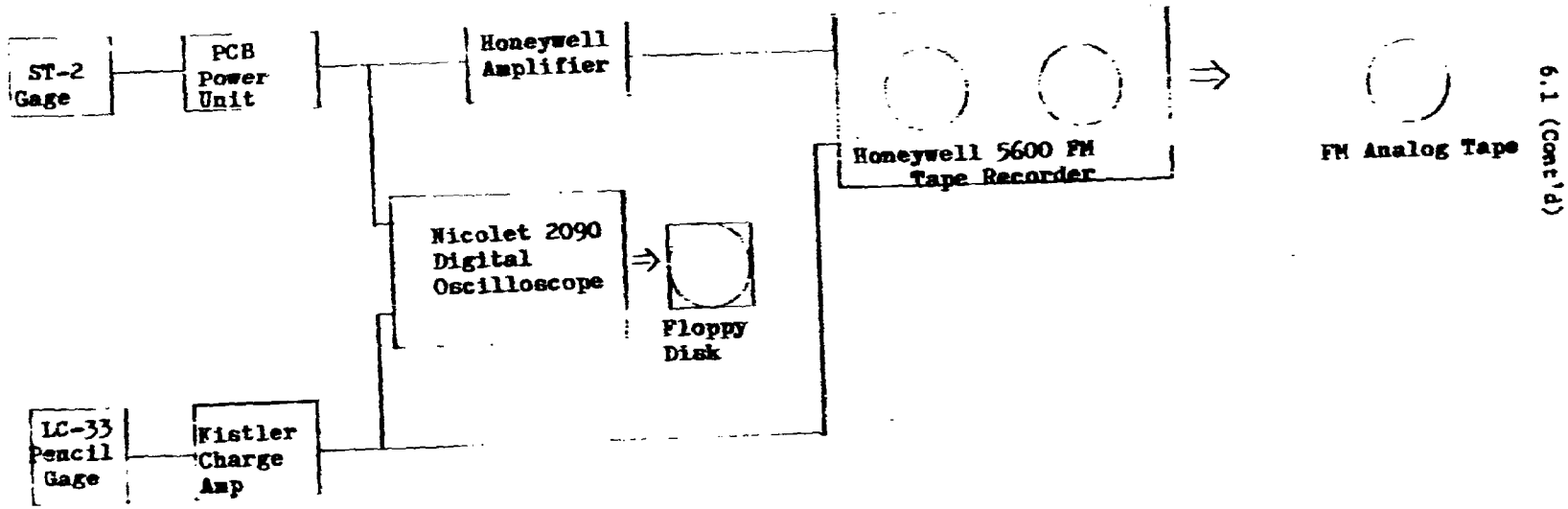

Data Acquisition Instrumentation

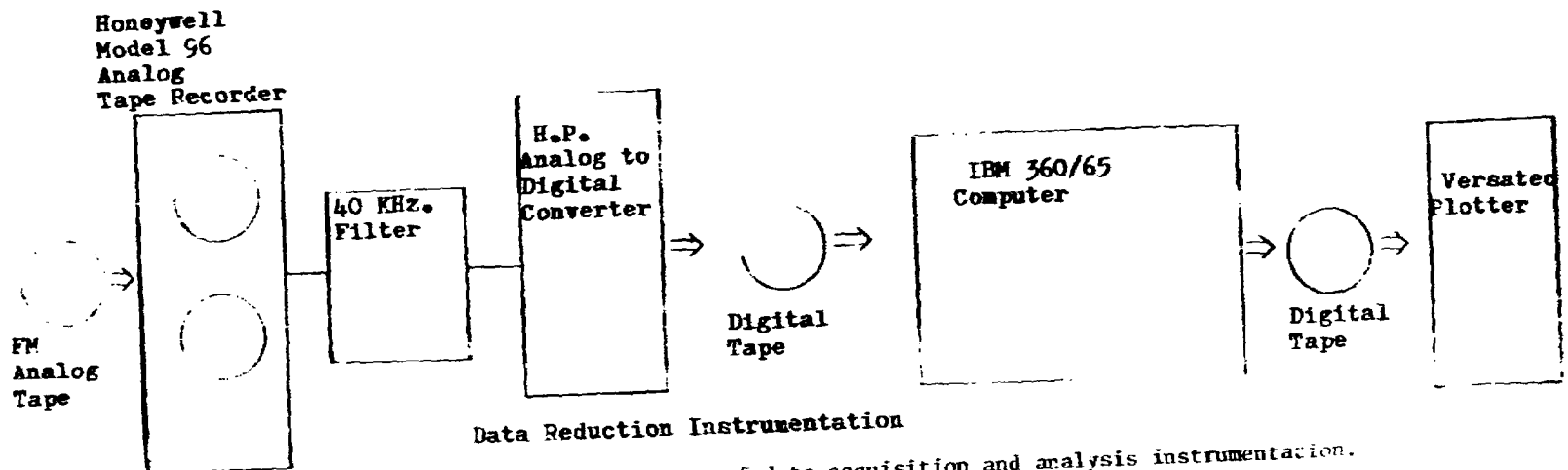

Data Reduction Instrumentation

Figure 6.1-1. Block diagram of data acquisition and analysis instrumentation.

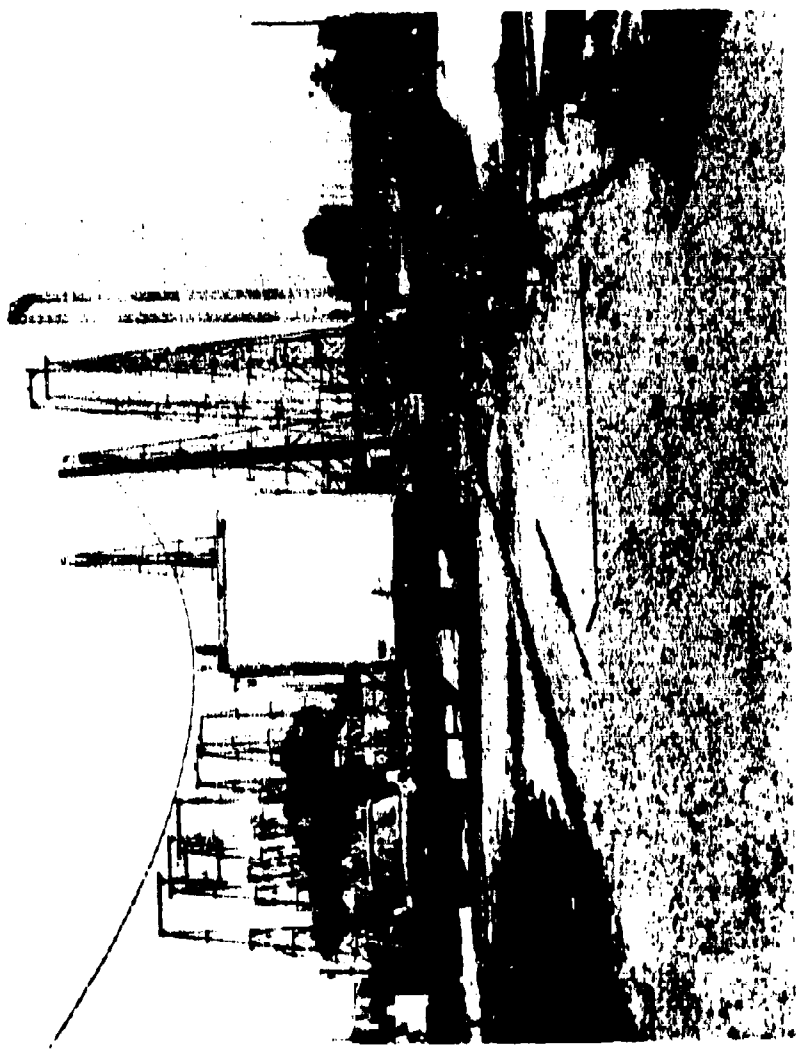

Figure 6.1-2. Photograph of data-acquisition trailer for field measurements.

Fig. 1 (Cont'd)

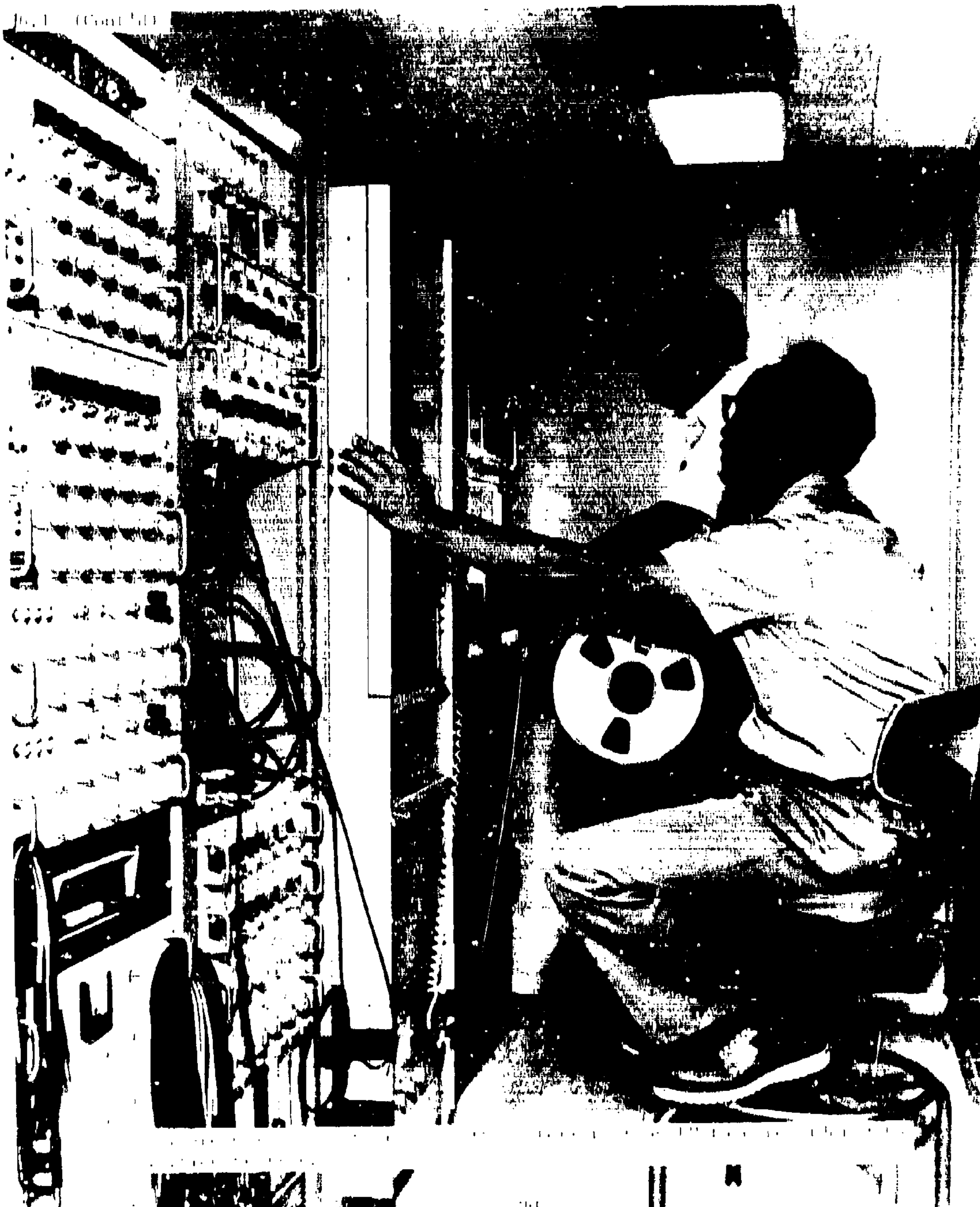

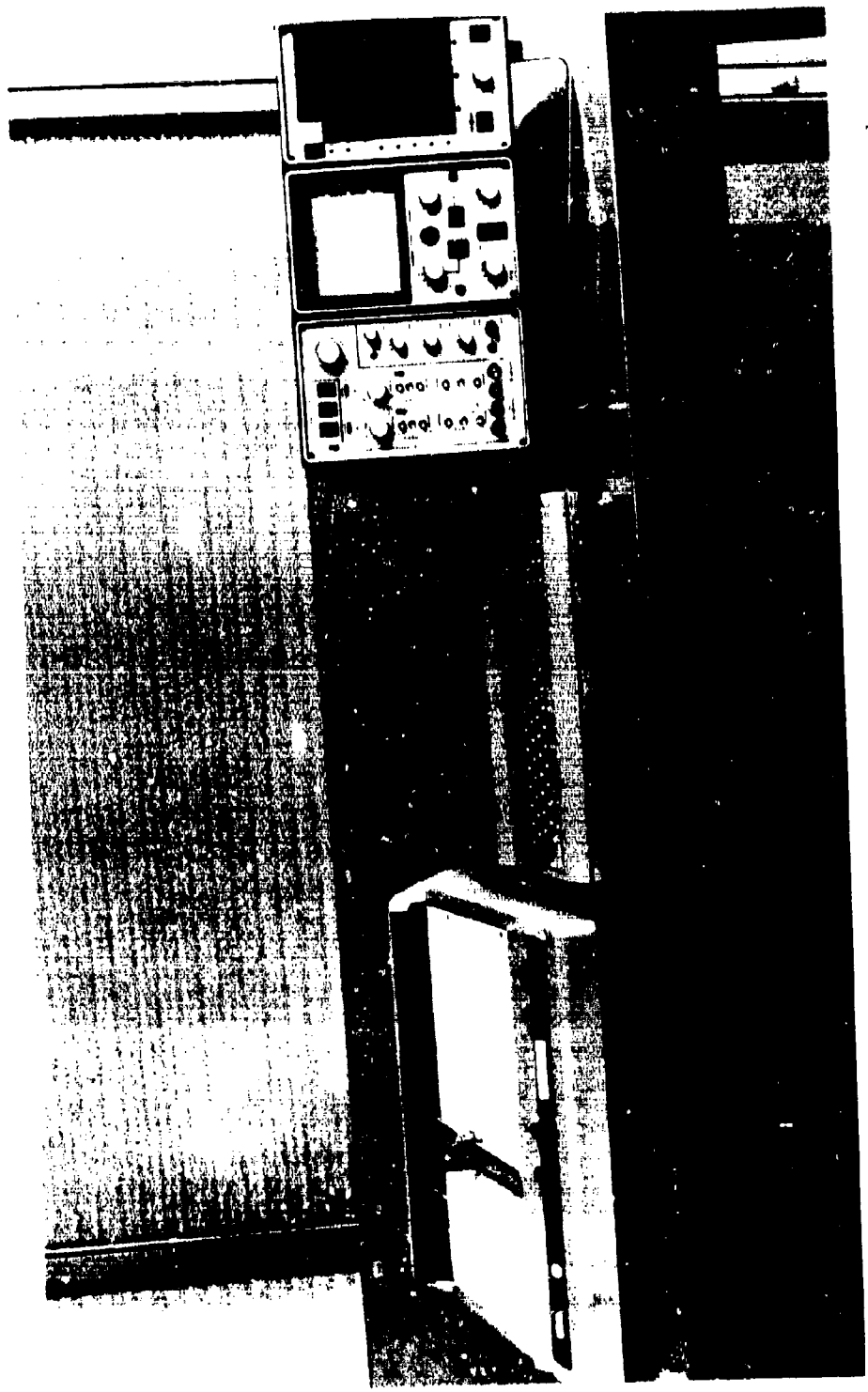

Figure 6.1-5. Photograph of digital transient recorder, desk top calculator, and digital plotter.

6.2 EFFECTS OF FILTERS

Almost all analysis of blast overpressure is performed by digital computers. An anti-aliasing filter is required prior to digitizing analog waveforms that are produced by a magnetic tape or directly from the transducer.

Various filters are available for this purpose. Some are designed for optimum frequency response, others are designed for optimum transient response. Analysis of blast overpressure is normally done in the time domain, with considerable interest in the peak pressure. For these reasons, optimum transient response is desired.

Figure 6.2-1 shows the response of various 40 kHz filters to a step. Note that the Elliptic and Butterworth filters (which are designed for optimum frequency response) have severe overshoot. Note that the Bessel filter (which is designed for optimum transient response) has the least overshoot and the shortest rise time. Because of these qualities, the Bessel filter is specified in the standardized procedures for muzzle blast measurement (ref 4).

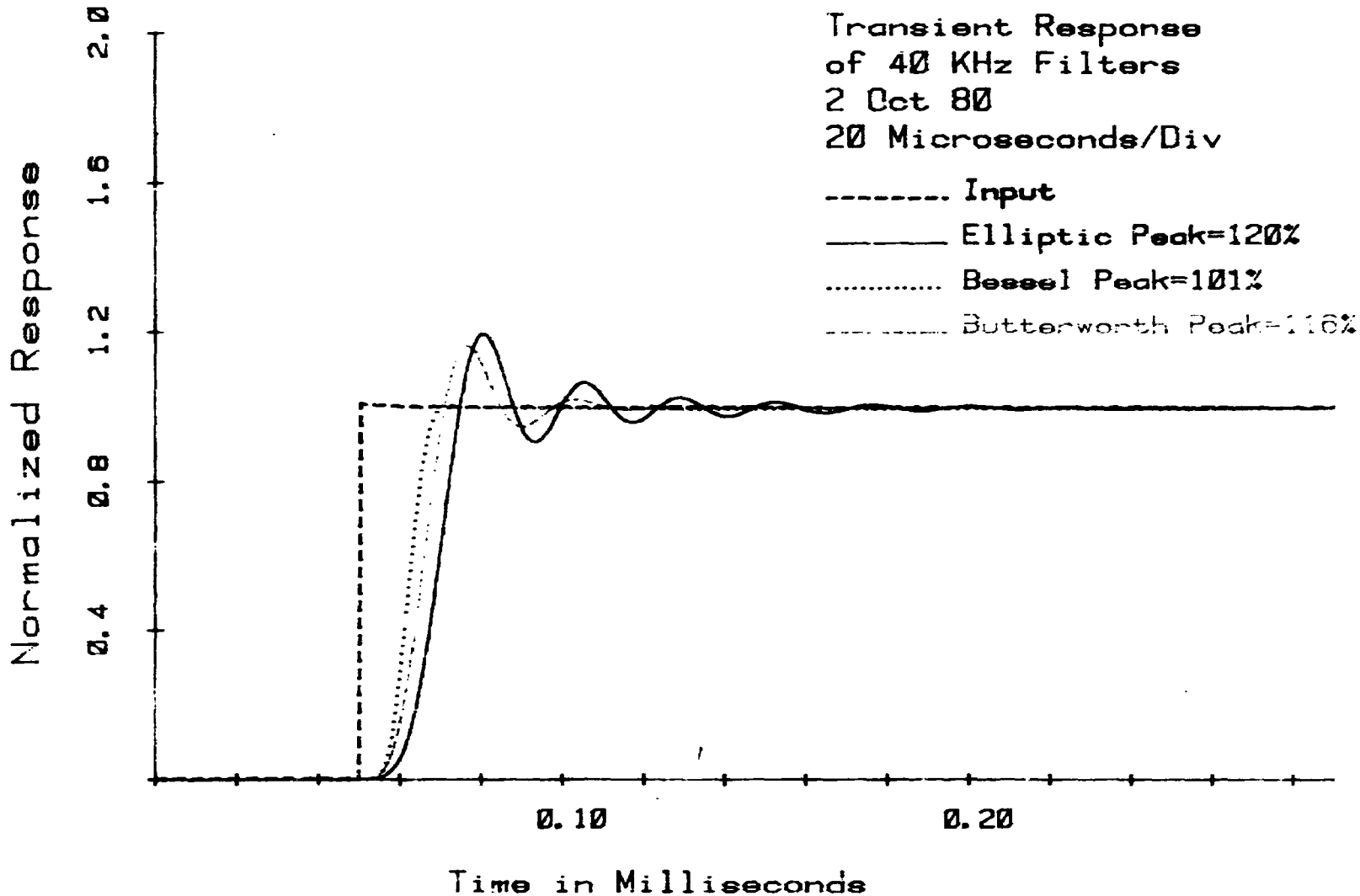

Figure 6.2-1. Transient response of 40 kHz filters. Bessel and Butterworth filters are 6 pole, 36 dB/octave initial rolloff. Elliptic filter is 6 pole, 6 zero, 80 db/octabe initial rolloff.

6.3 TAPE RECORDER EFFECTS

Some tape recorders have filters in the playback electronics that are user-selectable. The Honeywell 96 tape recorder has the option of optimum frequency response or optimum transient response in playback. As shown in figure 6.3-1, the optimum transient response is preferable for analysis of transients with short rise times, like blast waves.

Figure 6.3-2 shows a recording played back through a Bessel filter and the Bessel setting in the recorder playback electronics compared to the same recording with Butterworth filtering. Note that interpretation of the peak pressure of this recording can differ by 13%, depending upon how the filters are set.

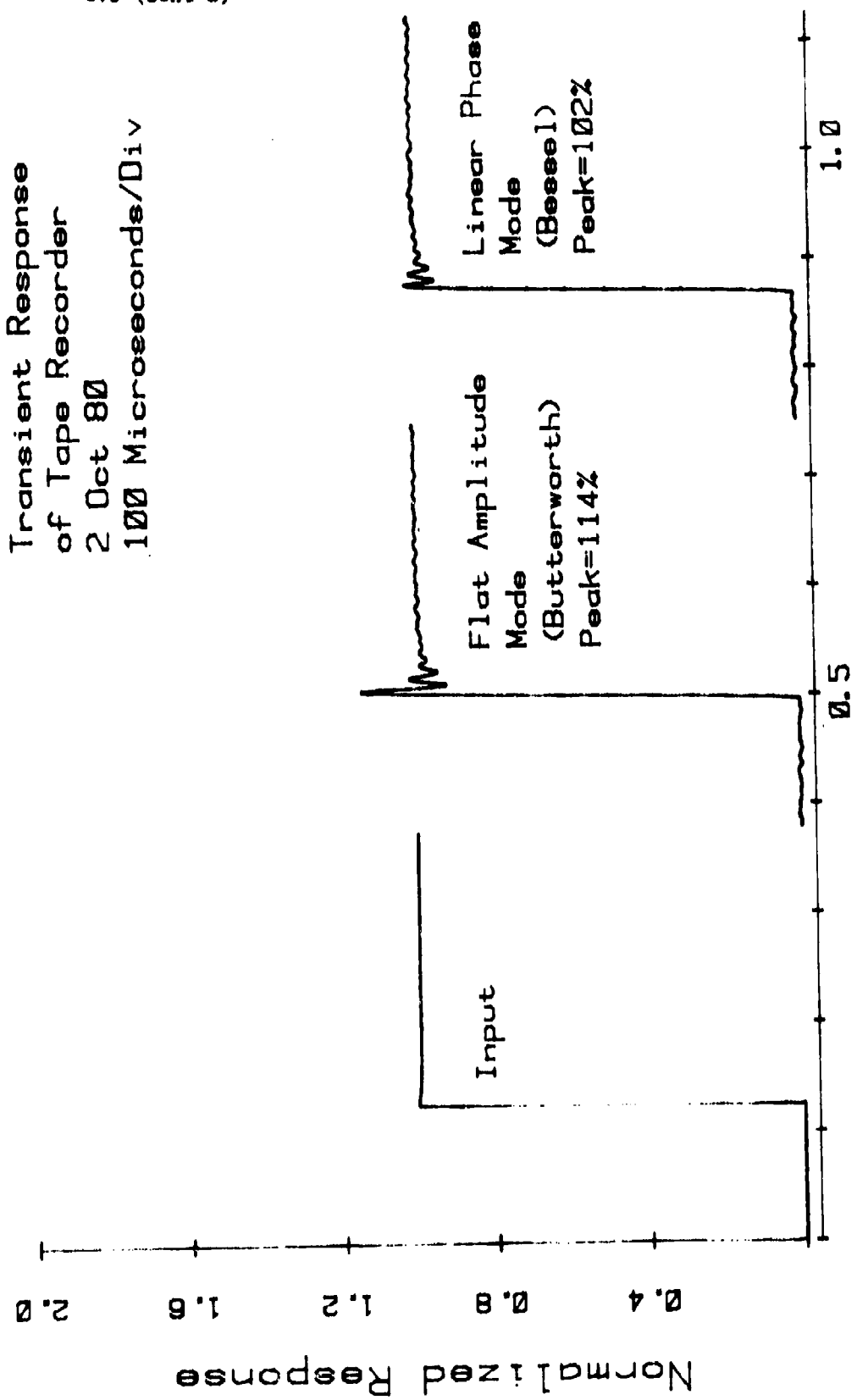

Figure 6.3-1. Transient response of Honeywell 96 tape recorder.

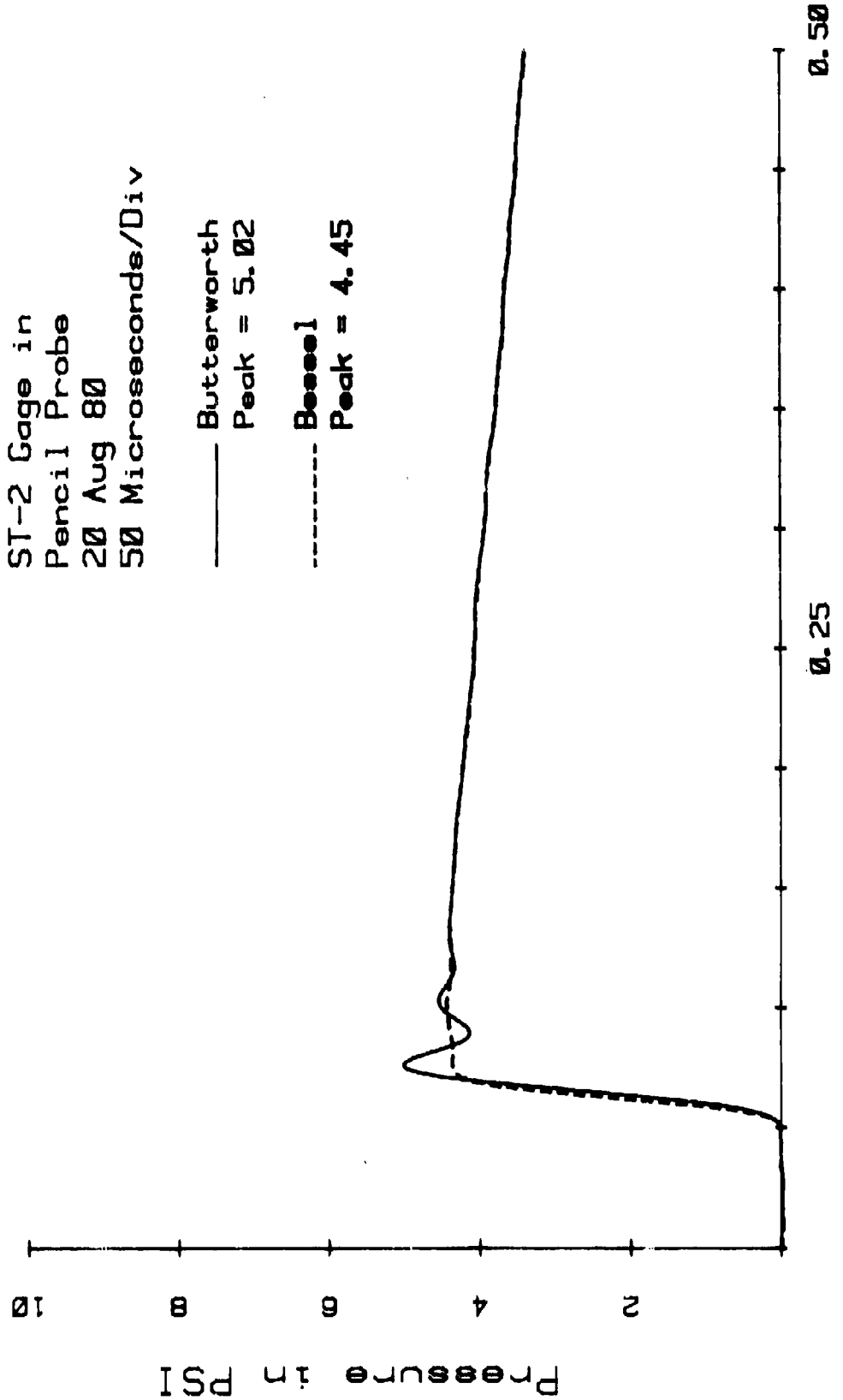

Figure 6.3-2. Comparison of Butterworth and Bessel filtering of the same measurement. Note 13% discrepancy in peak pressure.

6.4 COMPARISON OF RAW TRANSDUCER OUTPUT TO RECORDER AND FILTERED SIGNALS

Reference 4 requires that analysis of muzzle blast measurements be performed after the signal has been passed through a 40 kHz Bessel filter with 36 dB/octave rolloff. To compare the effect of filtered versus unfiltered signals, several measurements were simultaneously recorded on a digital transient recorder and an FM tape recorder. Figure 6.4-1 shows a block diagram of the instrumentation used to play back these recordings.

The tape recordings were made at 120 inches/second which produced a frequency response of 80 kHz. In figures 6.4-2 through 6.4-4, the unfiltered transducer output, the 80 kHz tape recording played back directly, and the tape recording played through a 40 kHz filter are compared.

Note that in a standard signal, such as shown in figure 6.4-2, there is less than 1% difference between the filtered signal and the signal directly out of the tape recorder. It is suspected that part of the 4% difference between the raw transducer output and the recorder output is due to some minor problem in the playback performance of the particular tape recorder used in this experiment.

Figure 6.4-3 shows larger discrepancies between the direct, tape, and filtered peak pressure values because the waveform has a sharper peak. The waveform shown in figure 6.4-4 has a very sharp peak, which produces very large discrepancies between the direct, tape, and filtered peak pressure values.

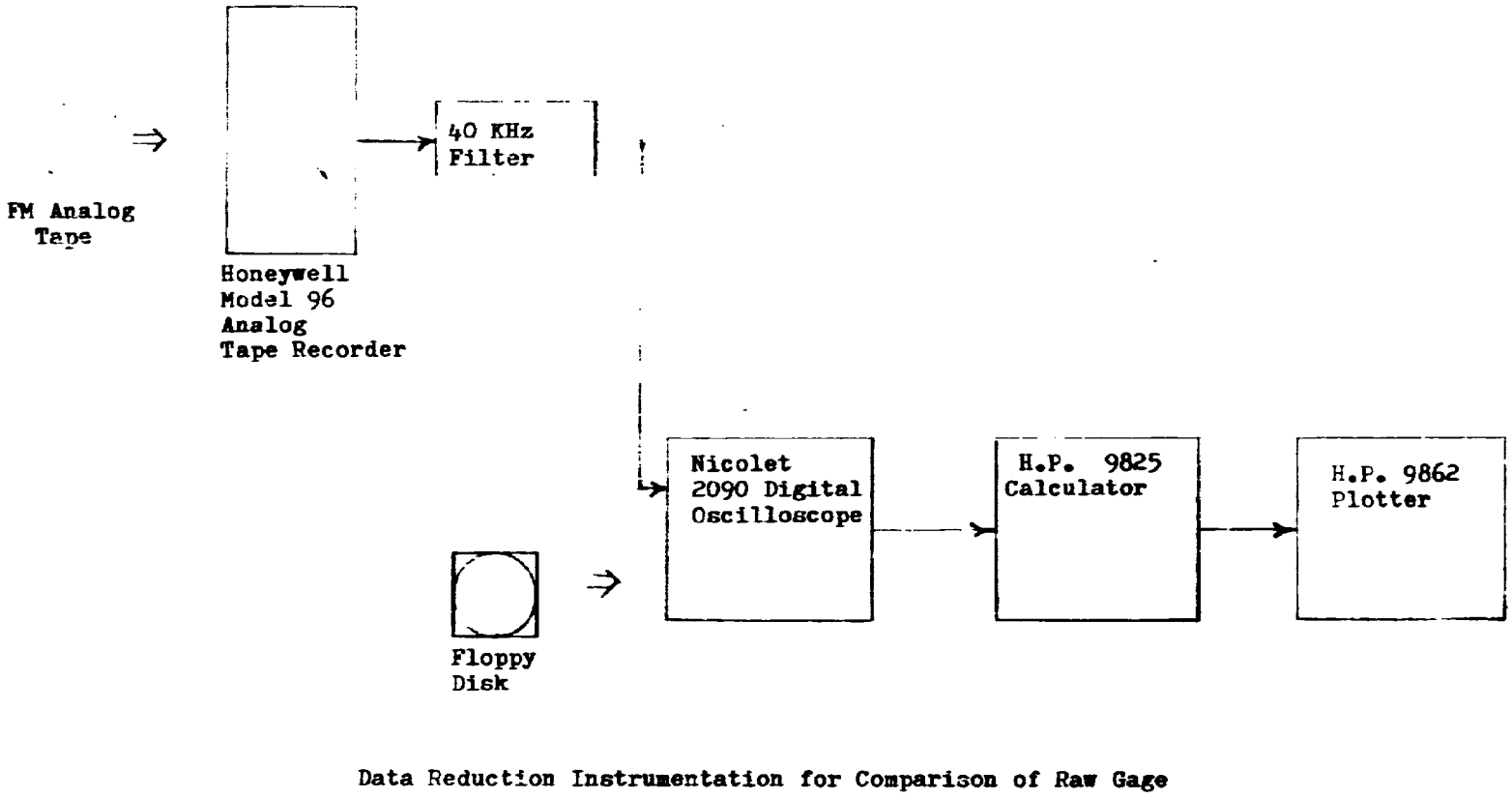

Data Reduction Instrumentation for Comparison of Raw Gage Output to Filtered Gage Output

Figure 6.4-1. Block diagram of instrumentation used to compare raw gage output to recorded and filtered signals.

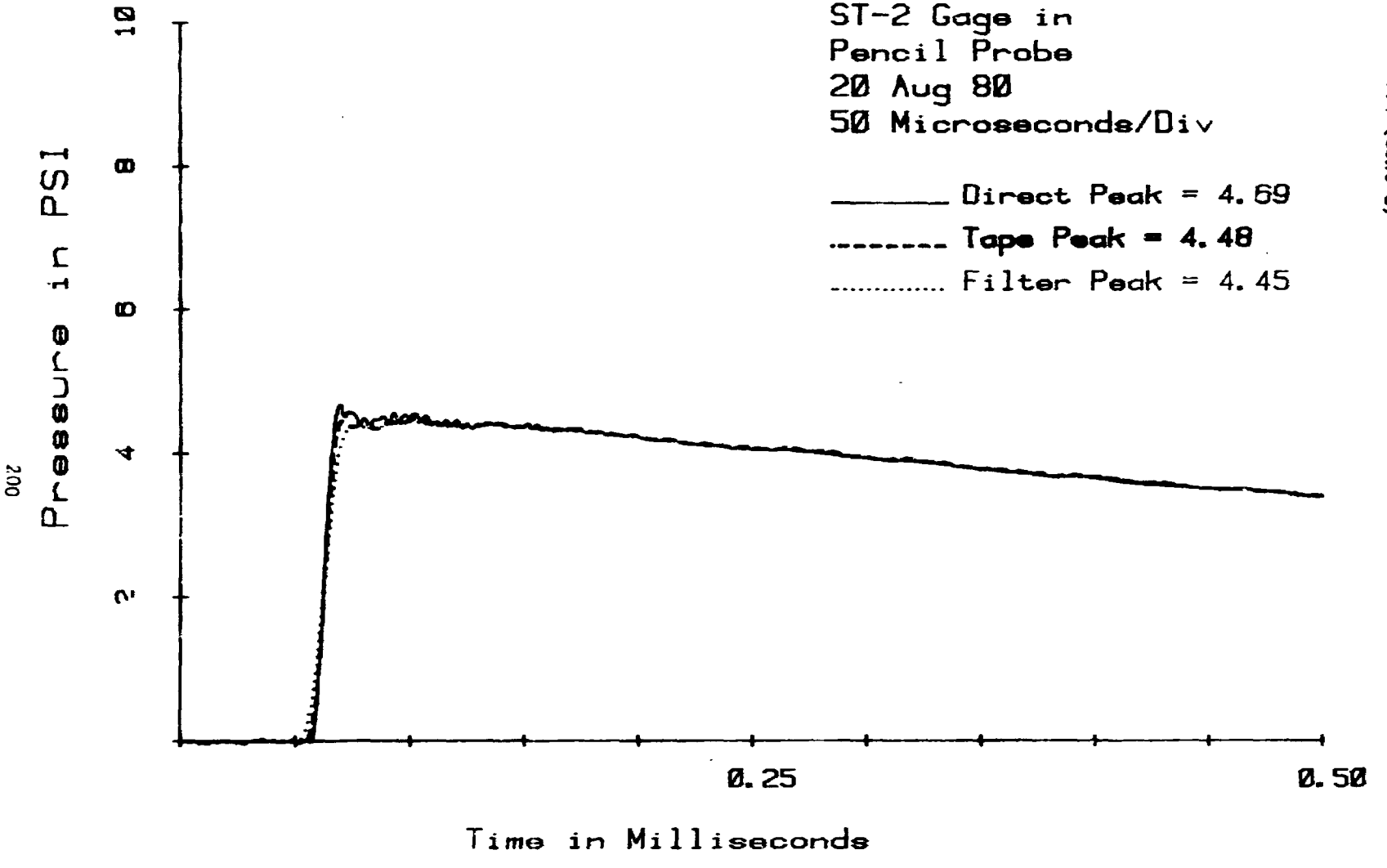

6.4 (Cont'd)

Figure 6.4-2. Comparison of raw gage output to filtered signal of a standard blast measurement.

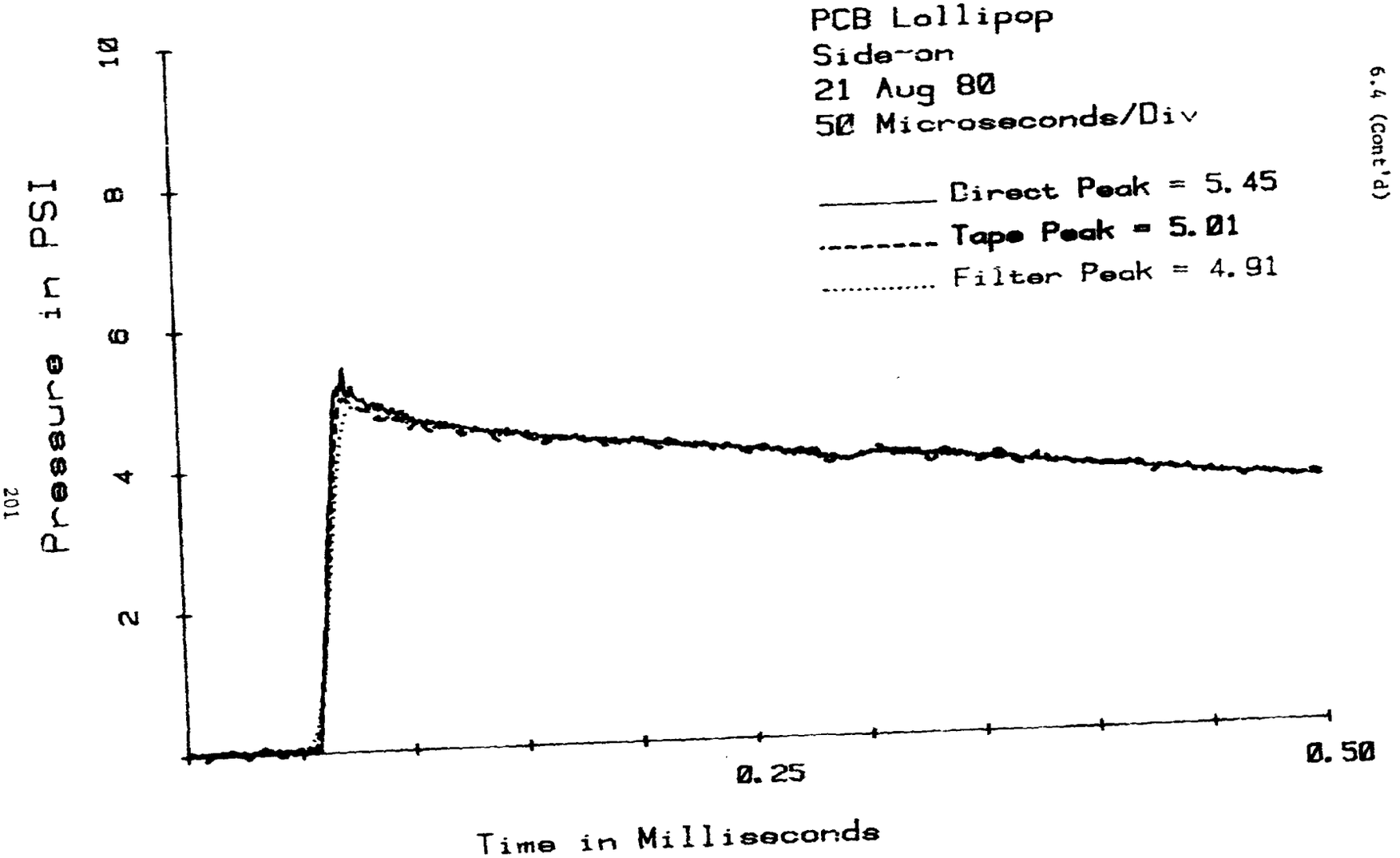

Figure 6.4-3. Comparison of raw gage output to filtered signal of a slightly peaked blast measurement.

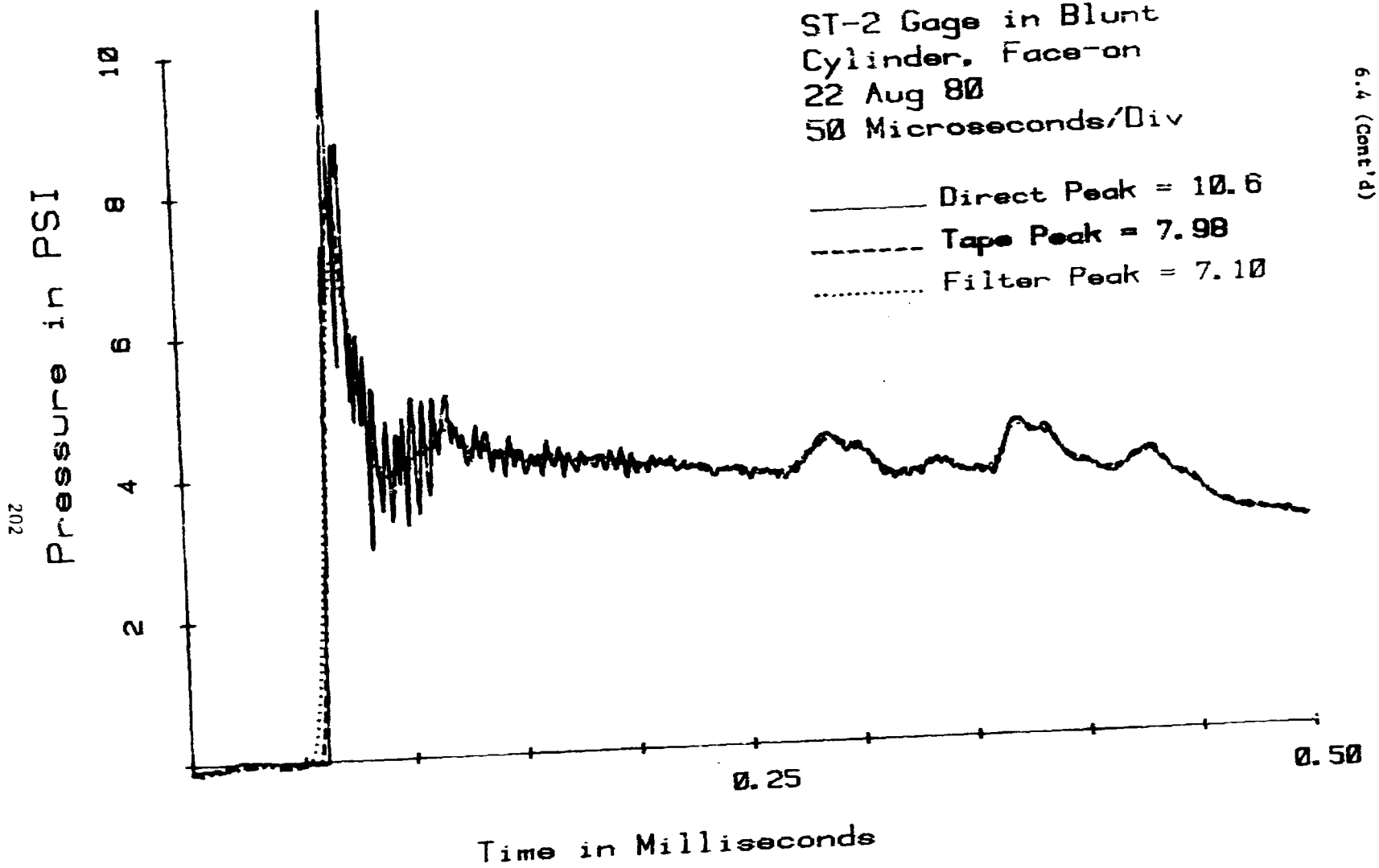

Figure 6.4-4. Comparison of raw gage output to filtered signal of a blast measurement with very sharp peaks.

6.5 EFFECT OF ELECTRICAL NOISE ON "B" DURATION

"B" duration is essentially the time required for the pressure versus time history to decay to less than 10% of the peak pressure value. Obviously, if the signal to noise ratio is 10:1 or less, the "B" duration will be infinite.

Signal to noise ratio is, therefore, critical to measurement of "B" duration. Figure 6.5-1 shows a pressure measurement made with an FM tape recorder. Note that the width of the baseline noise is roughly 2% of the peak pressure. Later in the record, the noise level increases for some unknown reason to roughly 7% of the peak pressure. Note that the "B" duration indicated in this plot is 45 milliseconds.

Figure 6.5-2 is a recording of the same waveform using digital data acquisition with a much larger signal to noise ratio. Note that with the excess electrical noise removed, the "B" duration is dramatically reduced to 27.5 milliseconds.

6.5 (Cont'd)

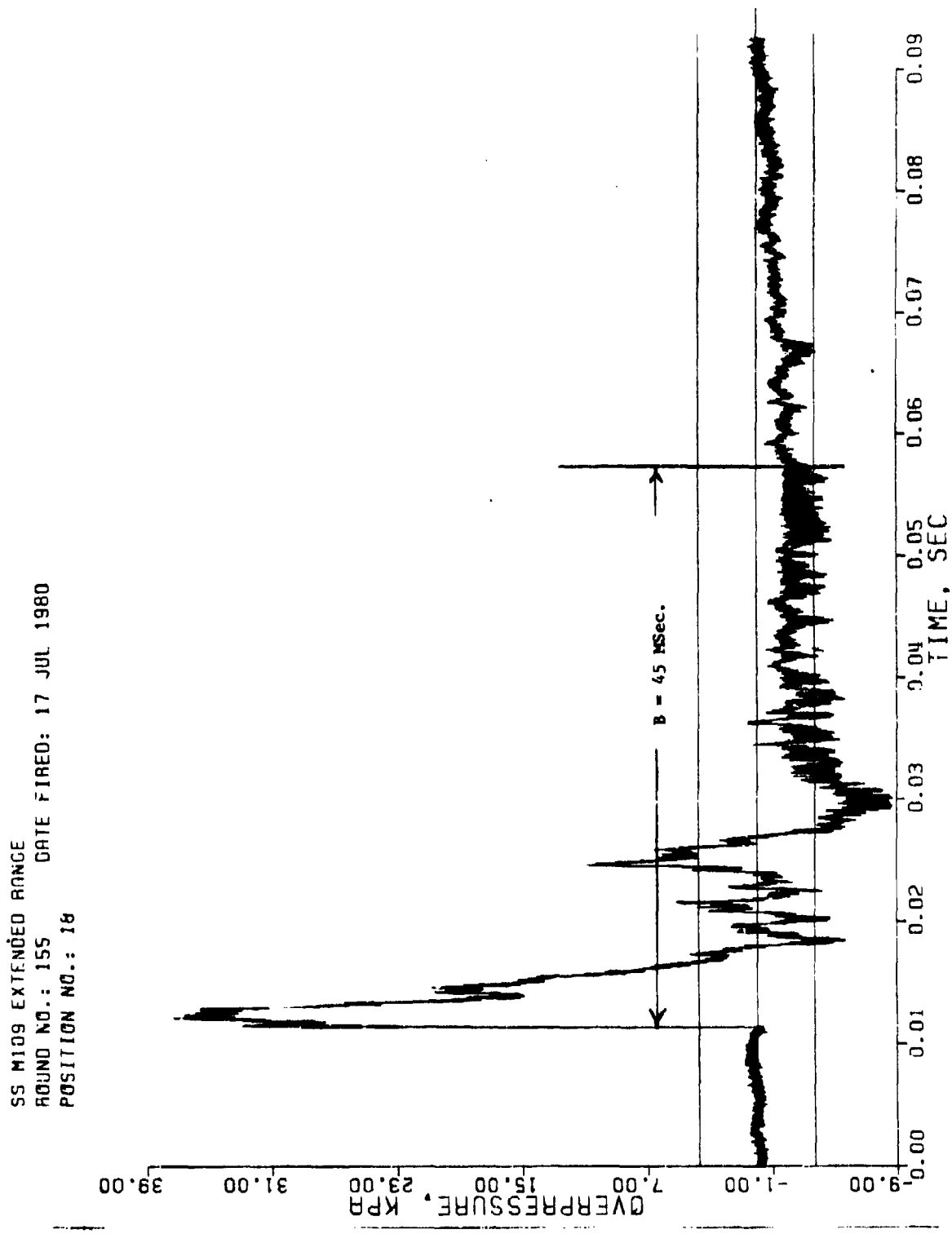

Figure 6.5-1. Pressure measurement with excessive electrical noise.

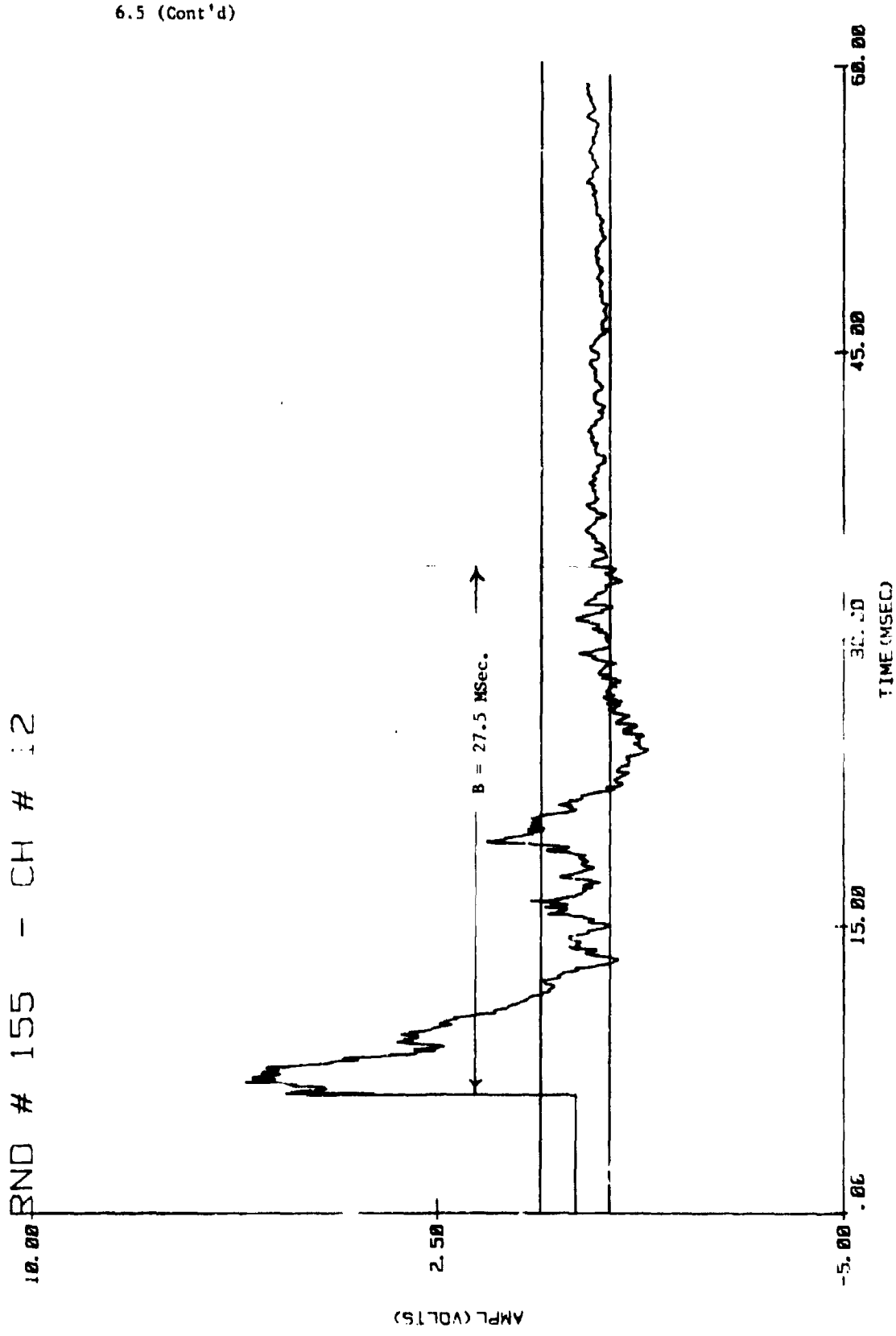

Figure 6.5-2. The same pressure measurement without excessive electrical noise.

(Page 206 Blank)

SECTION 7. APPENDICES

APPENDIX A - REFERENCES

1. Glasstone, Samuel, The Effects of Nuclear Weapons, US Atomic Energy Commission, April 1962.

2. MIL-STD-1474B (MI), Military Standard, Noise Limits for Army Materiel, 18 June, 197..

3. Garinther, Georges R.; Hodge, David C.; Chaiken, Gerald; Rosenberg, LTC Donald M.; Design Standards for Noise: A Review of the Background and Bases of MIL-STD-1474 (MI), Technical Memorandum 12-75, US Army Human Engineering Laboratory, Aberdeen Proving Ground, MD, March 1975.

4. Patterson, James; Coulter, George A.; Kalb, Joel; Garinther, George; Mozo, Benjamin; Gion, Edmund; Teel, George; Walton, W. Scott; Standardization of Muzzle Blast Overpressure Measurements, Special Publication ARBRL-AP-00014, US Army Armament Research and Development Command, Ballistic Research Laboratory, Aberdeen Proving Ground, MD, April 1980.

5. Cummings, Benjamin E., "I-81 mm Mortar Muzzle Blast Estimate," unpublished Disposition Form dated 18 May, 1979.

6. Gion, Edmund J.; Coulter, George R.; Shock Tube Tests of Muzzle Blast Transducers, Interim Memorandum Report No. 691, US Army Research and Development Command, Ballistic Research Laboratory, Aberdeen Proving Ground, MD, September 1980. (Note: final report of this work to be published at a later date.)

7. Goodman, H. J., Compiled Free - Air Blast Data on Bare Spherical Pentolite, Ballistic Research Laboratory Report No. 1092, US Army Ballistic Research Laboratories, Aberdeen Proving Ground, MD, February 1960.

8. Brode, Harold L., Review of Nuclear Explosion Phenomenon Pertinent to Protective Construction, Rand Document R-425-PR, DDC AD 601139, Rand Corporation, Los Angeles, CA, May 1964.

9. Hilten, John S.; Vezzetti, Carol F.; Mayo-Wells, J. Franklin; Lederer, Paul S.; A Test Method for Determining the Effect of Thermal Transients on Pressure - Transducer Response, NBS Technical Note 905, US Department of Commerce, National Bureau of Standards, Washington, DC, March 1976.

10. Hilten, John S.; Vezzetti, Carol F.; Mayo-Wells, J. Franklin; Lederer, Paul S.; Experimental Investigation of Means for Reducing the Response of Pressure Transducers to Thermal Transients, NBS Technical Note 961, US Department of Commerce, National Bureau of Standards, Washington, DC, January 1978.

11. Coulter, George A.; Dynamic Calibration of Pressure Transducers at the BRL Shock Tube Facility, BRL Memorandum Report No. 1843, US Army Ballistic Research Laboratory, Aberdeen Proving Ground, MD, May 1967.

APPENDIX B - DISTRIBUTION LIST

TECOM Project No. 7-CO-ILO-AP1-001

Addressee	Final Report
Commander Army Test and Evaluation Command ATTN: DRSTE-AD-M	1
DRSTE-AD-I	1
DRSTE-CM-F	1
DRSTE-SG-A	1
Aberdeen Proving Ground, MD 21005	
Commander US Army Materials and Mechanics Research Center ATTN: DRXMR-ER (Mr. Joe Prifti) Watertown, MA 02172	1
Commander US Army Environmental Hygiene Agency ATTN: HSE-OB (Mr. Felix Sachs) Bldg E2100 Aberdeen Proving Ground, MD 21010	1
Commander US Army Aeromedical Research Laboratory ATTN: SGRD-VAH-SP (Mr. James Patterson)	1
SGRD-UAH-SP (Mr. Ben Mozo)	1
PO Box 577 Fort Rucker, AL 36362	
Commander US Army Armament Research and Development Command ATTN: DRDAR-LCA-F (Mr. Loeb)	1
DRDAR-LCA-G (Mr. Dick Collett)	1
Dover, NJ 07801	
Commander US Army Yuma Proving Ground ATTN: STEYP-MTC (Mr. Welton Phillips) Yuma Proving Ground, AZ 85364	1
Project Manager - CAWS US Army Armament Research and Development Command ATTN: DACPM-CAWS (Mr. Barth) Dover, NJ 07801	1

Addressee	Final Report
Director US Army Ballistic Research Laboratory/ ARRADCOM	
ATTN: DRDAR-TS-ST	1
DRDAR-TSB-S	2
DRDAR-BLL (Mr. Ed Schmidt)	1
DRDAR-BLL (Mr. Ed Gion)	1
DRDAR-BLT (Mr. George Coulter)	1
DRDAR-BLT (Mr. George Teel)	1
Aberdeen Proving Ground, MD 21005	
Director US Army Human Engineering Laboratory	
ATTN: DRXHE-SP (Mr. Georges Garinther)	1
DRXHE-SP (Mr. Joel Kalb)	1
DRXHE-SP (Mr. Ben Cummings)	1
Aberdeen Proving Ground, MD 21005	
Director Division of Medicine WRAIR/WRAMC	
ATTN: SGRD-UWH-D (CPT Jaeger)	1
Washington, DC 20012	
Commander US Army Aberdeen Proving Ground	
ATTN: STEAP-MT-M	1
STEAP-MT-A (Mr. Lacy)	1
STEAP-MT-A (Mr. Jack Taylor)	1
STEAP-MT-G (Mr. Brady)	1
STEAP-MT-G (Mr. Bill Diegel)	1
STEAP-MT-G (Mr. Steiner)	1
STEAP-MT-G (Mr. Walton)	20
STEAP-MT-X	1
Aberdeen Proving Ground, MD 21005	
Administrator Defense Technical Information Center	
ATTN: DDA	2
Cameron Station Alexandria, VA 22314	

Distribution unlimited.